Roald N. Leif for the degree of Doctor of Philosophy in Oceanography presented on July 23, 1993.

Title: Laboratory Simulated Hydrothermal Alteration of Sedimentary Organic Matter from Guaymas Basin, Gulf of California

Redacted for Privacy

Abstract approved:_____

Bernd R. T. Simoneit

High temperature alteration of sedimentary organic matter associated with marine hydrothermal systems involves complex physical and chemical processes that are not easily measured in most natural systems. Many of these processes can be evaluated indirectly by examining the geochemistry of the hydrothermal system in the laboratory. In this investigation, an experimental organic geochemical approach to studying pyrolysis of sedimentary organic matter is applied to the hydrothermal system in the Guaymas Basin, Gulf of California.

A general survey of hydrothermal oils and extractable organic matter (bitumen) in hydrothermally altered sediments identified several homologous series of alkanones associated with a high temperature hydrothermal origin. The alkanones range in carbon number from C_{11} to C_{30} with no carbon number preference. Alkan-2-ones are in highest concentrations, with lower amounts of 3-, 4-, 5- (and higher) homologs. The alkanones appear to be pyrolysis products synthesized under extreme hydrothermal conditions.

Hydrous pyrolysis and confinement pyrolysis experiments were performed to simulate thermally enhanced diagenetic and catagenetic changes in the immature sedimentary organic matter. The extent of alteration was measured by monitoring the n-alkanes, acyclic isoprenoids, steroid and triterpenoid biomarkers, polycyclic aromatic hydrocarbons and alkanones. The results were compared to bitumen extracts from sediments which have been naturally altered by a sill intrusion and accompanied hydrothermal fluid flow. These pyrolysis experiments duplicated many of the organic matter transformations observed in the natural system. Full hopane and sterane

maturation occurred after 48 hr in experiments at 330°C with low water/rock mass ratios (0.29).

A variety of radical and ionic reactions are responsible for the organic compound conversions which occur under extreme hydrothermal conditions. Short duration pyrolysis experiments revealed that a portion of the hydrocarbons generated from kerogen was observed to go through alkene intermediates, and the rate of alkene isomerization was influenced by the ionic strength and catalytic mineral phases. Confinement of the organic pyrolysate to the bulk sediment accelerated the rates of the biomarker epimerization reactions, suggesting that these reactions are influenced strongly by the association of the inorganic matrix, and that the relative rates of some ionic and radical reactions can be influenced by the water/rock ratio during the pyrolysis experiments.

LABORATORY SIMULATED HYDROTHERMAL ALTERATION OF SEDIMENTARY ORGANIC MATTER FROM GUAYMAS BASIN, GULF OF CALIFORNIA

by

Roald N. Leif

A THESIS

submitted to

Oregon State University

in partial fulfillment of
the requirement for the
degree of

Doctor of Philosophy

Completed July 23, 1993
Commencement June 1994

APPROVED:

Redacted for Privacy

Professor of Oceanic and Atmospheric Sciences in charge of major

Redacted for Privacy

Head of Department of Oceanic and Atmospheric Sciences

Redacted for Privacy

Dean of Graduate School

Date thesis is presented_____July 23, 1993_____

Typed by researcher for _____Roald N. Leif_____

To my parents
and
Yen-Wen

ACKNOWLEDGMENTS

TABLE OF CONTENTS

LIST OF FIGURES

LIST OF TABLES

LABORATORY SIMULATED HYDROTHERMAL ALTERATION OF SEDIMENTARY ORGANIC MATTER FROM GUAYMAS BASIN, GULF OF CALIFORNIA

CHAPTER 1

Introduction

The process of convective cooling of ridge-crest systems, known as seafloor hydrothermal circulation, was first proposed by Anderson and co-workers (1977) to explain the deficiency of conductive heat loss observed at ridge axes in the Indian Ocean. It was also in 1977 that the first observations were made of seafloor hydrothermal venting at the Galapagos spreading center (Corliss et al., 1979). The phenomenon of hydrothermal venting at seafloor spreading centers is now considered a widespread and common process (Von Damm, 1990 and references therein).

Hydrothermal systems can be broadly classified as sedimented or unsedimented. Fig. 1.1 shows the hydrothermal systems of the Eastern Pacific. Of the hydrothermal areas documented so far on this tectonic system, Middle Valley, Escanaba Trough and Guaymas Basin are classified as sedimented rift systems, with the Guaymas Basin being the most thoroughly studied active, sediment-covered hydrothermal vent system.

Guaymas Basin is the largest of the enclosed basins in the Gulf of California with dimensions of approximately 240 x 60 km (Fig. 1.2). The two deepest areas are the parallel spreading centers which are 3 to 5 km wide and approximately 100 m deeper than the surrounding sea floor. These are the northern and southern axial rift valleys (40 and 20 km long, respectively) that overlap at a non-transform offset (Lonsdale and Becker, 1985).

The high sedimentation rate of 1 to 4 m / kyr (van Andel, 1964; Calvert, 1966; Curray et al., 1982) is much higher than typical pelagic rates over other spreading centers. The diatomaceous nanofossil ooze from the plankton blooms (Calvert, 1966) and clastic rich turbidites that pour into the two troughs fill the basin with a sediment cover (Einsele and Kelts, 1982) estimated at 500 m thick (Lonsdale and Lawver,

1980). The reducing conditions in the sediments and low bottom water oxygen concentrations contribute to a total organic carbon content of 3 to 4% (Goldhaber, 1974). Fig. 1.3 is a schematic of the hydrothermal convection of seawater through the sediment cover.

The thick sediment cover prevents extrusion of fresh basalt onto the seafloor. Instead the newly accreted material solidifies as intrusions intercalated within the sediments (Moore, 1973; Williams et al., 1979; Einsele et al., 1980; Gieskes et al., 1982a,b). The results of this process are shown schematically in Fig. 1.4. Two distinct types of hydrothermal systems are operating in Guaymas Basin (Kastner, 1982). A minor system consists of intrusions of hot sills into the highly porous cold sediments (150-200°C), and a major hydrothermal circulation system consists of a relatively shallow magma chamber driving large scale circulation (300±50°C). Both of these processes heat and pyrolyze the sedimentary organic matter to produce petroleum (Simoneit and Lonsdale, 1982). This process of hydrothermal petroleum generation has been documented at other sedimented rift systems (Kvenvolden et al., 1986, 1988; Kvenvolden and Simoneit, 1990; Simoneit et al., 1992; Simoneit, 1990, 1993).

The hydrothermal fluids of the Guaymas Basin hydrothermal system transport large amounts of hydrocarbons to the seafloor, primarily of thermogenic origin (Simoneit and Lonsdale, 1982; Simoneit, 1985). Previous analyses have shown that there is a large variation in the character of the hydrothermal oils. These oils can differ in the amounts of saturated, branched, aromatic and polar components present (Simoneit and Lonsdale, 1982; Kawka, 1990). But in general, the oils formed by this hydrothermal alteration of sedimentary organic matter are characteristically more polar, with a relatively high proportion of aromatic components (Simoneit, 1984; Kawka and Simoneit, 1990).

This study was a continuation of the research into hydrothermal petroleum generation at the Guaymas Basin hydrothermal system. It was conducted to elucidate some of the chemical pathways that control the distributions of the major compounds present in oils from the Guaymas Basin hydrothermal system. This research involved an extension of the survey of oils and sediment extracts to include the polar nitrogen, sulfur and oxygen-containing (NSO) fraction, identifying the major resolved compounds in this fraction. In addition to the survey, laboratory heating experiments by closed system pyrolysis on Guaymas Basin sediments were conducted, and the changes in the content of the solvent extractable organic matter that is resolvable by

gas chromatography was monitored. Specifically, two primary objectives were pursued:

(1) perform a survey of the polar (NSO) fraction of hydrothermally derived oils from Guaymas Basin and identify the major oxygen-containing compounds; and

(2) duplicate some key aspects of oil generation by hydrothermal processes using laboratory hydrous pyrolysis.

This research is motivated by the need to understand the factors that control the transformation of sedimentary organic matter to petroleum. A more complete characterization of the oils and sediment extracts, combined with laboratory pyrolysis studies, should aid in elucidating some of the major chemical pathways by which contemporary organic matter is transformed into oil. An understanding of high temperature pyrolytic conversion is a prerequisite to continued research on this system or other sedimented ridge systems, where different sources of organic matter and inorganic mineral assemblages could influence the pyrolysis products. How the study outlined above relates to hydrothermal conversion of marine sedimentary organic matter conversion is discussed below.

Survey of hydrothermal oils and sediment extracts from the Guaymas Basin hydrothermal system. The previous investigations into the compositions of hydrothermal petroleum have also involved the search for organic compounds that are characteristic of a hydrothermal mode of formation, and could therefore be used as indicators of the quick, high temperature mode of organic matter maturation. Correlations have been made between the high thermal stresses encountered in the Guaymas Basin hydrothermal system and Diels' hydrocarbon (1,2-(3'-methylcyclopenteno)phenanthrene), a triaromatic steroid hydrocarbon common in Guaymas Basin oils. This compound has been used as an indicator of rapid hydrothermal petroleum generation processes (Kawka, 1990; Simoneit et al., 1992), although downcore investigations of sediments thermally altered by contact metamorphism from sill intrusions have found lower amounts in these areas than what is expected from the analyses of seabed oils (Kawka, 1990). These previous investigations have focused primarily on the aliphatic and aromatic components, with

only cursory mention of some polar components of the hydrothermal oils (Gieskes et al., 1988).

As the next step in characterizing petroleum generated by hydrothermal processes, a survey was undertaken of the GC resolved components of the polar NSO fractions in oils and thermally-altered sediment extracts. This survey identified some major oxygenated compounds that appear to be uniquely associated with a high temperature hydrothermal mode of formation. The analyses of the polar NSO fractions were correlated to the aliphatic and aromatic fractions. A description of the samples used in the survey and a summary of the results are presented in Chapter 2. A complete display of the gas chromatograms from this survey is presented in Appendices 1 - 3.

Simulated hydrothermal alteration of sedimentary organic matter by laboratory hydrous pyrolysis. Extensive laboratory research has been performed to further our understanding of the chemical transformations which occur during the maturation of sedimentary organic matter. In simulating the natural oil generation process, high temperature experiments are performed to compensate for the lower temperatures and longer durations during natural petroleum generation. The procedure of laboratory hydrous pyrolysis is one method used to study the transformations of sedimentary organic matter. This procedure is defined as the pyrolysis of a sample in contact with liquid water (Lewan et al., 1979), with the water / sediment ratio adjusted to insure that the sample is completely submerged in the liquid phase at the reaction temperature (Lewan, 1992). Hydrous pyrolysis is commonly used to further our understanding of the oil generation process by assessing the maturation level of petroleum and sedimentary organic matter after different time / temperature intervals (Lewan, 1993 and references therein).

Hydrous pyrolysis is well suited for simulating hydrothermal processes since hydrothermal oils are the result of natural hydrous pyrolysis occurring at high temperature over a relatively short time (Simoneit, 1992). A detailed investigation was undertaken to study the major reactions occurring under simulated hydrothermal conditions using pure organic compounds and an organic-rich shale. The results are presented in Chapter 3. By combining these results with the knowledge of the actual organic chemical reactions which occur on mineral surfaces (Solomon, 1968; Wilson et al., 1986; Regtop et al., 1985; Kissin, 1987; Weres et al., 1988; Lao et al., 1989; Smith et al., 1989) and under high temperature aqueous conditions (Blouri et al., 1981; Breslow, 1991; Depeyre and Flicoteaux, 1991; Siskin and Katritzky, 1991 and

references therein), a more detailed model of organic conversions under hydrous pyrolysis conditions was developed.

A series of hydrous pyrolysis experiments was performed on a surface sediment from Guaymas Basin. The effects of temperature on the nature and concentrations of selected components in the pyrolysates were documented. The results of this study are presented in Chapter 4.

A modified pyrolysis technique was developed which was better suited towards simulating the natural conditions during hydrothermal alteration of sedimentary organic matter. Using this method, three Guaymas Basin sediment samples which have undergone different amounts of diagenesis were pyrolyzed. These heating experiments were compared to downcore sediment sequences that have been thermally altered by a sill intrusion. The results are presented in Chapter 5.

Aliphatic ketones are highly correlated with high temperature pyrolysis conditions, both natural and simulated. In addition to some selected results from the previous pyrolysis experiments, the results from additional heating experiments are summarized in Chapter 6. Simulation of the natural hydrothermal pyrolysis process by laboratory hydrous pyrolysis techniques provides information regarding the mode of alkanone formation.

A summary of the overall results is presented in Chapter 7. The insight gained from the study of laboratory methods for simulating hydrothermal oil generation has better defined the experimental design and conditions necessary which best suit the simulation processes, and application of these results to the natural hydrous pyrolyses broaden our understanding of the conditions which control the formation of oil by high temperature hydrothermal processes.

The reader of this thesis should be aware that the chapters of this thesis are written in manuscript format to facilitate submission of the chapters for publication. As such, there is unavoidably some duplication of material from chapter to chapter.
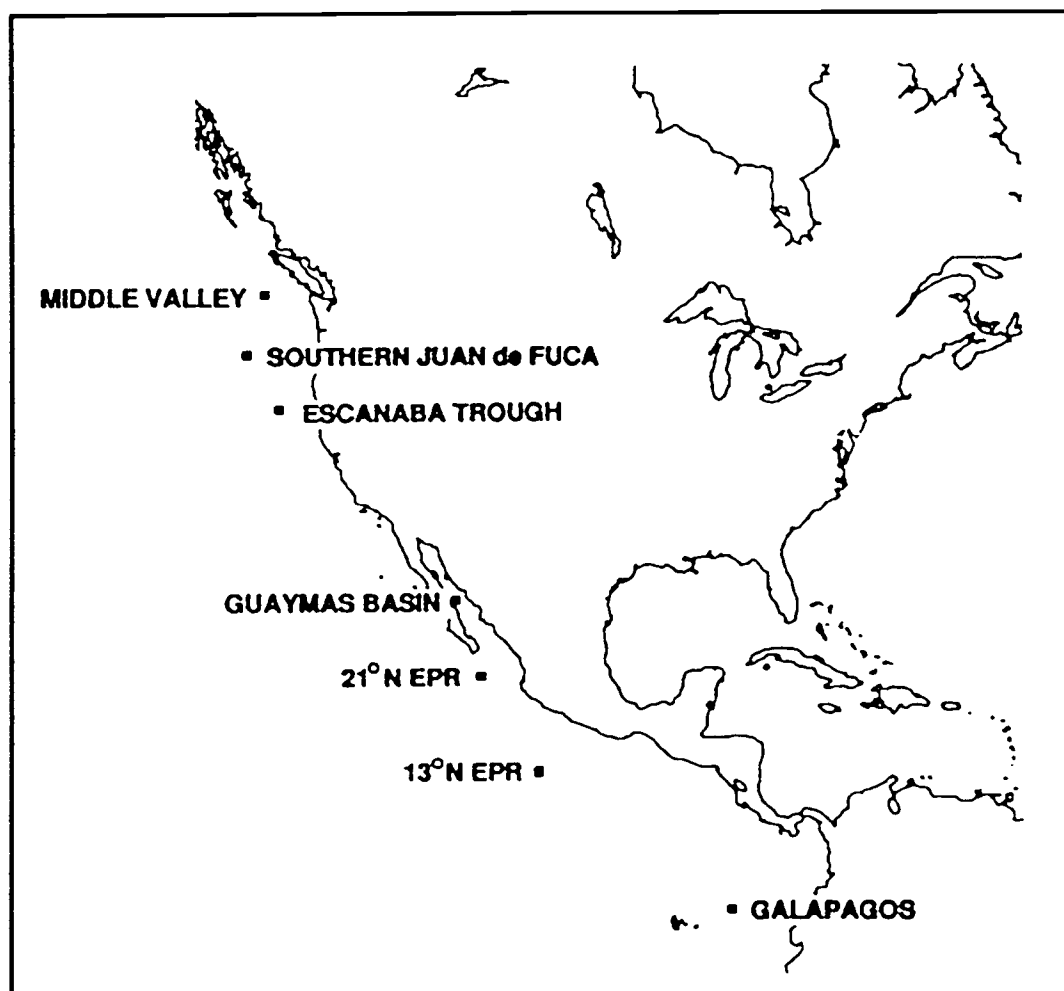
Figure 1.1. Map of discovered submarine hydrothermal systems of the Eastern Pacific (Von Damm, 1991).
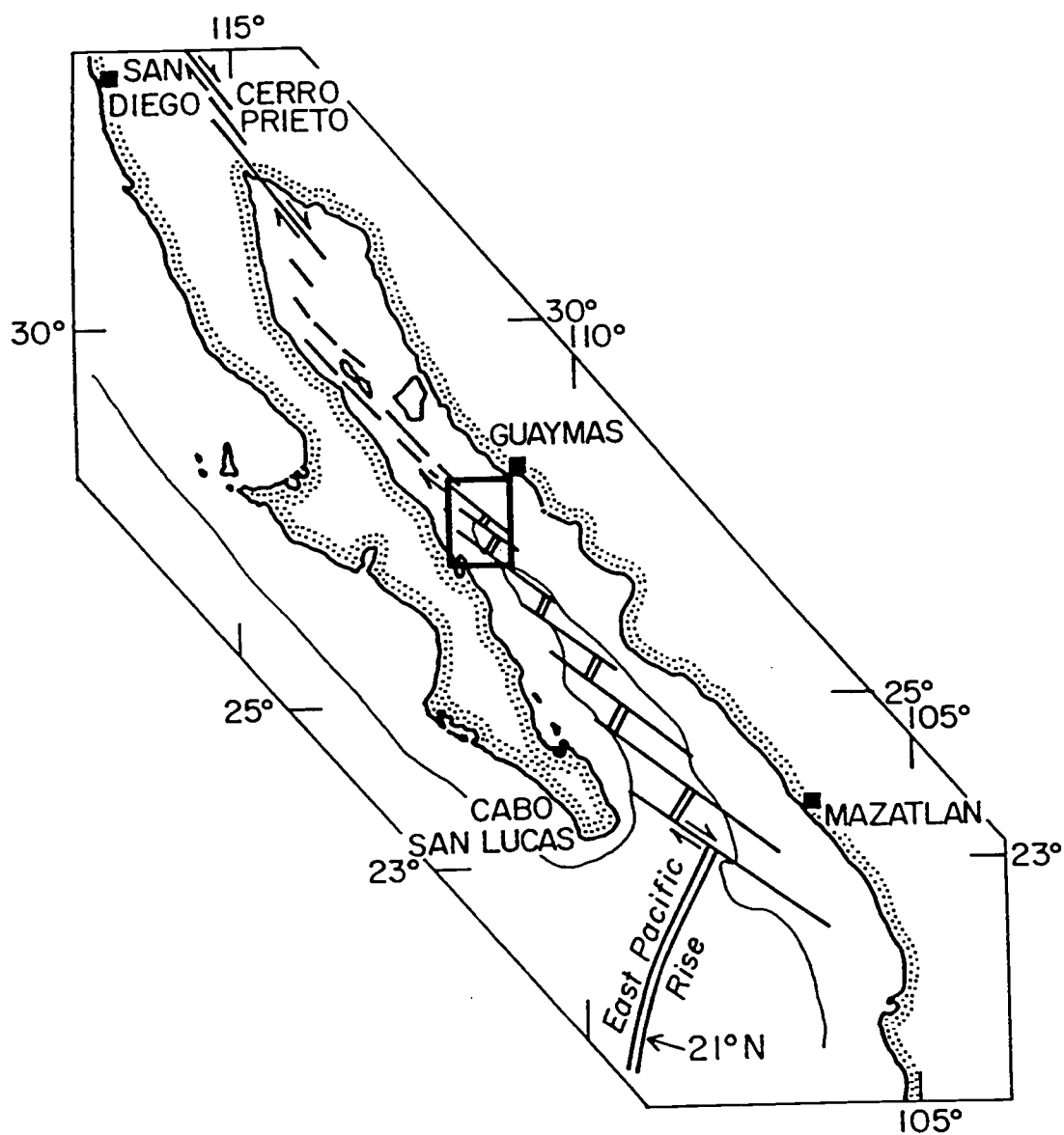
Figure 1.2. Map of the Guaymas Basin hydrothermal system, Gulf of California (Gieskes et al., 1991).
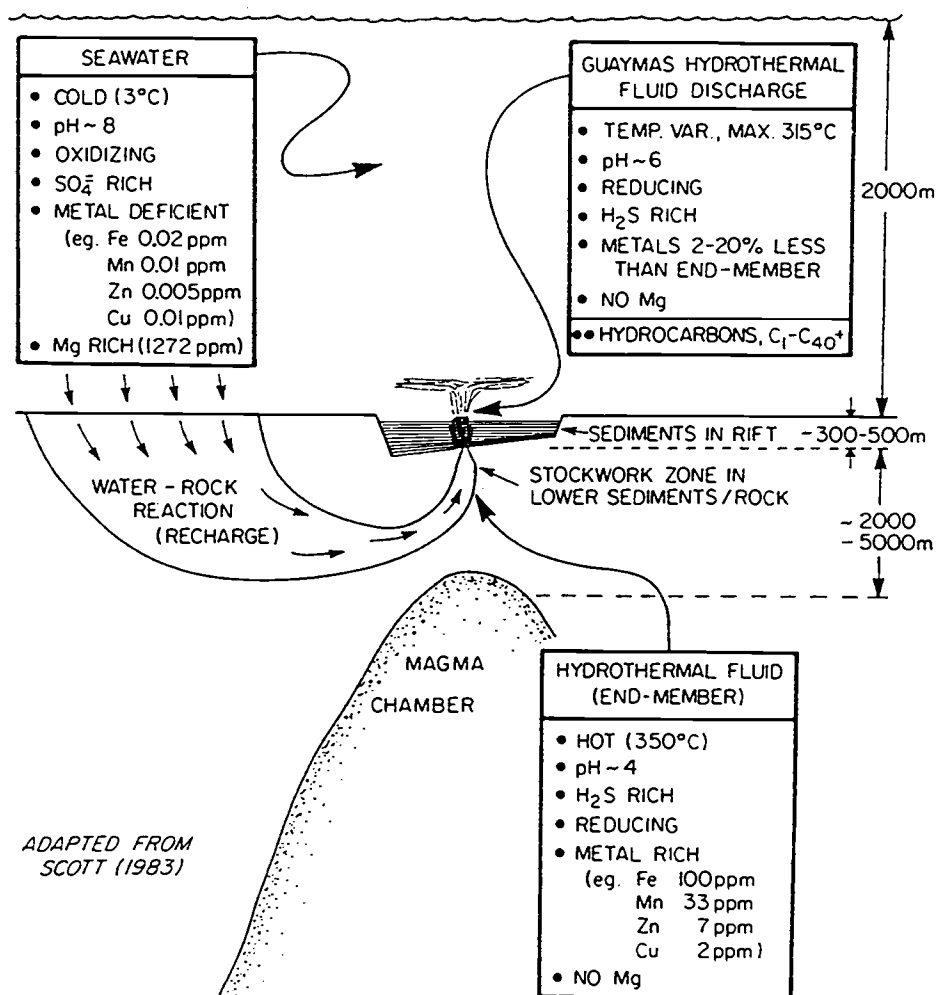
Figure 1.3. Diagram showing the hydrothermal convection of seawater in a sediment-covered spreading center (adapted from Scott, 1983; Simoneit, 1985).
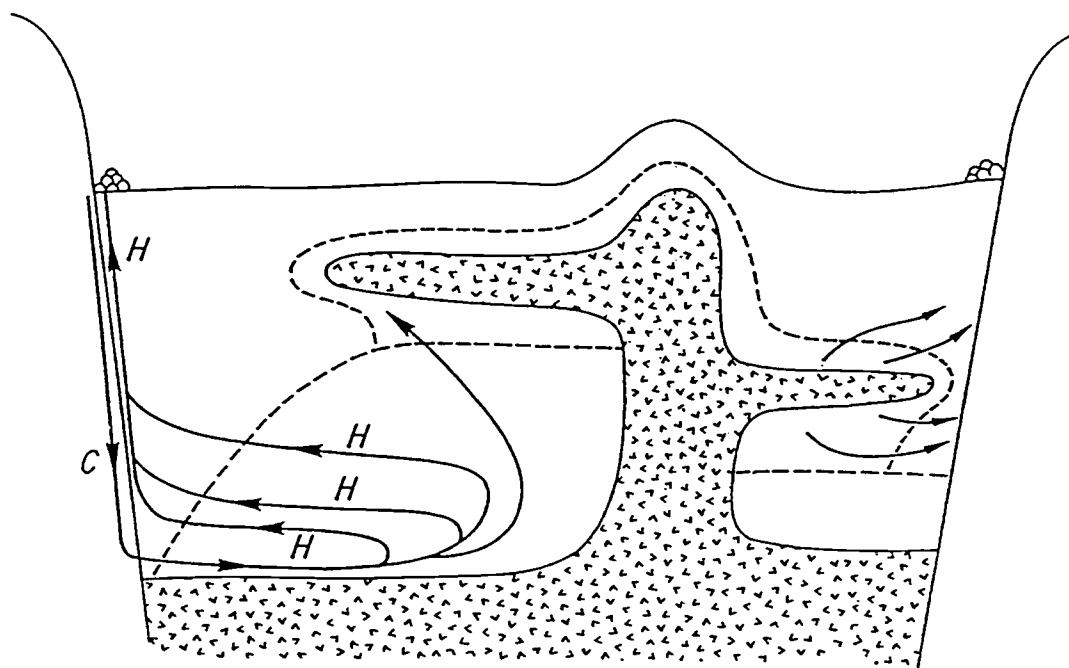
Figure 1.4. Schematic version of hydrothermal systems in Guaymas Basin , Gulf of California. C = cold water advected down through fault zones. H = hot water advected through sediments and fault zones (Adapted from Gieskes et al., 1982b).

CHAPTER 2

Survey of the Polar (NSO) Fractions of Seabed Oils and Sediment Extracts

ABSTRACT

The aliphatic, aromatic and polar (NSO) fractions of seabed oils and sediment extracts from the Guaymas Basin hydrothermal system have been analyzed by gas chromatography and gas chromatography - mass spectrometry. The oils were collected from the interiors and exteriors of high temperature hydrothermal vents and represent hydrothermal pyrolysates that have migrated to the seafloor by hydrothermal fluid circulation. The downcore sediments are representative of both thermally unaltered and thermally altered sediments. The survey has revealed the presence of oxygenated compounds correlated with samples exhibiting a high degree of thermal maturity. Several homologous series of related ketone isomers are enriched in the interiors of the hydrothermal vent samples or in hydrothermally-altered sequences of the downcore sediments The ketones range in carbon number from C_{11} to C_{31} with a C_{max} from C_{15} to C_{23}, distributions that are similar to those of the $\underline{n}$-alkanes. The alkan-2-ones are usually in highest concentrations, with lower amounts of 3-, 4-, 5-, 6-, 7- (and higher) homologues. The alkanones possess no carbon number preference. A second class of oxygenated compounds found in these same samples are the phenols. A series of methyl-, dimethyl- and trimethyl-isoprenoid phenols are present in all of the seabed NSO fractions, with the methyl- and dimethyl-isoprenoid phenols present as major components, and a trimethyl-isoprenoid phenol as a minor component. A homologous series of $\underline{n}$-alkylphenols have also been found in the seabed oils. The alkanones and phenols are derived from the hydrothermal alteration of sedimentary organic matter. The ketones and $\underline{n}$-alkylphenols are most likely synthesized under hydrothermal conditions, but the isoprenoid phenols are probably hydrothermal alteration products of natural product precursors. The suite of normal ketones should be useful tracers of high temperature hydrothermal processes.

INTRODUCTION

Hydrothermal activity is common at tectonic spreading ridges throughout the world. The Guaymas Basin, Gulf of California is a spreading center under a thick cover of diatomaceous oozes and mud turbidites. The combination of plate accretion by dike and sill intrusions into the sediments and accompanying high temperature hydrothermal fluids pyrolyze the sedimentary organic matter to produce petroleum. The petroleum can be transported to the seafloor by hydrothermal fluid migration. ^{14}C ages for selected petroleum samples range from 4240 to 5705 years B. P. indicating that a significant proportion of the hydrothermal petroleum is derived from Recent organic detritus (Peter et al., 1991). Hydrothermal petroleum derived from shallow sediments are characteristically enriched in polar constituents and have a high polycyclic aromatic hydrocarbon content (Simoneit, 1983, 1984; Kawka and Simoneit; 1990). Guaymas Basin is the most thoroughly studied sediment-covered spreading center. Although extensive research has been performed on the characterization of the aliphatic and aromatic fractions of these hydrothermal oils (Simoneit and Lonsdale, 1982; Simoneit, 1985, 1990), little is known about the polar nitrogen, sulfur and oxygen (NSO) fraction.

This chapter is an organic geochemical survey of the NSO fractions of representative oils and sediment extracts from the Guaymas Basin hydrothermal system. Comparisons are made to the aliphatic and aromatic fractions of the oils and sediment extracts. Specifically, two types of samples were studied : (1) seabed oils associated with high temperature seafloor hydrothermal vents that have been migrated with the hydrothermal fluids and condensed in the vent spires; and (2) extractable organic matter in downcore sediments representative of unaltered and hydrothermally altered regions. The objective of this research is to characterize some of the components in one of the major fractions of the oils, the polar (NSO) fraction.

EXPERIMENTAL

Samples. The seabed oils for this study were sampled from the interiors and exteriors of hydrothermal vents collected during the dives of the Deep Submergence Vessel (D.S.V.) *Alvin* in March, 1988. Figure 2.1 is a location map of the Guaymas Basin hydrothermal system located in the Gulf of California. Figure 2.2 is a detailed bathymetric chart of Guaymas Basin showing the general locations of *Alvin* dives 1981-1984. The transponder array with its x,y coordinates is also indicated (Simoneit, 1988). The x,y coordinates of the oil covered hydrothermal vents are listed in Table 2.1.

The subsurface sediment samples analyzed in this study were collected during Leg 64 of the Deep Sea Drilling Project (DSDP) from December, 1978 to January, 1979. The selected downcore samples were taken from Holes 477 and 481A. Locations of the two drill sites are shown in Figure 2.1. The lithologic columns for Sites 477 and 481A are shown in Figure 2.3. The sample listings, depths and descriptions are summarized in Table 2.2.

Extraction and fractionation. The frozen hydrothermal vent samples were brought to room temperature and oil samples were collected from the interiors and exteriors of each specimen. They were diluted in chloroform and filtered to remove any debris and passed through an activated copper column to remove the elemental sulfur. The samples were reduced to 2 mL by rotary evaporation.

The DSDP samples have been freeze dried and stored at room temperature until analysis. Powdered sediments ranging in size from 10 to 40 g were extracted for 72 hours with methanol / methylene chloride in a Soxhlet extractor. The extract was combined with 100 mL water and the aqueous phase acidified with 6N HCl. The organic phase was collected and the aqueous phase was extracted with two 50 mL portions of methylene chloride. The three organic extracts were combined and solvent removed to near dryness by rotary evaporation.

The whole oils and sediment extracts were deasphalted with 100 mL heptane. The asphaltenes were allowed to precipitate for 24 hrs and removed by filtration. The deasphalted fractions were reduced to 4 mL and fractionated by column chromatography (30 cm x 1 cm) packed with 3.8 g alumina (fully active) over 3.8 g silica gel (fully active). The samples were separated into three fractions by elution with 50 mL heptane (aliphatic, F1), 50 mL toluene (aromatic, F2) and 25 mL methanol (polar NSO, F3).

Quantitation was by the addition of $\underline{n}$-$C_{24}D_{50}$ for aliphatic fractions and D_{10}-pyrene for aromatic and polar fractions.

Gas chromatography. Gas chromatography (GC) of the oil fractions was performed with a Hewlett Packard 5890A equipped with a 30 m x 0.25 mm i.d. DB-5 open tubular column (0.25 μm film thickness). The GC oven was heated using the following program : isothermal for 2 min. at 65°C, 4°/min. to 310°C, and isothermal for 30 min., with the injector at 290°C, detector at 325°C, and helium as the carrier gas.

Gas chromatography-mass spectrometry. The gas chromatography-mass spectrometry (GC-MS) was performed on a Finnigan 9610 gas chromatograph coupled to a Finnigan 4021 quadrupole mass spectrometer operated at 70 eV over the mass range 50-650 dalton and a cycle time of 2.0 s. The GC oven temperature was programmed at isothermal for 2 min. at 65°C, 3°/min. to 310°C, and isothermal for 30 min., with the injector at 290°C, and helium as the carrier gas. The MS data were processed with an on-line Finnigan-Incos 2300 computer data system.

RESULTS AND DISCUSSION

Seabed oils. The results of the bulk chromatographic separations into the compound classes for the four hydrothermal vent samples are listed in Table 2.3 and shown in Fig. 2.4 (a-d) . Samples 1972-CH1, 1983-CH1 and 1984-CH1 show a consistent difference between their interior and exterior oils. The exterior oils all show a decrease in the proportion of the aliphatic fractions with an accompanying increase in the aromatic, polar and asphaltene fractions relative to the interior oils. The interior and exterior samples from 1984-CH2 have essentially the same proportions of the four fractions. These compositional differences between the interior and exterior oils are more clearly shown in Fig. 2.5 which is a ternary diagram of the gross oil compositions where the NSO and asphaltene fractions have been combined into one compound class. Included on the ternary diagram are seabed oil samples from Guaymas Basin collected during previous Alvin dives and dredge sampling expeditions (Kawka and Simoneit, 1987).

The variations in the distribution of the oils from the interiors and the exteriors of the high temperature hydrothermal vents reflect the process of biodegradation occurring after migration to the seafloor (Kawka and Simoneit, 1987). With the exception of oil 1984-CH2, whose interior and exterior oils are almost identical in composition, the seabed oils have a significant decrease in the aliphatic portion of the bulk composition. Water washing, the removal of water-soluble components, is another likely factor working in combination with biodegradation to alter the bulk compositions of the oils and thus enrich the NSO fractions (Tissot and Welte, 1984).

The aliphatic, aromatic and polar NSO fractions of the eight seabed oils have been analyzed by gas chromatography. The complete set of gas chromatograms are located in Appendix 1. The hydrothermal oils from 1972-CH1 were selected as representative oils for discussing the major characteristics of the seabed samples. The gas chromatograms of the aliphatic, aromatic and NSO fractions from the hydrothermal oils of 1972-CH1 are presented in Fig. 2.6 and 2.7.

The hydrocarbon patterns of the aliphatic fractions are typical of other normal hydrothermal seabed oils previously reported (Simoneit, 1984). The aliphatic fractions of these oils have smooth n-alkane distributions (carbon preference index, CPI = 1) with the other major components being the isoprenoids, with the isoprenoids pristane and phytane in highest concentrations. The n-alkanes range in carbon number from 11 to 25, with the 1984-CH1 oils containing hydrocarbons up to C_{29}. The

pristane /phytane ratios range from 1.1 to 1.7. However, there is a consistent trend of the exterior oils having a decreased amount of normal hydrocarbons relative to the isoprenoid hydrocarbons, characteristic of having undergone slight biodegradation relative to the corresponding oil from the interior of the vent. This is most pronounced in the oils from 1972-CH1 (Fig. 2.6a and 2.7a), where the pristane/$\underline{n}$-C_{17} and phytane/$\underline{n}$-C_{18} ratios of the exterior oil are 4.25 and 3.31 respectively, but the pristane/$\underline{n}$-C_{17} and phytane/$\underline{n}$-C_{18} ratios of the interior oil are 0.79 and 0.51 respectively. The molecular parameters for these oils are summarized in Table 2.4. In slightly and moderately biodegraded oils, the $\underline{n}$-alkanes are the first class of compounds to be removed, leaving the isoprenoid hydrocarbons relatively unaffected (Connan et al., 1980; Tissot and Welte, 1984). Although the $\underline{n}$-alkanes are present in all oils, there is a significant increase in the Pr/$\underline{n}$-C_{17} and Pr/$\underline{n}$-C_{18}, characteristic of the very early stages of biodegradation.

The aromatic fractions contain polycyclic aromatic hydrocarbons and alkylated polycyclic aromatic hydrocarbons common to other Guaymas Basin seabed oils (Simoneit and Lonsdale, 1982, Kawka and Simoneit, 1990). The GC traces of the aromatic fractions are characterized by a large unresolved complex mixture (UCM) which results in a large hump in the chromatogram, with the resolved components on this hump. Except for the oils from 1984-CH2, where the interior and exterior oils are very similar, the resolved component in highest concentrations in most of the aromatic fractions from the chimney exteriors is Diels' hydrocarbon (1,2-(3'-methylcyclopenteno)phenanthrene), a triaromatic steroid hydrocarbon common in Guaymas Basin oils and an indicator of rapid hydrothermal petroleum generation processes (Kawka, 1990; Simoneit et al., 1992a). Diels' hydrocarbon (DHC) and some of the other major resolved polycyclic aromatic hydrocarbons (PAH) are identified in the aromatic fractions of the 1972-CH1 oils (Fig. 2.6 and 2.7).

The polar NSO fractions, similar to the aromatic fractions, are dominated by a large UCM, with the resolved components on this hump. Two classes of homologous oxygenated compounds, alkanones and phenols, have been identified as the major resolved components of the NSO fractions.

The alkanones occur as several homologous series which range in carbon number from C_{11} to C_{31} with a C_{max} from C_{15} to C_{23}. These oils contain alkan-2-ones in highest concentrations, with lower amounts of 3-, 4-, 5-, 6-, 7- (and higher) alkanones. These compounds possess no carbon number preference and are enriched in the interiors of the hydrothermal vent spires indicating the ketones have a pyrolytic

origin at depth or are formed by reaction with the hot hydrothermal fluids, and do not originate from an external biogenic deposition. The relative decrease of the aliphatic ketones of the polar fractions of the exterior oils is likely due to preferential microbial utilization of straight-chain aliphatic components. Fig. 2.8 shows the distribution of ketones present in a representative oil, the interior oil from vent 1972-CH1.

The second class of oxygenated compounds are the phenols. A series of methyl-, dimethyl- and trimethyl-isoprenoid phenols were present in all of the NSO fractions, with the methyl- and dimethyl-isoprenoid phenols present as major components, and a trimethyl-isoprenoid phenol as a minor component. The tentative structure assignments were made by interpretation of the mass spectra of the parents and silylated derivatives and by the similarities to the mass spectra of the mono-, di- and trimethylchromans (Sinninghe Damsté et al., 1987), structurally related compounds possessing an isoprenoid side chain. The two compounds in highest concentration exhibited characteristic mass spectra with ions at m/z 107, 122, 135, 161 and 388 (molecular ion, M^+) and m/z 121, 136, 149 and 402 (M^+). These compounds are labeled A and B in Fig. 2.6 - 2.7. A third phenol, compound C, is found in trace levels and has a characteristic mass spectrum of m/z 135, 150, 194, 374 and 416 (M^+). Fig. 2.9 shows the mass fragmentograms of the characteristic ions of these compounds. The mass spectra of compounds A, B and C, and the proposed structures are shown in Fig. 2.10, which were present in interior oil of chimney 1972-CH1 F3, a representative oil sample. Treating this oil with a silylating agent (BSTFA, Pierce Chemical Co.) produced the trimethylsilane derivatives of compounds A, B and C (labeled A', B' and C') with characteristic ions of 179, 194, 207 and 460 (M^+), 193, 208, 221 and 474 (M^+) and 193, 222, 266 and 488 (M^+), respectively. The mass fragmentograms of the characteristic ions of these three derivatives are shown in Fig. 2.11, and mass spectra of the three derivatized phenols are shown in Fig. 2.12.

Present in much lower concentrations are homologous series of n-alkylphenols. These series are shown in Fig. 2.13. Representative mass fragmentograms of the C_{27} to C_{29} n-alkylphenols is shown in Fig. 2.14, and mass spectra are shown in Fig. 2.15.

Downcore sediment extracts from DSDP Site 477. Site 477 is located in the southern rift of Guaymas Basin. A total of 191 meters was cored. A massive dolerite sill was encountered between 58 and 105.5 m below seafloor (mbsf). The sediments above the sill consist primarily of olive-brown hemipelagic diatom oozes and mud turbidites. Extensive hydrothermal alteration of the sediments has occurred below the sill resulting in grey claystones and sandstones, with dolomite, pyrite and quartz

(Curray et al., 1982). Three sediment samples above the sill and twelve sediment samples below the sill were extracted and analyzed by GC. A few samples were selected for analysis by GC-MS. The complete set of the gas chromatograms for the total extracts and the aliphatic, aromatic and NSO fractions are located in Appendix 2. An extensive analysis of the aliphatic and aromatic fractions of sediments altered by the emplacement of the dolorite sill has previously been reported (Kawka, 1990). Therefore, only a brief discussion of some representative samples will be presented.

Sample 477-2-2 (145-150) is representative of a typical near-surface sediment, dominated by long-chain n-alkanes with a CPI=3.9, characteristic of a terrigenous source for these n-alkanes (Brassell et al., 1978). The major aromatic component is perylene, a diagenetically-derived PAH (Louda and Baker, 1974). Both sample 477-7-1 (88-90) and 477-7-1 (106-108) resemble other samples from Guaymas Basin that have undergone thermally-enhanced diagenesis (Simoneit et al., 1984, 1992b), where the total extract is dominated by pristane, phytane, the C_{25} isoprenoid thiophenes and the steroid biomarkers. The polar fractions of both samples contain a large UCM with few resolved components. Two samples near the sill contact zone, 477-16-2 (140-145) and 477-16-2 (145-150), are fully mature organic extracts. The CPI=1 for the n-alkanes and the aromatic fractions contain the full suite of PAH and alkylated-PAH. Of interest is the presence of the alkyl ketones. The alkanones occur as several homologous series which range in carbon number from C_{11} to C_{33}. As with the seabed oils, these sediment extracts contain 2-, 3-, 4-, 5-, 6-, 7- (and higher) alkanones. There is no carbon number preference and their correlation with the oil zone suggests that the ketones have a high temperature pyrolytic origin. Deeper in the sediment column the alteration is extensive, resulting in low yields in the extractable organic matter from the sediments. The total extracts are dominated by the aromatic components. The ketones are not present or are in lower concentrations in these sediments. It is interesting to note that samples 477-16-4 (135-140) and 477-17-1 (145-150) have a bimodal n-alkane distribution with maxima at C_{10} and C_{23}. The low molecular weight component is from a condensate and contains the diamondoid hydrocarbons adamantane, diadamantane, triadamantane and their alkylated derivatives, analogous to petroleum condensates (Wingert, 1992). This portion of the sediment column was apparently an active flow channel for the condensate.

Downcore sediment extracts from DSDP Site 481A. Site 481A is located in the northern rift of Guaymas Basin. A total of 384 meters was cored. A massive chert and dolerite sill complex was encountered between 169.5 and 200 mbsf. The

sediments above the sill consist primarily of olive-brown diatomaceous muds with intercalations of grey, muddy sands (Curray et al., 1982). Hydrothermal alteration of the sediments has occurred in contact zones above and below the sill. Seven sediment samples above the sill and nine sediment samples below the sill were extracted and analyzed by GC. The complete set of the gas chromatograms for the total extracts and the aliphatic, aromatic and NSO fractions are located in Appendix 3. From this set of samples, eight were chosen for analysis by GC-MS. They are representative of sediments that are unaltered, partially altered and extensively altered by the sill intrusion.

A listing of the samples along with various parameters of the aliphatic fractions is given in Table 2.5. The n-alkane CPI, a measure of the maturation, ranges from approximately 5.5 in the sediments furthest away from the sill to 1 in the sediments nearest to the contact zone. The ratio of pristane to phytane (Pr/Ph) is usually around 0.5 in unaltered sediments, but becomes inverted in the oils and thermally altered sequences. Therefore, these two molecular parameters are useful in distinguishing the unaltered sequences from the altered sequences. The CPI and Pr/Ph are plotted versus depth in Fig. 2.16a and 2.16b, respectively.

The mass fragmentograms m/z 191, representative of the triterpenoid hydrocarbons, are presented in Fig. 2.17a - 2.17h for the eight samples. The samples away from the sill are dominated by triterpenes and $\beta\beta$-hopanes, products of diagenesis. The samples close to the sill have undergone thermal maturation, but a measure of the C_{31} (S/(S+R)) parameter of the C-22 carbon for the samples closest to the sill range from 0.37 to 0.49. These ratios are not at the equilibrium ratio of 0.6 (Ensminger et al., 1974, 1977; Seifert and Moldowan, 1978) and indicate that full thermal maturation has not been achieved.

Fragmentograms representative of the steroid hydrocarbons are presented in Fig. 2.18a - 2.18h. As with the triterpenoids, the steroids away from the sill are diagenetic products, primarily sterenes. The steroid distributions near the sill are dominated by C_{27} to C_{29} steranes, primarily the 5α(H),14α(H),17α(H)-20R isomers, with lower amounts of the less stable 5β(H),14α(H),17α(H)-20R isomers, a distribution commonly found in hydrothermal oils (Kawka and Simoneit, 1987). A dominance of the C_{29}(20R) isomer in sample 481A-12-4 (55-65) suggests greater contribution of a terrestrial steroid component (Huang and Meinschein, 1979).

Histograms of concentrations of the major PAH for the eight sediment samples are shown in Fig. 2.19a - 2.19h. These distributions range from perylene dominated in

the unaltered sequences to phenanthrene dominated in the altered sequences. Perylene is primarily a diagenetically formed PAH (Louda and Baker, 1984) which is not stable under hydrothermal conditions and is destroyed in the altered zones. The other PAH in the histograms are derived pyrolytically and therefore the change from perylene-rich to phenanthrene rich is another useful thermal maturity indicator. Diels' hydrocarbon, a triaromatic steroid hydrocarbon used as a tracer of hydrothermal alteration of organic matter, was detected in the altered zones, but the concentrations were low compared to the concentrations found in seabed oils (Kawka, 1990).

The survey of the NSO fraction focused on the search for the ketones and the isoprenoid phenols, the major components of the polar fractions of the seabed oils. The fragmentograms representative of the alkanones are given in Fig. 2.20a - 2.20h. Alkanone distributions resembling those in the oils were found only in samples 481A-12-4 (55-65) and 481A-13-2 (118-127). As with the seabed oils, the ketones in these two altered sequences are present as several homologous series of 2-, 3-, 4-, 5-, 6-, 7-(and higher) alkanones. They have no carbon number preference and the correlation of their presence with the oil zone suggests that these ketones were formed during the hydrothermal alteration of the sedimentary organic matter.

The isoprenoid phenols were found in samples 481A-12-4 (55-65) and 481A-18-1 (30-32) but not in the altered sediment of 481A-13-2 (118-127). The mass fragmentograms of m/z 122 and m/z 136, representative of the methyl and dimethyl isoprenoid phenols, are presented in Fig. 2.21.

Downcore variations in the aliphatic and aromatic compositions in Hole 481A show a direct relationship to the thermal alteration of the sedimentary organic matter from sill emplacement. The alkanones and isoprenoid phenols present in the seabed oils were found only in the altered zones. Ketones are absent or occur in trace amounts in oils (Tissot and Welte, 1984), although the homologous series of alkan-2-ones are common constituents of recent and older marine sediments, they are generally present with an odd-carbon number predominance (Brassell et al., 1980; Cranwell, 1977; Simoneit, 1978, 1979; Volkman et al., 1983). The ketones in the seabed oils and thermally altered zones of the downcore sections are unique in that they are major resolved components of the polar fractions exhibiting a smooth distribution, analogous to the smooth n-alkane distributions of the oils. Aliphatic ketones are commonly found in oil shale pyrolysates (Regtop et al, 1982; Rovere et al., 1983), but only recently have ketones been detected in sedimentary rocks exhibiting a CPI = 1 (George and Jardine, 199?). In that study the ketones have been found in the

thermally altered sediments adjacent to a Proterozoic sill, indicating that there is a link between the high temperature igneous alteration of sedimentary organic matter and ketone formation.

The n-alkylphenols present in the seabed oils in several homologous series also exhibit a smooth distribution (CPI = 1) characteristic of a pyrolytic origin. But the isoprenoid phenols present in the oils and altered sedimentary sequences occur only as a few discrete isomers, structurally related to the tocopherols and sedimentary chromans (Sinninghe Damsté et al., 1987). This suggests that these compounds or related precursors could lead to the isoprenoid phenols. Of these two classes of compounds, the chromans are more likely to be converted directly to the isoprenoid phenols since they lack the additional phenolic hydroxyl groups present in the tocopherols. Chromans have been identified in Guaymas Basin sediments (Kawka, 1990). A survey of the aromatic fractions of sediment extracts of Hole 481A has also identified these compounds, but in only trace amounts in the thermally-unaltered zones. The most abundant isomer of the chroman series has three methyls on the aromatic ring structure, but the most abundant isomer of the isoprenoid phenolic series has only one methyl on the aromatic ring. These results argue against sedimentary chromans being precursors to the isoprenoid phenols. One possible mode of origin is that the isoprenoid phenols are bound to the kerogen matrix and preferentially released under high temperature hydrothermal conditions. Thus, the presence of these phenolic compounds is probably highly dependent on the organic source material and they are therefore not good candidates as universal indicators of high temperature hydrothermal processes.

However, if tocopherol or chroman related compounds are found to be precursors of the isoprenoid phenols, it does indicate the preferential cleavage of the ether bridge of the precursor structure, an indication that an acid-catalyzed reaction under relatively extreme conditions is necessary (Siskin et al., 1990) for the reaction to proceed. This is important because it identifies a type of ionic reaction, as opposed to radical cracking reactions, as operating in the breakdown of the kerogen structure, a class of chemical reactions often overlooked and only recently being emphasized as possibly significant to the petroleum generation process (Siskin and Katritzky, 1991).

CONCLUSIONS

A survey of the polar fractions of the seabed oils and sediment extracts of hydrothermally-altered sequences has revealed that there are two major classes of oxygenated compounds present, the ketones and the phenols. The smooth distributions of the n-alkylphenols and the alkanones (CPI = 1) indicate a pyrolytic source, analogous to the origin of n-alkanes from the pyrolysis of sedimentary organic matter. Their presence in the thermally-altered downcore sediments suggests that they are formed by the sill intrusions and transported to the seabed by hydrothermal fluid circulation. The isoprenoid phenols, occurring as a few isomers, are likely hydrothermal alteration products of natural product precursors in the sediments. The proposed structures of the isoprenoid phenols suggest that the precursors are structurally related to the sedimentary chromans or tocopherols present in these sediments.

Table 2.1. Location of oil covered hydrothermal vent samples.

Vent [a]	Location [b]
1972-CH1	not available
1983-CH1	4935, 4712
1984-CH1	4929, 4687
1984-CH2	4009, 3578

[a] Number refers to Alvin dive number, CH = chimney sample

[b] Locations are given in transponder coordinates within the 1988 transponder array

Table 2.2a. Sample summary for DSDP Site 477.

Sample	Depth [a] (mbsf)	Description [b]
a) 477-2-2 (145-150)	3.97	Olive brown diatomaceous ooze
b) 477-7-1 (88-90)	49.39	Diatomaceous ooze
c) 477-7-1 (106-108)	49.57	Diatomaceous ooze
d) 477-16-2 (140-145)	117.93	Hydrothermally-altered clay siltstone
e) 477-16-2 (145-150)	117.98	Hydrothermally-altered clay siltstone
f) 477-16-4 (130-135)	120.83	Hydrothermally-altered clay siltstone
g) 477-16-4 (135-140)	120.88	Hydrothermally-altered clay siltstone
h) 477-17-1 (145-150)	125.98	Hydrothermally-altered silty siltstone
i) 477-19-1 (130-135)	144.83	Hydrothermally-altered siltstone
j) 477-19-1 (135-140)	144.88	Hydrothermally-altered siltstone
k) 477-20-1 (135-140)	154.37	Hydrothermally-altered claystone
l) 477-21-1 (52-57 + 91-96)	163.25	Hydrothermally-altered silty clay
m) 477-22-1 (110-115)	173.12	Hydrothermally-altered silty clay
n) 477-23-1 (90-95)	182.47	Hydrothermally-altered silty clay
o) 477-23-1 (CC)	182.80	Hydrothermally-altered silty clay

[a] Depth (meters below seafloor) calculated according to DSDP convention (Curray et al., 1982)

[b] Sample descriptions are from Curray et al. (1982)

Table 2.2b. Sample summary for DSDP Site 481A.

Sample [a]	Depth [a] (mbsf)	Description [b]
a) 481A-4-2 (93-98)	73.0	Olive-brown Diatomaceous ooze
b) 481A-6-5 (118-120)	98.2	Grayish-olive diatomaceous mud
c) 481A-6-5 (124-135)	98.3	Grayish-olive diatomaceous mud
d) 481A-7-6 (71-80)	107.3	Muddy diatomaceous ooze
e) 481A-8-7 (top of pipe)	108.5	Grayish-olive diatomaceous mud
f) 481A-12-4 (55-65)	151.6	Olive- to brownish-black silty clay
g) 481A-13-2 (118-127)	158.7	Brownish-black clay- and sandstone
h) 481A-18-1 (30-32)	203.8	Brownish-grey sandy clay
i) 481A-18-1 (CC)	204.1	Brownish-grey sandy clay
j) 481A-20-1 (110-115)	223.6	Diatomaceous mudstone
k) 481A-22-1 (65-70)	242.2	Diatomaceous mudstone
l) 481A-22-7 (top of pipe)	250.5	Mudstone
m) 481A-22-7 (97-101)	251.5	Mudstone
n) 481A-24-CC	269.9	Silty claystone
o) 481A-25-CC	279.4	Olive grey silty claystone
p) 481A-26-CC	288.9	Claystone to silty claystone

[a] Depth (meters below seafloor) calculated according to DSDP convention (Curray et al., 1982)

[b] Sample descriptions are from Curray et al. (1982)

Table 2.3. Bulk characterization of seabed chimney oils.

Sample	F1 (%)	F2 (%)	F3 (%)	Asphaltenes (%)
1972-CH1 Interior	63.8	4.8	15.8	15.6
1972-CH1 Exterior	39.9	12.3	20.0	27.8
1983-CH1 Interior	68.5	5.8	20.5	5.2
1983-CH1 Exterior	54.6	10.2	25.3	9.9
1984-CH1 Interior	71.0	3.4	20.3	5.3
1984-CH1 Exterior	36.1	15.2	29.3	19.4
1984-CH2 Interior	31.1	15.8	31.5	21.6
1984-CH2 Exterior	29.8	16.3	32.7	21.2

Table 2.4. Summary of molecular parameters for hydrothermal vent oils.

Sample	Hydrocarbons					Ketones	
	$\underline{n}$-Alkane range	C_{max}	Pr/Ph	Pr/$\underline{n}$-C_{17}	Ph/$\underline{n}$-C_{18}	Ketone range	C_{max}
1972-CH1 Interior	12-27	18	1.3	0.79	0.51	12-29	22
1972-CH1 Exterior	12-25	18	1.3	4.25	3.31	15-25	20
1983-CH1 Interior	12-25	18	1.4	0.87	0.65	12-28	21
1983-CH1 Exterior	12-24	16	1.6	1.27	0.93	12-26	19
1984-CH1 Interior	12-29	20	1.1	0.94	0.70	12-31	23
1984-CH1 Exterior	12-28	19	1.4	1.37	0.87	12-30	21
1984-CH2 Interior	12-25	16	1.5	0.85	0.66	11-25	15
1984-CH2 Exterior	11-25	15	1.7	1.03	0.82	11-25	15

Table 2.5. Selected parameters for the aliphatic fractions of DSDP Leg 64 Hole 481A.

	Samples (Leg 64, Hole 481A)							
Parameter	4-2 (93-98)	8-7 (top)	12-4 (55-65)	13-2 (118-127)	18-1 (30-32)	20-1 (110-115)	22-7 (top)	26-CC
$\underline{n}$-alkane range	12-33	12-32	12-35	12-38	12-38	12-31	13-31	13-33
CPI	4.09	3.60	1.87	1.20	1.60	n.d.	4.13	5.46
C_{max}	29	29	29	15	15	15,29	29	29
Pr/Ph	n.d.	0.47	1.51	1.75	2.09	0.34	0.45	0.50
Pr/$\underline{n}$-C_{17}	n.d.	0.31	2.16	0.54	2.14	5.96	1.17	1.54
Ph/$\underline{n}$-C_{18}	n.d.	1.04	1.79	0.34	1.21	14.85	4.43	4.8
S/(S+R) C_{31}	-	-	0.37	0.49	.048	-	-	-
S/(S+R) C_{32}	-	-	0.42	.048	-	-	-	-
$\dfrac{29,30,31\text{H}}{29,30,31\text{M}}$	-	-	1.79	2.89	2.16	-	-	-
27R/29R	-	-	0.74	2.01	1.08	1.73	-	-
27R/28R	-	-	2.09	1.61	2.35	1.57	-	-
28R/29R	-	-	0.35	1.24	0.46	1.10	-	-

n.d. = not determined

S/(S+R) = C-22 S and R epimer ratios for C_{31} and C_{32} α-homohopanes

$$\frac{29,30,31 \text{ H}}{29,30,31 \text{ M}} = \frac{C_{29} + C_{30} + C_{31} \text{ } \alpha\text{-hopanes}}{C_{29} + C_{30} + C_{31} \text{ moretanes}} \qquad \frac{27R}{28R} = \frac{C_{27} \text{ 20 R } \alpha\alpha\alpha\text{-sterane}}{C_{28} \text{ 20 R } \alpha\alpha\alpha\text{-sterane}}$$

$$\frac{27R}{29R} = \frac{C_{27} \text{ 20 R } \alpha\alpha\alpha\text{-sterane}}{C_{29} \text{ 20 R } \alpha\alpha\alpha\text{-sterane}} \qquad \frac{28R}{29R} = \frac{C_{28} \text{ 20 R } \alpha\alpha\alpha\text{-sterane}}{C_{29} \text{ 20 R } \alpha\alpha\alpha\text{-sterane}}$$

Figure 2.1. (a) Map of Gulf of California showing geographic location of the sampling area, and (b) Map of Guaymas Basin showing its two rifts, with locations of DSDP Sites (Simoneit, 1991).
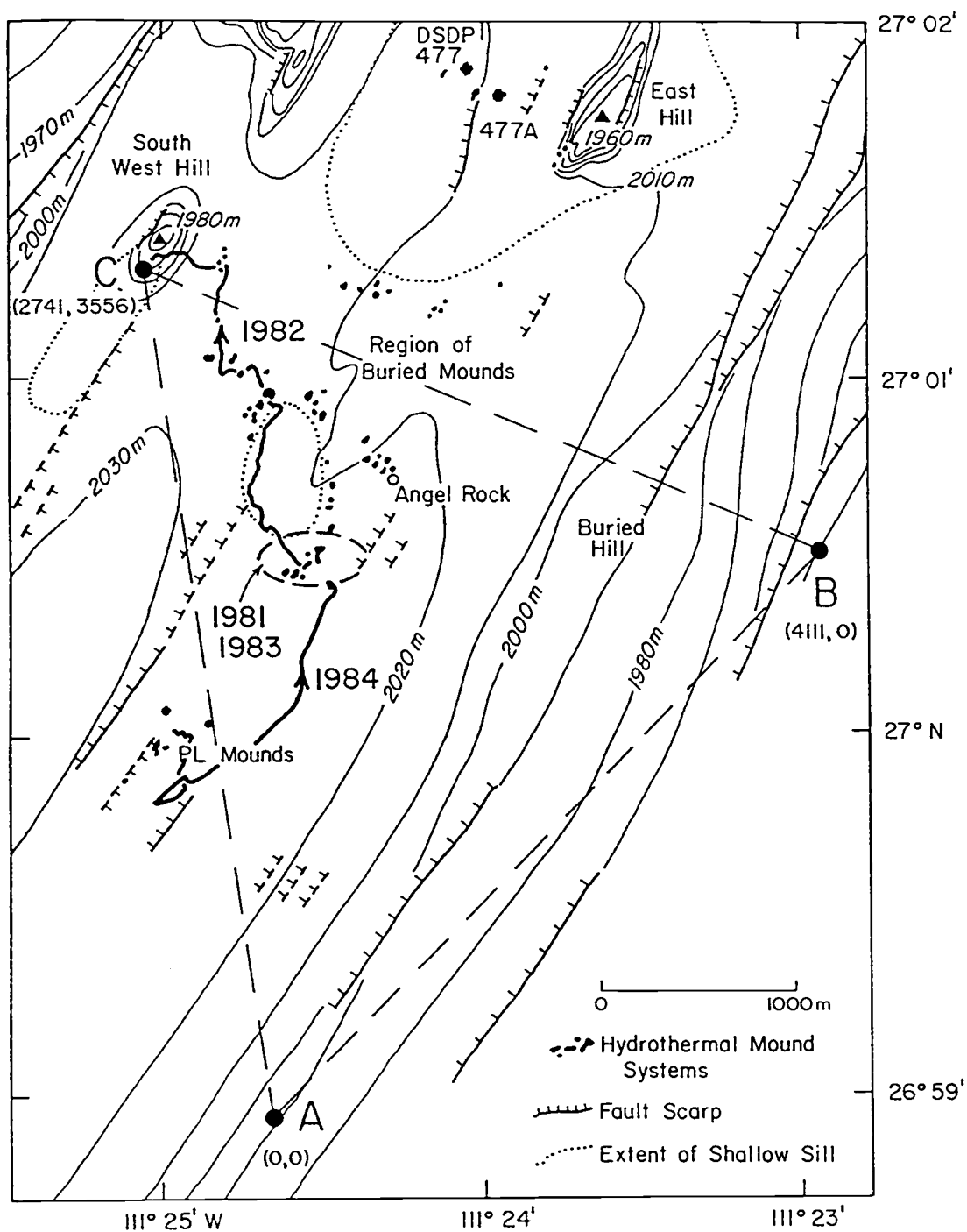
Figure 2.2. Bathymetric chart of the southern rift of Guaymas Basin with general study area of *Alvin* dives during March, 1988. The transponder array with its x,y coordinates is also indicated (Simoneit, unpublished report, 1988).
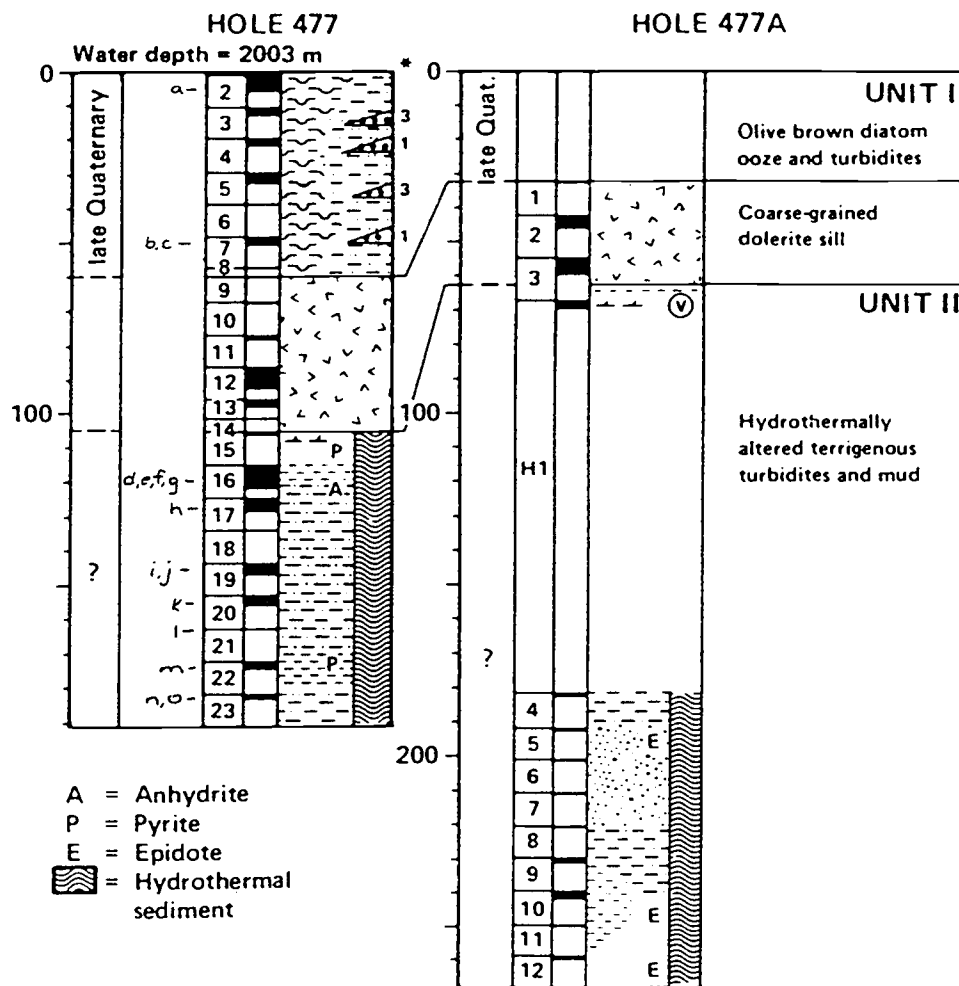
Figure 2.3a. Lithologic column for site DSDP Site 477, lowercase letters refer to sample locations listed in Table 2.2a (Curray et al., 1982).
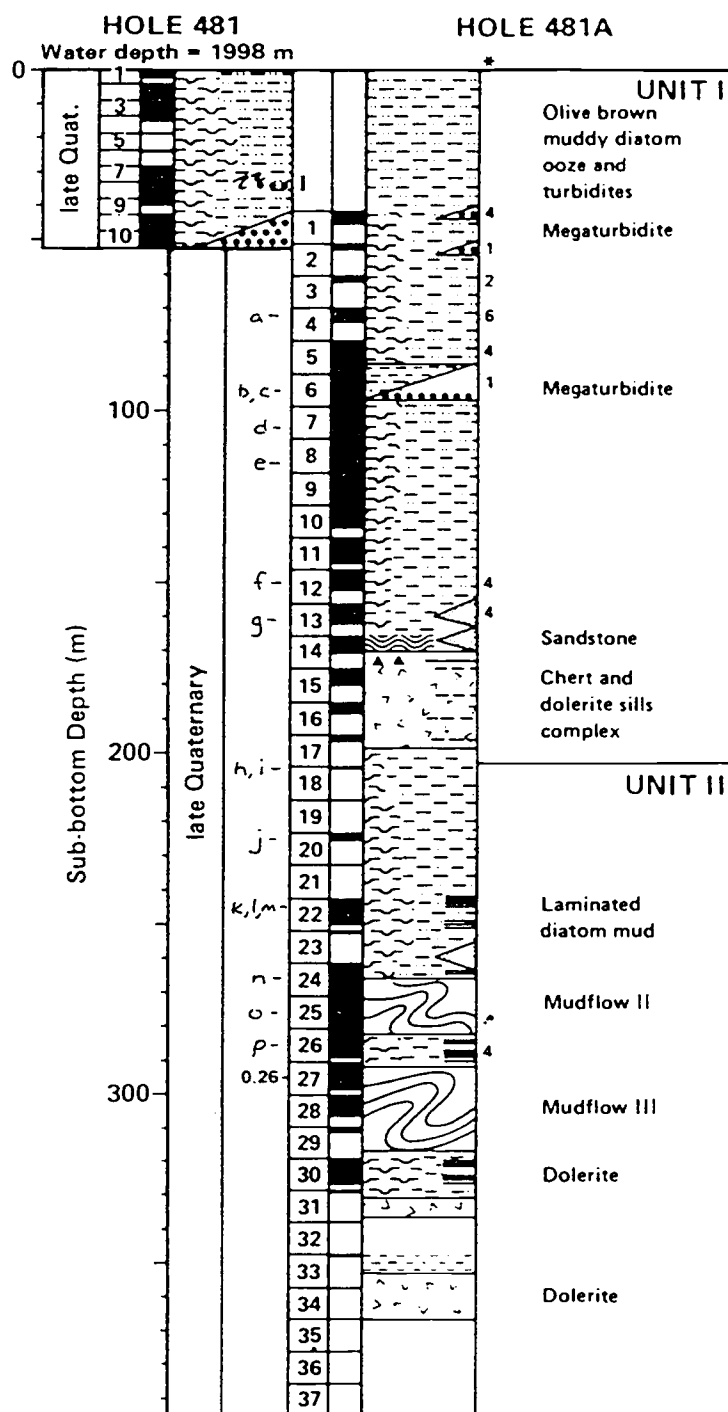
Figure 2.3b. Lithologic column for site DSDP Site 481A, lowercase letters refer to sample locations listed in Table 2.2b (Curray et al., 1982).
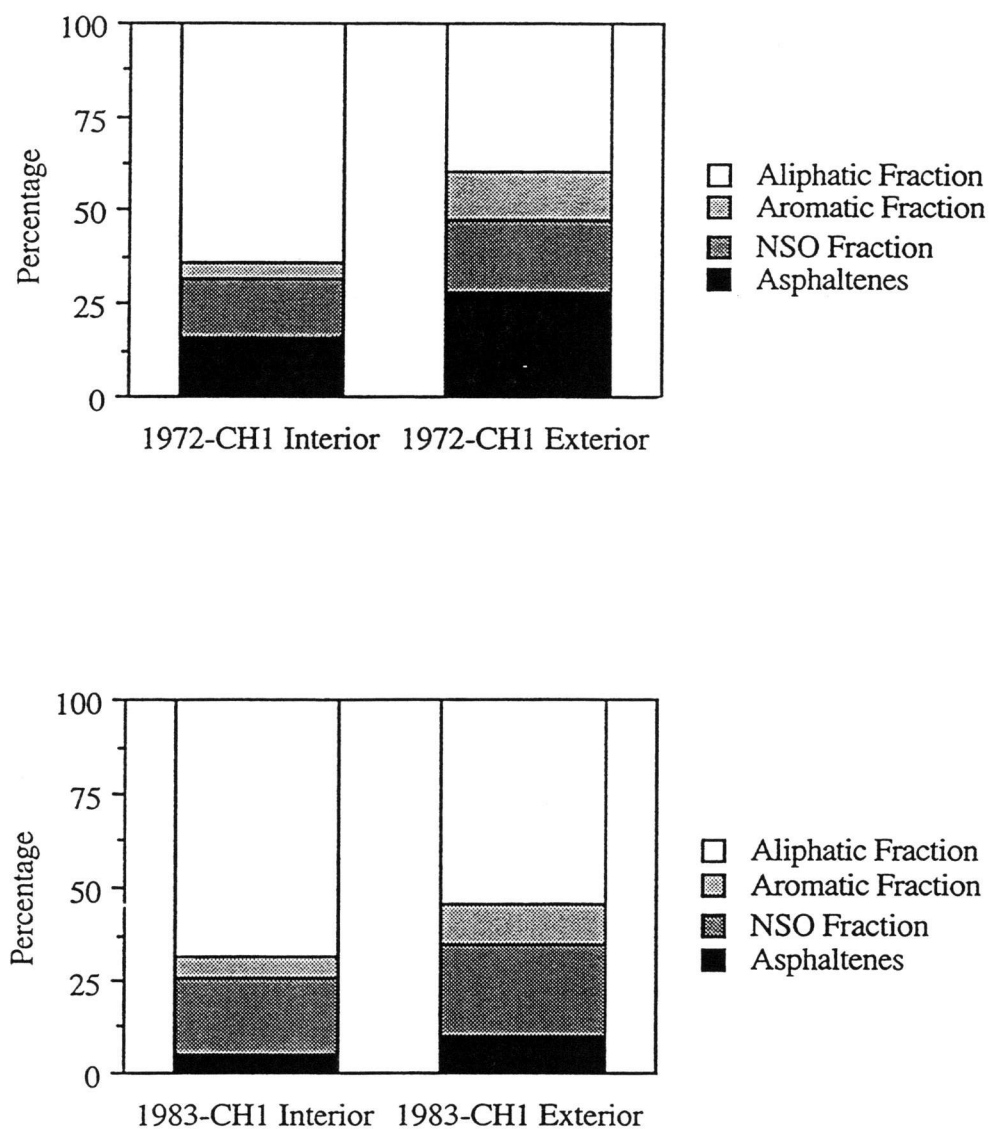
Figure 2.4. Histograms of bulk class percentages for chimney samples (a) 1972-CH1 and (b) 1983-CH1.
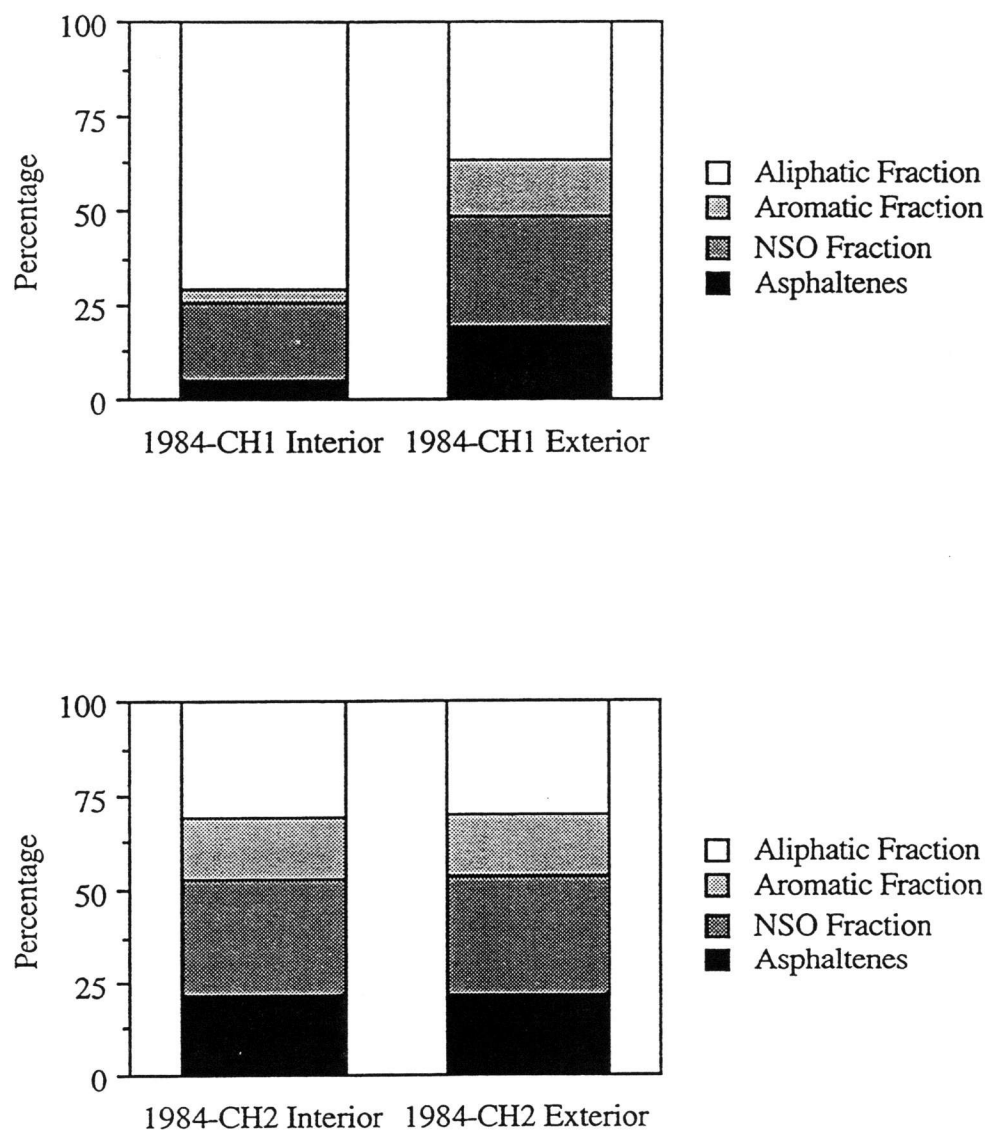
Figure 2.4. Histograms of bulk class percentages for chimney samples (c) 1984-CH1 and (d) 1984-CH2.
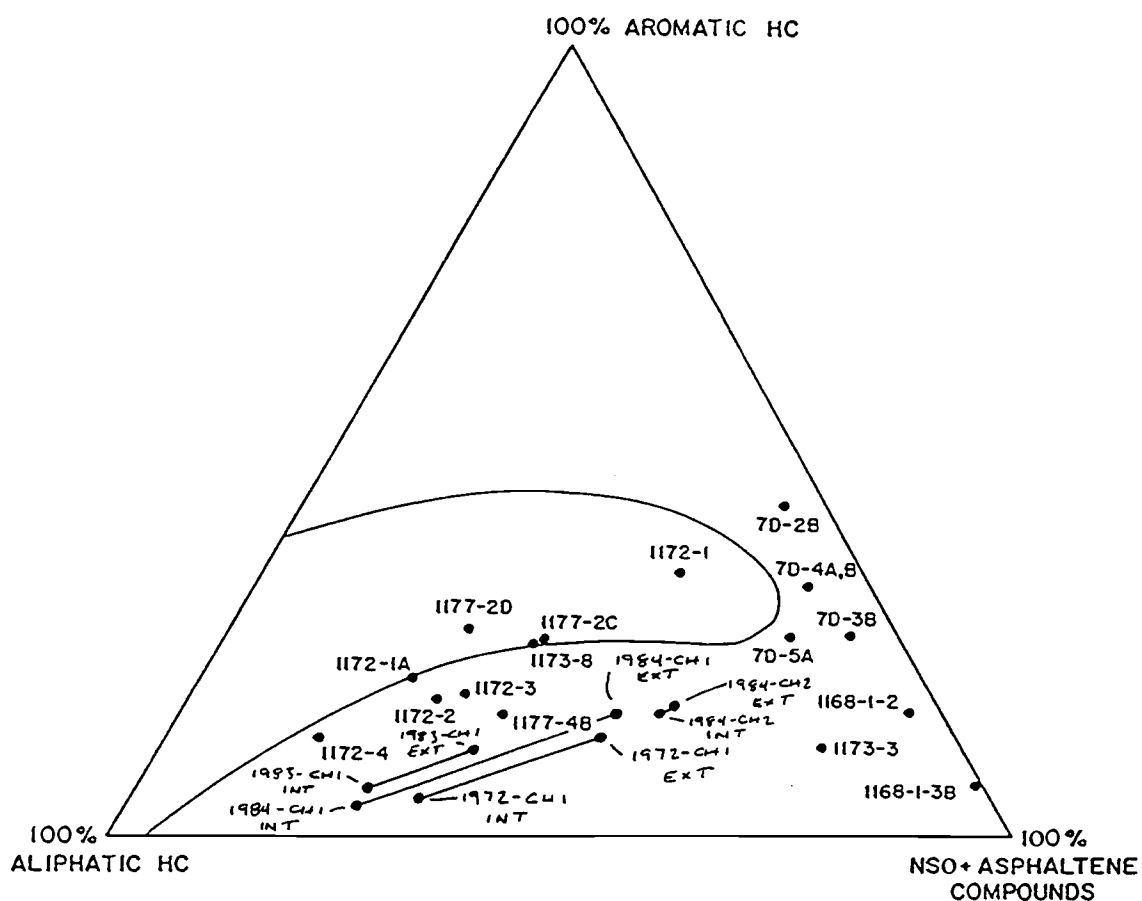
Figure 2.5. Ternary diagram of the bulk compositions for seabed hydrothermal oils. (adapted from Kawka and Simoneit, 1987).

1972-CH1 Interior
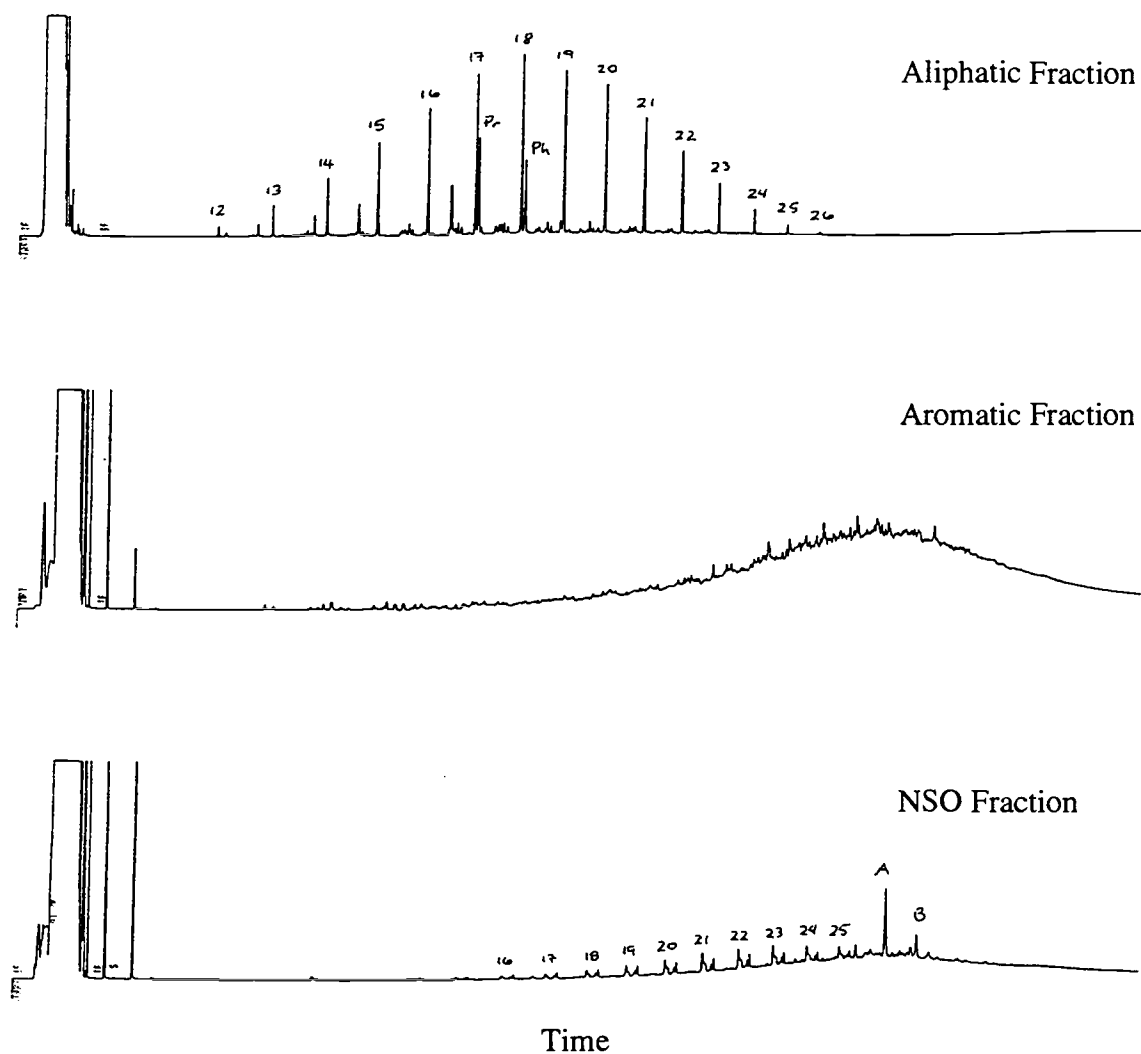
Figure 2.6. Gas chromatograms of 1972-CH1 Interior: (a) aliphatic fraction; (b) aromatic fraction; (c) NSO fraction. Numbers refer to carbon chain length of the n-alkanes and ketones, Pr = pristane, Ph = phytane, A = isoprenoid phenol (MW = 388), B = isoprenoid phenol (MW = 402).

1972-CH1 Exterior
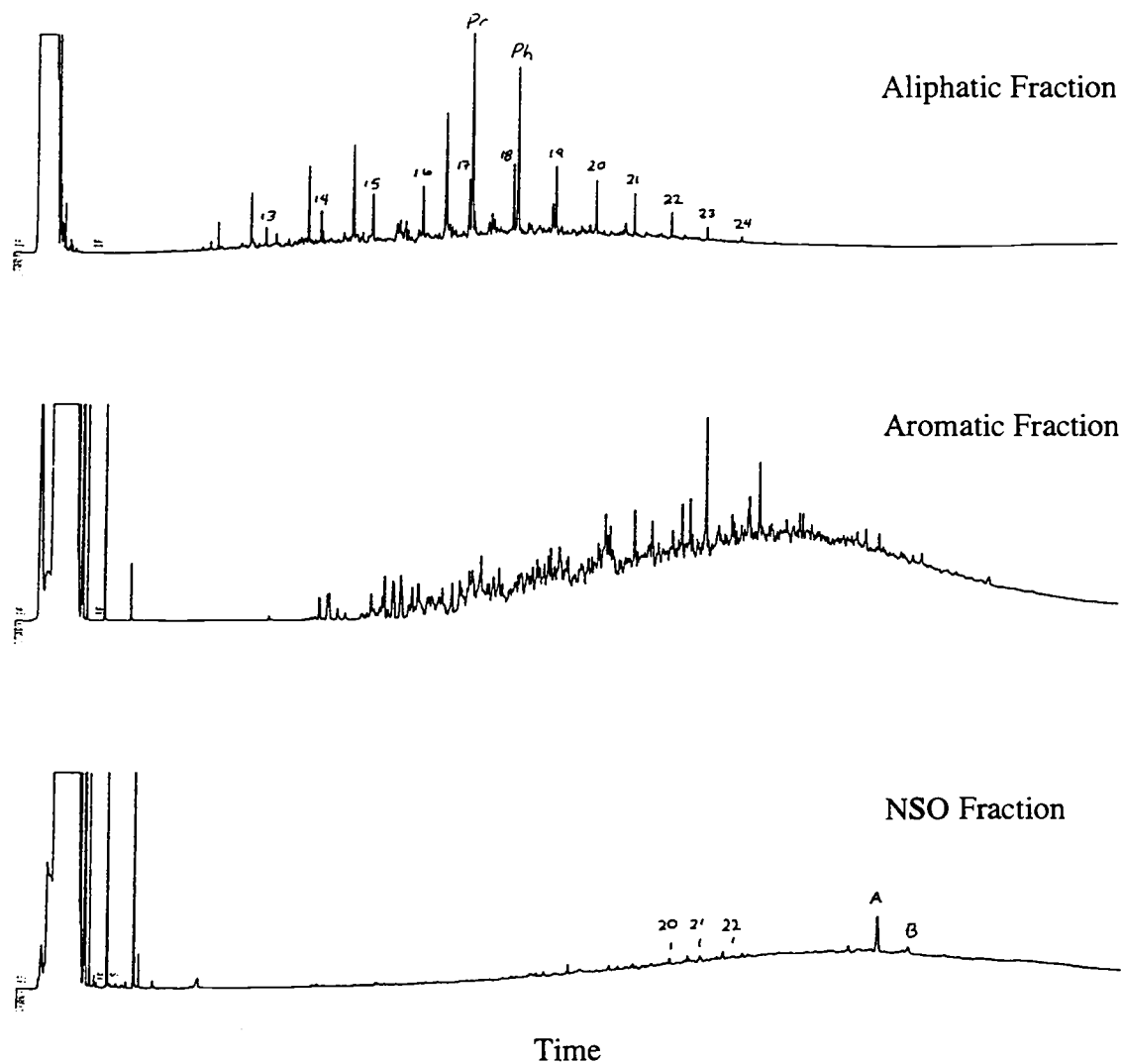
Figure 2.7. Gas chromatograms of 1972-CH1 Exterior: (a) aliphatic fraction; (b) aromatic fraction; (c) NSO fraction. Numbers refer to carbon chain length of the n-alkanes and ketones, Pr = pristane, Ph = phytane, A = isoprenoid phenol (MW = 388), B = isoprenoid phenol (MW = 402).
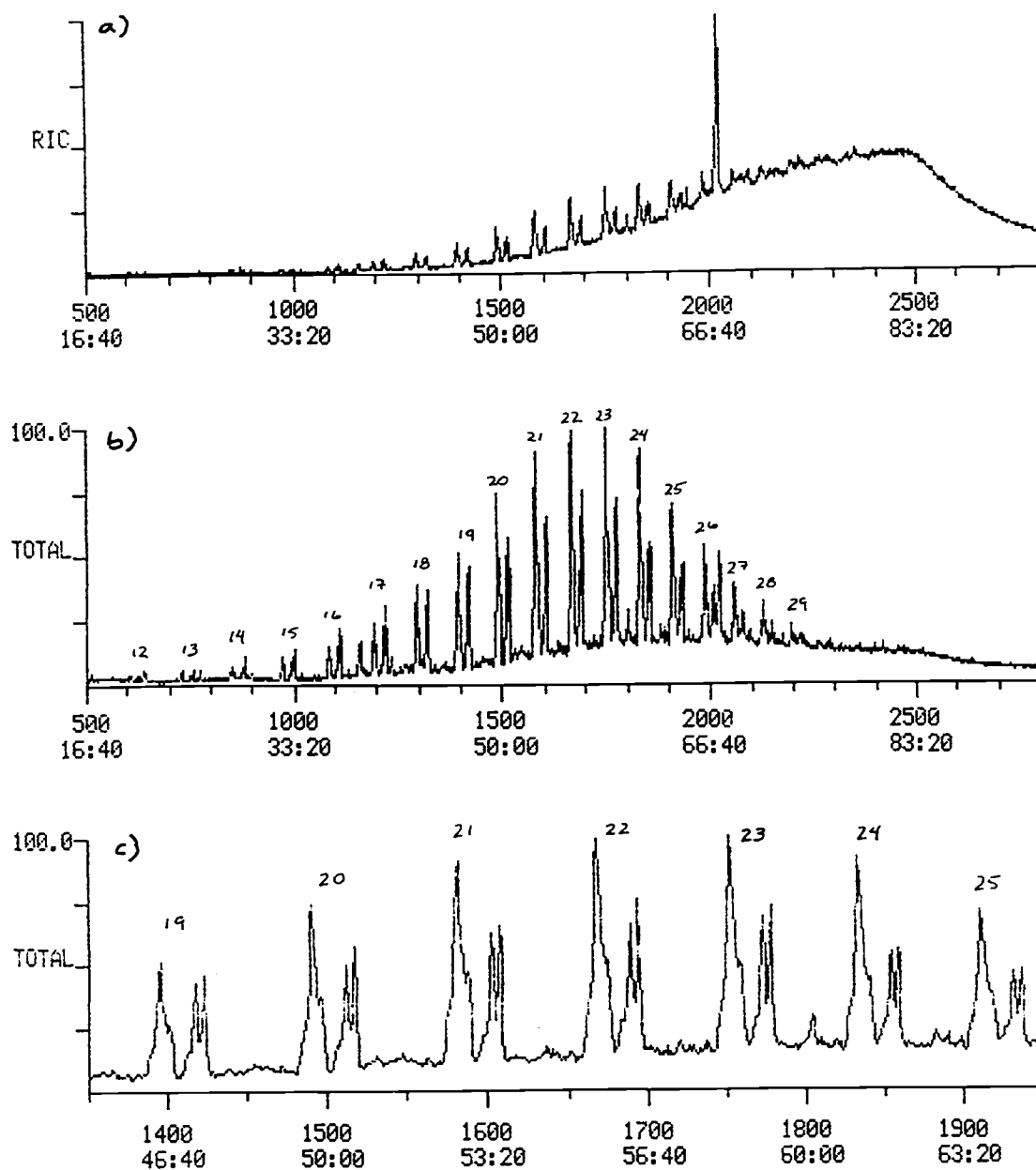
Figure 2.8. NSO fraction of hydrothermal oil from the interior of vent 1972-CH1: (a) reconstructed ion chromatogram (RIC) ; (b) representative mass fragmentograms for ketones (m/z 57 + 58 + 71 + 72) of oil covering the same scan range; (c) expanded scale identifying resolved ketone isomers. Numbers refer to carbon chain length.
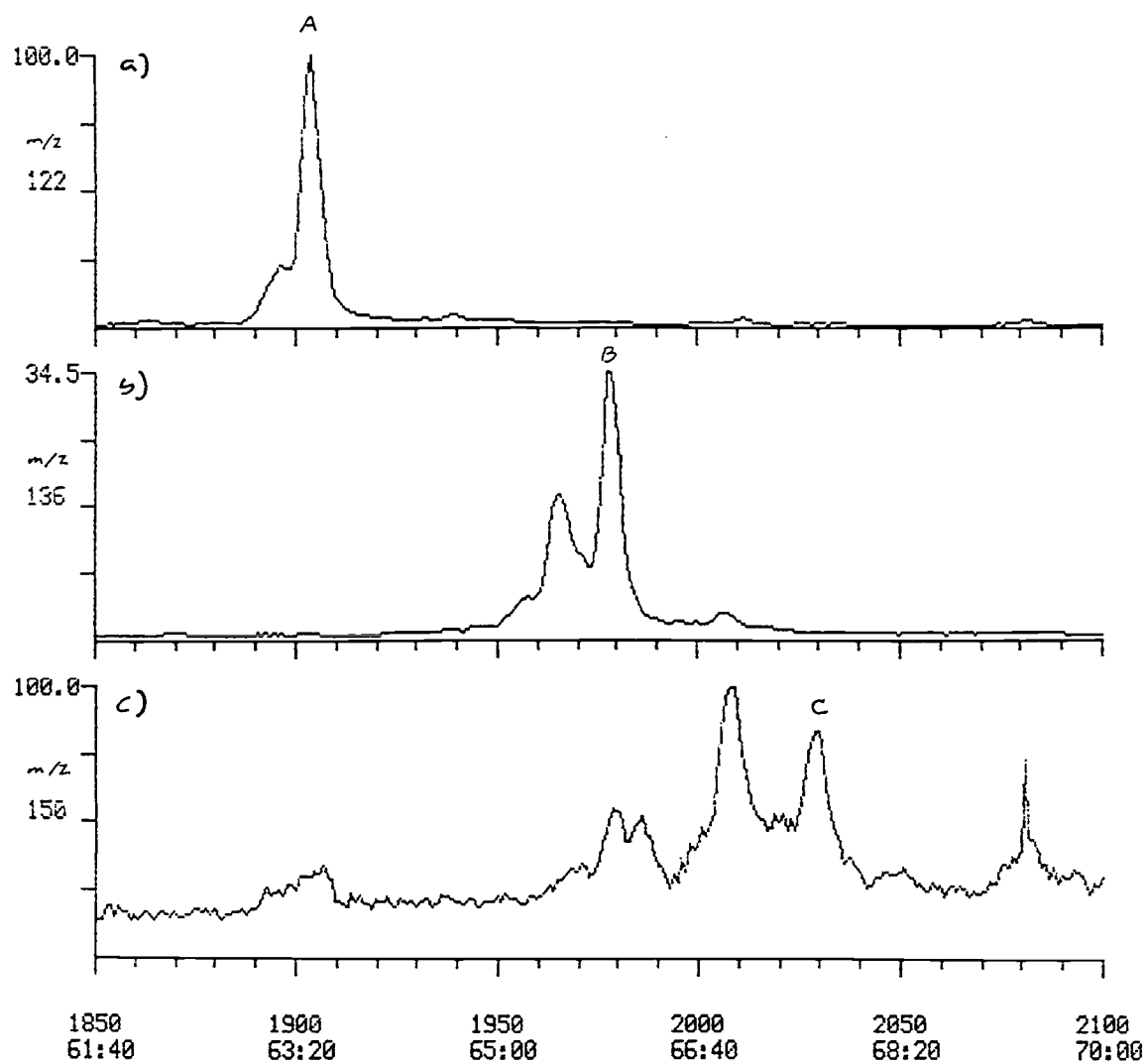
Figure 2.9. NSO fraction of hydrothermal oil from the interior of vent 1972-CH1: (a) representative mass fragmentogram for the isoprenoid phenol compound A (m/z 122); (b) representative mass fragmentogram for the isoprenoid phenol compound B (m/z 136); (c) representative mass fragmentogram for the isoprenoid phenol compound C (m/z 150).
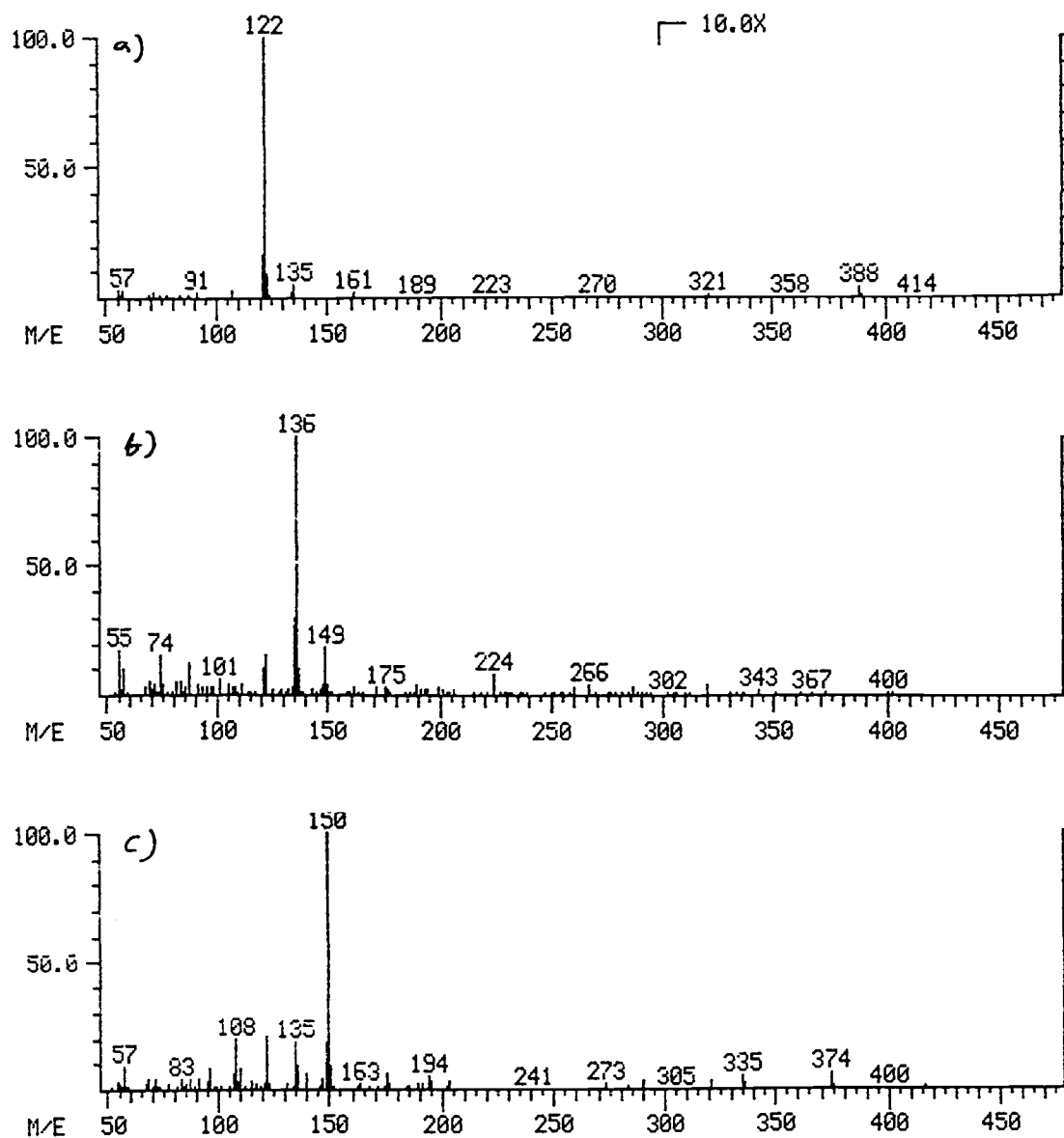
Figure. 2.10. Mass spectra and proposed structures of isoprenoid phenols present in NSO fraction of hydrothermal oil from the interior of vent 1972-CH1: (a) compound A; (b) compound B; (c) compound C. Mass spectra correspond to the peaks labeled in Fig. 2.9.
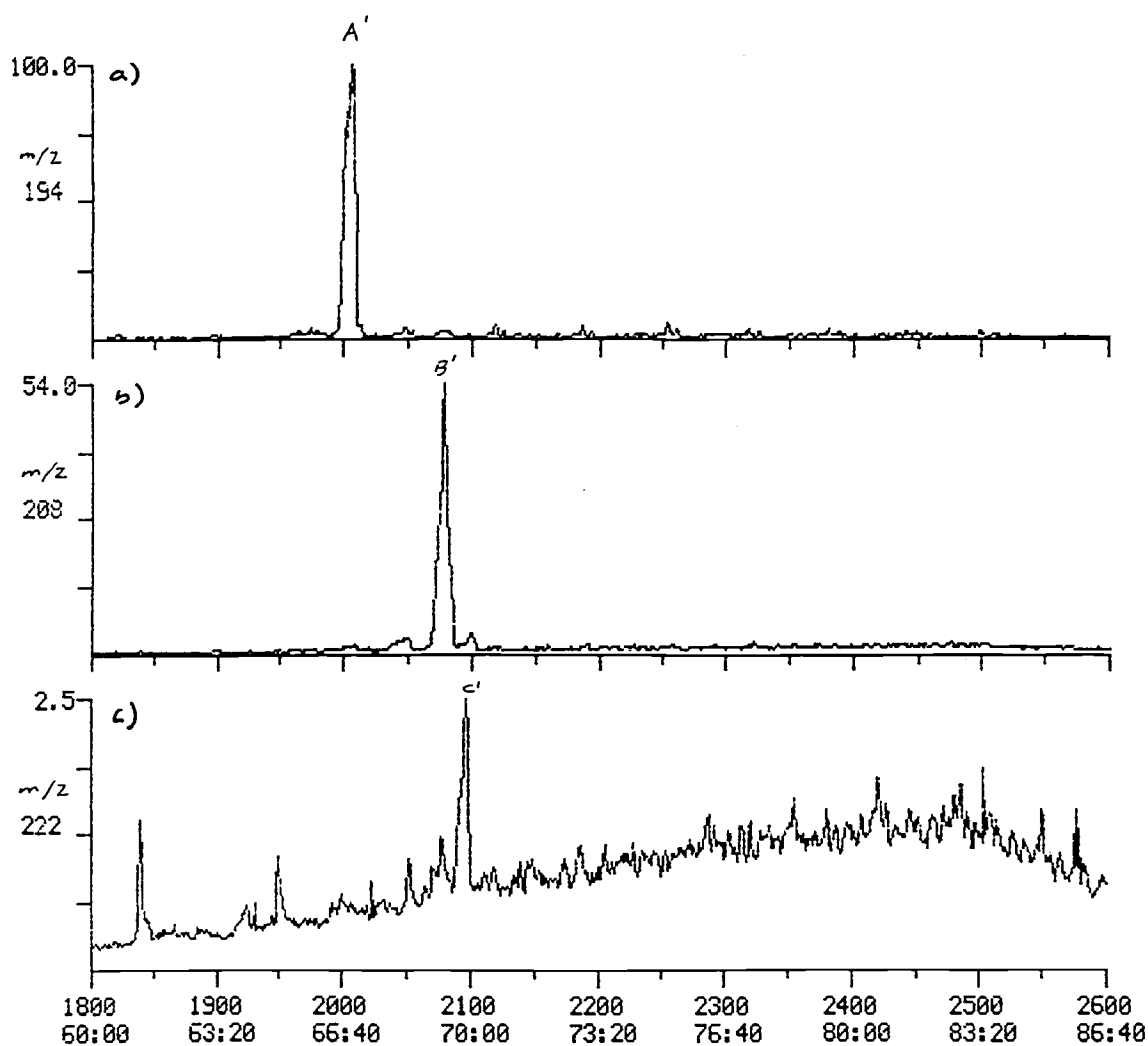
Figure 2.11. Silylated NSO fraction of hydrothermal oil from the interior of vent 1972-CH1: (a) representative mass fragmentogram for the isoprenoid phenol compound A' (m/z 194); (b) representative mass fragmentogram for the isoprenoid phenol compound B' (m/z 208); (c) representative mass fragmentogram for the isoprenoid phenol compound C' (m/z 222).
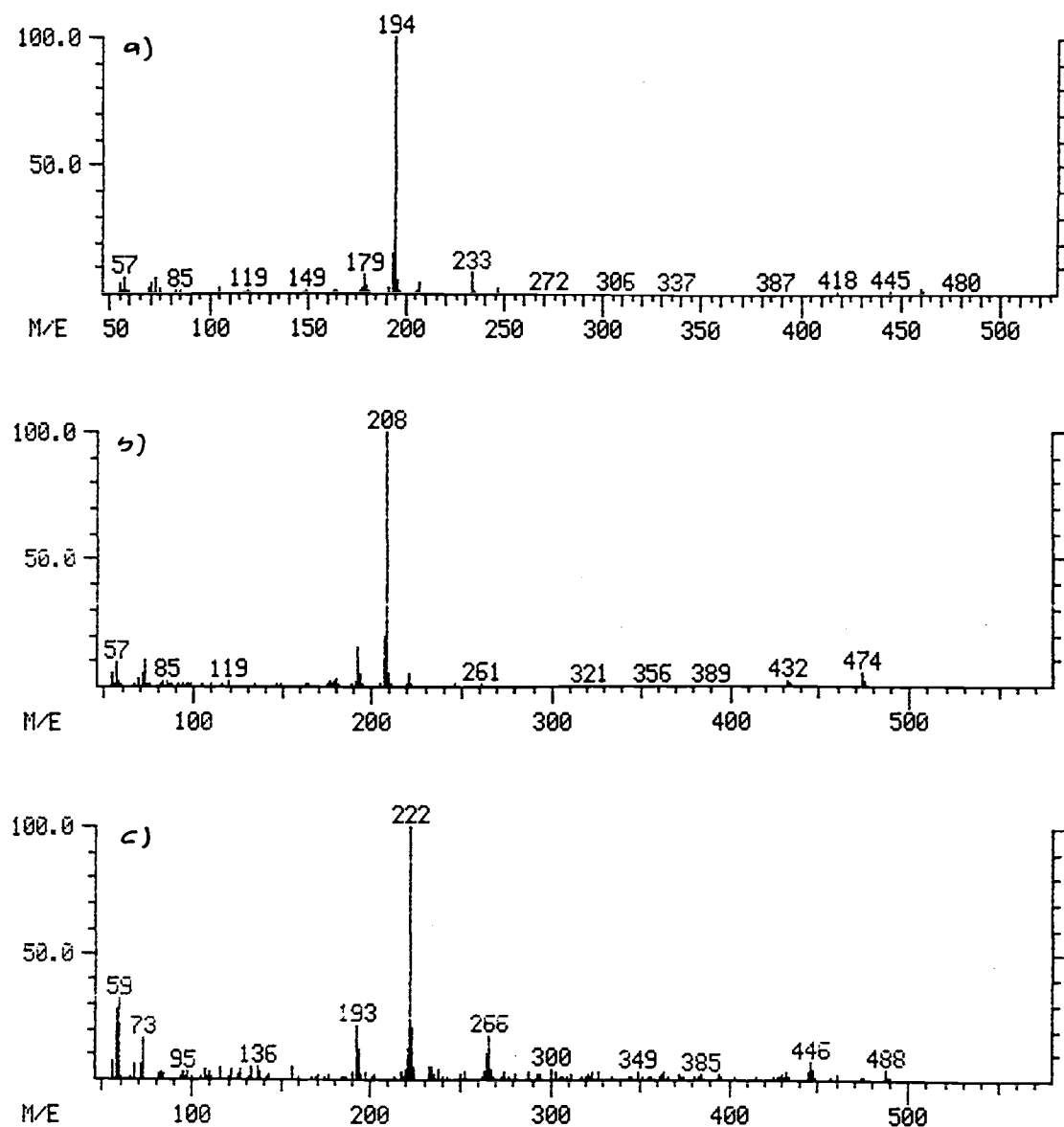
Figure. 2.12. Mass spectra of silylated isoprenoid phenols present in NSO fraction of hydrothermal oil from the interior of vent 1972-CH1: (a) compound A'; (b) compound B'; (c) compound C'. Mass spectra correspond to the peaks labeled in Fig. 2.11.
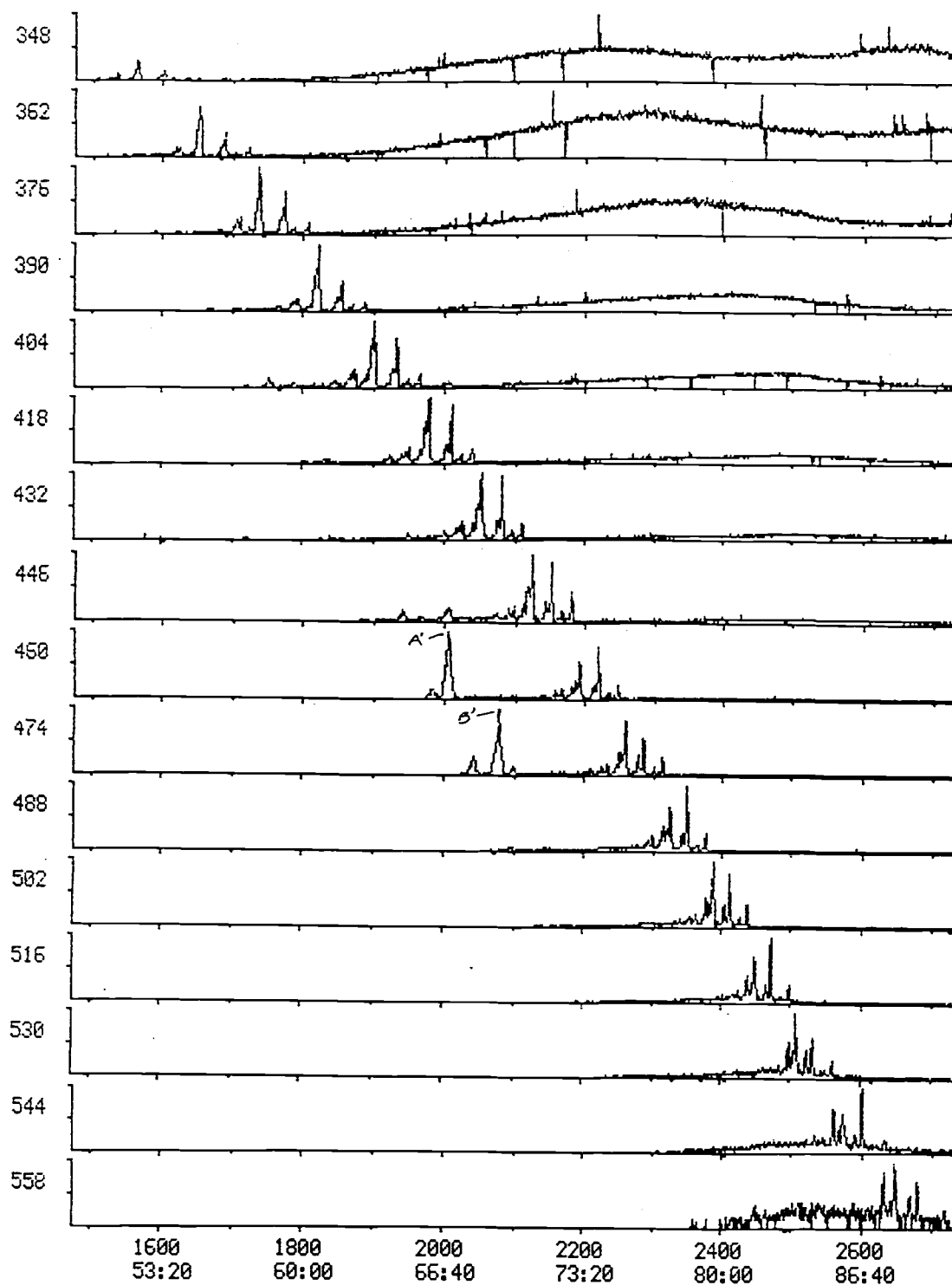
Figure 2.13. Representative mass fragmentograms (M$^+$) for the silylated derivatives of the extended C_{19} to C_{34} n-alkylphenols present in the NSO fraction of hydrothermal oil 1972-CH1 Interior. Compounds A' and B' refer to the isoprenoid phenols.
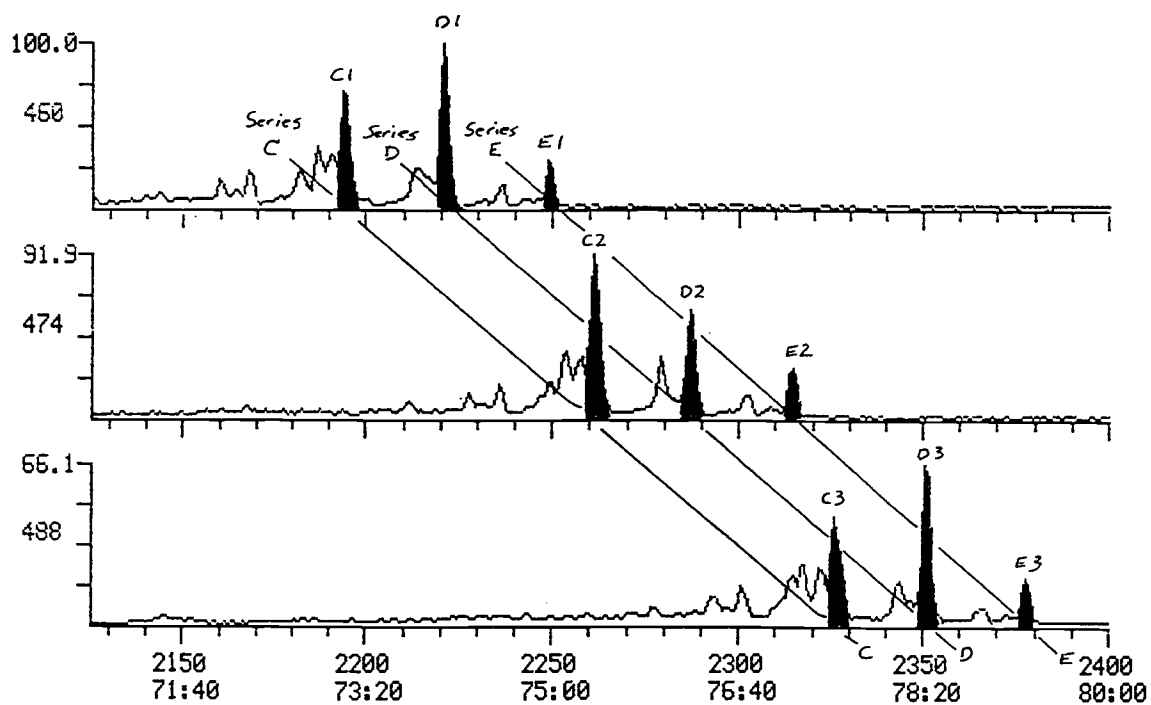
Figure 2.14. Representative mass fragmentograms (M+) for the silylated derivatives of the extended C_{27} to C_{29} n-alkylphenols present in the NSO fraction of hydrothermal oil 1972-CH1 Interior. Labeled in the figure are series C, D and E.
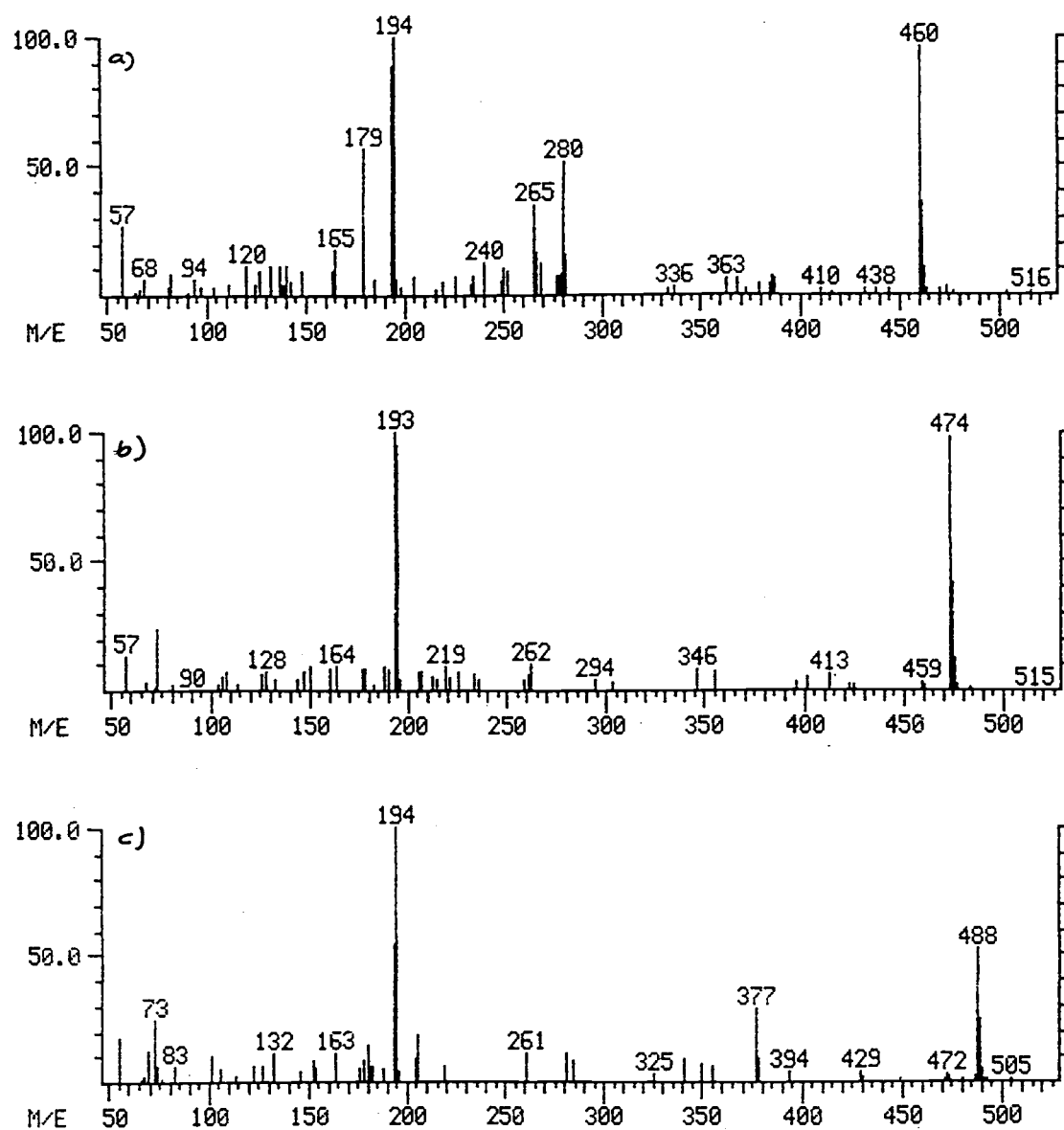
Figure 2.15. Mass spectra of silylated n-alkylphenols present in NSO fraction of hydrothermal oil from the interior of vent 1972-CH1: (a) compound C1; (b) compound C2; (c) compound C3. Mass spectra correspond to the peaks labeled in Fig. 2.14.
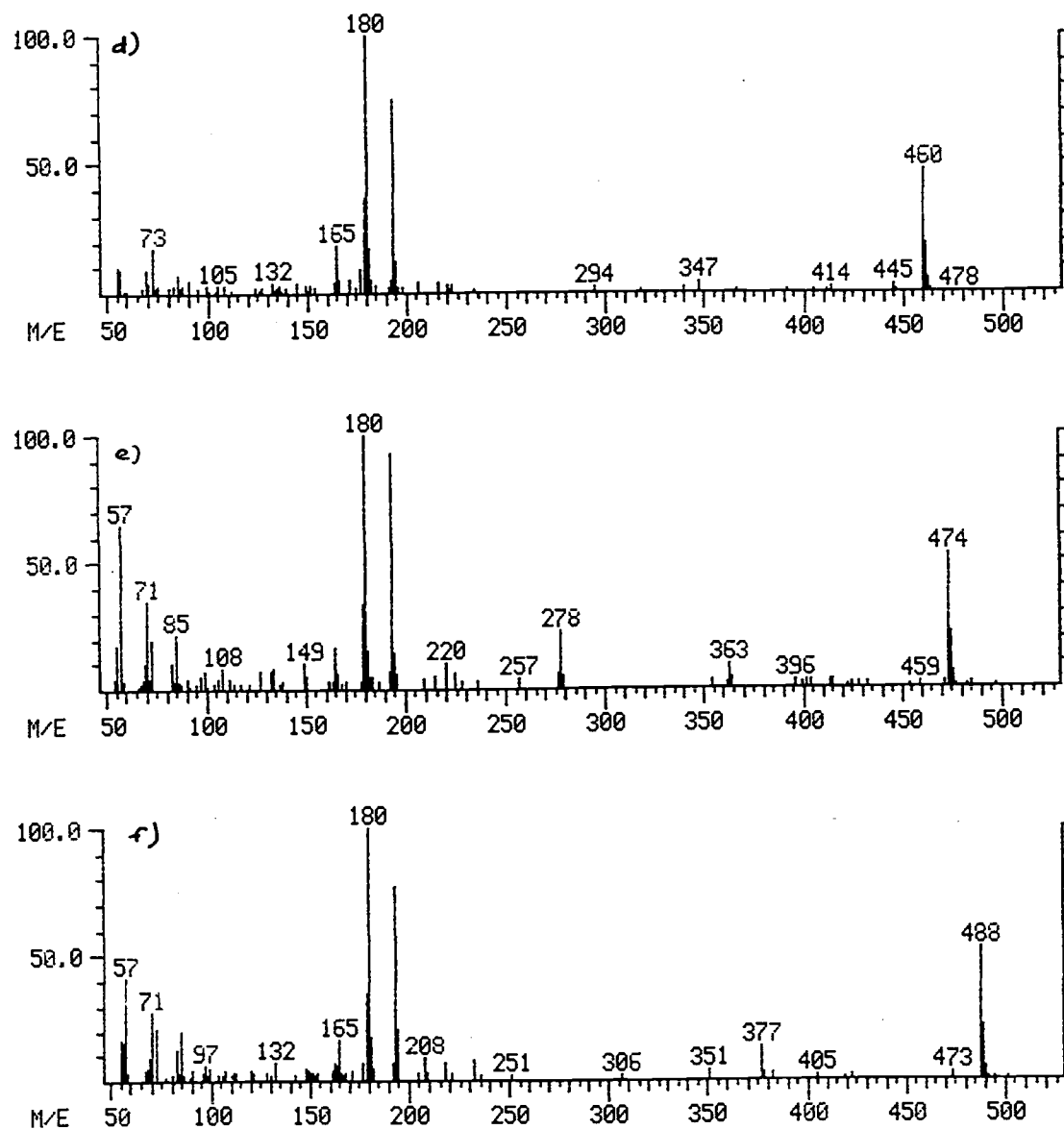
Figure 2.15. Mass spectra of silylated n-alkylphenols present in NSO fraction of hydrothermal oil from the interior of vent 1972-CH1: (d) compound D1; (e) compound D2; (f) compound D3. Mass spectra correspond to the peaks labeled in Fig. 2.14.
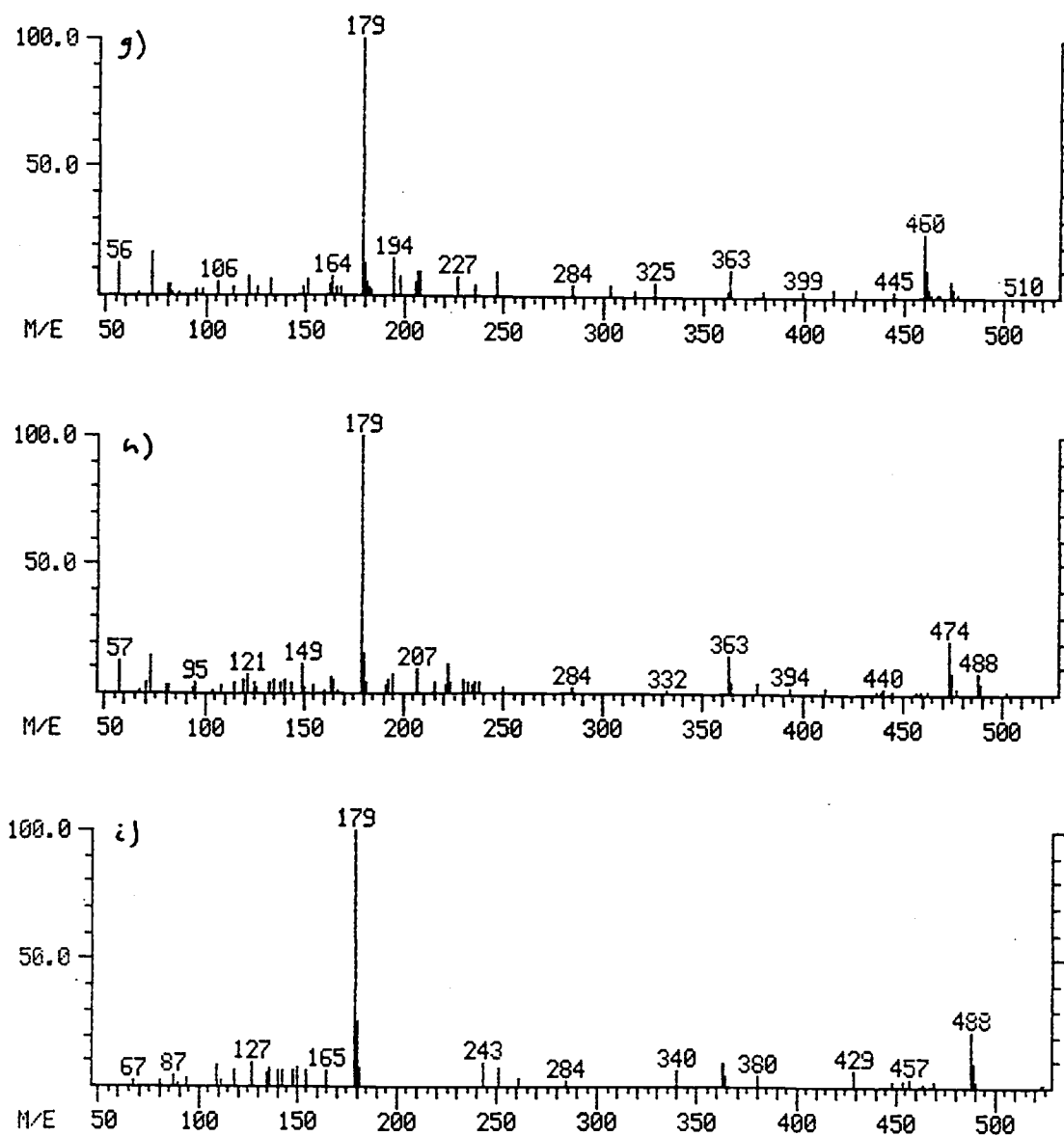
Figure 2.15. Mass spectra of silylated n-alkylphenols present in NSO fraction of hydrothermal oil from the interior of vent 1972-CH1: (g) compound E1; (h) compound E2; (i) compound E3. Mass spectra correspond to the peaks labeled in Fig. 2.14.
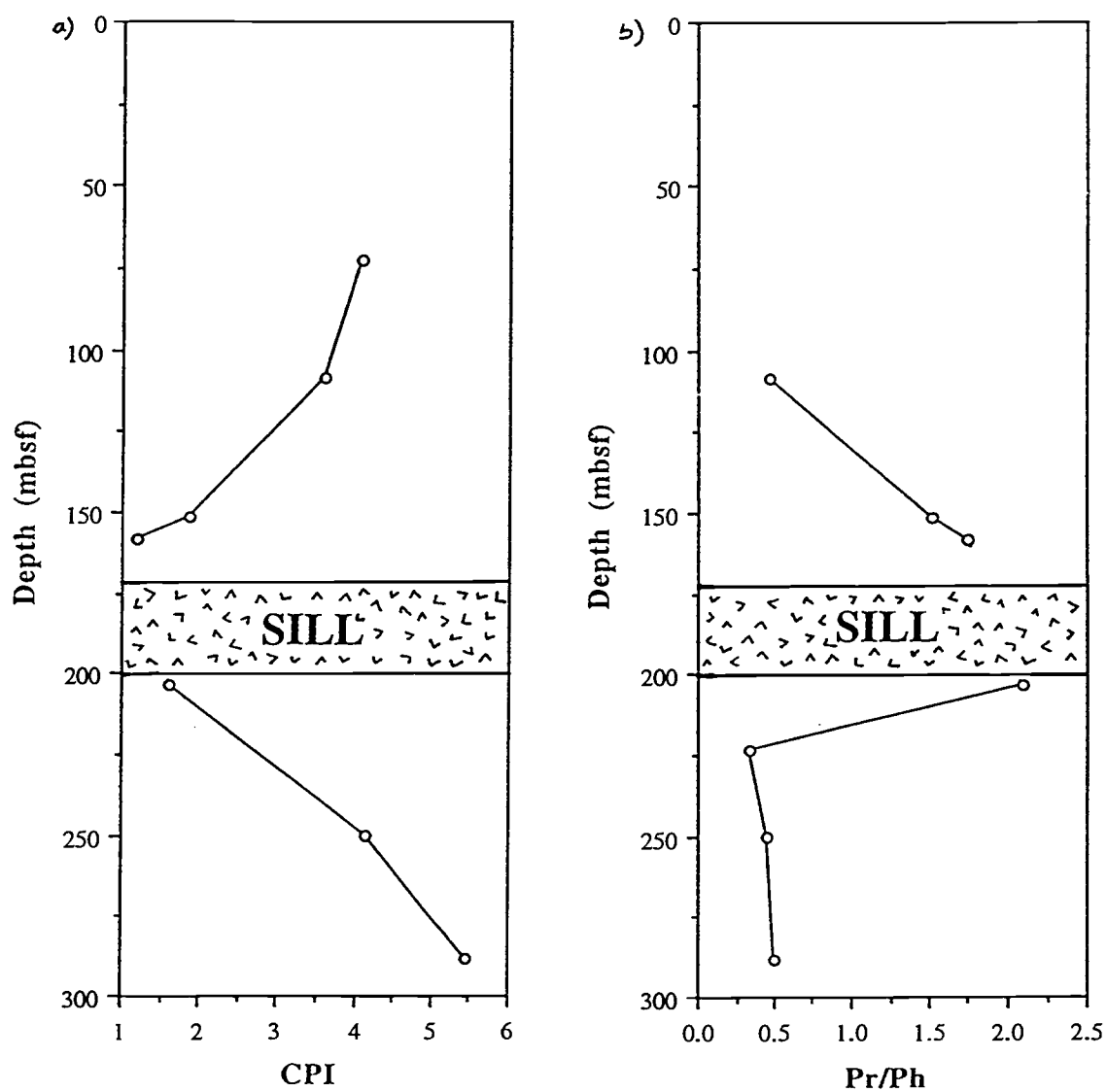
Figure 2.16. Plots of molecular parameters versus depth in DSDP Leg 64 Hole 481A: (a) CPI vs. Depth, meters below sea floor (mbsf) and (b) Pr/Ph vs. Depth (mbsf).
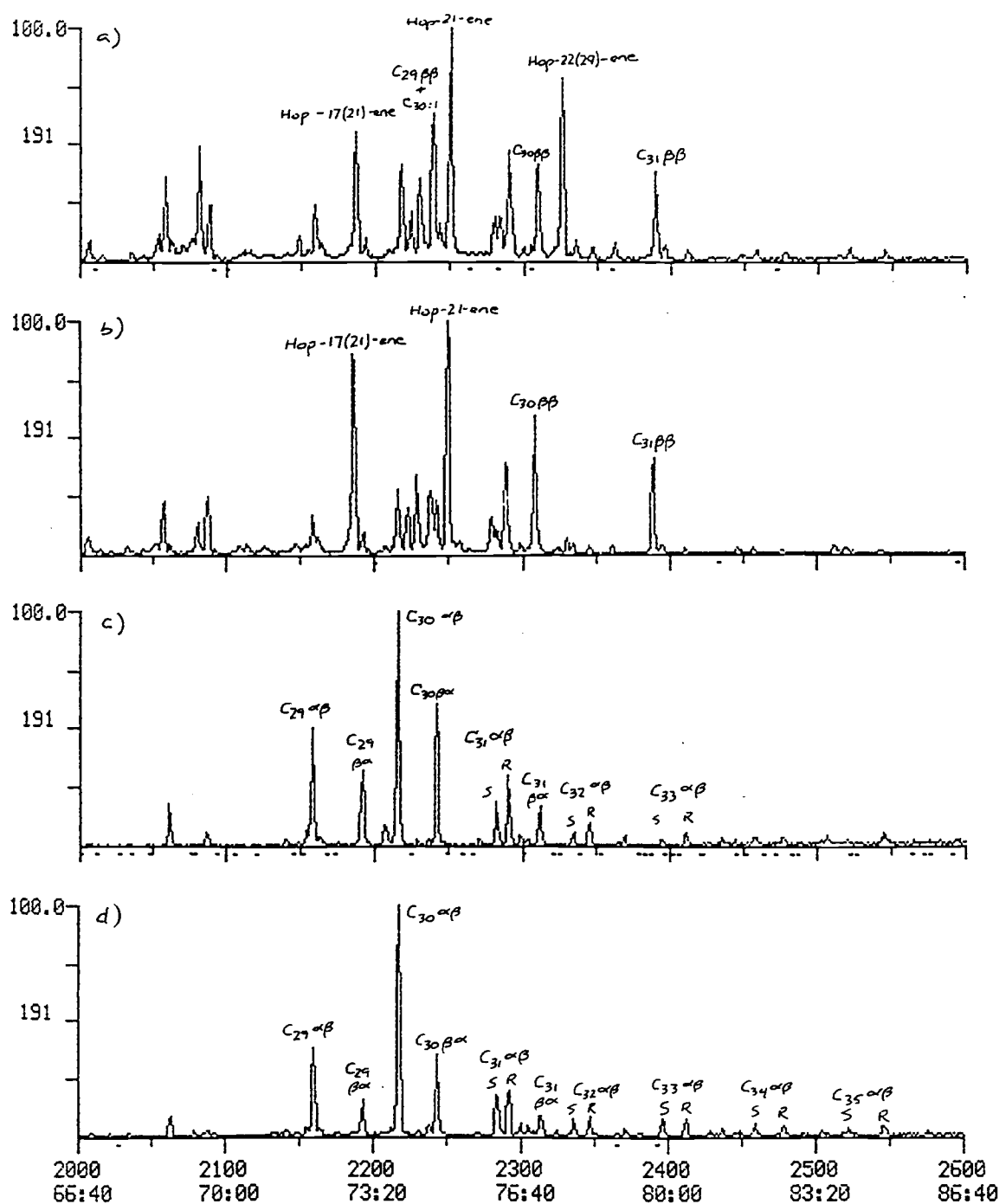
Figure 2.17. Representative mass fragmentograms m/z 191 for the triterpenoid hydrocarbons in the bitumen of DSDP Leg 64 sediments: (a) 481A-4-2 (93-98); (b) 481A-8-7 (top of pipe); (c) 481A-12-4 (55-65); (d) 481A-13-2 (18-27).
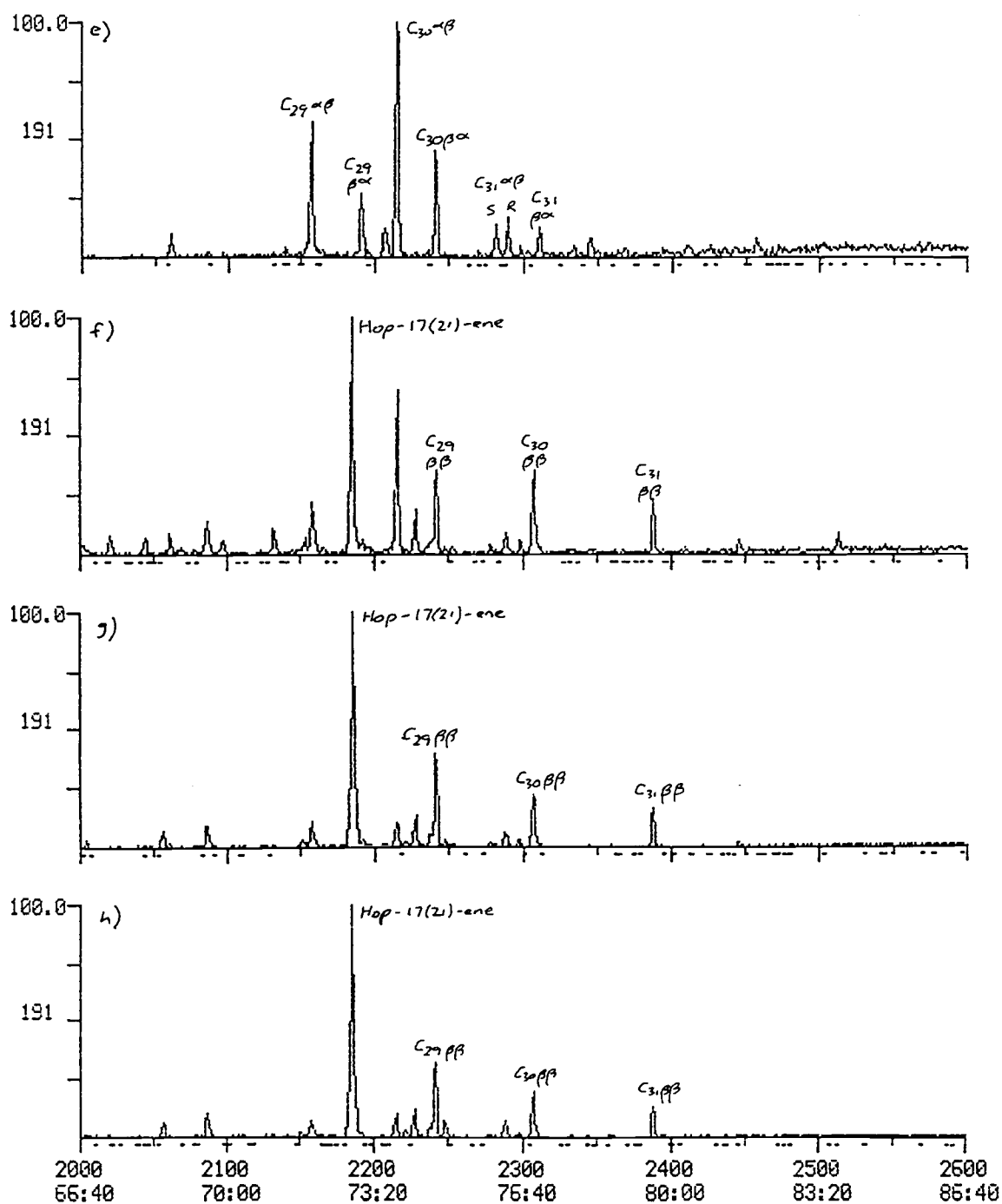
Figure 2.17. Representative mass fragmentograms m/z 191 for the triterpenoid hydrocarbons in the bitumen of DSDP Leg 64 sediments: (e) 481A-18-1 (30-32); (f) 481A-20-1 (110-115); (g) 481A-22-7 (top of pipe); (h) 481A-26-CC.
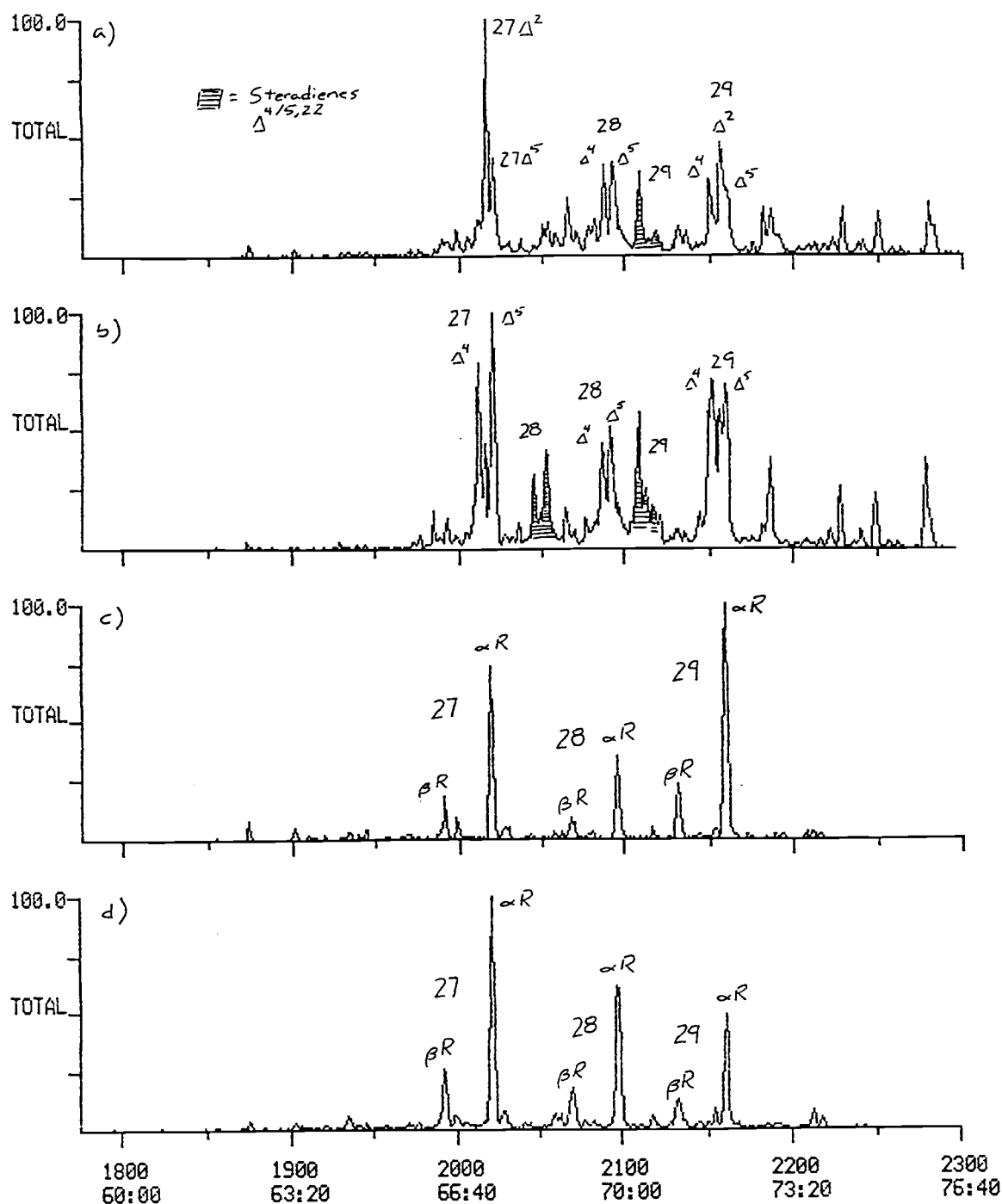
Figure 2.18. Representative mass fragmentograms (m/z 215, 217, 218, 257, 259) for the steroid hydrocarbons in the bitumen of DSDP Leg 64 sediments: (a) 481A-4-2 (93-98); (b) 481A-8-7 (top of pipe); (c) 481A-12-4 (55-65); (d) 481A-13-2 (18-27).
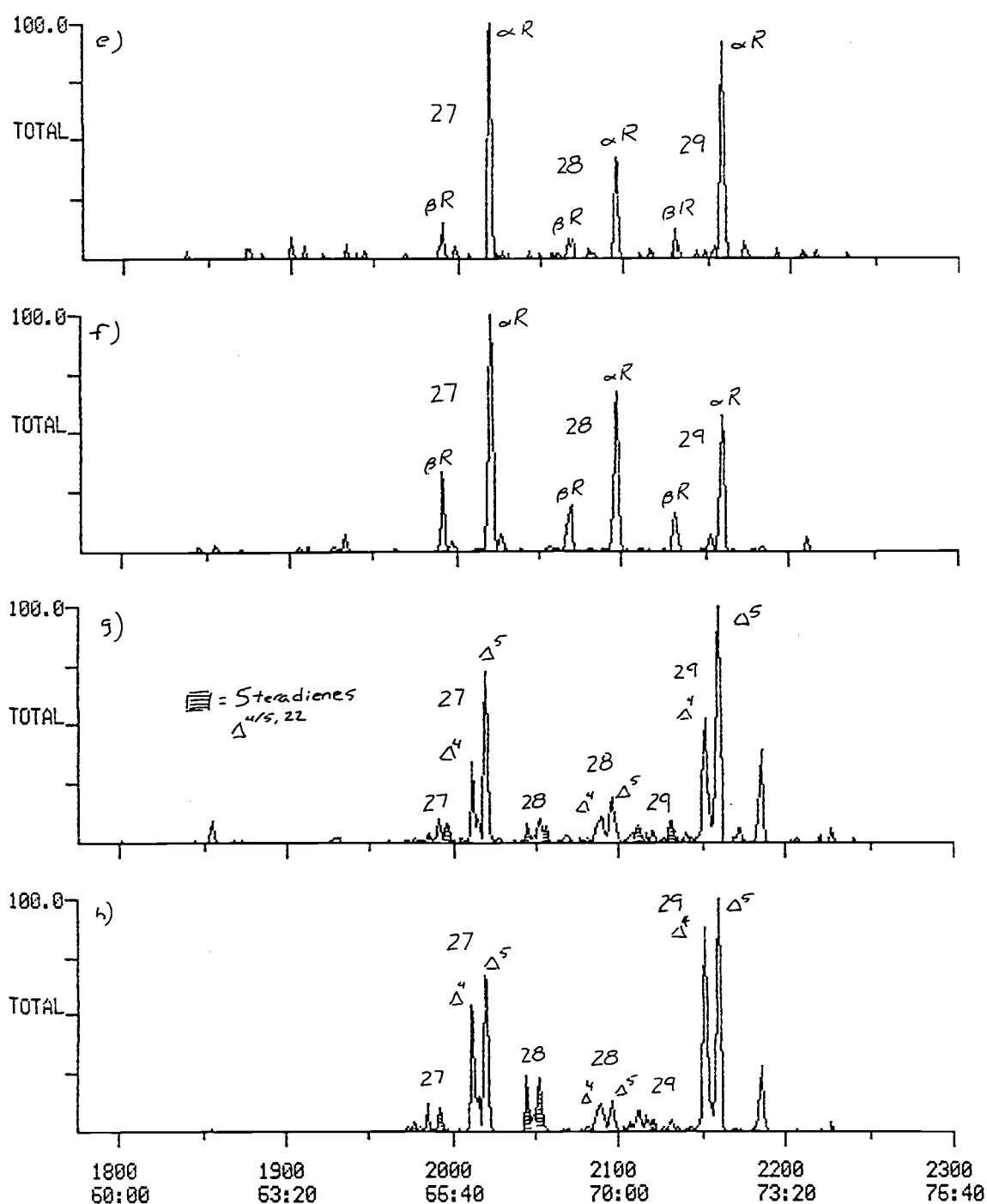
Figure 2.18. Representative mass fragmentograms (m/z 215, 217, 218, 257, 259) for the steroid hydrocarbons in the bitumen of DSDP Leg 64 sediments: (e) 481A-18-1 (30-32); (f) 481A-20-1 (110-115); (g) 481A-22-7 (top of pipe); (h) 481A-26-CC.
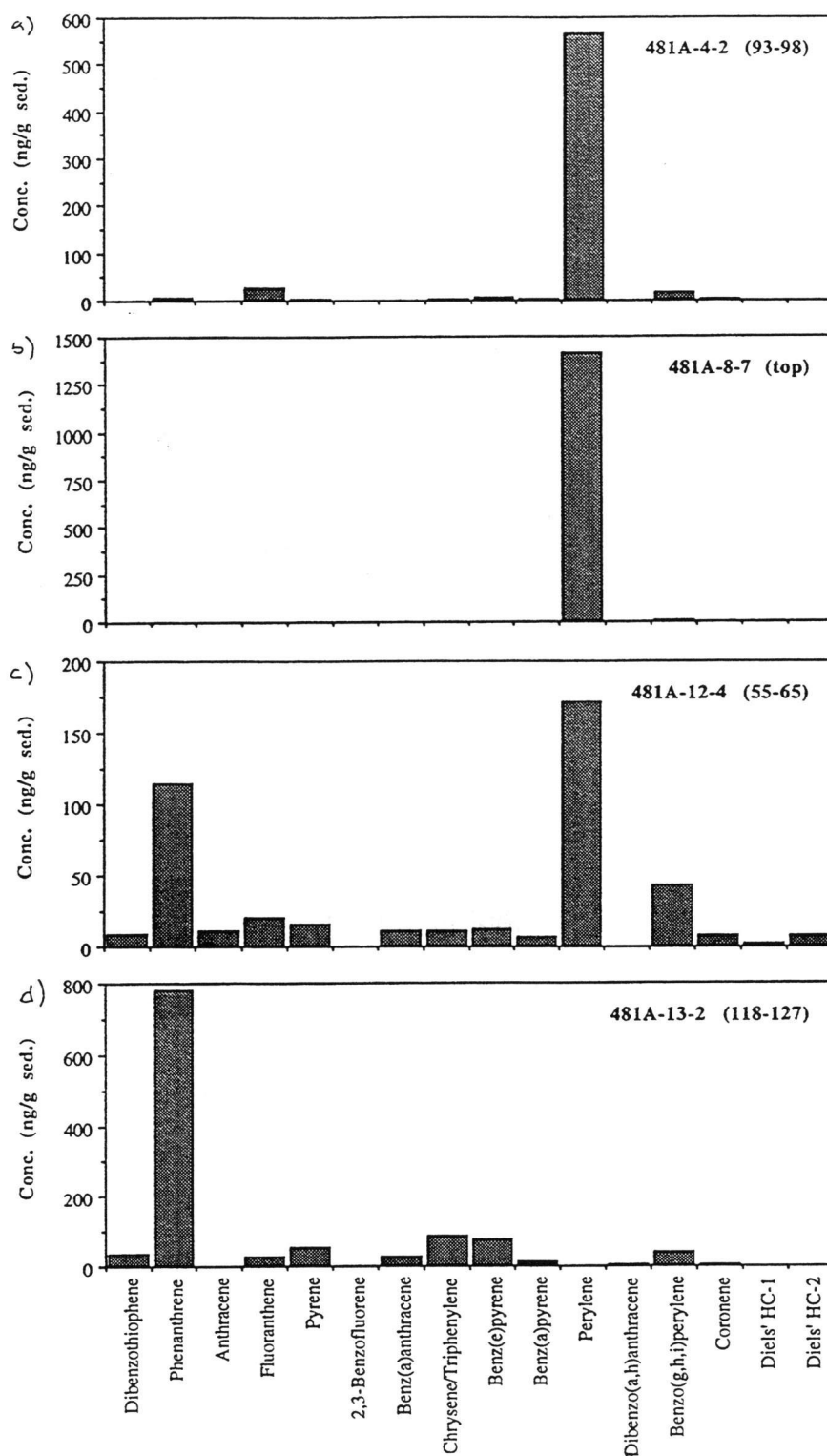
Figure 2.19. Histograms of the major aromatic compounds present in the bitumen of DSDP Leg 64 sediments: (a) 481A-4-2 (93-98); (b) 481A-8-7 (top of pipe); (c) 481A-12-4 (55-65); (d) 481A-13-2 (18-27).
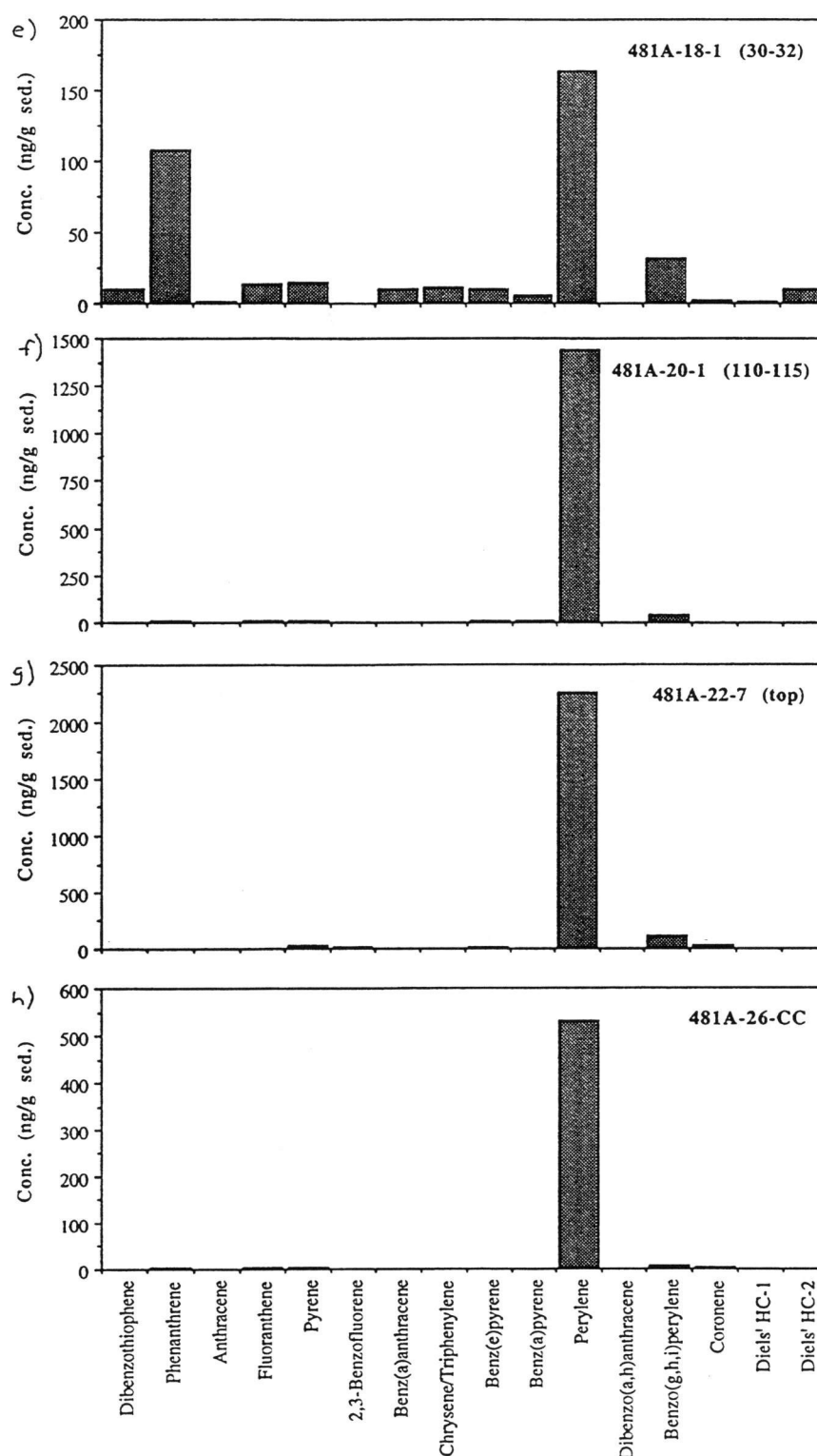
Figure 2.19. Histograms of the major aromatic compounds present in the bitumen of DSDP Leg 64 sediments: (e) 481A-18-1 (30-32); (f) 481A-20-1 (110-115); (g) 481A-22-7 (top of pipe); (h) 481A-26-CC.
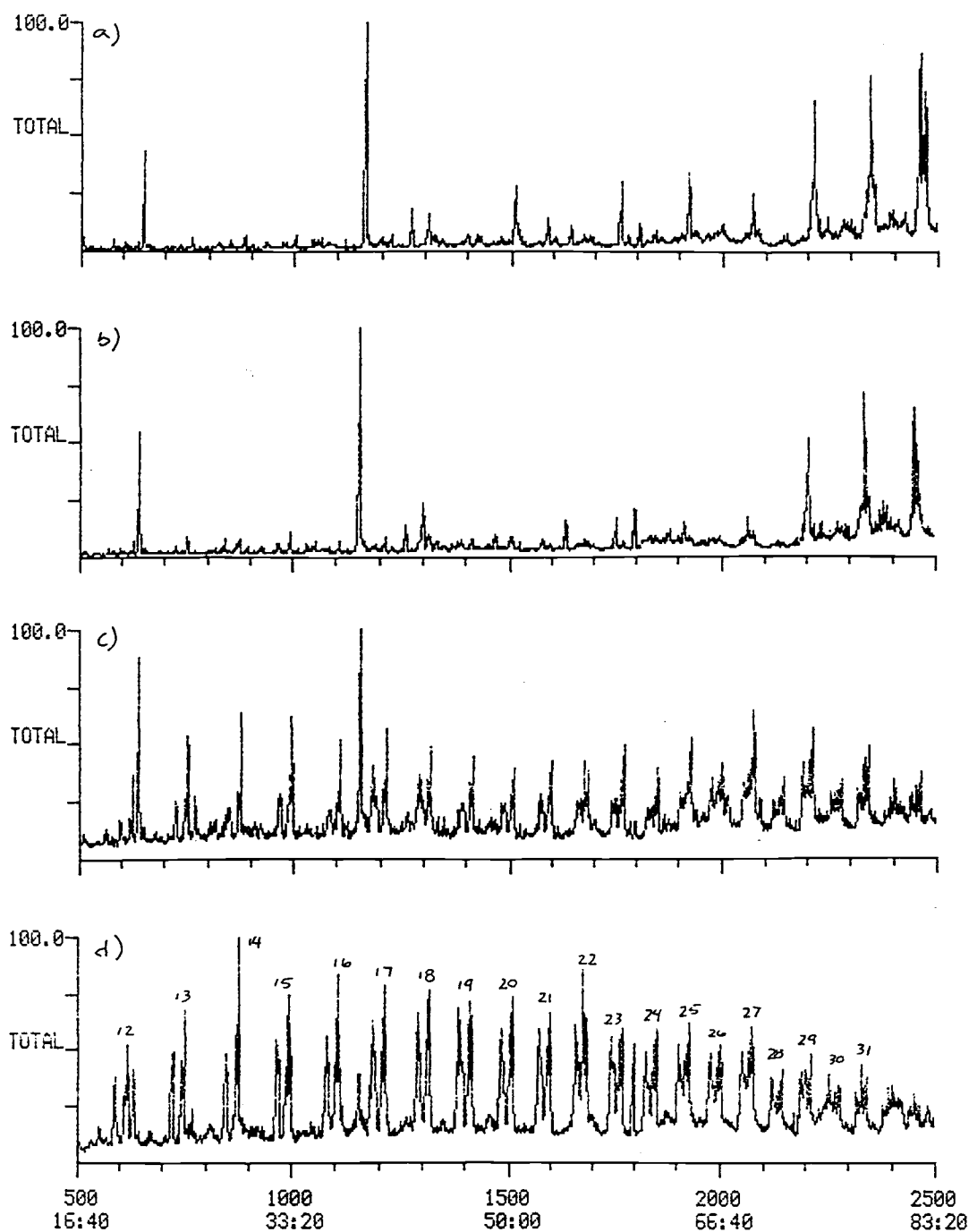
Figure 2.20. Representative mass fragmentograms (m/z 57, 58, 71, 72) for the ketones in the bitumen of DSDP Leg 64 sediments: (a) 481A-4-2 (93-98); (b) 481A-8-7 (top of pipe); (c) 481A-12-4 (55-65); (d) 481A-13-2 (18-27).
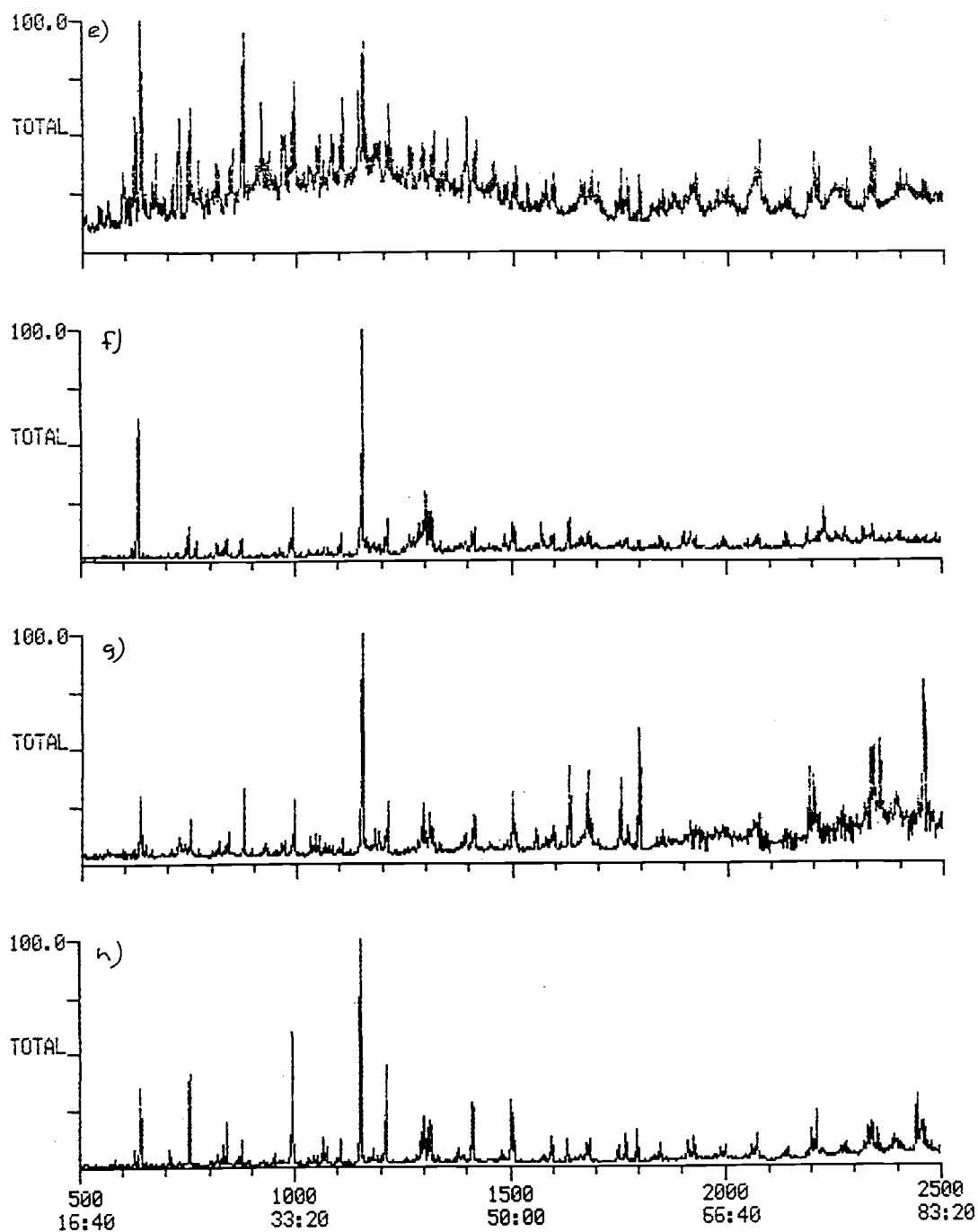
Figure 2.20. Representative mass fragmentograms (m/z 57, 58, 71, 72) for the ketones in the bitumen of DSDP Leg 64 sediments: (e) 481A-18-1 (30-32); (f) 481A-20-1 (110-115); (g) 481A-22-7 (top of pipe); (h) 481A-26-CC.
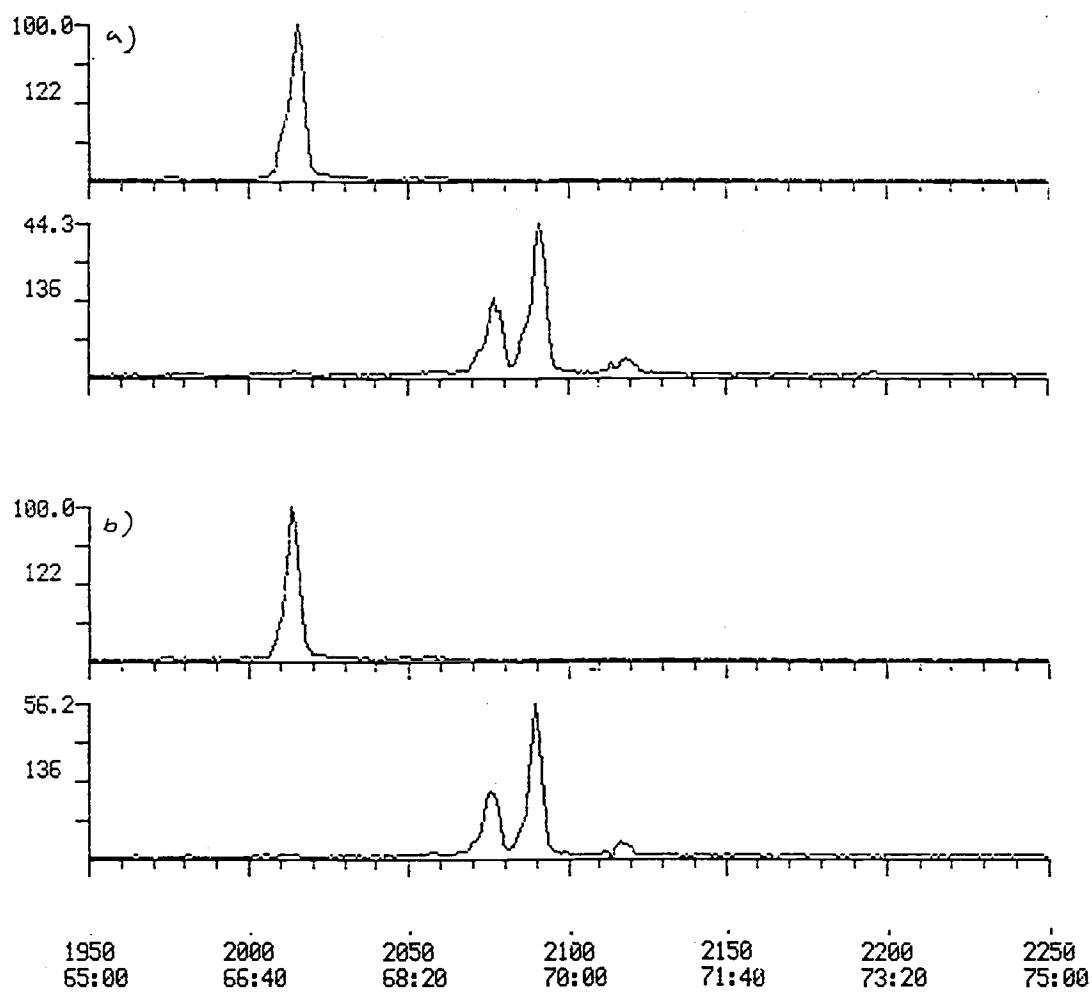
Figure 2.21. Representative mass fragmentograms (m/z 122 and m/z 136) for the isoprenoid phenols in the bitumen of DSDP Leg 64 sediments: (a) 481A-12-4 (55-65) and (b) 481A-18-1 (30-32).

CHAPTER 3

Radical and Ionic Reactions During Hydrothermal Pyrolysis of Organic Matter : Implications for the Simulation of Geochemical Processes

ABSTRACT

The heavy water pyrolysis experiments of Messel shale and model compounds performed by Hoering have demonstrated that there can be a large exchange of protons between water and organic compounds during hydrous pyrolysis. There has not been a satisfactory explanation for these results, especially the aspects of the extent of deuterium substitution in the n-alkanes and the enrichment of deuterium at only one end of some molecules.

The following mechanism accounts for the deuterium substitution observed in the hydrocarbons generated during Messel shale heavy water pyrolysis. Thermal cracking of the aliphatic kerogen network during hydrous pyrolysis generates n-alkanes and α-olefins. The α-olefins are quickly converted to internal olefins by acid-catalyzed double bond isomerization, a process which rapidly incorporates deuterium into the hydrocarbon skeleton. Deuterium exchange by direct homogeneous radical exchange with saturated hydrocarbons occurs at a much slower rate. The olefins are subsequently hydrogenated to fully saturated n-alkanes, but the rate of alkene isomerization is much greater than the rate of hydrogenation. Aliphatic moieties bound to the kerogen at one site can form a terminal double bond upon cleavage. Acid-catalyzed double bond isomerization followed by hydrogenation preferentially introduces deuterium at only one end of the molecule, resulting in hydrocarbons with unsymmetric patterns of deuterium incorporation. This mechanism accounts for the extensive deuterium substitution observed in the generated n-alkanes and also explains how deuterium substitution can occur at only one end of selected hydrocarbon species.

INTRODUCTION

The research by Hoering (1984) produced some interesting results concerning the role of water during laboratory hydrous pyrolysis. Presented below are some key aspects from that publication, a paper which was divided into three parts :

(1)   hydrous pyrolysis of shale kerogen to evaluate the similarities and differences between artificially derived oils and natural oils,

(2)   the pyrolysis experiments in D_2O with deuterium used as a tracer to understand how water interacts in the catagenetic reactions,

(3)   pure compound D_2O pyrolyses to aid in understanding the mechanisms of organic matter transformations.

Messel shale was selected for the experiments due to its low thermal history, its high organic carbon content, and having been a sample for numerous studies. The shale was powdered and extracted prior to heating. For each experiment the shale was combined with water or heavy water, sealed under nitrogen in a stainless steel reaction vessel and heated at 330°C for 72 h.

The n-alkanes from the D_2O pyrolysis were isolated and analyzed by mass spectrometry to determine the extent of deuterium incorporation. Fig. 3.1 is a histogram of an unweighted average deuterium distribution for the C_{17} to C_{29} n-alkanes generated from the kerogen by hydrous pyrolysis. The substitution ranged from 0 to at least 14 deuterium atoms for each n-alkane, with the highest relative abundances of 4 to 6 deuterium atoms. There was no obvious trend in substitution pattern as a function of chain length.

The analysis of isoprenoid and branched hydrocarbons generated by the D_2O pyrolysis experiments provided additional information about the nature of the deuterium exchange process. Fig. 3.2 is a histogram showing the relative abundances of the C_{13} ion fragments from the mass spectrum of pristane generated in the D_2O experiment. The bimodal distribution is consistent with a pristane molecule which has deuterium substituted at only one end of the molecule. The C_{13} fragment which contains no deuterium atoms would produce an ion fragment of m/z 183 while the C_{13} fragment containing the deuterium atoms would produce ion fragments greater than m/z 183, and in this case maximizes at m/z 190, corresponding to 7 deuterium substitutions as being the most abundant isomer. The preferential deuterium

enrichment to only one end of certain molecules was also evident in the analysis of iso- and anteiso-alkanes. Fig. 3.3 is the partial mass spectrum of 2-methyl heptadecane, a compound representative of the branched hydrocarbons produced in the pyrolysis experiments. The cluster of ion fragments maximizing at m/z 247 corresponds to loss of a methyl group with 8 deuterium substitutions being the most abundant. The cluster at m/z 216 is produced by the loss of a propyl group with 5 deuterium substitutions being the most abundant. These patterns of the mass fragments are also consistent with an enrichment of deuterium at one end of the molecule. But contrary to the original interpretation, this molecule appears to be enriched with deuterium at the end where the branching occurs. Analysis of sterane and triterpane hydrocarbons also revealed a preferential enrichment at one end of the molecule (Hoering, 1984).

In an attempt to understand the mechanism of deuterium enrichment in the hydrocarbons, pyrolyses of some model compounds were performed. Below is a discussion of the results from the alkane and alkene D_2O pyrolyses from the original Hoering (1984) publication.

Docosane was selected to study the degree of deuterium incorporation by simple homogeneous exchange. Under the same heating conditions as those in the Messel shale pyrolyses (72 hr @ 330°C) there was a small amount of deuterium exchange with the fully saturated alkane. Fig. 3.4a is a histogram of the results showing the relative amounts of the deuterium substituted isomers. Another experiment was conducted using the olefin 1-octadecene as the molecular probe. This compound was chosen since dry pyrolysis experiments usually generate a large amount of olefins. Under the same reaction conditions the olefin was hydrogenated to the saturated octadecane, indicating a strongly reducing environment inside the reaction vessel. Analysis of this product showed that a substantially higher amount of deuterium incorporation occurred before the olefin was converted into the fully saturated reaction product octadecane. A histogram of the relative amounts of the deuterium substituted isomers is shown in Fig. 3.4b. These results indicate that the deuterium exchange process is enhanced by the presence of a double bond, but the presence of only one double bond is not sufficient to explain the extent of deuterium substitution observed in the n-alkanes generated by the D_2O Messel shale pyrolysis, shown in Fig. 3.1.

To explain the deuterium substitution patterns in the pyrolysis experiments, a free radical chain mechanism was proposed. One set of reactions is shown in Fig. 3.5

(Hoering, 1984). This mechanism proposes that one part of the multiple deuteration could have occurred by the free radical migration of the olefin sites.

A re-examination of the Hoering (1984) deuterium isomer profile data by numerical modeling was performed by Ross (1992a,b). He concluded that one likely explanation for the deuterium isomer distribution in the n-alkanes generated in the D_2O Messel shale pyrolysis is by simultaneous deuterium exchange at more than one site. He suggested a combination of ionic and radical chemistry to explain the results, shown in Fig. 3.6 (Ross, 1992a), although the details of the actual chemical mechanisms to result in preferential deuterium substitution at one end of the molecule could still not be fully explained.

Recent research in pyrolysis and high temperature aqueous chemistry of hydrocarbons provides some insight into the major reactions that alkanes and alkenes undergo (Weres et al., 1988; Siskin et al., 1990; Kissin, 1987, 1990; Leif et al., 1992). These studies point to the importance of both radical and ionic reaction mechanisms during the pyrolysis of organic matter. This chapter duplicates the original Hoering (1984) Messel shale pyrolysis experiments and presents results from additional hydrous pyrolysis experiments which provide evidence for the chemical pathway by which hydrogen exchange occurs between water and aliphatic hydrocarbons.

EXPERIMENTAL

Chemicals and samples. H_2O pyrolysis experiments were performed using Burdick and Jackson ultrapure water, and D_2O pyrolysis experiments were done using D_2O from Cambridge Isotope Laboratories. The D_2O was glass distilled before using. Aliphatic compounds used in pyrolysis experiments were 1,13-tetradecadiene (purity > 97), 1-hexadecene (purity > 97%), eicosane (purity 99%), dotriacontane ($\underline{n}$-$C_{32}H_{66}$, purity > 97%), and low-density polyethylene (LDPE, purity > 99%). Sublimed elemental sulfur was used in one of the pyrolysis experiments. The Messel shale used in the experiments was powdered and Soxhlet extracted with methanol/methylene chloride for 72 hr prior to the pyrolysis studies. One surface sediment sample from Guaymas Basin, Gulf of California, was pyrolyzed at 350°C for 72 hr and extracted with methanol and methylene chloride prior to this study.

Hydrous pyrolysis experiments. Pyrolysis experiments were performed in Sno-Trik® T316 stainless steel high pressure pipes rated at 60,000 psig (4080 bar), sealed with end caps and heated in an air circulating oven set at 330° ±2°C. The reaction vessels with reactant mixtures were placed in a glove bag and flushed with five volumes of argon. Deoxygenated H_2O or D_2O, prepared by bubbling with argon gas for 45 minutes, was added and the vessels sealed. Durations of the heating experiments ranged from 1 hr to 72 hr (Table 3.1).

Extraction and fractionation. The reaction vessels were removed from the oven and cooled to room temperature upon completion of the heating cycle. The reaction vessels were extracted with two 1 mL portions of methanol followed by five 1 mL portions of methylene chloride. The solvents and water from each pyrolysis experiment were combined in a centrifuge tube and the organic fraction separated and collected. The water was extracted with two additional portions of methylene chloride and the two methylene chloride fractions were combined. The methylene chloride was dried with anhydrous sodium sulfate and was passed through an activated copper column to remove the elemental sulfur. The solvent was removed to near dryness using a rotary evaporator at 30°C. The total extract was made up to 2 mL of methylene chloride and deasphalted in 100 mL of heptane. The asphaltenes were allowed to precipitate overnight and removed by filtration. The deasphalted fractions were fractionated by column chromatography (30 cm x 1 cm) packed with 3.8 g alumina (fully active) over 3.8 g silica gel (fully active). The samples were separated into three fractions by elution with 50 mL heptane (nonpolar, F1), 50 mL toluene

(aromatic, F2) and 25 mL methanol (polar NSO, F3). Separation of the alkanes from the alkenes was done by argentation silica column chromatography. In one experiment the normal alkanes were isolated from the nonpolar fractions by urea adduction. Hydrogenation of selected samples was done by bubbling H_2 gas into the sample for 30 min. in the presence of platinum(IV) oxide (Adam's catalyst).

Gas chromatography. Gas chromatography (GC) of the pyrolysates was performed with a Hewlett Packard 5890A equipped with a 30 m x 0.25 mm i.d. DB-5 open tubular column (0.25 µm film thickness). The GC oven was heated using the following program : isothermal for 2 min. at 65°C, 3°/min. to 310°C, and isothermal for 30 min., with the injector at 290°C, detector at 325°C, and helium as the carrier gas.

Gas chromatography-mass spectrometry. Gas chromatography-mass spectrometry (GC-MS) was performed on a Finnigan 9610 gas chromatograph coupled to a Finnigan 4021 quadrupole mass spectrometer operated at 70 eV over the mass range 50-650 dalton and a cycle time of 2.0 s. The GC oven temperature was programmed at isothermal for 2 min. at 65°C, 4°/min. to 310°C, and isothermal for 30 min., with the injector at 290°C, and helium as the carrier gas. The MS data were processed with an on-line Finnigan-Incos 2300 computer data system.

Additional analyses were performed on a Hewlett Packard 5890 Series II GC coupled to a Hewlett Packard 5971 Series Mass Selective Detector (MSD). The GC was equipped with a 30 m x 0.25 mm i.d. DB-1 open tubular column (0.25 µm film thickness). The GC oven temperature was programmed at isothermal for 2 min. at 100°C, 5°/min. to 260°C, 10°C/min. to 300°C, and isothermal for 10 min., with an on-column injector, and helium as the carrier gas. The MS data were processed with a Hewlett Packard Vectra 486 PC.

RESULTS AND DISCUSSION

n-C$_{32}$H$_{66}$ pyrolysis experiments. To more fully understand the factors affecting the aqueous high temperature organic chemistry of heavy n-paraffins, pyrolysis of n-C$_{32}$H$_{66}$ with water only or water with inorganic additives has been studied (Leif et al., 1992). Each experiment was run at 350°C for 72 hr under a nitrogen atmosphere. It has been shown that extensive cracking, with varying degrees of alkene formation, occurred under the experimental conditions. The composition of the products was modified by pH and reactive species such as elemental sulfur and iron sulfides. Fig. 3.7 shows the gas chromatograms of the total extracts from these pyrolysis experiments. They are characterized by a broad distribution of cracking products with a large amount of unreacted starting material. The recovered cracking products ranged in carbon number from C$_9$ to C$_{31}$, there was a negligible amount of gas pressure in each of the reaction tubes which escaped upon opening. The cracking products in all of the experiments maximized at C$_{16}$, half the carbon number of the starting material. The aliphatic fraction consists n-alkanes and n-alkenes. Fig. 3.8a is the aliphatic fraction of the n-C$_{32}$H$_{66}$ - H$_2$O system, consisting of n-alkanes and several n-alkene isomers. Catalytic hydrogenation of the nonpolar fraction confirms the presence of only n-alkene isomers (Fig. 3.8b). The large number of n-alkene isomers is evidence of acid-catalyzed double bond isomerization. The experiment was repeated in an alkaline environment maintained by the addition of NaOH. The chromatograms of the nonpolar fraction and hydrogenated nonpolar fraction are shown in Fig. 3.9a and 3.9b. The low hydrogen ion concentration in the alkaline system inhibited double bond migration to give a product distribution dominated by terminal n-alkenes. These results show that the products from these pyrolysis experiments are the result of primary cracking of n-C$_{32}$H$_{66}$ to form terminal alkenes, followed by secondary acid-catalyzed reactions of these terminal n-alkenes to form a suite of internal n-alkenes. The extent of double bond isomerization in the water system indicates that there can be significant proton exchange between water and hydrocarbons by this pathway.

To measure the amount of proton exchange that can occur by acid-catalyzed double bond isomerization, the above experiments were repeated using D$_2$O. The chromatograms of the n-C$_{32}$H$_{66}$ -D$_2$O system are shown in Fig. 3.10. As before, the products consist of n-alkanes and several n-alkene isomers. The saturated and unsaturated hydrocarbons were separated by AgNO$_3$ column chromatography.

Deuterium substitution in the n-alkanes was negligible while there was extensive deuterium substitution in the alkenes. Figure 3.11 shows the mass spectrum of n-C_{17} of the alkane fraction (Fig. 3.11a) and the mass spectrum of n-C_{17} from the hydrogenated alkene fraction (Fig. 3.11b). Fig. 3.12 shows the results from the n-$C_{32}H_{66}$ -D_2O - NaOD system. The alkaline system greatly reduced the amount of deuterium substitution in the hydrocarbons. Figure 3.13 shows the mass spectrum of n-C_{17} of the alkane fraction (Fig. 3.13a) and the mass spectrum of n-C_{17} from the hydrogenated alkene fraction (Fig. 3.13b). These results indicate that no deuteration occurred under these conditions, neither in the alkane fraction nor in the alkene fraction. Since alkaline conditions should inhibit the acid-catalyzed chemistry but not affect the free radical chemistry, the above experiments indicate that direct exchange between D_2O and n-alkanes does not occur under these conditions. The major pathway for the deuterium exchange under these conditions appears to be an ionic rather than a radical mechanism.

Pyrolysis of 1,13-tetradecadiene, 1-hexadecene and eicosane in D_2O. A time series in D_2O was conducted to measure the relative rates of deuterium incorporation for an alkadiene, an alkene and an alkane. The gas chromatograms for the aliphatic fractions are shown in Fig. 3.14. Hydrogenation of this fraction produced only alkanes (Fig. 3.15). The patterns of deuterium incorporation for the three hydrocarbons for each experiment are shown in Figs. 3.16 to 3.20.

Low density polyethylene pyrolysis. Pyrolysis experiments investigating the aqueous organic hydrothermal chemistry was extended to include low density polyethylene (LDPE), a highly cross-linked aliphatic polymer. This polymer was chosen since its structure resembles the chemically resistant aliphatic biopolymer material of kerogen thought to be the most important precursor of n-alkanes in crude oils (Burlingame et al., 1969; Simoneit and Burlingame, 1973; Goth et al., 1988; Tegelaar et al., 1989a,b,c). Hydrous pyrolysis of LDPE was performed under alkaline conditions to inhibit the secondary acid-catalyzed reactions of the alkene pyrolysis products. No gas pressure was detected at the termination of the reaction. Fig. 3.21a is the gas chromatogram of the aliphatic fraction. The products are dominated by homologous series of terminal n-alkenes and n-alkanes ranging from C_{10} to C_{37}, maximizing at C_{16}. The absence of any appreciable amount of ethylene is due to the predominance of thermal degradation reactions of the aliphatic polymer network rather than depolymerization reactions. This distribution of pyrolysis products resembles the product distributions from flash pyrolysis experiments of LDPE

(Sugimura and Tsuge, 1978). Catalytic hydrogenation of this fraction is shown in Fig. 3.21b, showing a smooth, homologous series of n-alkanes almost indistinguishable from distributions found in the n-$C_{32}H_{66}$ pyrolyses or any highly aliphatic oil. The results from this experiment indicate that hydrous pyrolysis of LDPE produces n-alkanes and terminal n-alkenes as primary cracking products, with a small amount of branched hydrocarbons formed.

Pyrolysis of 1,13-tetradecadiene polymerization product. Polymerization of 1,13-tetradecadiene occurred during a 330°C pyrolysis experiment with D_2O, the first 72 hr pyrolysis experiment done in the small reaction vessels. The polymer lined the walls of the reaction vessel but was easily removed without breakage. It was a thin, flexible, translucent polymer. It is likely that the interior of the vessel was catalytically active and aided in the polymerization of the α,ω-olefin into presumably an aliphatic and highly cross-linked polymer. A portion of the polymer was pyrolyzed under identical time and temperature conditions with H_2O as the medium. The results of the pyrolysis experiment are shown in Fig. 3.22. The m/z 99 mass fragmentogram, characteristic of n-alkanes, shows that the major pyrolysis products of the C_{14} polymer are n-alkanes.

The previous pyrolysis experiments with n-$C_{32}H_{66}$ and aliphatic polymers have demonstrated that hydrous pyrolysis of aliphatic material produces n-alkanes and terminal n-alkenes. Secondary reactions of the alkenes (i.e. bond isomerization reactions) can rapidly introduce protons (or deuterons) from the water (or heavy water) into the hydrocarbons. To test whether this is a feasible chemical pathway for the deuterium incorporation observed in the original Hoering (1984) pyrolyses of Messel shale with D_2O, the pyrolysis was repeated under the same time and temperature conditions. Since only saturated hydrocarbons were observed in the original pyrolyses, time series experiments were run to determine the relative rates of alkene isomerization versus alkene hydrogenation and deuterium incorporation.

Messel shale pyrolysis - repeat of Hoering (1984) experiment. The Messel shale - D_2O pyrolysis experiments of Hoering (1984) were repeated using the Parr reaction vessel and the stainless steel reaction pipes. The extent of deuterium incorporation into the n-alkanes was measured and there was no difference in the extent of deuterium substitution from the Parr reaction vessel or the pipe reactors. The deuterium substitution for the C_{17} to C_{29} n-alkanes is shown in Table 3.2. Shown in Fig. 3.23 is an unweighted average of the C_{17} to C_{29} n-alkane deuterium substitution distribution. Comparing these results to the original Hoering distribution shown in

Fig. 3.1, there is a difference in the distribution of deuterium substitution, primarily in the D0 to D3 range. These results suggest that there was a much smaller amount of n-alkanes formed in the D0 to D3 range than in the experiment performed by Hoering (1984). But in general a very large amount of deuterium incorporation has occurred in the n-alkanes that were generated in the heating experiments.

Messel shale H_2O pyrolyses - composition of aliphatic molecular probes. Two time series experiments were performed involving Messel shale in the pipe reaction vessels. The first series in H_2O was conducted to measure the relative rates of alkene isomerization versus hydrogenation for an alkadiene and an alkene when pyrolyzed in the presence of Messel shale. The gas chromatograms for the aliphatic fractions are shown in Fig. 3.24. Hydrogenation of this fraction produced alkanes and a minor amount of branched/cyclic compounds (Fig. 3.25). Data from this series are found in Table 3.3 and show that the rate of acid-catalyzed alkene isomerization is much faster than the rate of hydrogenation.

Messel shale D_2O pyrolyses - composition of aliphatic molecular probes. The second time series was conducted in D_2O to measure the relative rates of alkene isomerization and deuterium incorporation for an alkadiene, an alkene and an alkane when pyrolyzed in the presence of Messel shale. The gas chromatograms for the aliphatic fractions are shown in Fig. 3.26. Hydrogenation of this fraction produced alkanes (Fig. 3.27). The patterns of deuterium incorporation for the three hydrocarbons for each experiment are shown in Figs. 3.28 to 3.32, and data from this series are summarized in Table 3.4. This series has shown that the rate of acid-catalyzed alkene isomerization is slightly slower in D_2O than in H_2O. Deuterium was incorporated in the saturated alkane, interpreted as being due exclusively to a radical exchange process, but the degree of deuterium incorporation in the saturated hydrocarbon is much slower than in either of the olefin species.

Messel shale H_2O and D_2O pyrolyses - composition of aliphatic hydrocarbons released from kerogen. Additional information about the process of hydrous pyrolysis was obtained in the time series experiments by looking at the n-alkanes and triterpenoid hydrocarbons released from the Messel shale kerogen. Fig. 3.33 shows the range of pyrolysis products starting at n-$C_{23}H_{48}$ to n-$C_{32}H_{66}$. Fig. 3.34 shows the GC traces of the 1, 5, and 10 hr experiments at higher concentrations. After 1 hr a homologous series of terminal n-alkenes and n-alkanes are generated from the kerogen in an approximate ratio of 1:2. The 5 and 10 hr experiments shows evidence of alkene

isomerization and a decrease in the alkene to alkane ratio. Alkenes were not detected in either the 36 or the 72 hr reactions.

Free alkenes were also detected in the triterpenoid hydrocarbons released from the kerogen. Fig. 3.35 is the m/z 191 mass fragmentograms characteristic of the triterpenoid hydrocarbons released in the Messel shale H_2O time series experiments. After 1 hr the dominant compounds in the m/z 191 fragmentogram are the hopenes. The mass spectra of the hopenes indicate that the points of unsaturation all occur in the D or E rings of the C_{29} and C_{30} hopanes, and in the alkyl side chains of the hopanes C_{31} or greater. This is consistent with being bound to the kerogen at this end of the pentacyclic structure. The hopenes are were not detected after 10 hr. These triterpenoid biomarker distributions show the progression from an thermally immature distribution to one characteristic of the earliest stages of oil generation. After 10 hr there is not much change in the biomarker pattern, the only obvious trends are the progressive change in the T_s / T_m ratio and the slight isomerization of the $C_{31}\alpha\beta(R)$ hopane to the $C_{31}\alpha\beta(S)$.

Fig. 3.36 is the m/z 191 mass fragmentogram showing the triterpenoid hydrocarbons released in the Messel shale after 72 hr in D_2O. Selected mass spectra of the major hopanes are presented in Fig. 3.37. These mass spectra confirm that the deuterium incorporation has occurred in the D and E rings or the side chains of the hopane structures. The most likely explanation for these substitution patterns is deuterium incorporation has occurred by both isomerization and during the process of saturating the double bond. A homogeneous radical exchange process would produce a random deuterium distribution pattern in all rings of the pentacyclic structure, which would be distinguishable from the mass spectra.

Guaymas Basin sediment D_2O pyrolysis - composition of aliphatic molecular probes. One 10 hr experiment was performed where the three aliphatic probes were spiked on a sediment from the Guaymas Basin hydrothermal system. The deuterium substitution patterns for the three molecular probes are shown in Fig. 3.38. No deuterium was incorporated in the saturated eicosane but a large amount of deuterium was incorporated in the alkenes. These deuterium substitution patterns are unique in that they show that extensive deuterium incorporation has occurred in those alkenes that have isomerized. This suggests that there is a strong catalytic effect associated with the sediments which promotes extensive double bond isomerization once the alkenes begin to isomerize.

<u>Elemental sulfur D$_2$O pyrolysis - composition of aliphatic molecular probes.</u>
One 10 hr experiment was performed where the three aliphatic probes were combined
with 0.5 g elemental sulfur. The deuterium substitution patterns for the three
molecular probes are shown in Fig. 3.39. Although this was only a 10 hr experiment,
extensive deuteration occurred, even in the saturated alkane. This set of results
demonstrates the large degree to which sulfur can greatly accelerate both the ionic and
radical exchange processes.

The procedure of laboratory hydrous pyrolysis is one method used to study the
transformations of sedimentary organic matter and source rocks to petroleum. These
experiments are performed over short durations but at elevated temperatures to
compensate for the lower temperature organic reactions which occur over geological
time scales. The presence of water is generally regarded as an important component
of pyrolysis simulations by generating aliphatic-rich pyrolysates which are very low or
absent in olefins, as opposed to the olefin rich pyrolysates formed by dry pyrolyses
(Lewan et al., 1979). Ever since Lewan and co-workers (1979) used water in their
experiments and named the procedure hydrous pyrolysis, the actual role of water has
been a point of controversy, especially when oil-like pyrolysates have been formed
under anhydrous conditions (Comet et al., 1986). But it has been shown that in
general under aqueous conditions, these pyrolysates resemble natural oils (Eglinton et
al., 1986; Eglinton and Douglas, 1988; Lewan, 1983; Lewan et al., 1986). Water also
has the important ability of facilitating the ionic mineral reactions which are primarily
responsible for fixing the Eh and pH of a system (Eugster, 1986; Shock, 1990).
Although Lewan and co-workers (1979) have shown that water does not increase the
amount of hydrogen to the organic material, hydrogen exchange between water and
hydrocarbons can occur.

The original D$_2$O pyrolysis experiments performed by Hoering (1984)
identified the extent to which deuterium from the D$_2$O is exchanged with organic
matter and incorporated into the aliphatic hydrocarbons generated under hydrous
pyrolysis conditions for 72 hr at 330°C. By using D$_2$O as a medium instead of H$_2$O,
insight into what role water plays in this simulated maturation process was obtained.
But the free radical mechanism proposed does not explain the degree to which the
deuterium is incorporated (Ross, 1992a,b). The experiments performed by Hoering
were duplicated in this study and additional experiments were performed with H$_2$O
and D$_2$O.

In the present series of experiments the major types of chemical reactions and their relative rates leading to the pyrolysate distributions of aliphatic material have been identified. During hydrous pyrolysis the primary products generated by the thermally-induced bond cleavages of the aliphatic components are n-alkanes and terminal n-alkenes, the same products generated during the Curie-point pyrolyses of hydrocarbons and aliphatic-rich materials (Tegelaar et al., 1989a,b,c). The terminal n-alkenes can undergo secondary isomerization and hydrogenation reactions. The relative rates of the primary and the two competing secondary reactions depend on the experimental conditions. Thermal destruction of the aliphatic kerogen network should also produce double bonds in the kerogen which can undergo isomerization reactions by which deuterium is directly incorporated into the kerogen network.

Fig. 3.40 shows the proposed chemical pathways by which n-$C_{32}H_{66}$ reacts in the presence of H_2O and H_2O - NaOH. Fig. 3.41 presents the analogous reactions when performed in D_2O, showing the pathway in which deuterium is incorporated into the aliphatic hydrocarbon by acid-catalyzed double bond isomerization. When two double bonds are present, as in the molecular probe experiments in D_2O involving 1,13-tetradecadiene, acid-catalyzed double bond isomerization occurs simultaneously to greatly accelerate the amount of deuterium incorporated into the hydrocarbon (Fig. 3.42).

When these molecular probes were pyrolyzed on a sediment from the Guaymas Basin, a deuterium distribution pattern resulted which did not resemble those for samples pyrolyzed in water only. This distribution is interpreted to have resulted from the catalyzed isomerization by the clay minerals present in the sediments. Those alkenes which were isomerized were extensively isomerized and incorporated a large amount of deuterium (Fig. 3.43). There was still a large amount of alkene that was not isomerized.

A proposed pathway for the generation of n-alkanes and terminal n-alkenes during the hydrous pyrolysis of LDPE is shown in Fig. 3.44. This pathway was proposed since primarily n-alkanes and terminal n-alkenes are generated, and no appreciable amounts of α,ω-alkadienes were observed. The weakest bonds of an aliphatic cross-linked polymer such as LDPE are at the branch points, where there is a tertiary carbon. Thermal homolytic bond dissociation at one of these branch points is shown in Fig. 3.44. A hydrogen abstraction by the released primary radical results in the formation of an n-alkane with a secondary radical somewhere in the polymer network. The secondary radicals in the polymeric network, formed by the bond

scissions or H-abstractions, would then undergo β-scission, breaking the aliphatic cross-link to form an alkane chain and a terminal alkene chain still bonded to the polymer. With the weakest links still being the tertiary carbons, bond breaking at the branch points would still be favored and the process would continue, resulting in n-alkanes and terminal n-alkenes. The gas chromatograms of the LDPE pyrolysis in Fig. 3.21 show the production of other pyrolysis products, presumably branched hydrocarbons, but these were minor products and most likely the result of other competing radical cracking or isomerization reactions. Compared to Curie-point pyrolysis, the pyrolysis temperatures used in this study are comparatively milder and therefore bond cleavages can be more selective, preferentially breaking at branch points. Curie-point pyrolyses of LDPE (Wampler and Levy, 1987; Wampler, 1989) and aliphatic-rich kerogen (Goth et al., 1988) produce three homologous series, n-alkanes, terminal n-alkenes and α,ω-alkadienes, indicating a more random thermal destructive process breaking secondary and tertiary carbon-carbon bonds.

The proposed chemical pathway for the hydrous pyrolysis of LDPE can be used to explain the extent of deuterium incorporation observed in the D_2O Messel shale pyrolyses. The resulting pyrolysate compositions are interpreted to be due to radical cracking of the polymethylene chains from the kerogen. The carbon - carbon bond scission produces free n-alkanes and terminal n-alkenes, but also saturated and terminally unsaturated alkyl chains still bound to the kerogen. Acid-catalyzed double bond isomerization of the double bonds occurs at a rate faster than hydrogenation of the double bond (Fig. 3.24), and when the pyrolysis experiment is performed in D_2O, deuterium can be rapidly incorporated into the aliphatic hydrocarbons and polymethylene kerogen network. Once the alkyl chain is hydrogenated, it is relatively unreactive and deuterium incorporation occurs by radical exchange, a chemical pathway where the rate of exchange is much slower (Figs. 3.28 - 3.32).

The results suggest that the primary mode of deuterium incorporation into hydrocarbons occurs during acid-catalyzed double bond isomerization of alkene intermediates by 1,2-shifts of carbocations. Radicals would not be expected to undergo 1,2-shifts because in the rearranging radical, one electron must go into the antibonding orbital in the three-centered transition state, and therefore the transition state would be destabilized (Wilt, 1973). The formation of intermediate branched and isoprenoid alkenes, terminal n-alkenes, and even α,ω-alkadienes from kerogen is consistent with the findings from the structure elucidations of kerogens by chemical methods. Carboxylic acids, branched carboxylic acids, α,ω-dicarboxylic acids, and

isoprenoid acids are common products from kerogen oxidations (Burlingame et al., 1969; Djuricic et al., 1971; Simoneit and Burlingame, 1973; Vitorovic, 1980). Since branching points are susceptible to oxidation, monocarboxylic acids and isoprenoid acids would be formed from alkyl groups and isoprenoid groups, respectively, attached to the kerogen matrix at one point. α,ω–Dicarboxylic acids would be formed as a result of an alkyl "bridge" which is attached to the kerogen at two points. Curie-point pyrolysis confirms that this highly aliphatic polymer is present in Messel shale kerogen (Goth et al., 1988). The conditions during hydrous pyrolysis experiments may cause similar fragments, but release primarily n-alkanes and terminal n-alkene groups, analogous to the proposed pathway for the thermal destruction of LDPE under hydrous pyrolysis conditions. These double bonds, in the free pyrolysates and the bound aliphatic network, would then undergo acid-catalyzed double bond isomerization prior to hydrogenation of the double bond. Fig. 3.45 is a sequence of reactions which shows the proposed primary mode of deuterium incorporation into hydrocarbons during Messel shale pyrolysis with D_2O.

Water is seen as a medium in which the rate at which the inorganic ionic reactions occur is accelerated relative to dry pyrolysis. The system is driven more rapidly to equilibrium in the presence of water. Under these temperature and pressure conditions, water is also a good solvent for organic molecules. When hydrous pyrolysis is performed with reduced minerals (i.e. reduced sulfur species) the whole system can quickly become reducing, favoring the hydrogenation of unsaturated hydrocarbons. But this hydrogenation process is most likely a surface process, similar to the process of catalytic hydrogenation. So even under reducing conditions, as in the pyrolyses of Messel shale where iron sulfides are present, the hydrogenation of n-alkenes becomes a diffusion limited reaction, and the rate of acid-catalyzed double bond isomerization can be much faster than the rate of hydrogenation. The balance of competing radical and ionic reactions is important when trying to simulate geological processes under greatly accelerated laboratory conditions.

CONCLUSIONS

The pyrolysis of Messel shale in D_2O generates hydrocarbons with a large amount of deuterium. The exchange process is explained by double bond isomerization of alkenes formed by the pyrolytic breakdown of the aliphatic kerogen network. The major points are :

(1)   deuterium exchange between D_2O and saturated alkanes is negligible relative to the exchange which occurs by acid-catalyzed isomerization of a double bond under the same conditions,

(2)   the extent of deuterium substitution during the Messel shale D_2O pyrolysis experiment can be explained by acid-catalyzed double bond isomerization of intermediate alkene species,

(3)   the preferential deuterium enrichment at one end of a molecule would result from deuterium exchange at the site of one double bond,

(4)   the formation of alkene species has been observed during the hydrous pyrolysis of Messel shale,

(5)   the formation of intermediate alkene species is consistent with the results from the structural elucidations of kerogens by chemical oxidation, Curie-point pyrolysis experiments and hydrous pyrolysis of hydrocarbons and synthetic polymers under various conditions.

This mechanism explains the amount of deuterium incorporation into alkanes during Messel shale pyrolyses with D_2O and explains how deuterium can become enriched at one end of a molecule. By studying simple systems, relevant chemical pathways can be proposed and applied to the understanding of more complex systems.

Table 3.1. Hydrous pyrolysis experiments performed at 330°C.

Duration (hr)	Reactants
72	D_2O, $\underline{n}$-$C_{32}H_{66}$
72	D_2O, $\underline{n}$-$C_{32}H_{66}$, NaOD
72	H_2O, LDPE
72	D_2O, 1,13-tetradecadiene
72	H_2O, C_{14} polymer
72	Messel Shale, D_2O
1	D_2O, 1,13-tetradecadiene, 1-hexadecene, eicosane
5	D_2O, 1,13-tetradecadiene, 1-hexadecene, eicosane
10	D_2O, 1,13-tetradecadiene, 1-hexadecene, eicosane
36	D_2O, 1,13-tetradecadiene, 1-hexadecene, eicosane
72	D_2O, 1,13-tetradecadiene, 1-hexadecene, eicosane
1	Messel Shale, H_2O, 1,13-tetradecadiene, 1-hexadecene, eicosane
5	Messel Shale, H_2O, 1,13-tetradecadiene, 1-hexadecene, eicosane
10	Messel Shale, H_2O, 1,13-tetradecadiene, 1-hexadecene, eicosane
36	Messel Shale, H_2O, 1,13-tetradecadiene, 1-hexadecene, eicosane
72	Messel Shale, H_2O, 1,13-tetradecadiene, 1-hexadecene, eicosane
1	Messel Shale, D_2O, 1,13-tetradecadiene, 1-hexadecene, eicosane
5	Messel Shale, D_2O, 1,13-tetradecadiene, 1-hexadecene, eicosane
10	Messel Shale, D_2O, 1,13-tetradecadiene, 1-hexadecene, eicosane
36	Messel Shale, D_2O, 1,13-tetradecadiene, 1-hexadecene, eicosane
72	Messel Shale, D_2O, 1,13-tetradecadiene, 1-hexadecene, eicosane
10	Guaymas Basin Sediment , D_2O, 1,13-tetradecadiene, 1-hexadecene, eicosane
10	Sulfur, D_2O, 1,13-tetradecadiene, 1-hexadecene, eicosane

Table 3.2. Extent of deuterium substitution in normal hydrocarbons produced from the pyrolysis of Messel shale at 330°C for 72 hr with D_2O.

Deuterium Abundance	Carbon Number												
	17	18	19	20	21	22	23	24	25	26	27	28	29
D0	10	21	4	7	6	5	4	6	3	5	5	7	8
D1	30	41	28	25	27	27	55	17	10	14	18	26	11
D2	54	53	49	65	45	46	26	27	83	31	47	37	25
D3	84	68	76	82	68	75	100	83	48	99	67	46	34
D4	87	96	82	96	82	85	66	78	83	93	79	52	52
D5	100	99	100	100	86	100	66	89	94	93	84	78	62
D6	92	100	89	87	100	99	68	100	98	96	100	100	54
D7	89	97	92	87	91	85	59	92	94	81	79	91	100
D8	86	95	53	88	70	95	54	85	100	90	89	88	79
D9	79	73	74	74	80	81	50	76	83	100	53	81	62
D10	72	68	76	70	62	69	39	71	73	78	81	66	66
D11	59	64	62	49	55	58	32	63	54	60	50	75	52
D12	42	56	33	39	44	42	36	53	65	49	48	43	32
D13	37	54	71	47	39	45	22	49	52	49	44	60	43
D14	16	31	38	34	25	25	15	24	40	36	27	22	37
D15	11	27	31	27	22	25	9	14	25	19	23	19	18
D16	8	12	20	19	10	14	4	10	10	31	19	15	12
D17	7	15	11	10	12	12	0	10	15	19	10	15	10
D18	8	6	9	4	7	10	0	10	8	4	8	9	12
D19	2	8	7	2	3	5	0	10	6	12	8	6	3
D20	0	0	4	0	0	3	0	0	4	9	3	9	6
D21	0	0	0	0	0	0	0	0	0	0	0	3	0
D22	0	0	0	0	0	0	0	0	0	0	0	0	0

Table 3.3. Data from the pyrolysis of 1,13-tetradecadiene and 1-hexadecene molecular probes with Messel in H_2O at 330°C.

Time (hr)	1,13-tetradecadiene		1-hexadecene	
	% Isomerized	% Hydrogenated	% Isomerized	% Hydrogenated
1	12.6	0	5.7	0
5	89.9	11.6	70	22.2
10	96.2	13.6	84.8	33
36	97.2	50.5	91.9	65.8
72	100	94	100	96

Table 3.4. Data from the pyrolysis of 1,13-tetradecadiene and 1-hexadecene molecular probes with Messel in D_2O at 330°C.

	1,13-tetradecadiene		1-hexadecene	
Time (hr)	% Isomerized	% Hydrogenated	% Isomerized	% Hydrogenated
1	9.9	0	5.5	0
5	74.4	0	45.1	13.6
10	85.3	33.1	58.7	25.6
36	n.d. [a]	67	n.d. [a]	71
72	n.d. [a]	88.3	n.d. [a]	87.9

[a]   Not determined due to poor chromatographic peak shape as a result of deuterium substitution.
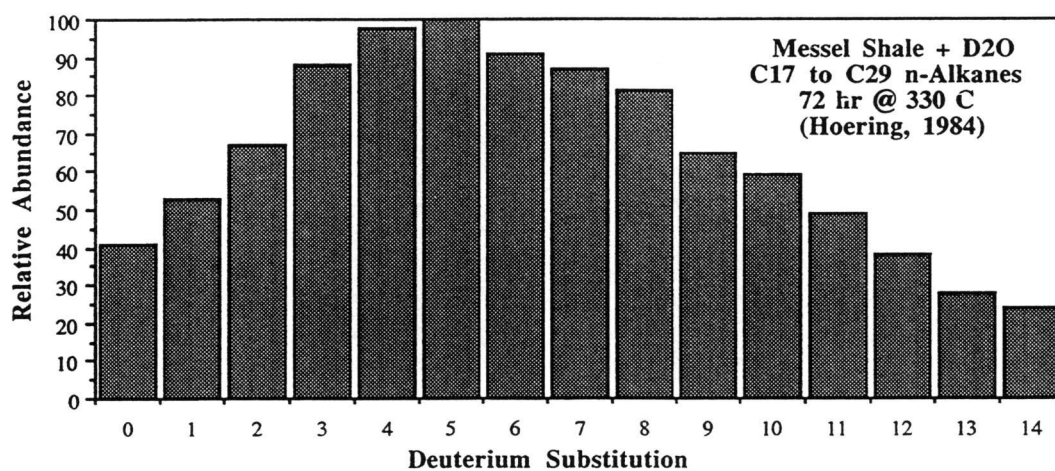
Figure 3.1. Overall average distribution of deuterium substitution in n-alkanes from C_{17} to C_{29} generated from the D_2O pyrolysis of Messel shale (after Hoering, 1984).
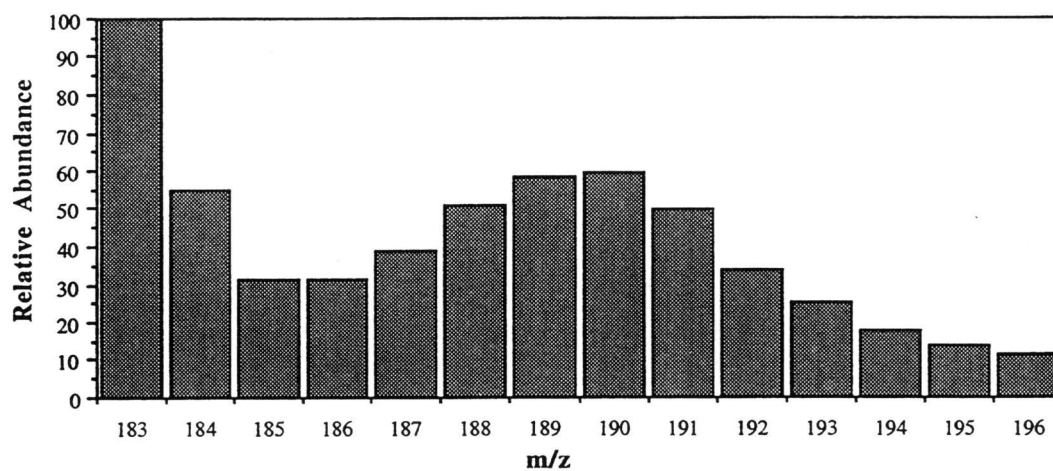
Figure 3.2. Distribution of the relative abundances of C_{13} ion fragments from pristane generated in the Messel shale D_2O pyrolysis (after Hoering, 1984).
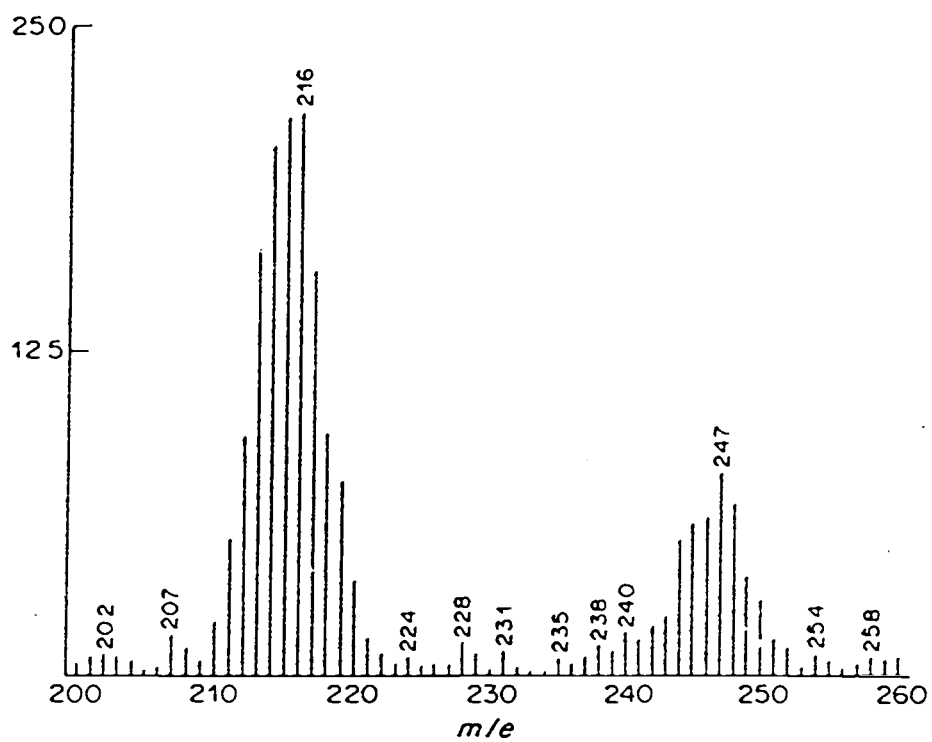
Figure 3.3. The partial mass spectrum of deuterated 2-methylheptadecane which was generated in the Messel shale D_2O pyrolysis (Hoering, 1984).
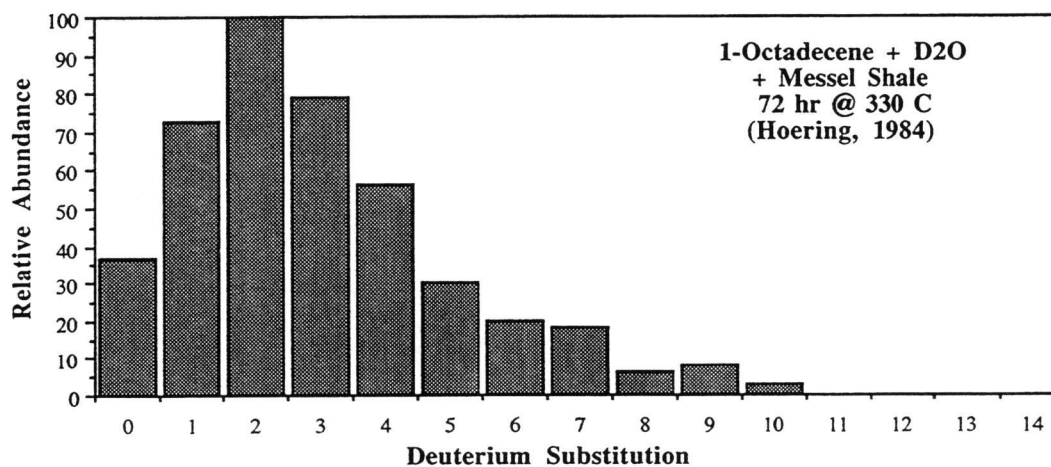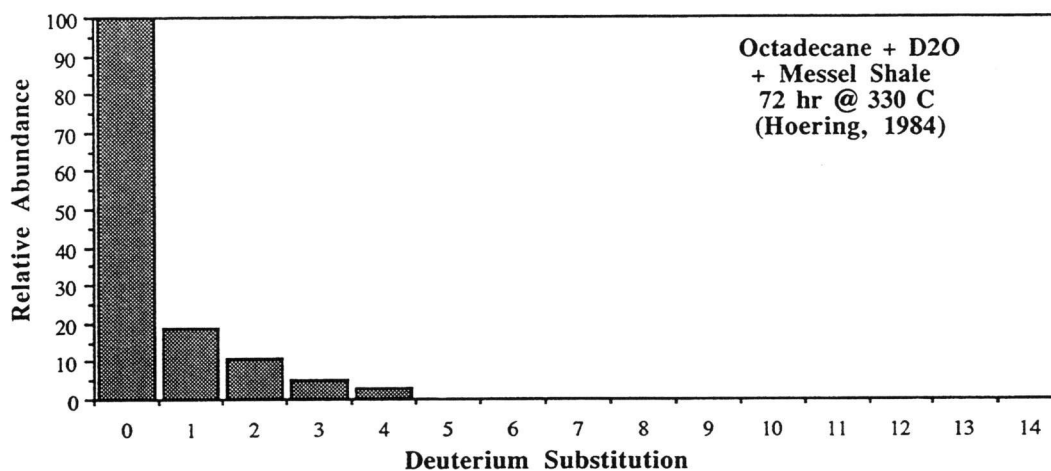
Figure 3.4. Distribution of deuterium substitution in the products of the molecular probe experiments, 330°C for 72 h : (a) pyrolysis of docosane and D₂O and (b) pyrolysis of 1-octadecene and D₂O (after Hoering, 1984).
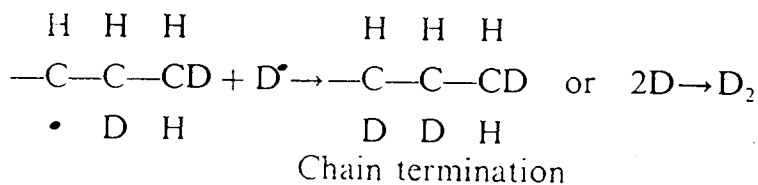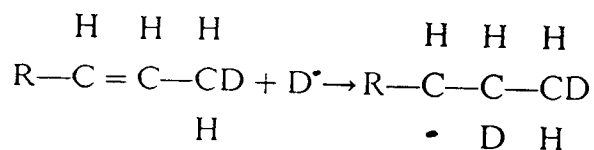
$$H\bullet + D_2O \rightleftharpoons D\bullet + HDO.$$

Primary radical

Olefin formation and chain propagation

$$\begin{array}{ccc} H & H & H \\ R\!-\!C\!-\!C\!-\!C^\bullet \\ H & H & H \end{array} \longrightarrow \begin{array}{ccc} H & H & H \\ R\!-\!C\!-\!C=CH+H^\bullet \\ H \end{array}$$

$$\begin{array}{ccc} H & H & H \\ R\!-\!C\!-\!C=CH + D^\bullet \rightarrow R\!-\!C\!-\!C\!-\!CD + H^\bullet \\ H & & H \;\bullet\; H \end{array}$$

$$\begin{array}{ccc} H & H & H \\ R\!-\!C\!-\!C\!-\!CD \rightarrow R\!-\!C=C\!-\!CD + H^\bullet \\ H \;\bullet\; H & & H \end{array}$$

$$\begin{array}{ccc} H & H & H \\ R\!-\!C=C\!-\!CD + D^\bullet \rightarrow R\!-\!C\!-\!C\!-\!CD \\ H & & \bullet\; D \;\; H \end{array}$$

$$\begin{array}{ccc} H & H & H \\ -\!C\!-\!C\!-\!CD + D^\bullet \rightarrow -\!C\!-\!C\!-\!CD \quad or \quad 2D\rightarrow D_2 \\ \bullet\; D \;\; H & & D \;\; D \;\; H \end{array}$$
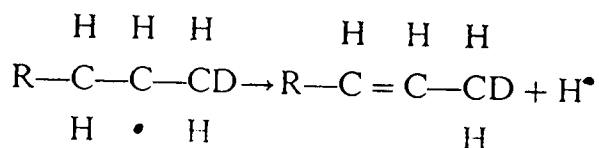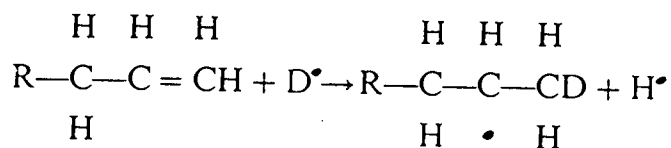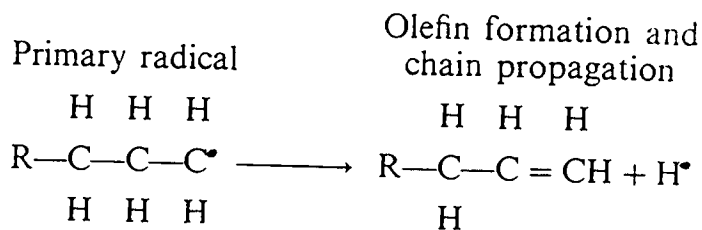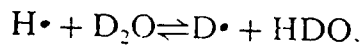
Chain termination

Figure 3.5. Set of reactions proposed by Hoering (1984) to explain the deuterium exchange process, includes only free radical chemistry.
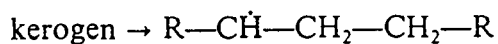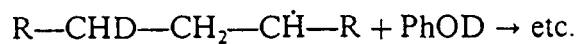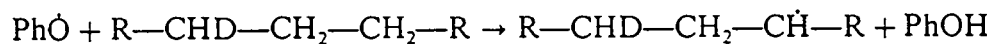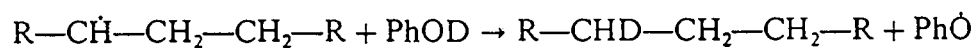
Initiation

$$\text{kerogen} \rightarrow \text{R—C}\overset{\cdot}{\text{H}}\text{—CH}_2\text{—CH}_2\text{—R}$$

Propagation

$$\text{D}_2\text{O} + \text{PhOH} \rightarrow \text{HOD} + \text{PhOD}$$

$$\text{R—C}\overset{\cdot}{\text{H}}\text{—CH}_2\text{—CH}_2\text{—R} + \text{PhOD} \rightarrow \text{R—CHD—CH}_2\text{—CH}_2\text{—R} + \text{Ph}\overset{\cdot}{\text{O}}$$

$$\text{Ph}\overset{\cdot}{\text{O}} + \text{R—CHD—CH}_2\text{—CH}_2\text{—R} \rightarrow \text{R—CHD—CH}_2\text{—C}\overset{\cdot}{\text{H}}\text{—R} + \text{PhOH}$$

$$\text{R—CHD—CH}_2\text{—C}\overset{\cdot}{\text{H}}\text{—R} + \text{PhOD} \rightarrow \text{etc.}$$
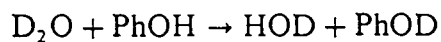
Figure 3.6. Set of reactions proposed by Ross (1992a) to explain the deuterium exchange process, includes ionic and free radical chemistry.

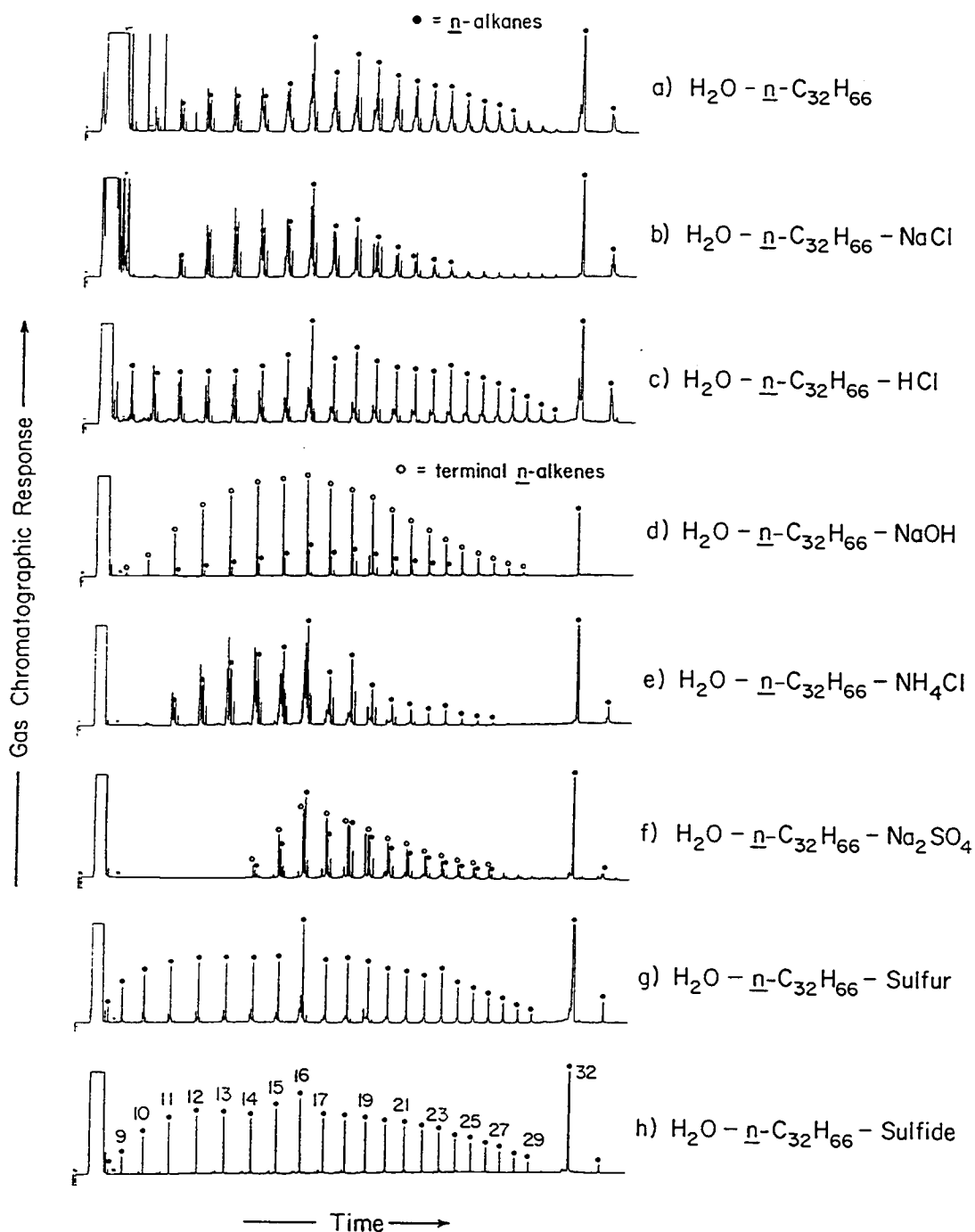Figure 3.7. Gas chromatograms of the total extracts from the hydrous pyrolysis experiments of n-C32H66 at 350°C : (a) H2O - n-C32H66;(b) H2O - n-C32H66 - NaCl; (c) H2O - n-C32H66 - HCl;(d)H2O - n-C32H66 - NaOH;(e)H2O - n-C32H66 - NH4Cl; (f) H2O - n-C32H66- Na2SO4; (g) H2O - n-C32H66- Sulfur;(h) H2O - n-C32H66- Sulfide. Numbers refer to carbon chain lengths of n-alkanes.

Figure 3.8. Gas chromatograms of the H_2O - $\underline{n}$-$C_{32}H_{66}$ system : (a) nonpolar fraction before catalytic hydrogenation; (b) nonpolar fraction after catalytic hydrogenation. Numbers refer to carbon chain lengths of $\underline{n}$-alkanes.
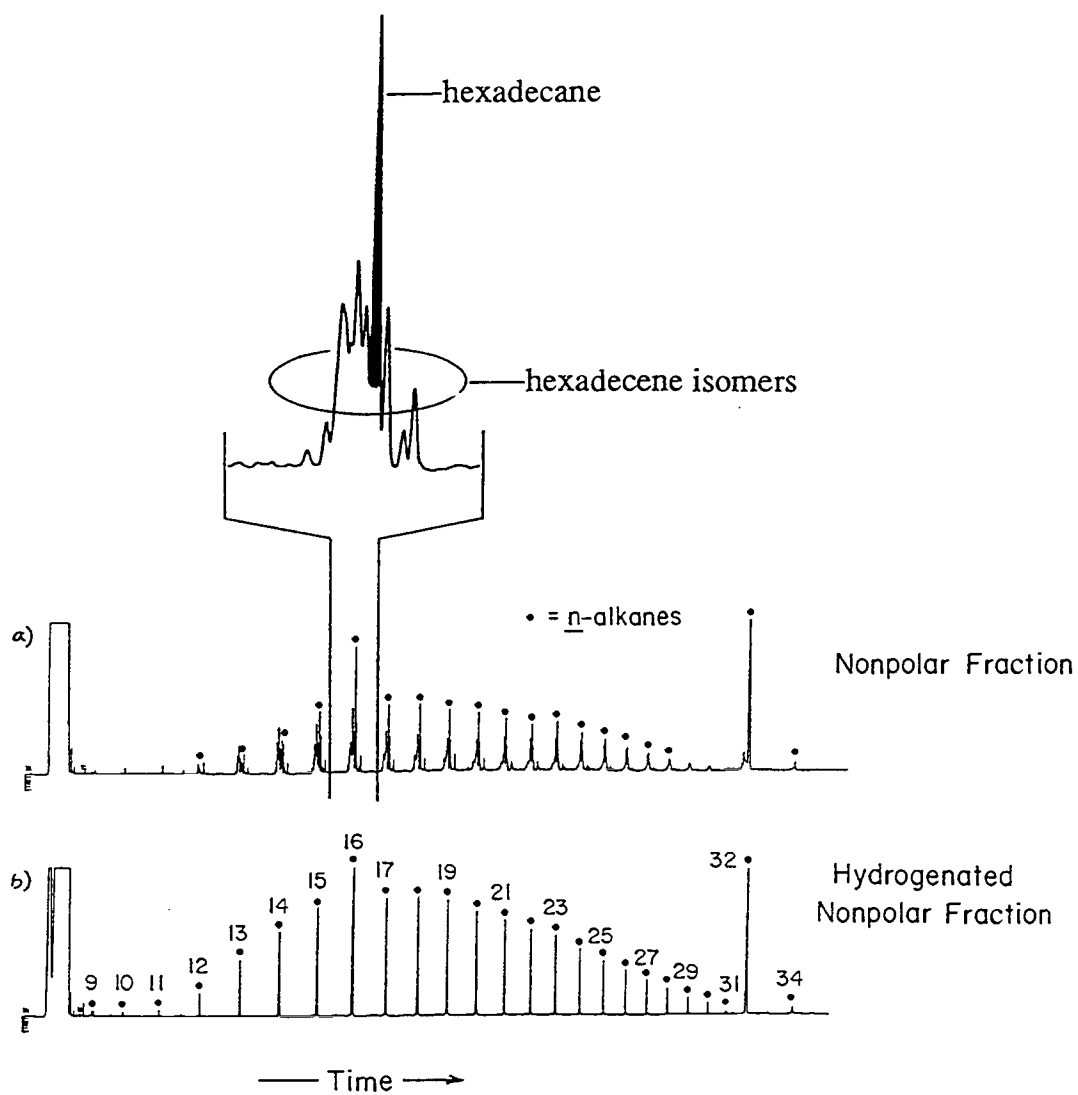
Figure 3.9. Gas chromatograms of the H_2O - n-$C_{32}H_{66}$ - NaOH system : (a) nonpolar fraction before catalytic hydrogenation; (b) nonpolar fraction after catalytic hydrogenation. Numbers refer to carbon chain lengths of n-alkanes.
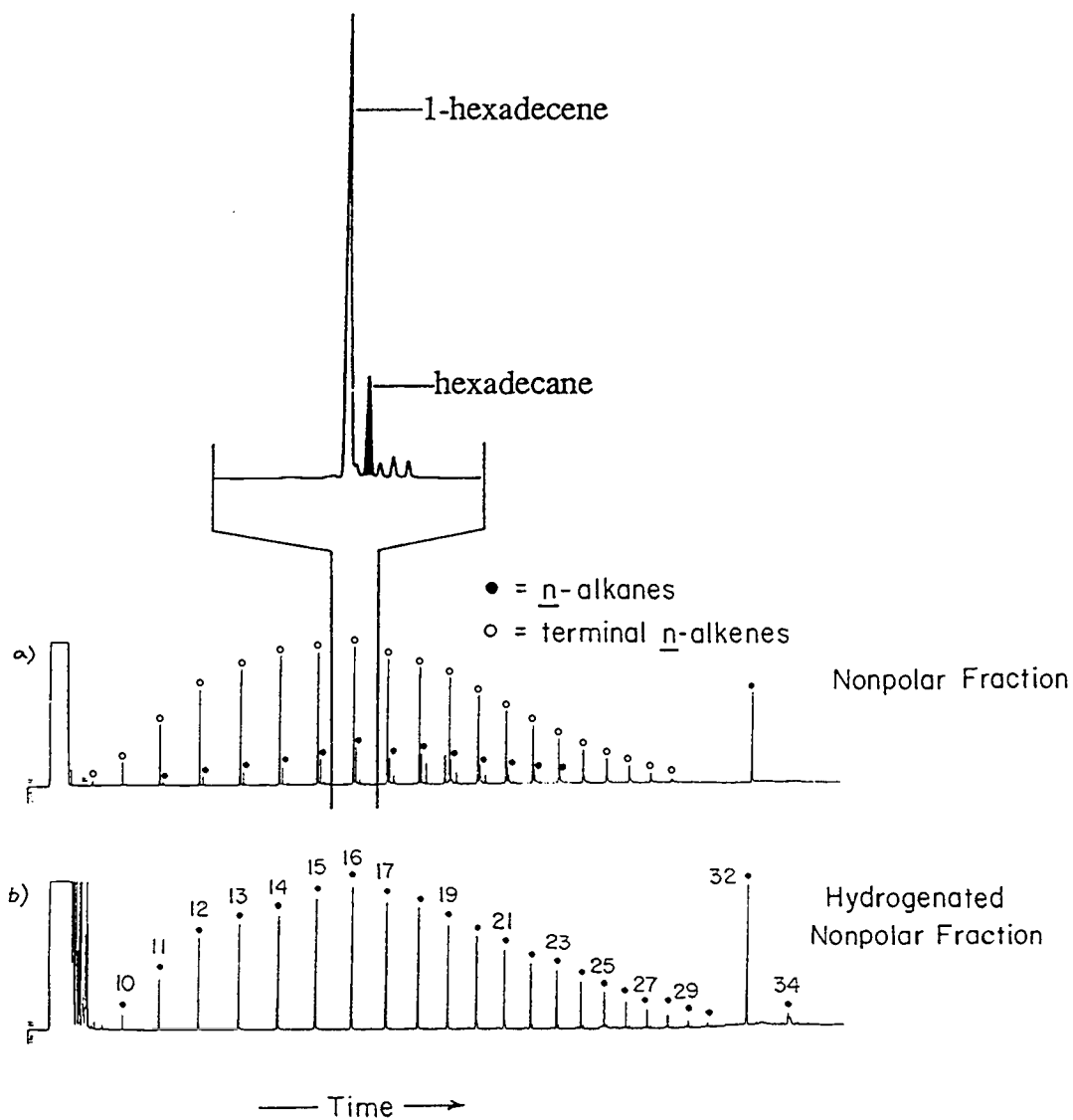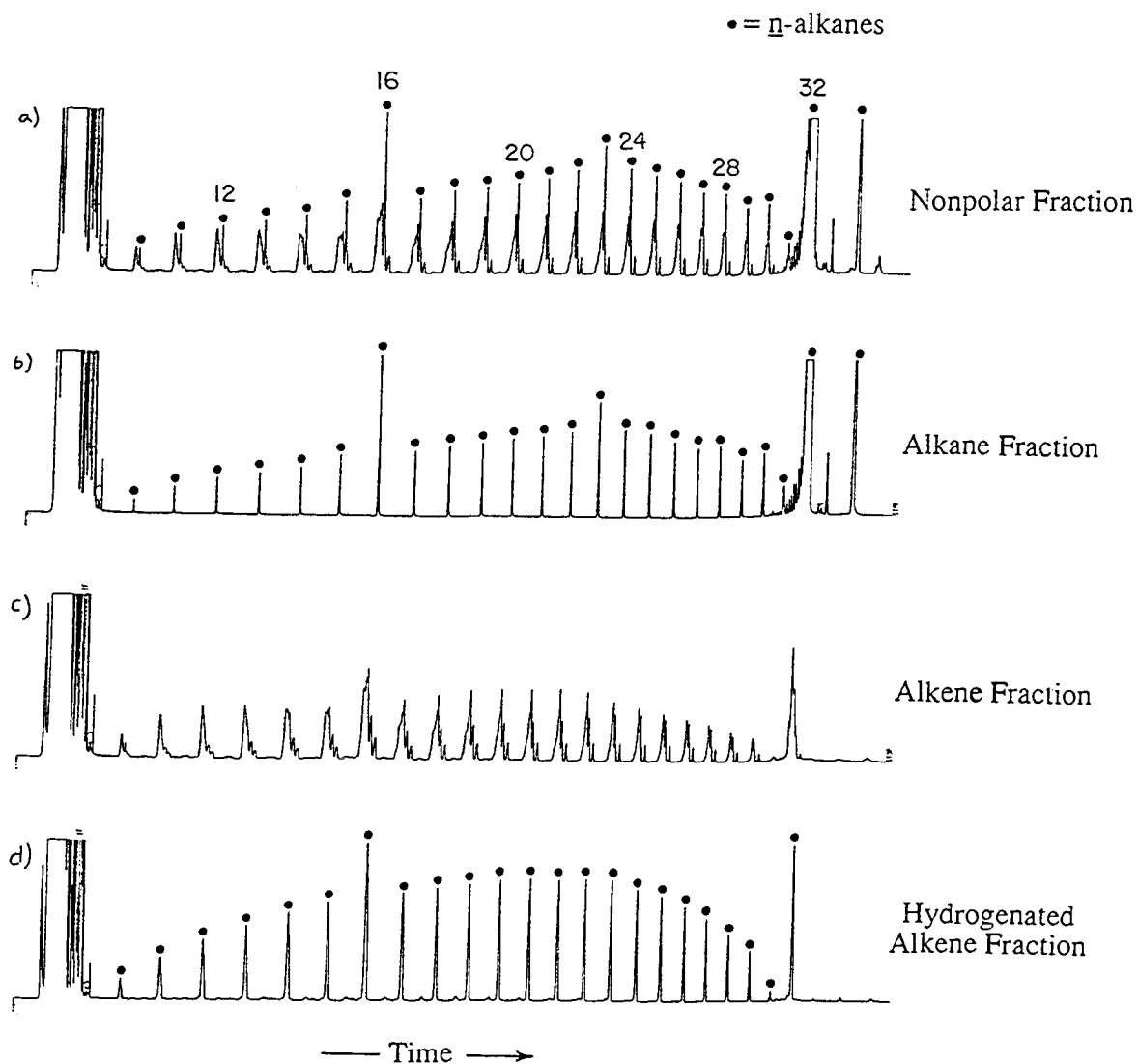
Figure 3.10. Gas chromatograms of the D_2O - n-$C_{32}H_{66}$ system :(a) nonpolar fraction; (b) alkane fraction; (c) alkene fraction; (d) alkene fraction after catalytic hydrogenation. Numbers refer to carbon chain lengths of n-alkanes.

Figure 3.11. Mass spectra of n-C₁₇H₃₆ from the D₂O - n-C₃₂H₆₆ system :(a) alkane fraction; (b) hydrogenated alkene fraction.

• = n-alkanes

o = terminal n-alkenes
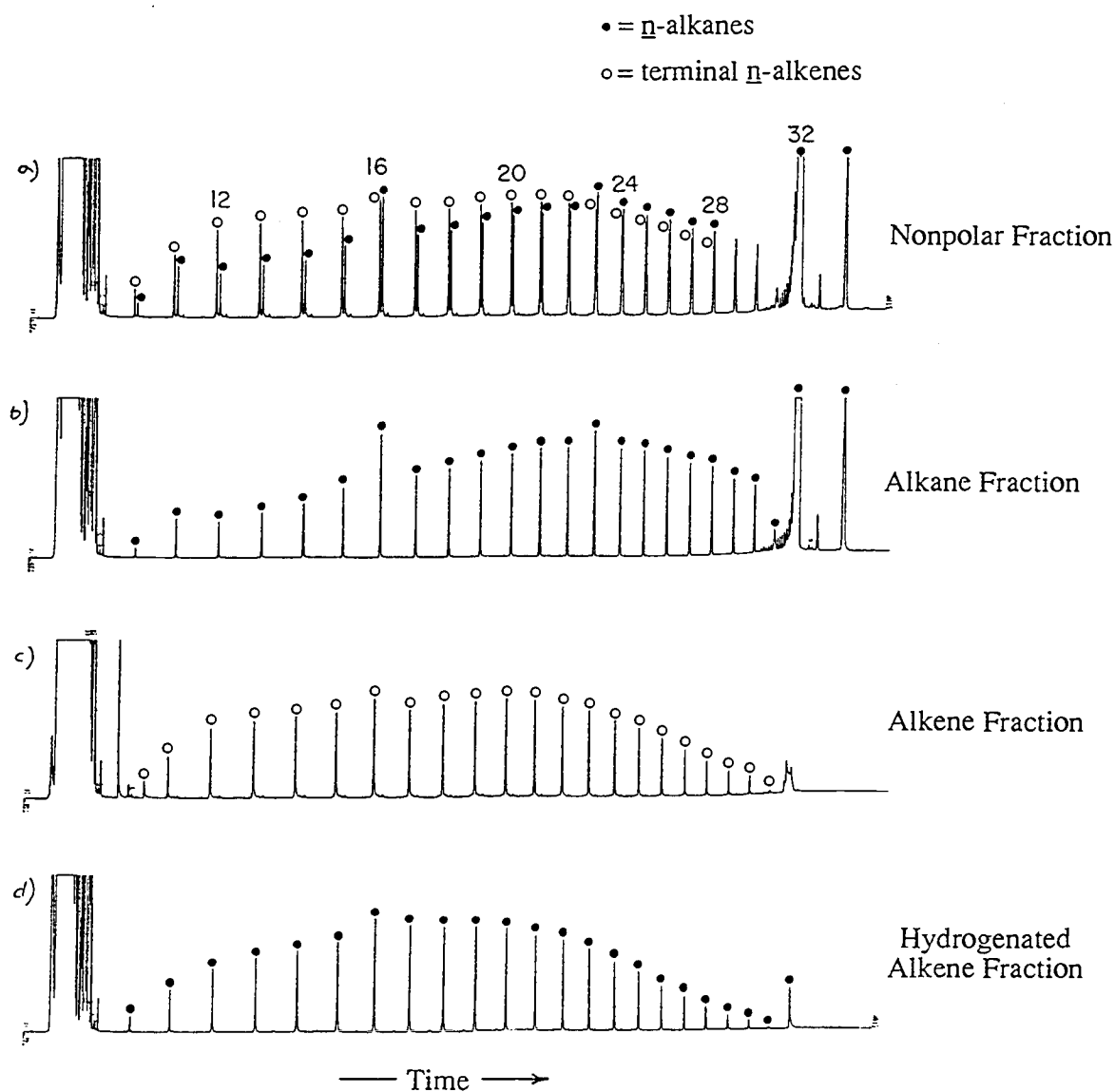
Figure 3.12. Gas chromatograms of the D_2O - n-$C_{32}H_{66}$ - NaOD system :(a) nonpolar fraction; (b) alkane fraction; (c) alkene fraction; (d) alkene fraction after catalytic hydrogenation. Numbers refer to chain lengths of n-alkanes.
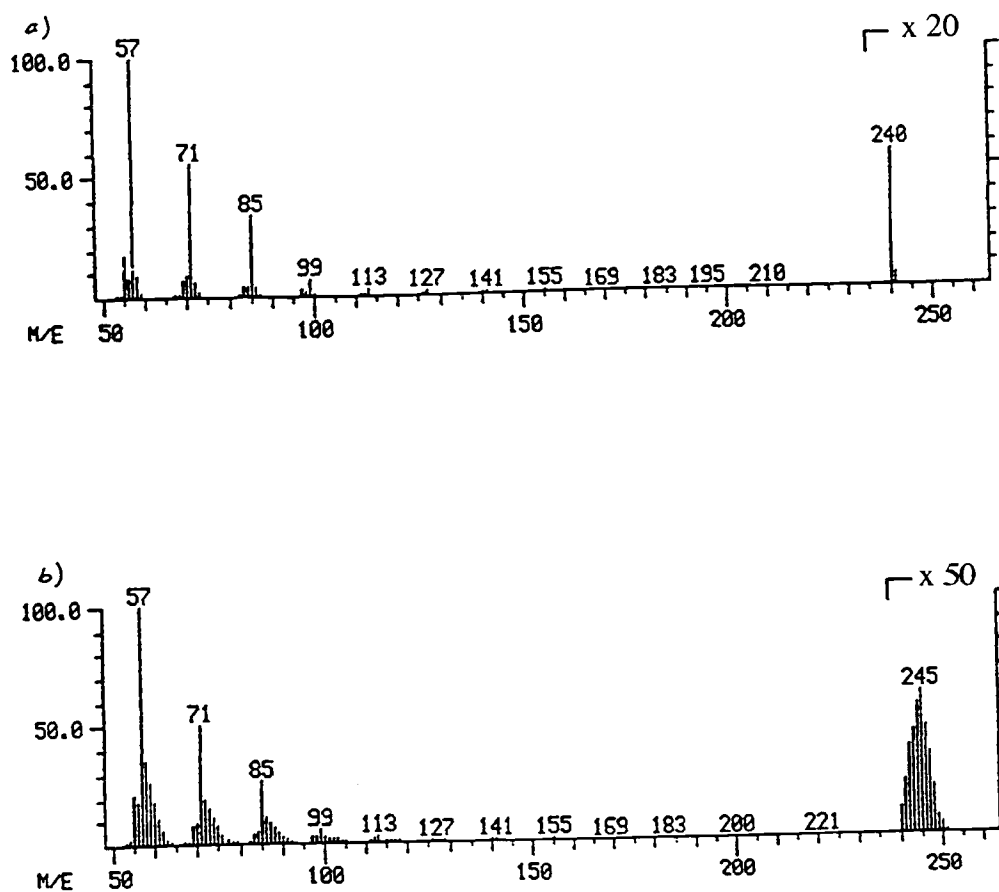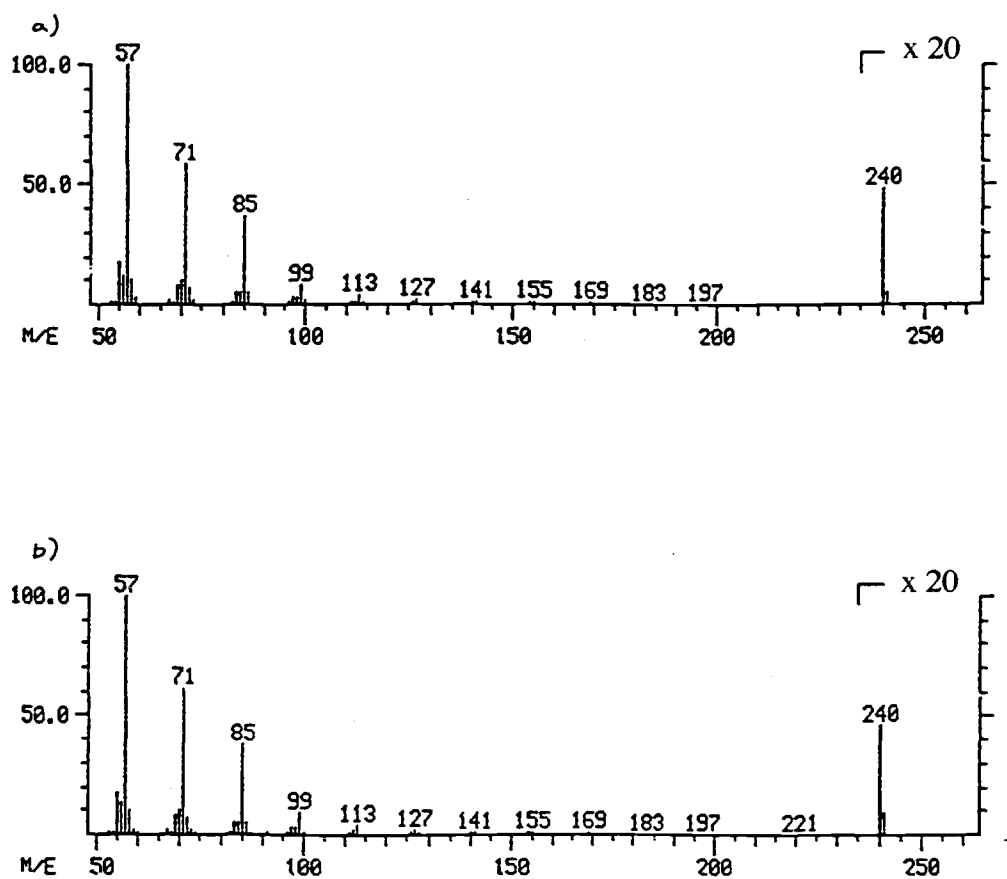
Figure 3.13. Mass spectra of $\underline{n}$-$C_{17}H_{36}$ from the D_2O - $\underline{n}$-$C_{32}H_{66}$ -NaOD system :(a) alkane fraction; (b) hydrogenated alkene fraction.
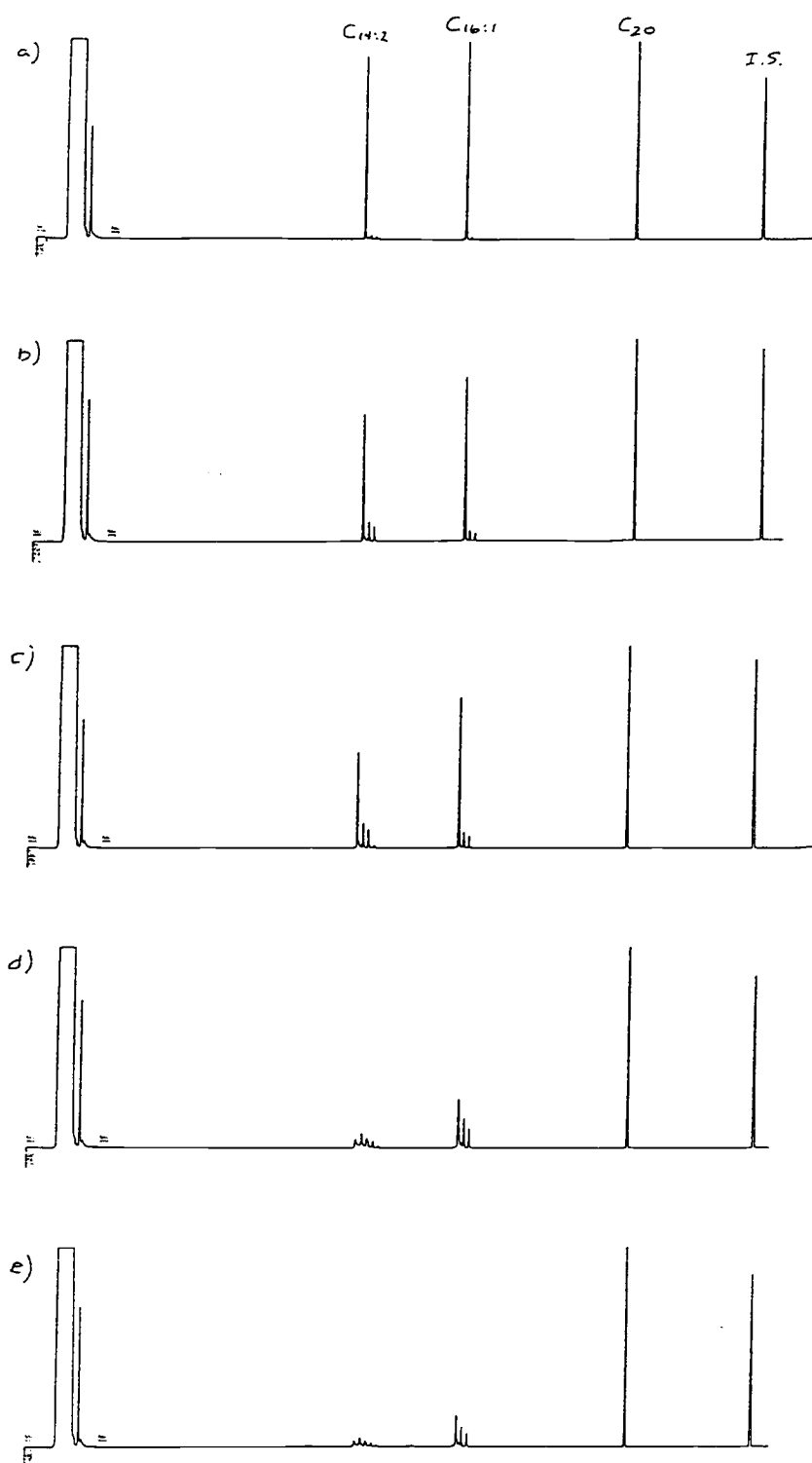
Figure 3.14. Gas chromatograms of the aliphatic fraction from the pyrolyses of 1,13-tetradecadiene, 1-hexadecene and eicosane with D_2O at 330°C: (a) 1 hr; (b) 5 hr; (c) 10 hr; (d) 36 hr; (e) 72 hr. I.S. = internal standard ($C_{24}D_{50}$).
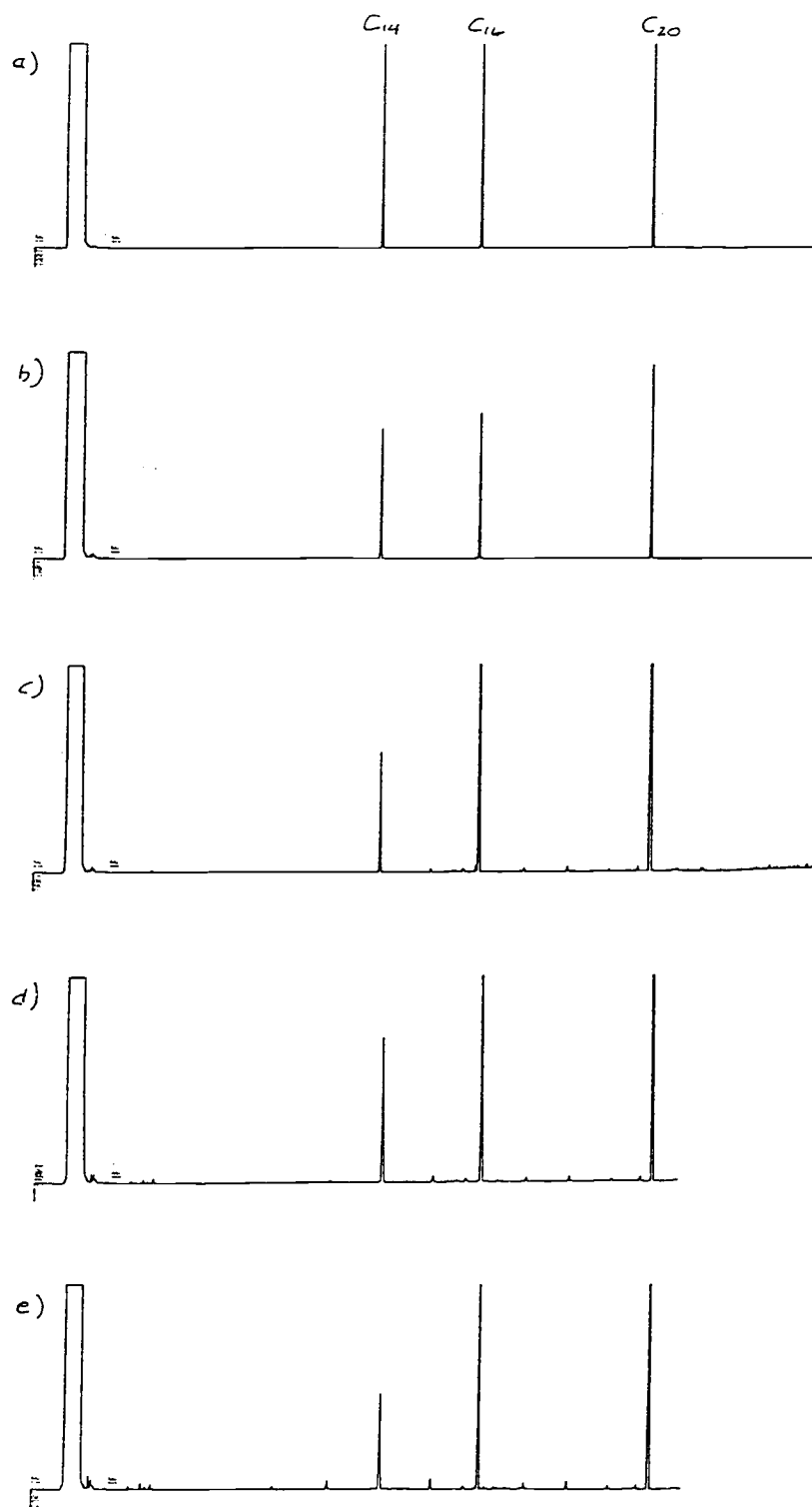
Figure 3.15. Gas chromatograms of the hydrogenated aliphatic fraction from the pyrolyses of 1,13-tetradecadiene, 1-hexadecene and eicosane with D_2O at 330°C: (a) 1 hr; (b) 5 hr; (c) 10 hr; (d) 36 hr; (e) 72 hr.

Figure 3.16. Histograms showing the extent of deuterium substitution after pyrolysis in D_2O for 1 hr at 330°C : (a) 1,13-tetradecadiene; (b) 1-hexadecane; (c) eicosane.
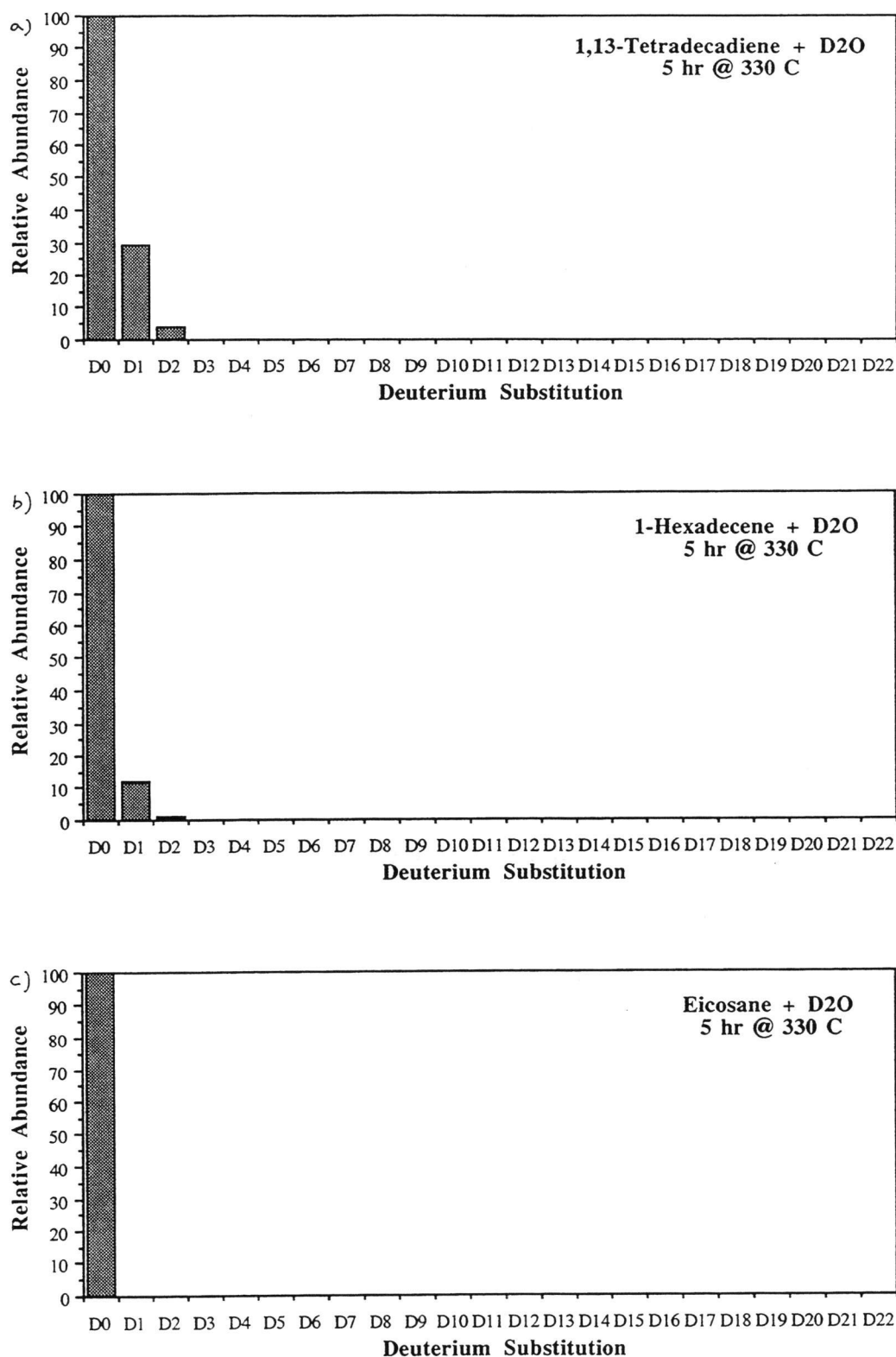
Figure 3.17. Histograms showing the extent of deuterium substitution after pyrolysis in D_2O for 5 hr at 330°C : (a) 1,13-tetradecadiene; (b) 1-hexadecane; (c) eicosane.
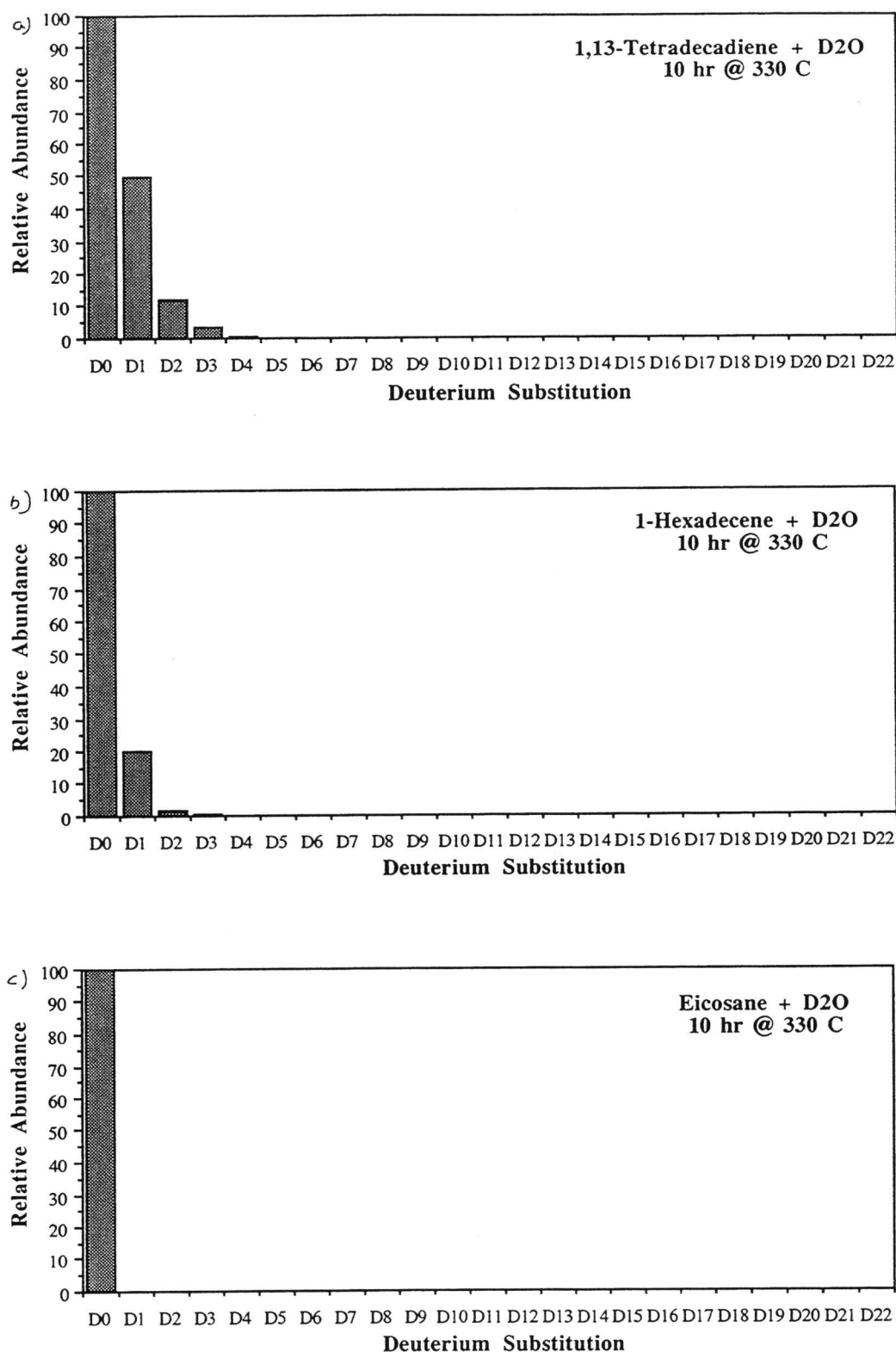
Figure 3.18. Histograms showing the extent of deuterium substitution after pyrolysis in D_2O for 10 hr at 330°C : (a) 1,13-tetradecadiene; (b) 1-hexadecane; (c) eicosane.
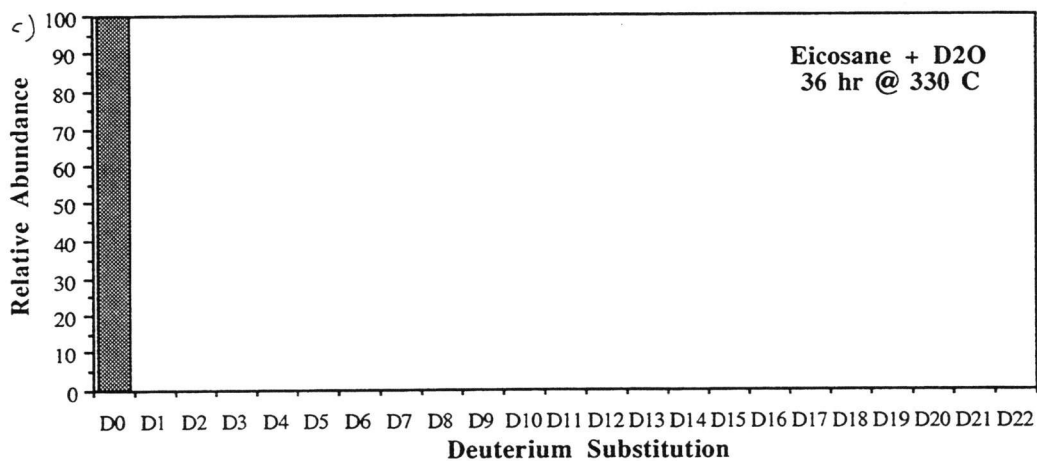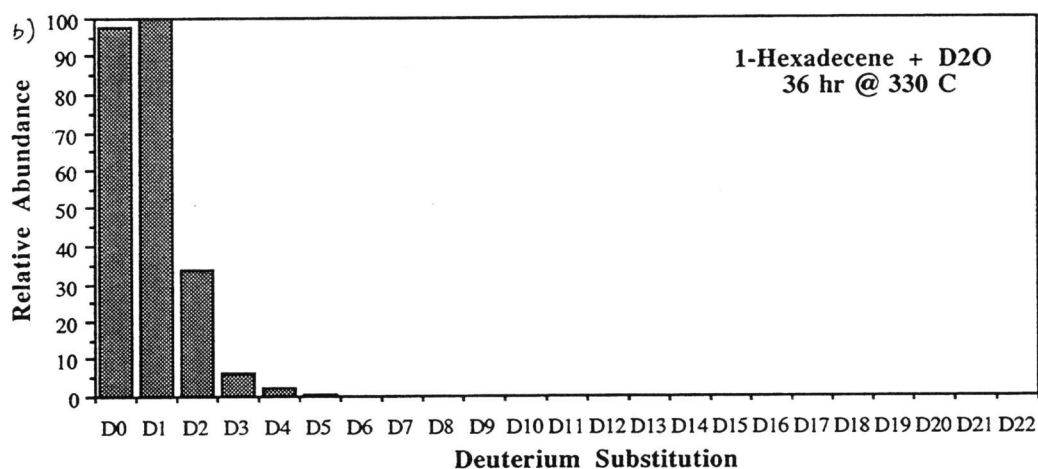
Figure 3.19. Histograms showing the extent of deuterium substitution after pyrolysis in D_2O for 36 hr at 330°C : (a) 1,13-tetradecadiene; (b) 1-hexadecane; (c) eicosane.

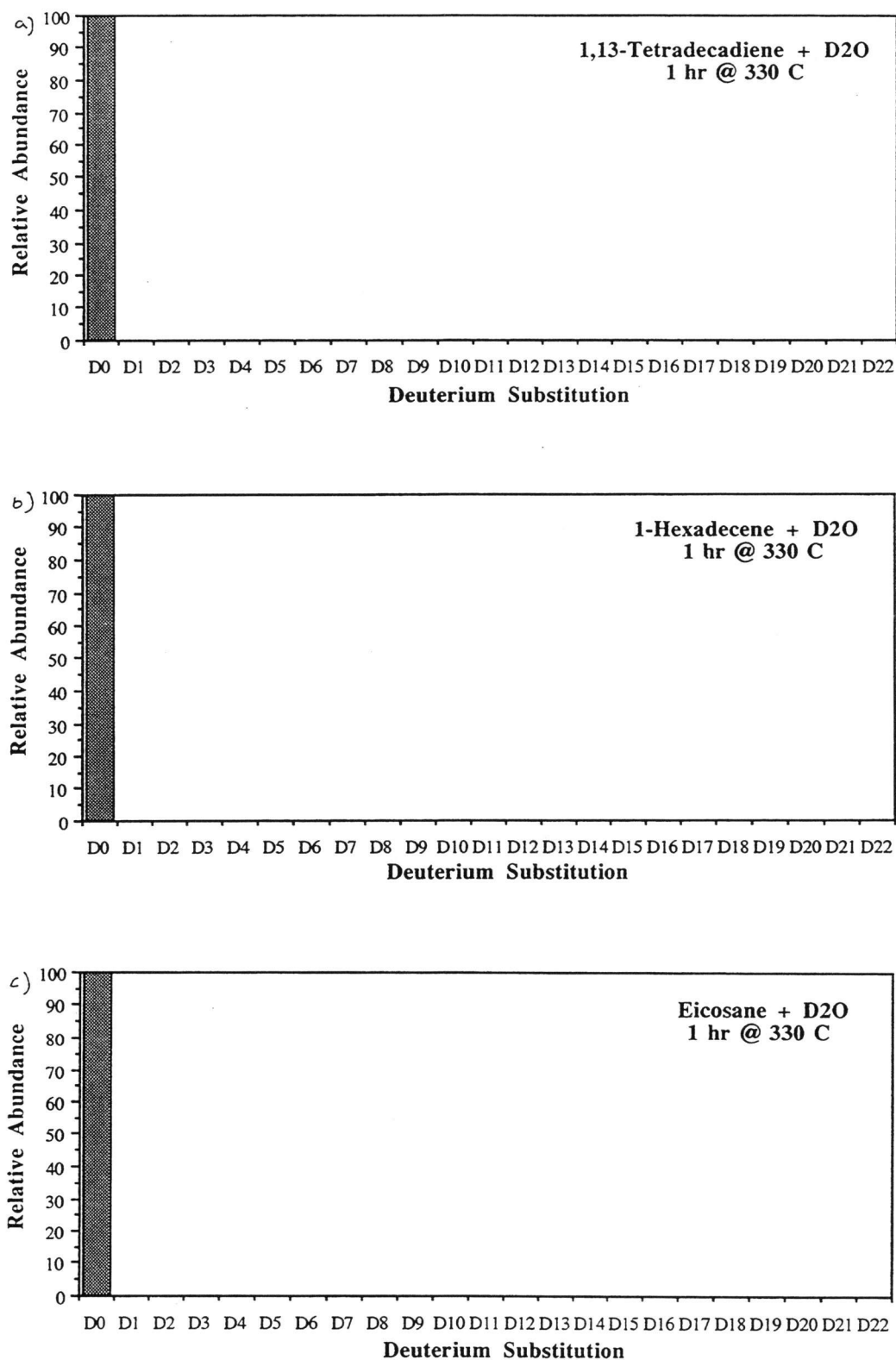Figure 3.20. Histograms showing the extent of deuterium substitution after pyrolysis in D_2O for 72 hr at 330°C : (a) 1,13-tetradecadiene; (b) 1-hexadecane; (c) eicosane.
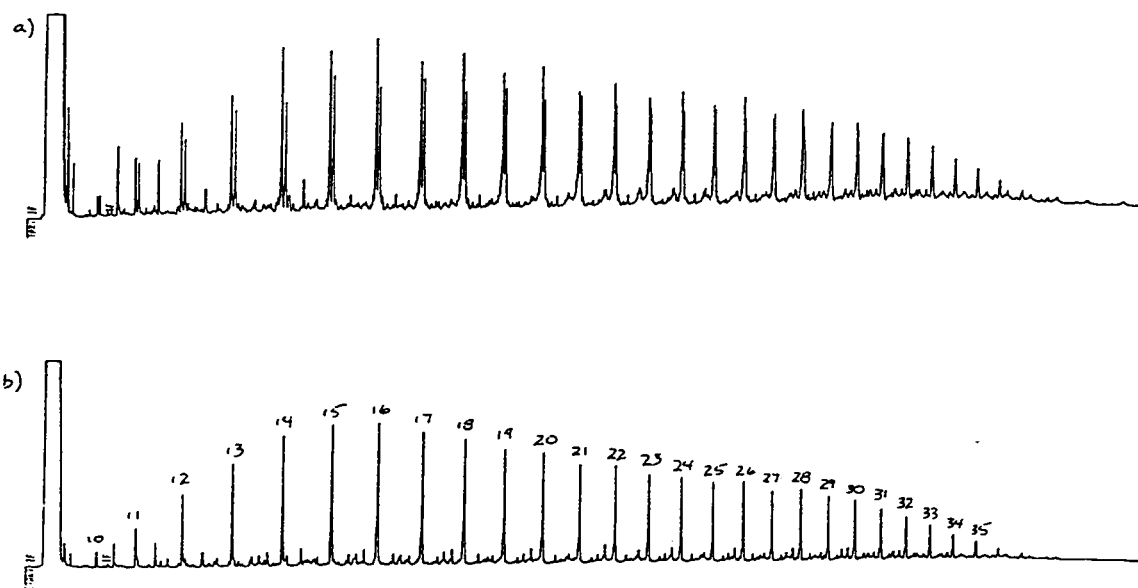
Figure 3.21. Gas chromatograms from the pyrolysis of LDPE in H_2O for 72 hr @ 330°C: (a) aliphatic fraction; (b) hydrogenated aliphatic fraction. Numbers refer to carbon chain lengths of n-alkanes.
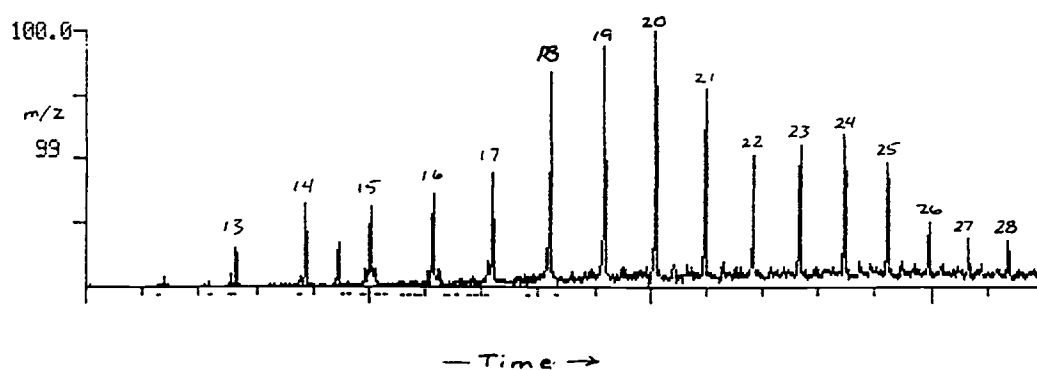
Figure 3.22. Mass fragmentogram m/z 99, representative of n-alkanes, for the pyrolysis of the C_{14} polymer. Numbers refer to carbon chain lengths of n-alkanes.
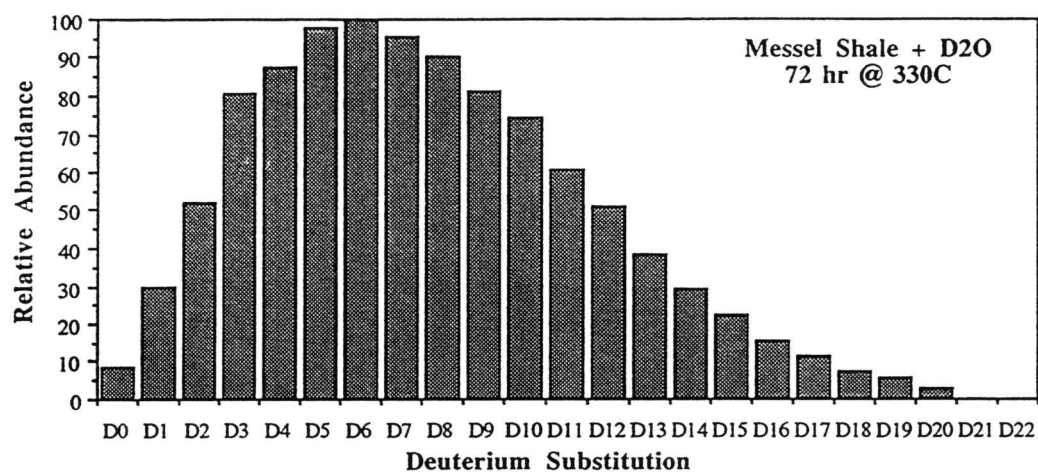
Figure 3.23. Overall average distribution of deuterium substitution in n-alkanes from C_{17} to C_{29} generated from the D_2O pyrolysis of Messel shale (this research).
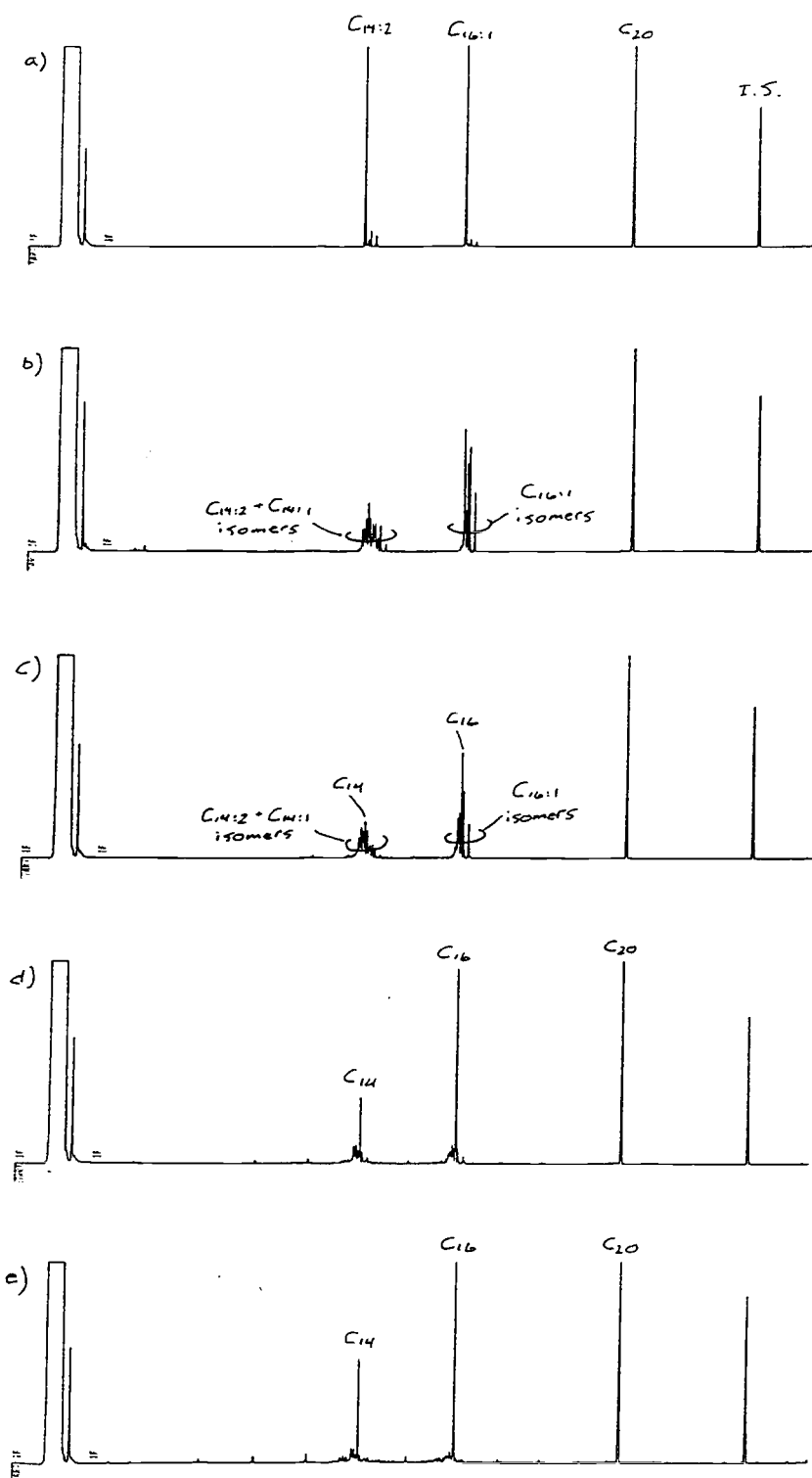
Figure 3.24. Gas chromatograms of the aliphatic fraction from the pyrolyses of 1,13-tetradecadiene, 1-hexadecene and eicosane spiked on Messel shale in H_2O at 330°C: (a) 1 hr; (b) 5 hr; (c) 10 hr; (d) 36 hr; (e) 72 hr. I.S. = internal standard ($C_{24}D_{50}$).
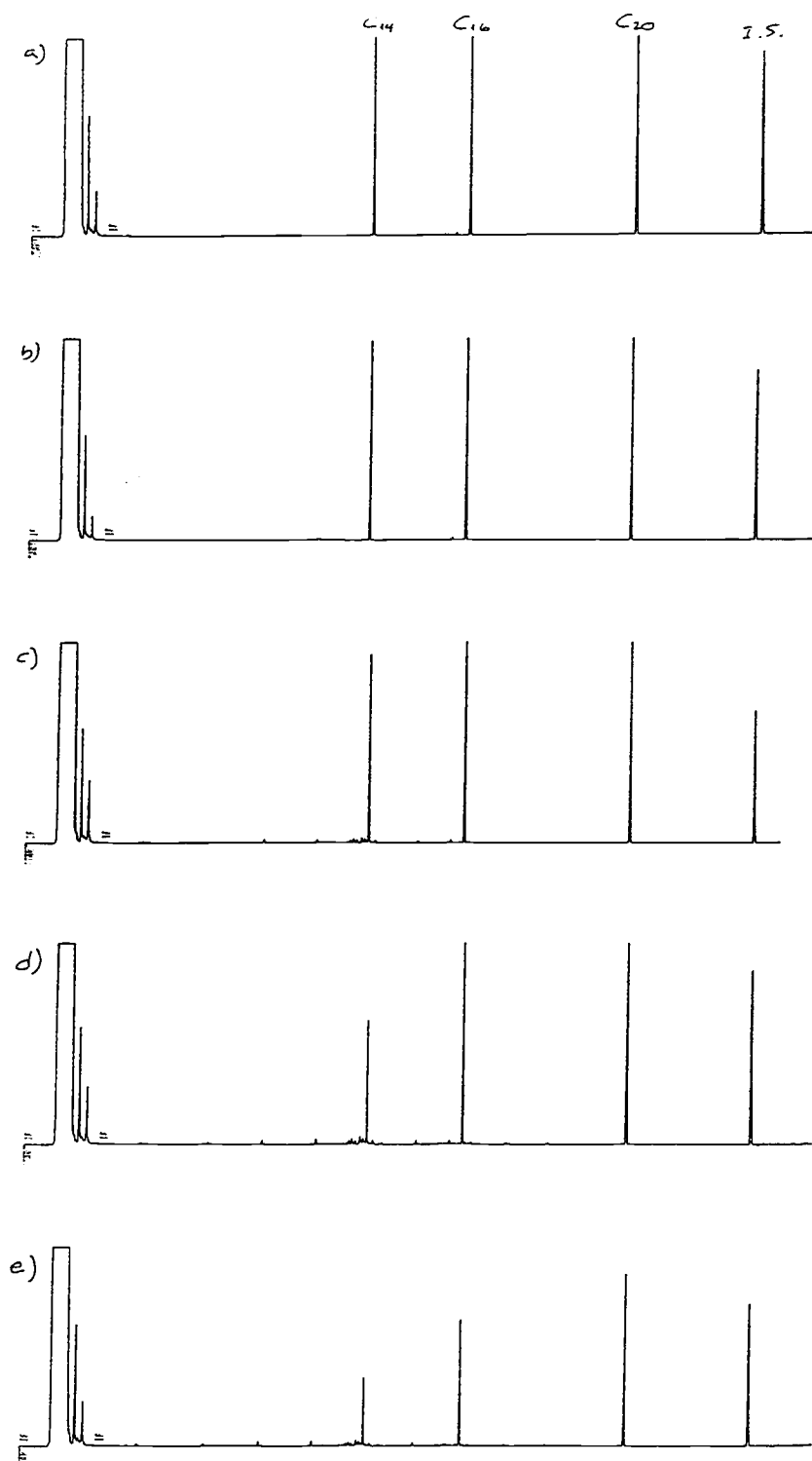
Figure 3.25. Gas chromatograms of the hydrogenated aliphatic fraction from the pyrolyses of 1,13-tetradecadiene, 1-hexadecene and eicosane spiked on Messel shale in H_2O at 330°C: (a) 1 hr; (b) 5 hr; (c) 10 hr; (d) 36 hr; (e) 72 hr. I.S. = internal standard ($C_{24}D_{50}$).
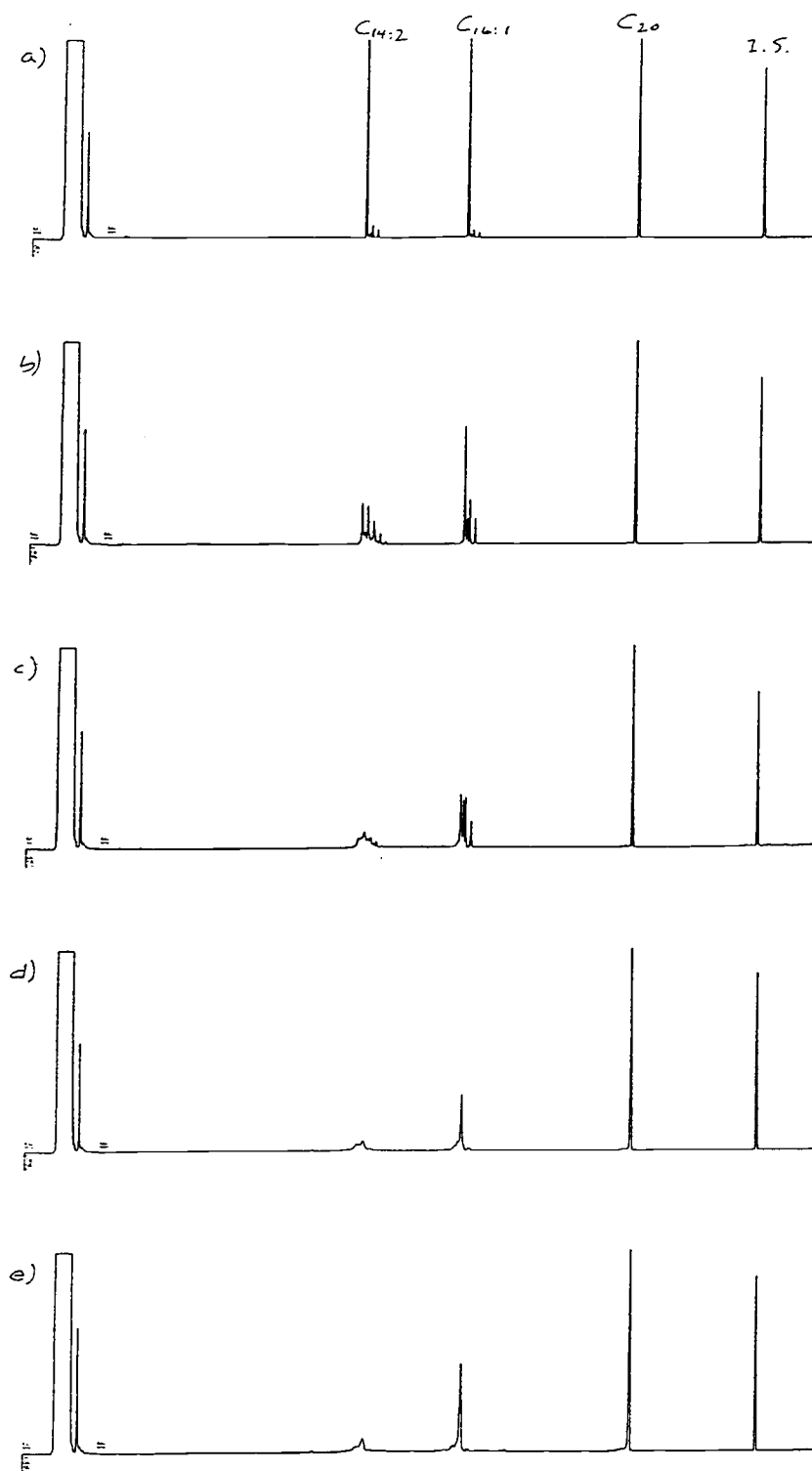
Figure 3.26. Gas chromatograms of the aliphatic fraction from the pyrolyses of 1,13-tetradecadiene, 1-hexadecene and eicosane spiked on Messel shale in D_2O at 330°C: (a) 1 hr; (b) 5 hr; (c) 10 hr; (d) 36 hr; (e) 72 hr. I.S. = internal standard ($C_{24}D_{50}$).
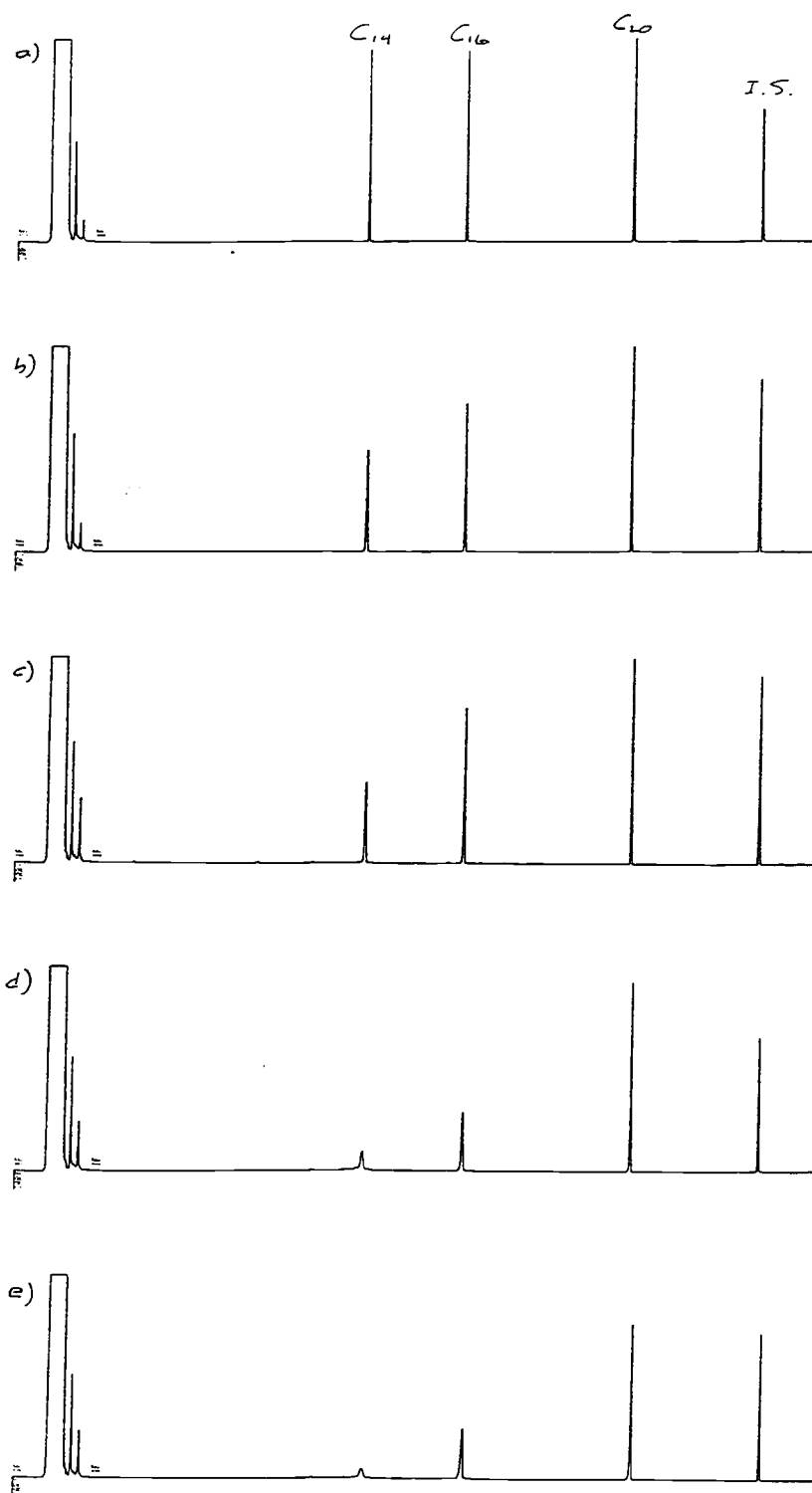
Figure 3.27. Gas chromatograms of the hydrogenated aliphatic fraction from the pyrolyses of 1,13-tetradecadiene, 1-hexadecene and eicosane spiked on Messel shale in D_2O at 330°C: (a) 1 hr; (b) 5 hr; (c) 10 hr; (d) 36 hr; (e) 72 hr. I.S. = internal standard ($C_{24}D_{50}$).
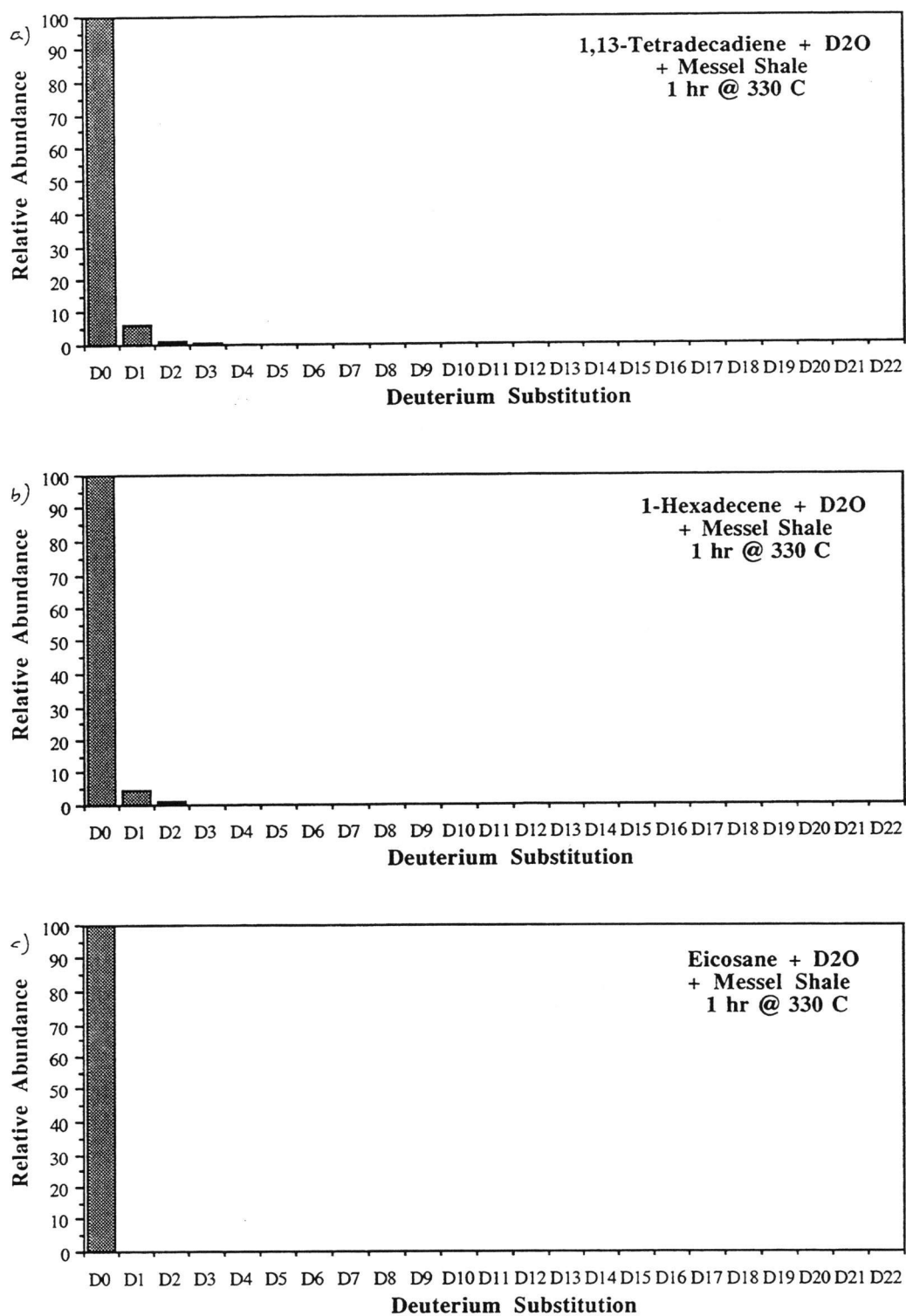
Figure 3.28. Histograms showing the extent of deuterium substitution after pyrolysis on Messel shale in D_2O for 1 hr at 330°C : (a) 1,13-tetradecadiene; (b) 1-hexadecane; (c) eicosane.
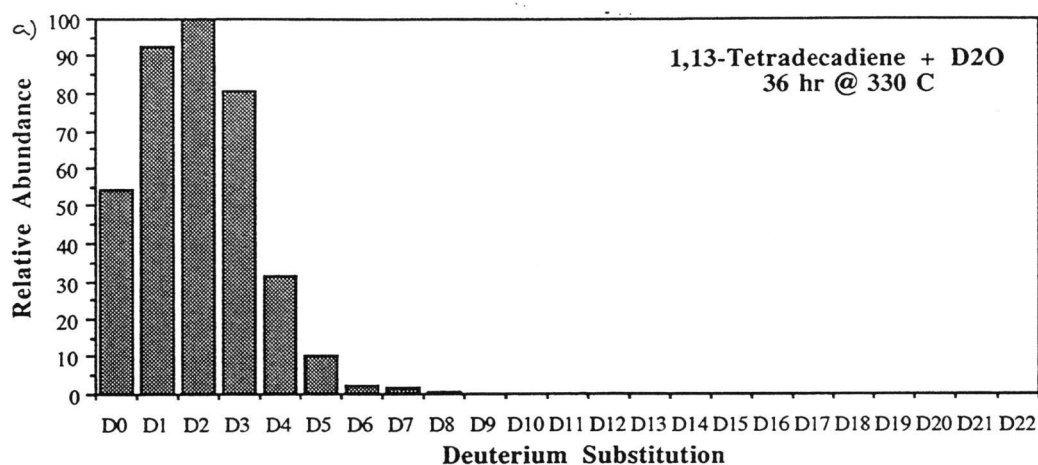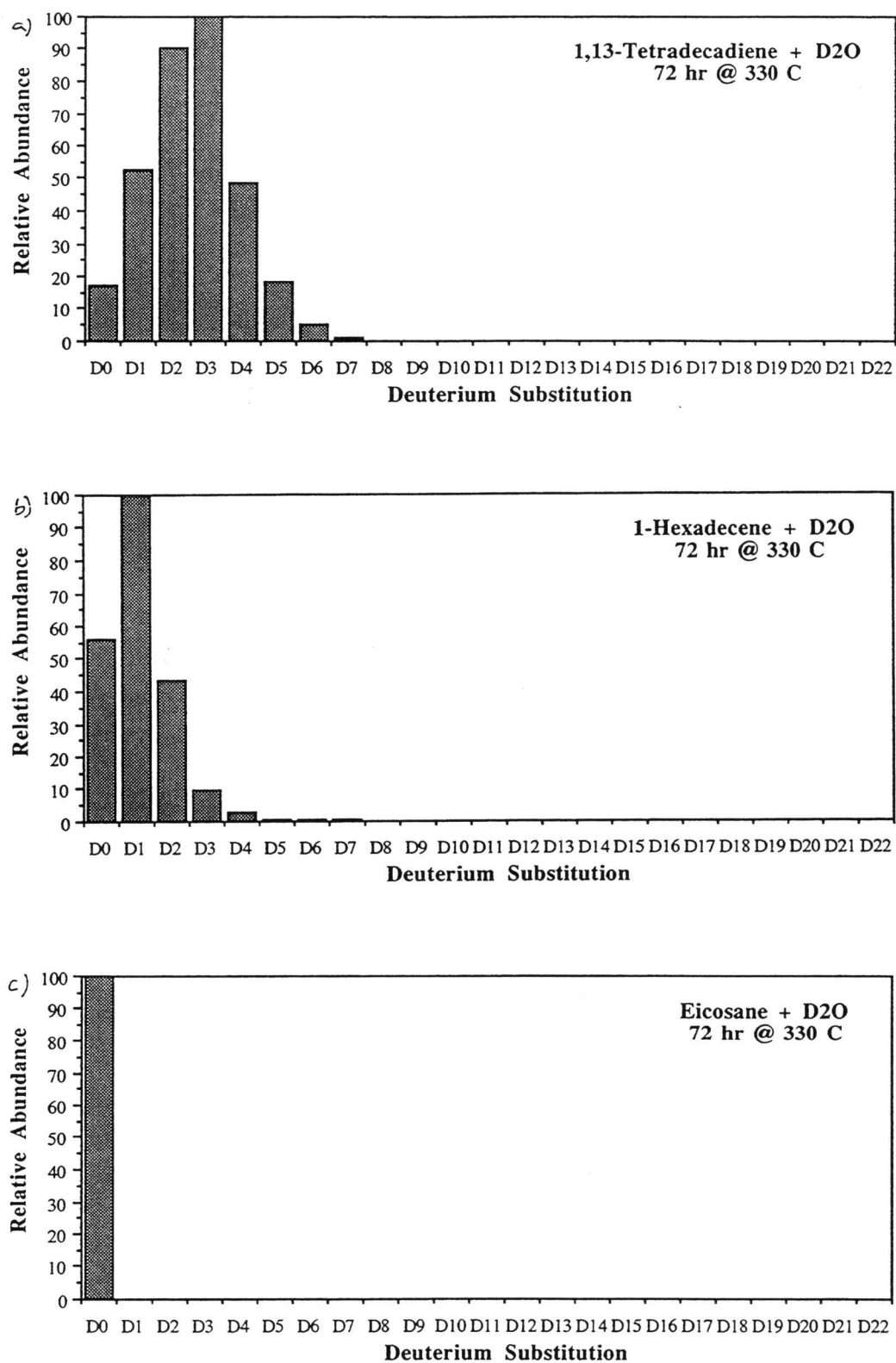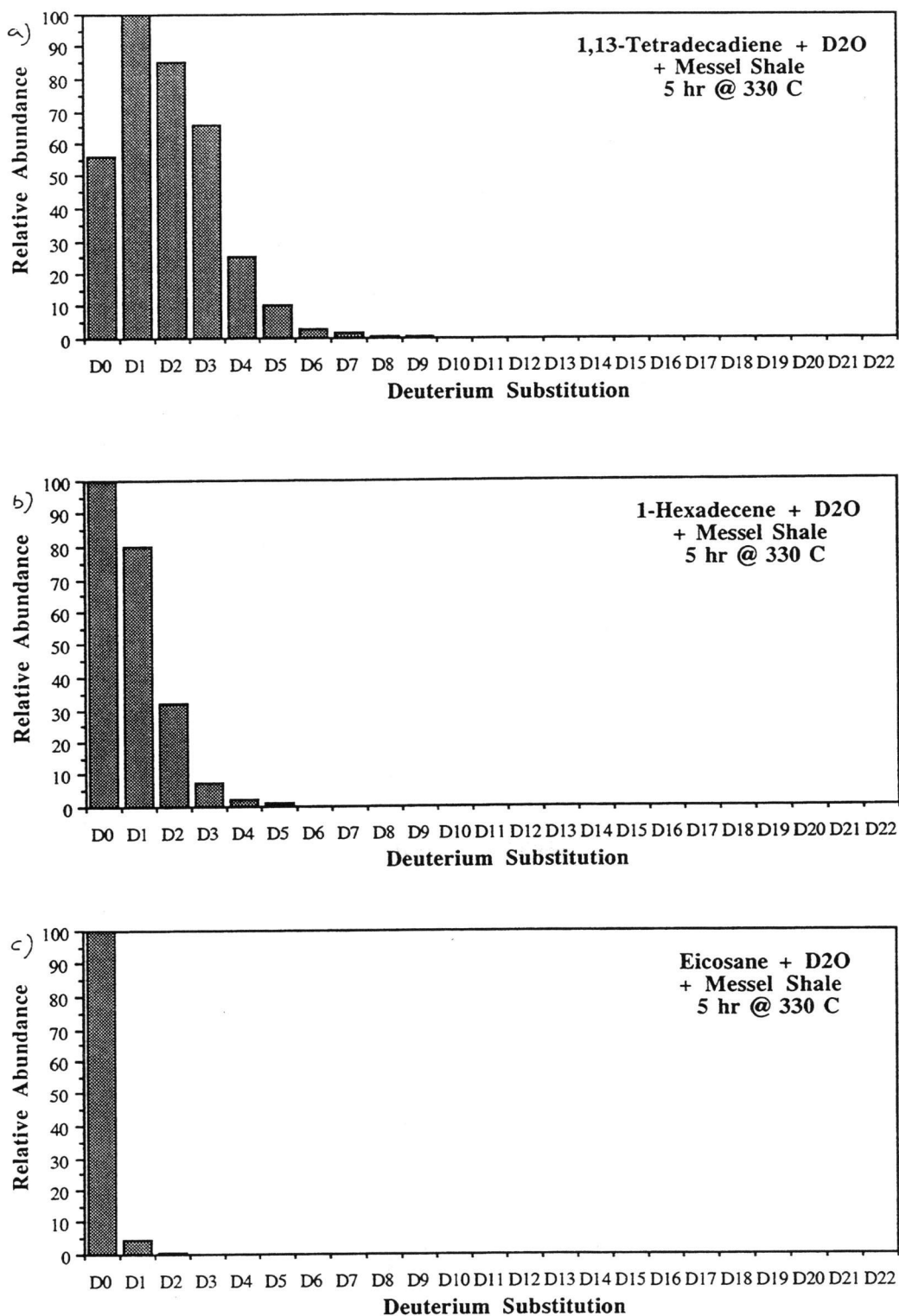
Figure 3.29. Histograms showing the extent of deuterium substitution after pyrolysis on Messel shale in D_2O for 5 hr at 330°C : (a) 1,13-tetradecadiene; (b) 1-hexadecane; (c) eicosane.
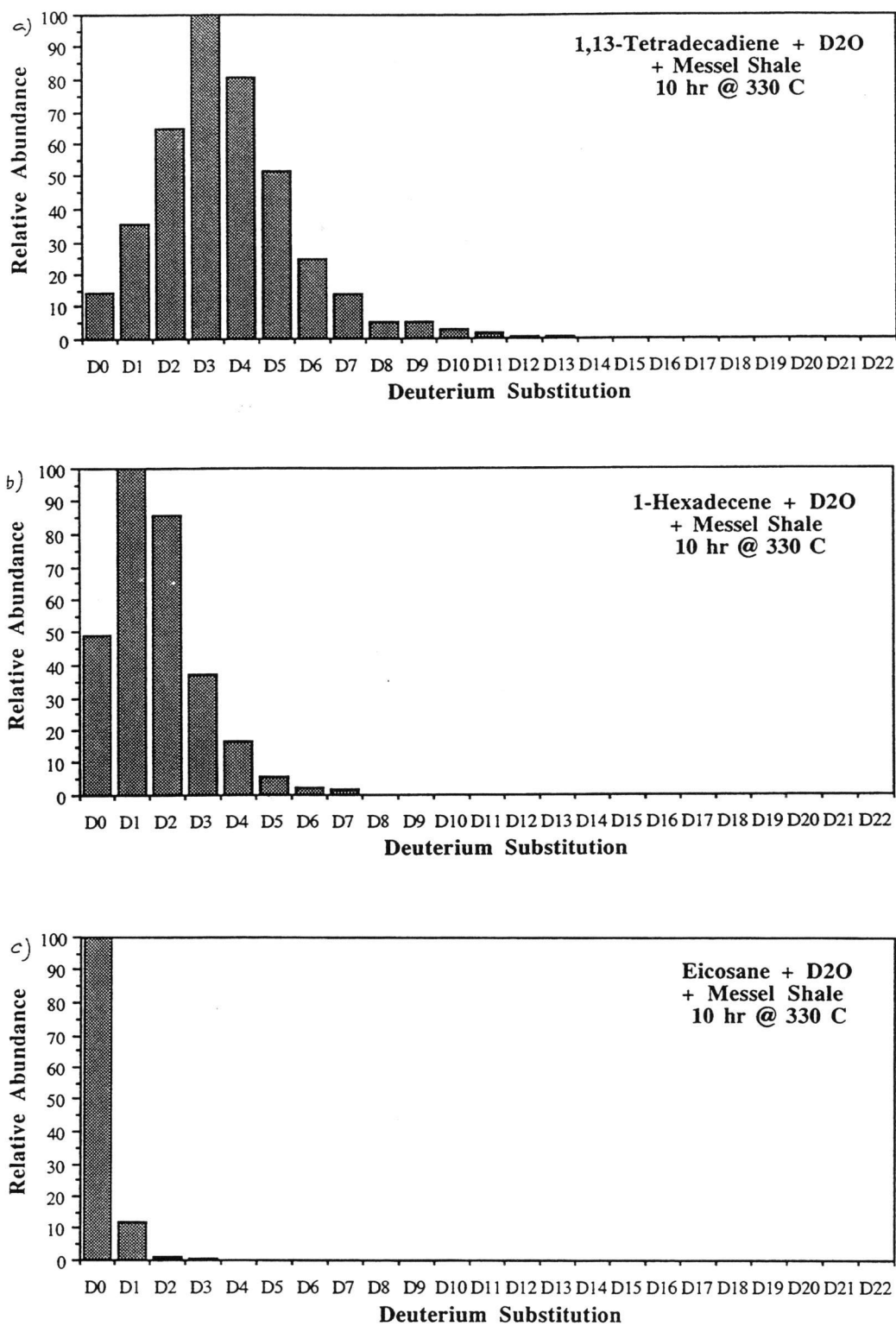
Figure 3.30. Histograms showing the extent of deuterium substitution after pyrolysis on Messel shale in D_2O for 10 hr at 330°C : (a) 1,13-tetradecadiene; (b) 1-hexadecane; (c) eicosane.
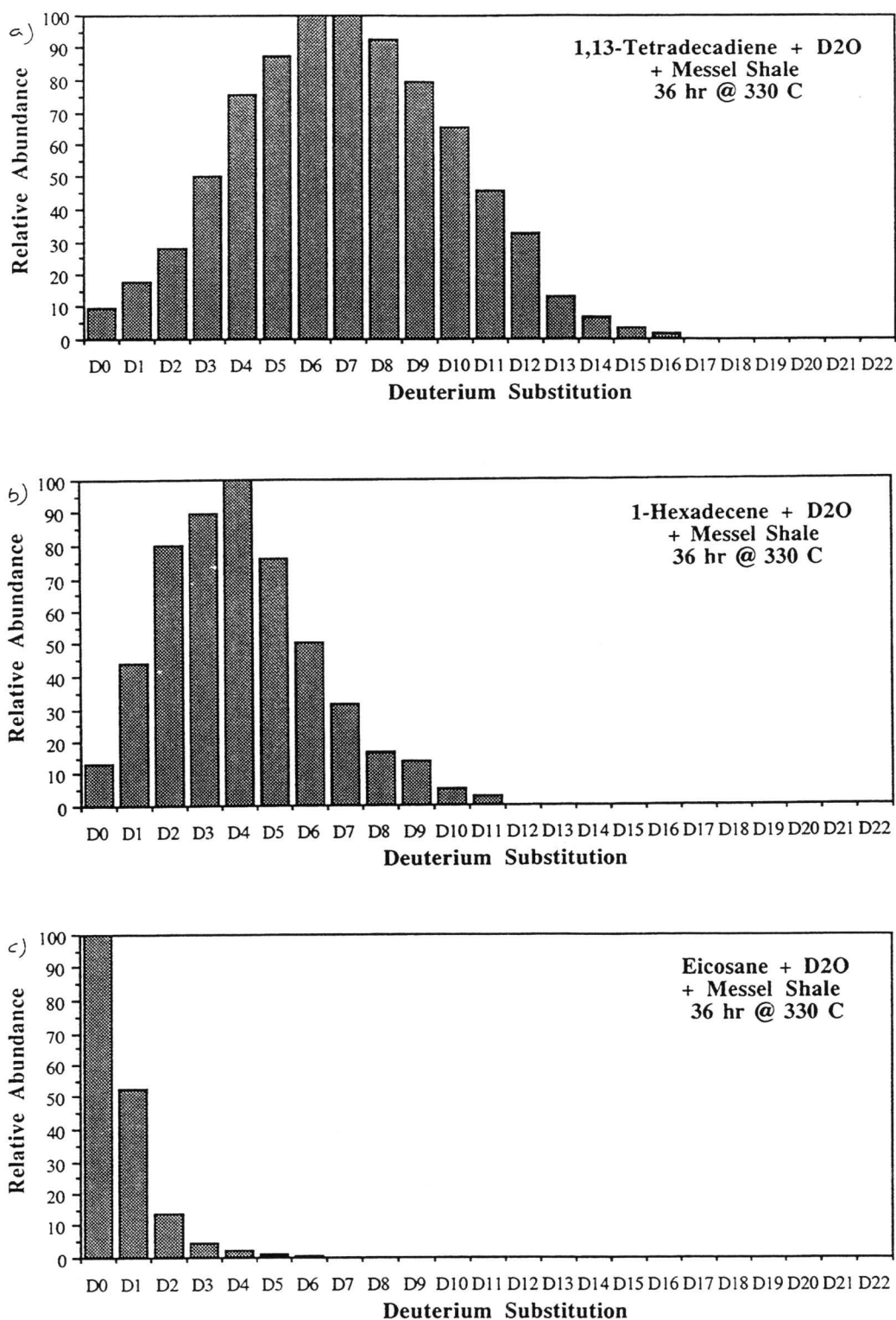
Figure 3.31. Histograms showing the extent of deuterium substitution after pyrolysis on Messel shale in D_2O for 36 hr at 330°C : (a) 1,13-tetradecadiene; (b) 1-hexadecane; (c) eicosane.
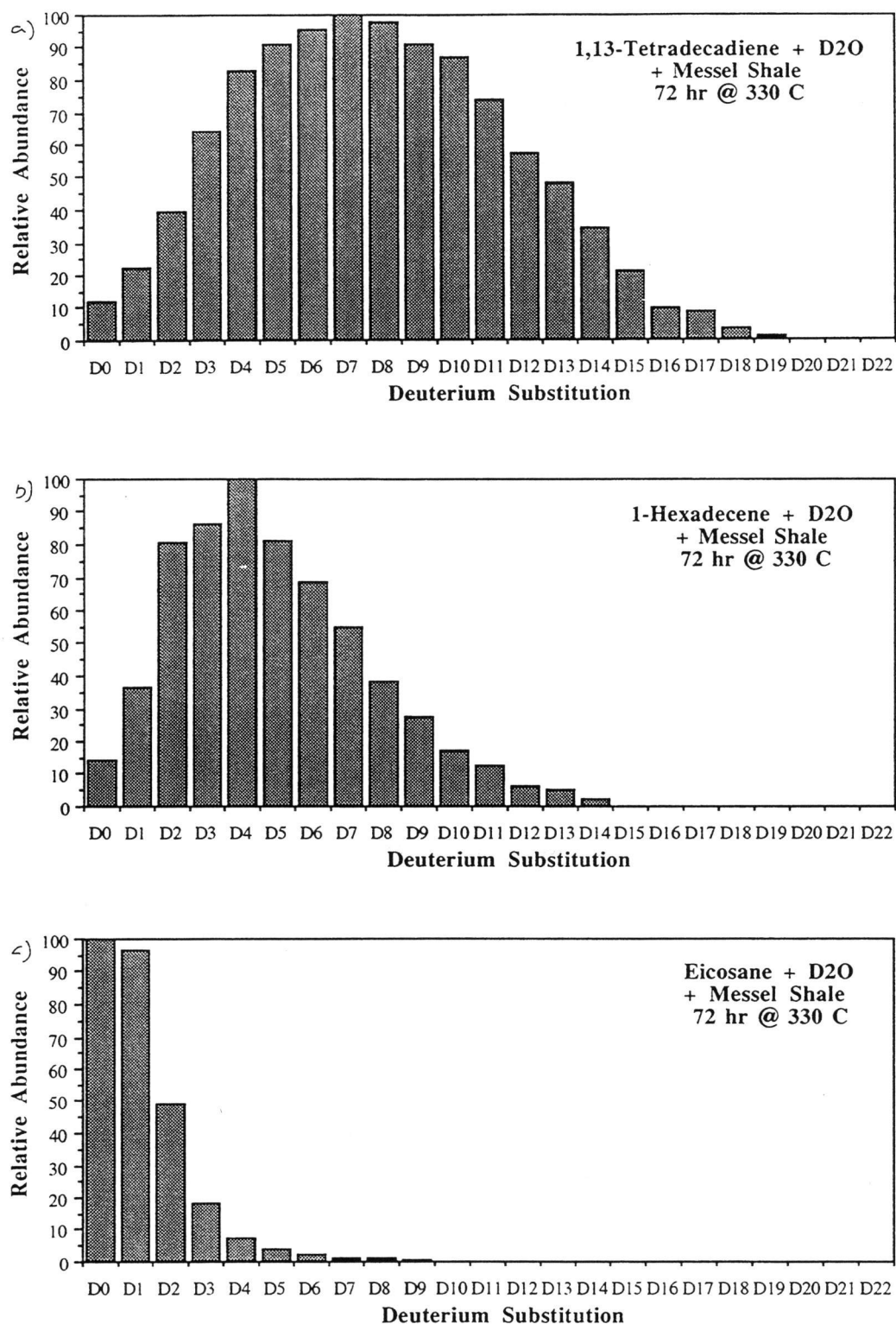
Figure 3.32. Histograms showing the extent of deuterium substitution after pyrolysis on Messel shale in D_2O for 72 hr at 330°C : (a) 1,13-tetradecadiene; (b) 1-hexadecane; (c) eicosane.
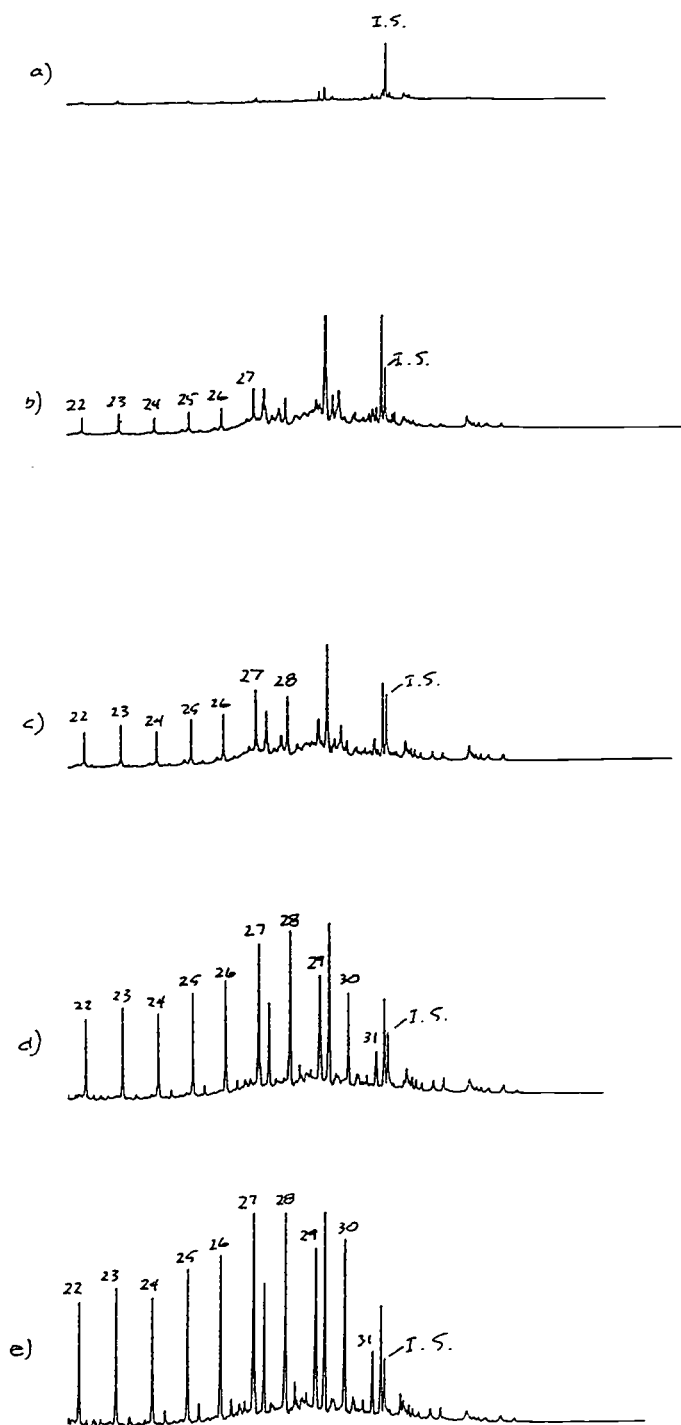
Figure 3.33. Gas chromatograms for the pyrolysis products released from the Messel shale kerogen during the pyrolyses in H_2O at 330°C: (a) 1 hr; (b) 5 hr; (c) 10 hr; (d) 36 hr; (e) 72 hr. Numbers refer to carbon chain lengths of n-alkanes. I.S. = internal standard (n-$C_{32}D_{66}$).
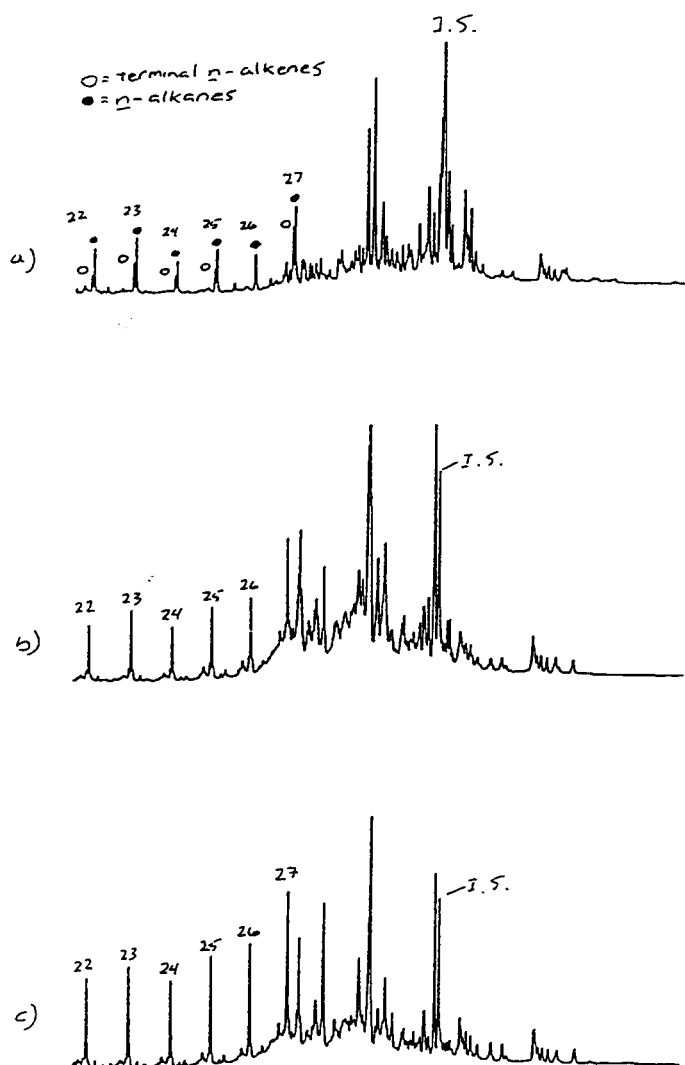
Figure 3.34. Gas chromatograms for the pyrolysis products released from the Messel shale kerogen during the pyrolyses in H_2O at 330°C: (a) 1 hr; (b) 5 hr; (c) 10 hr. Same samples as in Fig. 3.33 but concentration increased to show components in lower concentration. Numbers refer to carbon chain lengths of n-alkanes. I.S. = internal standard (n-$C_{32}D_{66}$).
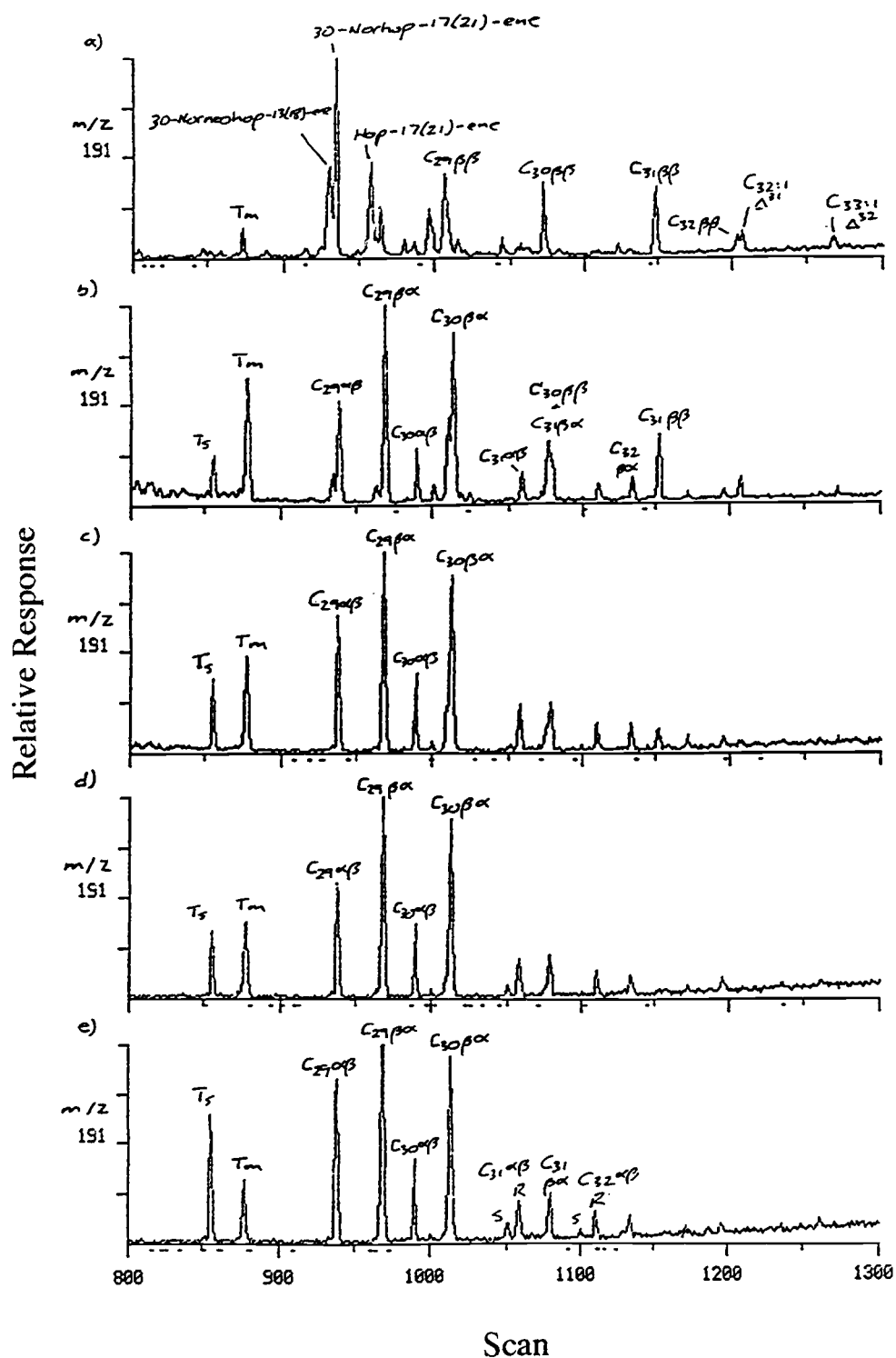
Figure 3.35. Mass fragmentogram m/z 191 representing triterpenoid hydrocarbons released from the Messel shale kerogen during the pyrolyses in H_2O at 330°C:-(a) 1 hr; (b) 5 hr; (c) 10 hr; (d) 36 hr; (e) 72 hr.
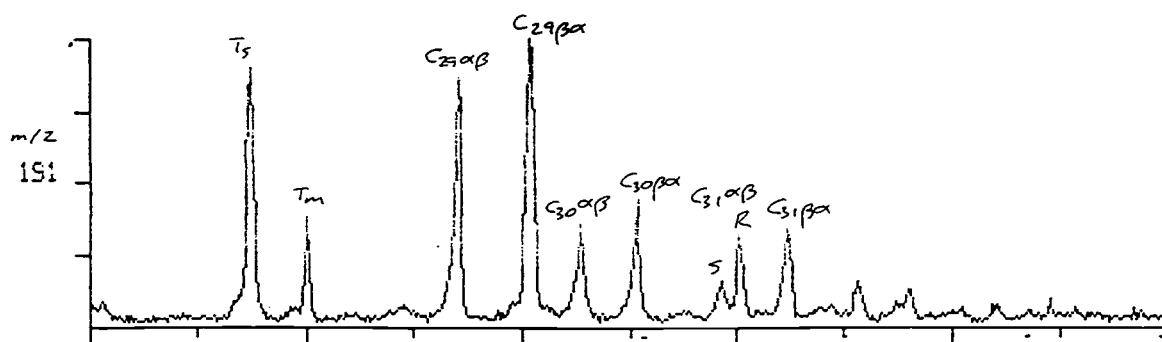
Figure 3.36. Mass fragmentogram m/z 191 representing triterpenoid hydrocarbons released from the Messel shale kerogen during the pyrolyses in D_2O for 72 hr at 330°C.
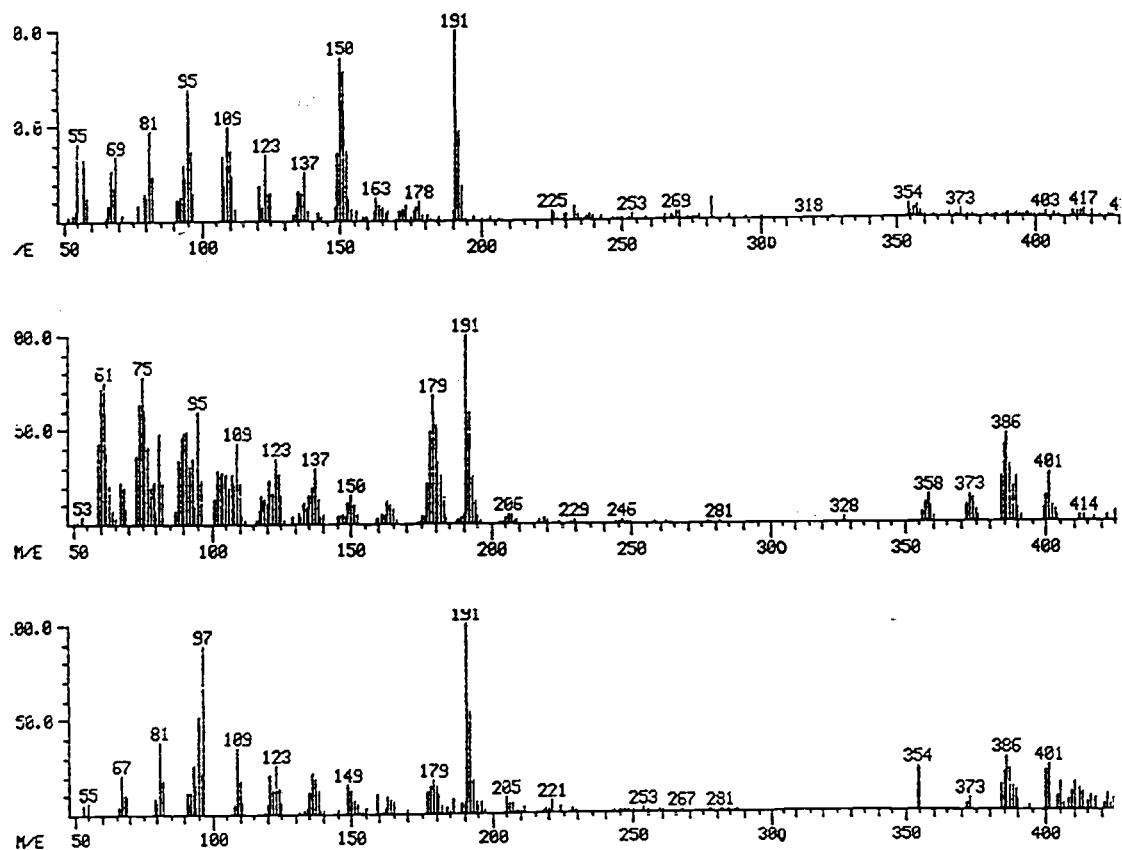
Figure 3.37. Selected mass spectra of polydeuterated triterpenoid hydrocarbons generated in the D_2O pyrolysis of Messel shale for 72 hr at 330°C.
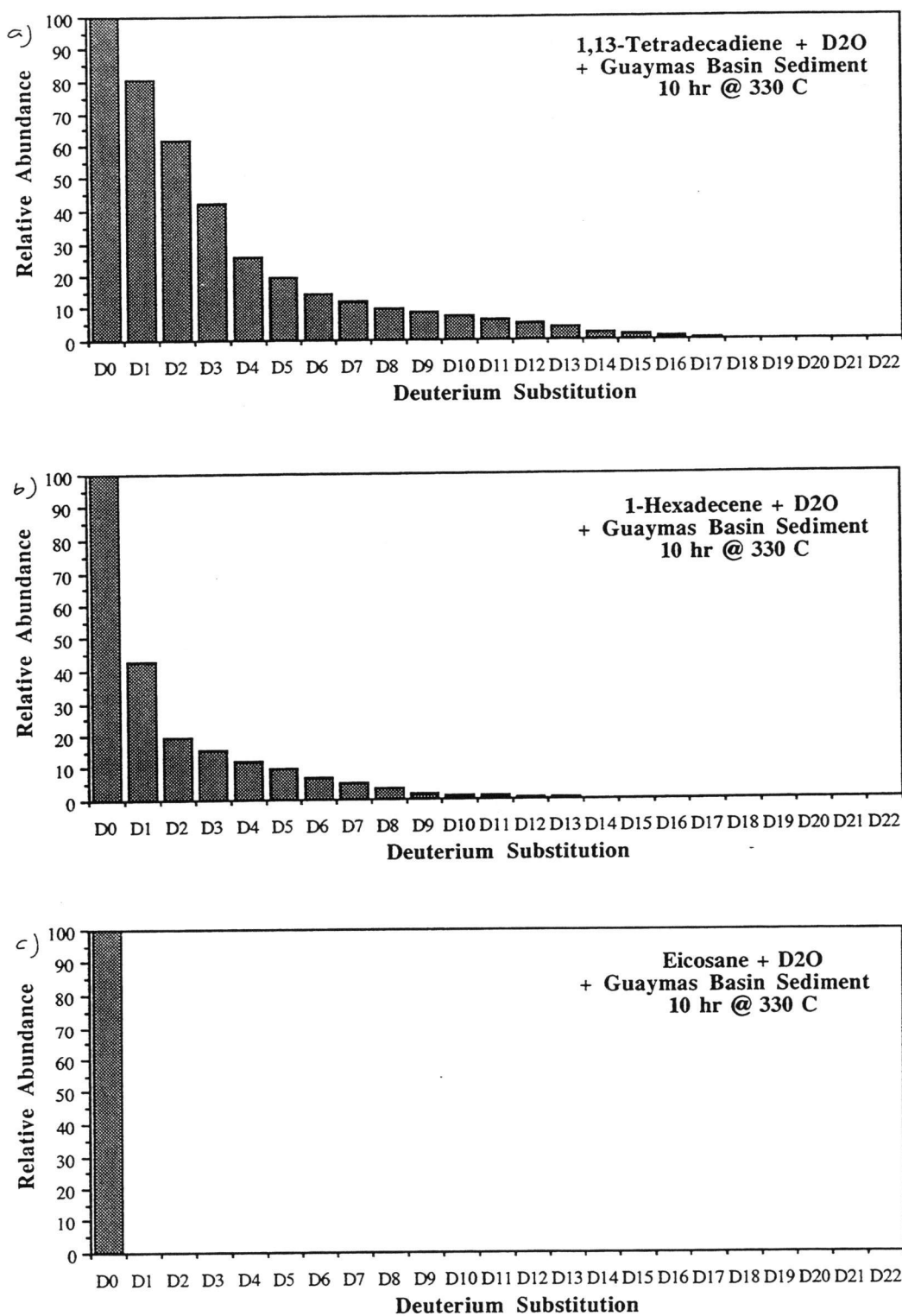
Figure 3.38. Histograms showing the extent of deuterium substitution after pyrolysis of molecular probes on Guaymas Basin sediment in D_2O for 10 hr at 330°C : (a) 1,13-tetradecadiene; (b) 1-hexadecane; (c) eicosane.
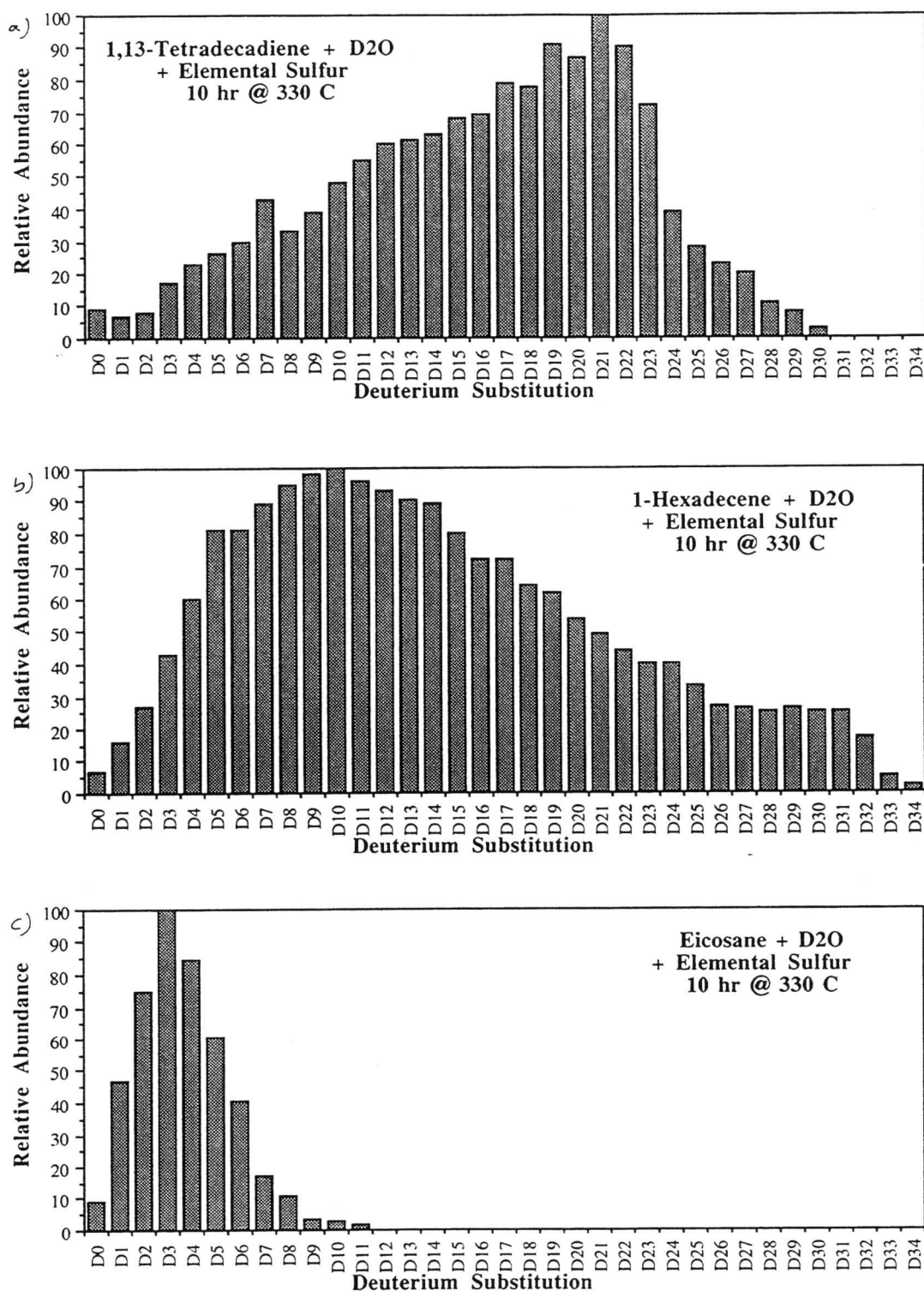
Figure 3.39. Histograms showing the extent of deuterium substitution after pyrolysis of molecular probes with 0.50 g elemental sulfur in D_2O for 10 hr at 330°C : (a) 1,13-tetradecadiene; (b) 1-hexadecane; (c) eicosane.

$\underline{n}\text{-}C_{32}H_{66}$

Radical C-C bond breaking

$\underline{n}$-alkane

α-olefin

no ionic
reactions

H^+ catalyzed double
bond isomerization

internal olefin
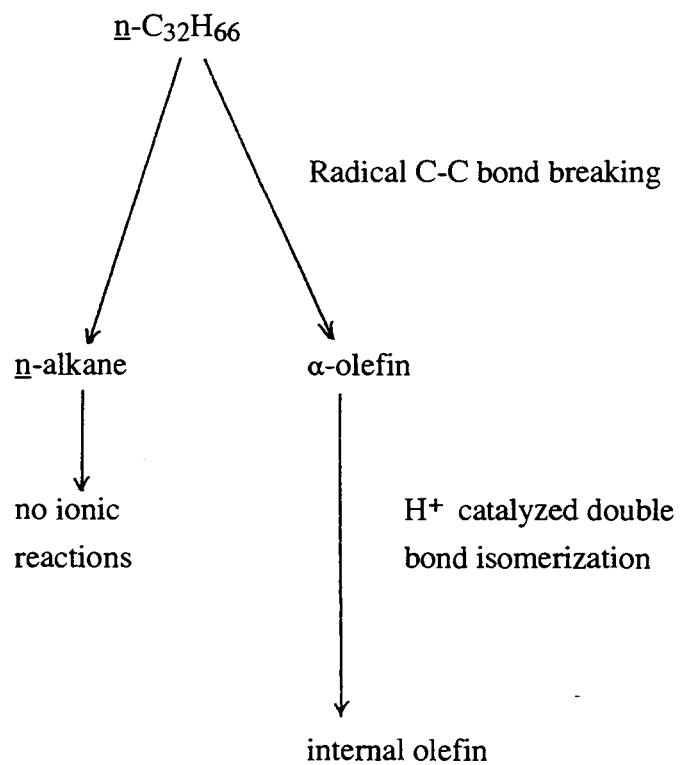
Figure 3.40. Set of proposed reactions showing a simplified version of the major primary and secondary reactions occurring during the pyrolysis of $\underline{n}\text{-}C_{32}H_{66}$ in H_2O.

$\underline{n}$-C$_{32}$H$_{66}$

Radical C-C bond breaking

$\underline{n}$-alkane α-olefin

no ionic   D$^+$ catalyzed double

reactions   bond isomerization

internal olefin (partially deuterated)
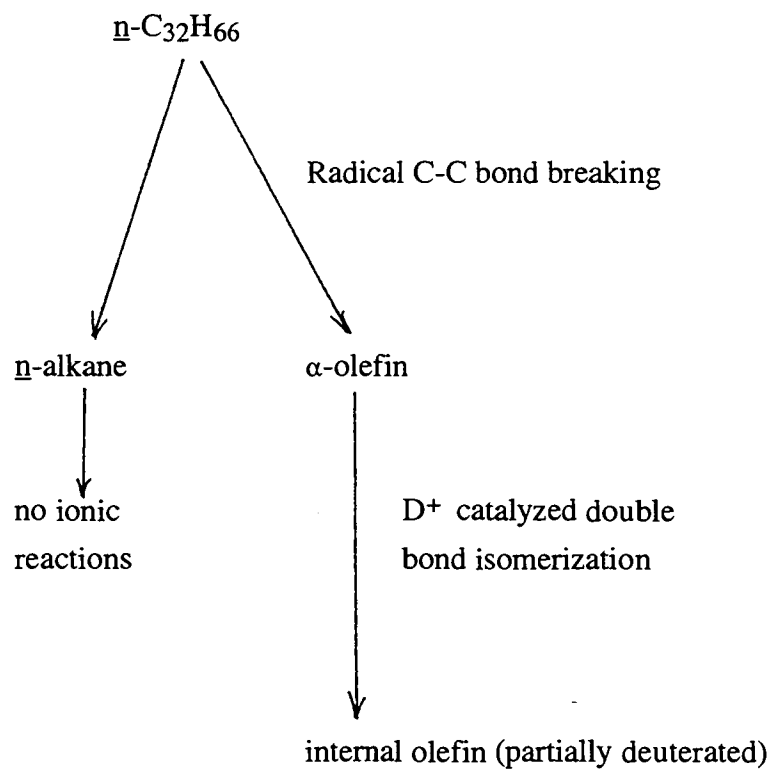
Figure 3.41. Set of proposed reactions showing a simplified version of the major primary and secondary reactions occurring during the pyrolysis of $\underline{n}$-C$_{32}$H$_{66}$ in D$_2$O.

Figure 3.42. Set of proposed reactions showing a simplified version of the deuterium exchange reactions occurring during the pyrolysis of 1,13-tetradecadiene in D_2O.

$$C = C - C - (CH_2)_8 - C - C - C = C$$

$$+$$

D$^+$ D$^+$ D$^+$ D$^+$ D$^+$ ← adsorbed/exchanged ions

C L A Y

↓ accelerated isomerization

C - C - C = C - C - C - C - C - C ≡ C - C - C - C - C

D D D   D$^+$ D$^+$ D$^+$ D$^+$ D D D D

C L A Y

↓

isomerized tetradecadiene (partially deuterated)

+

C L A Y
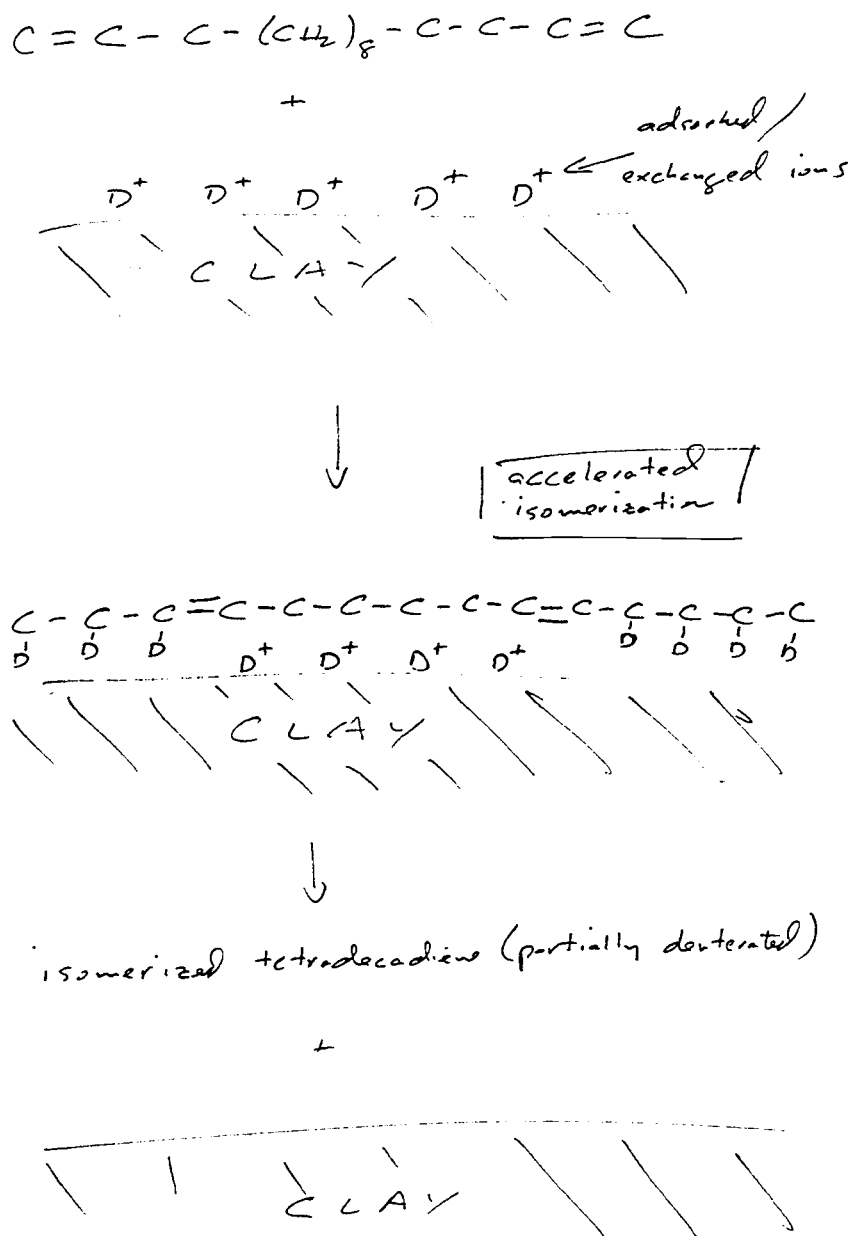
Figure 3.43. Set of proposed reactions showing a simplified version of the deuterium exchange reactions occurring during the pyrolysis of 1,13-tetradecadiene in D$_2$O spiked on Guaymas Basin sediments.
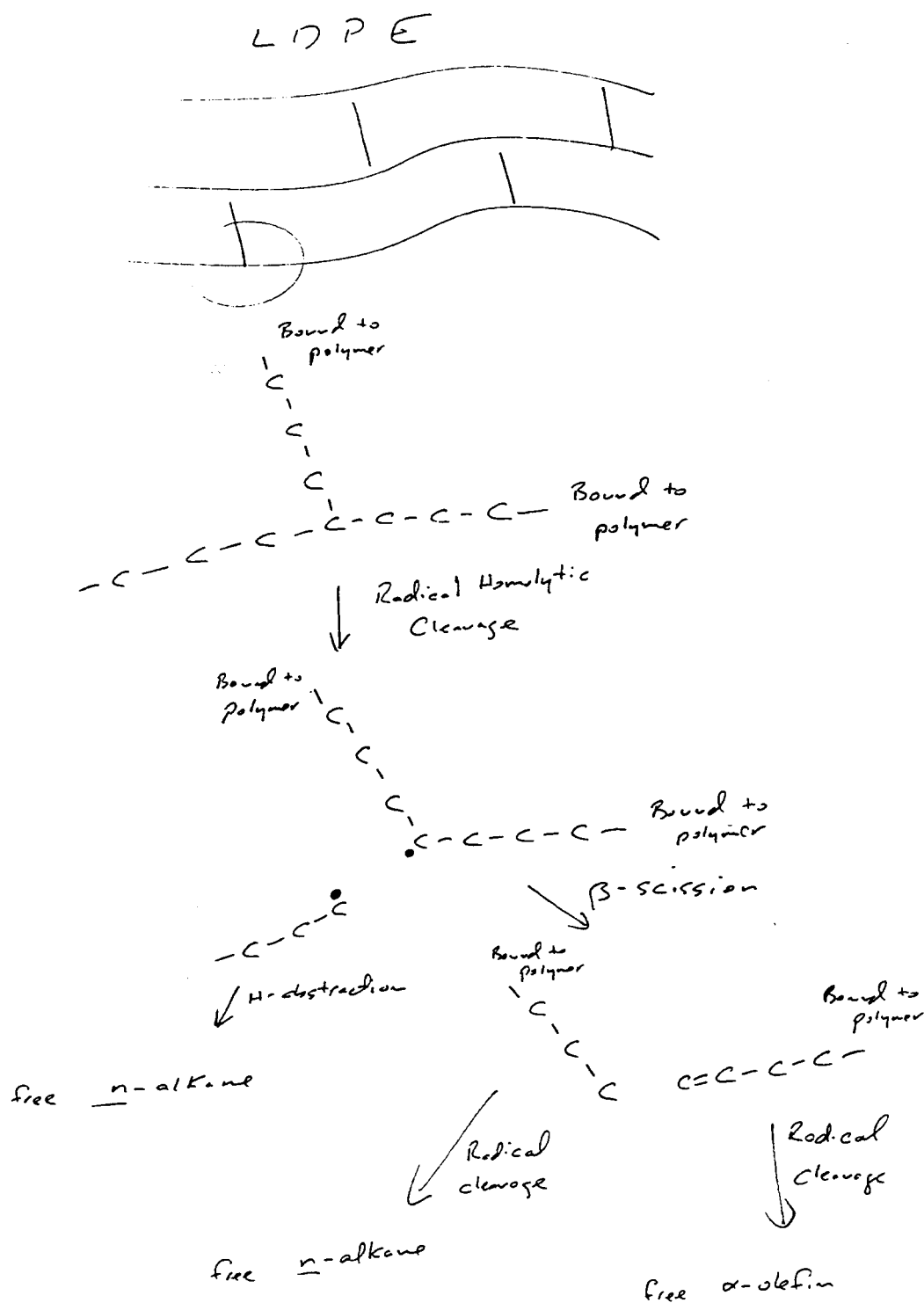
Figure 3.44. Set of proposed reactions showing a simplified version of the thermal breakdown of LDPE under hydrous pyrolysis conditions.

Messel Shale Kerogen

Aliphatic Network

Heat
Thermal Breakdown of
aliphatic network

n-alkanes + terminal n-alkenes

Homogeneous
Radical D
exchange
(s~11)

Hydrogenation

D^+ catalyzed double
Bond isomerization

n-alkane
(D-subst)

n-alkane

internal alkene
(D-subst)

Hydrogenation

n-alkane
(D-subst)

Figure 3.45. Proposed reaction pathway for the thermal alteration and deuterium exchange processes occurring during the D_2O pyrolysis of Messel shale.

CHAPTER 4

Simulation of Thermally-Enhanced Diagenetic and Catagenetic Transformations of Organic Matter in Surface Sediments from the Southern Trough of Guaymas Basin

ABSTRACT

In a preliminary study to simulate the hydrothermal petroleum generation process, a series of hydrous pyrolysis experiments (24 hr at 200, 250, 300 and 350°C) was conducted using a thermally unaltered sediment from Guaymas Basin, Gulf of California. The volatile hydrocarbons and bitumen were analyzed to monitor the changes in the compositions as a function of thermal stress. Some diagenetic and catagenetic alterations of organic matter observed in near surface sediments of the Guaymas Basin hydrothermal system have been duplicated by these short duration hydrous pyrolysis experiments.

The production of typical thermogenic hydrocarbons was accompanied by the production of an unusually large amount of volatile alkenes, with the proportion of alkenes to alkanes decreasing with temperature. Significant $\underline{n}$-alkane generation only occurred in the 350°C experiment. A progressive change was observed in the Carbon Preference Index (CPI) from 6.42 in the unaltered sediment to 1.4 in the 350°C experiment. Diploptene (hop-22(29)-ene) was the major component of the triterpenoid hydrocarbons of the unaltered sediment. In the 200°C experiment diploptene disappeared and hop-17(21)-ene became the major component of the triterpenoid series. The 250°C and 300°C experiments resulted in an overall decrease of the triterpenes, but there was the appearance of C_{27} to C_{32} hopanes (C_{28} missing) and the emergence of the C_{32} benzohopane with a minor amount of C_{33} benzohopane. The benzohopanes were not detected in the 350°C experiment, where the triterpen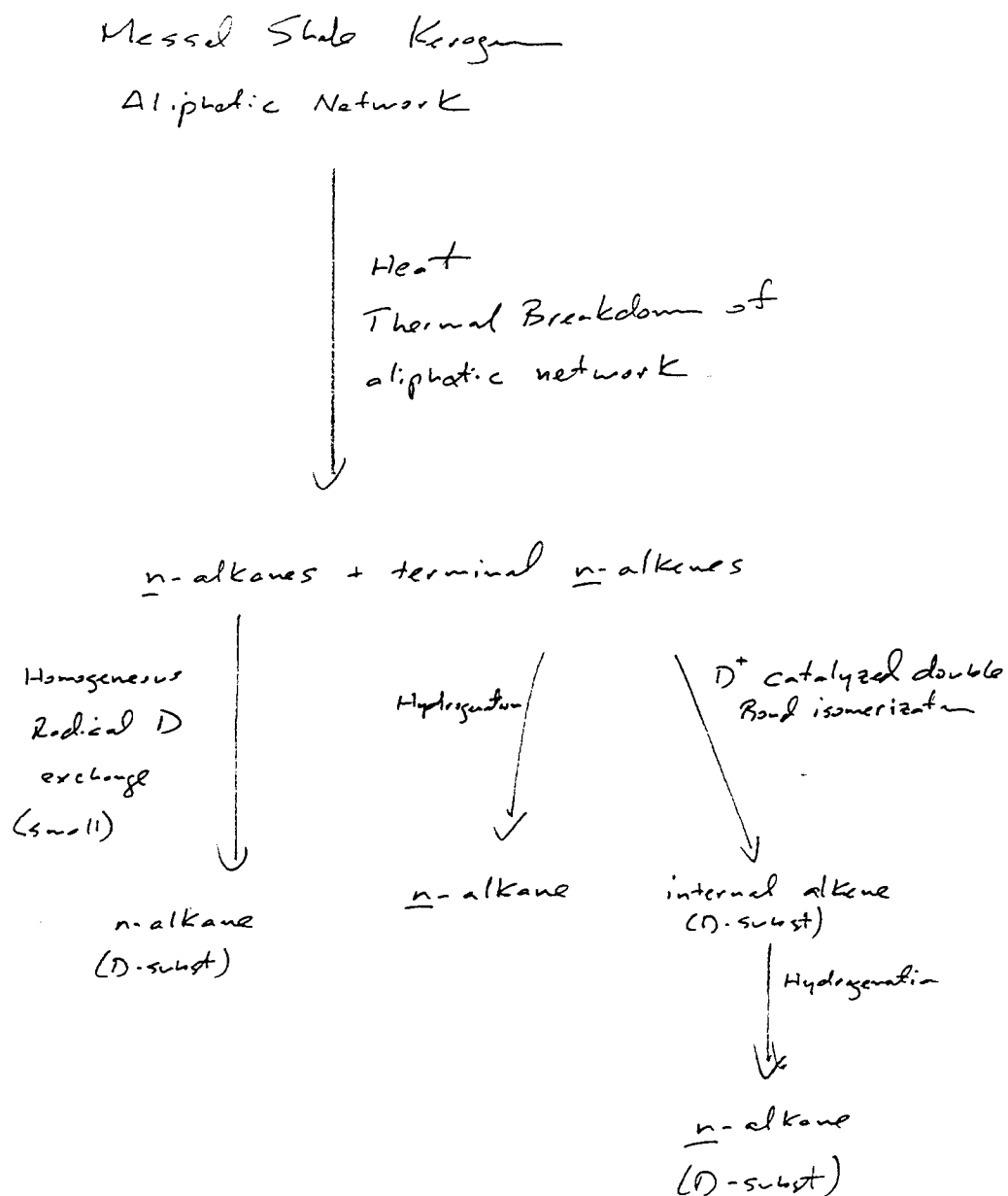oid distribution was dominated by $\alpha\beta$- and $\beta\alpha$-hopanes. The overall polycyclic aromatic hydrocarbon (PAH) distribution was similar to a thermally immature sediment. Perylene dominated and its concentration increased from 52 ng/mg bitumen in the unaltered sediment to 117 ng/mg bitumen in the 300°C experiment. Significant destruction of perylene occurred in the 350°C experiment. Diels' hydrocarbon, a C_{18} compound in the short-alkyl-chain series of triaromatic steroid hydrocarbons and a proposed indicator of rapid hydrothermal petroleum generation processes, was generated during the 250°C and higher experiments.

The biomarker transformations and PAH distributions in this series of experiments are more representative of hydrothermally-enhanced diagenesis, indicating that higher temperatures and/or longer heating durations are necessary to generate the types of petroleum products found in the Guaymas Basin hydrothermal system.

INTRODUCTION

The Guaymas Basin, Gulf of California is an actively spreading basin formed by the diverging Pacific and North America plates. The rift zones in the basin are distinguished from most spreading centers by having a thick sediment cover of diatomaceous oozes and mud turbidites. Petroleum generation occurs primarily by dike and sill intrusions into these sediments (Einsele et al., 1980; Lonsdale, 1985; Simoneit, 1983). ^{14}C ages for selected petroleum samples range from 3200 to 6600 years B. P. (Peter et al., 1991; Simoneit and Kvenvolden, 1993) indicating a significant amount of contemporary organic detritus has been converted to petroleum. Hydrothermal petroleums sourced from such recent sediments are characteristically enriched in polar constituents with a high polycyclic aromatic hydrocarbon (PAH) content (Simoneit, 1984; Simoneit et al., 1992a; Kawka and Simoneit, 1990). The quick, high temperature hydrothermal petroleum generation process is well suited for studying by laboratory methods such as hydrous pyrolysis, a closed system pyrolysis technique where the organic source material is kept submerged under water for the duration of the heating experiment (Lewan et al., 1979). This procedure was adapted in an attempt to simulate the hydrothermal petroleum generation process. The pyrolysates formed in the heating experiments were analyzed and the results were compared to oils and naturally-altered sediment extracts taken from the Guaymas Basin hydrothermal system.

EXPERIMENTAL

Samples. Fig. 4.1a is a map showing the Guaymas Basin trough system located in the Gulf of California. Fig. 4.1b is an enlargement of the Southern Trough of Guaymas Basin. The surface sediment sample used in the experiments came from site PC-1 of the Southern Trough of Guaymas Basin. Also shown is the location of the comparison core, PC-6, an 8 meter piston core which sampled a hydrothermally altered sediment (Simoneit et al., 1992b). The water depths at these locations are approximately 2000 m.

Hydrous pyrolysis experiments. The piston core PC-1 sampled an area not affected by hydrothermal activity. The surface sediment recovered with this core was transferred to a Nalgene® bottle and immediately frozen. Prior to the heating experiments the whole sediment was thawed, homogenized and split into 25g portions. These fractions were placed in the freezer until needed for the hydrous pyrolysis experiments.

A 250 mL T316 stainless steel pressure vessel (Parr Instrument Co.) with gage block designed for hydrothermal studies to 600°C and 6000 psig (408 bar) was used in the heating experiments. The reaction vessel and thawed sediment sample was placed in a glove bag and flushed with five volumes of N_2. The sediment was transferred to the reaction vessel and water was added to result in a water to sediment ratio of 3 to 1. The vessel was sealed and placed in a heater, temperature was controlled to $\pm$ 3°C. The temperatures used for the experiments ranged from 150° to 350°C at 50°C intervals and pressures from 290 to 2400 psig (20 to 163 bar). Each experiment lasted 24 hrs.

Extraction and fractionation. The reaction vessel was removed from the heater and cooled to room temperature upon completion of the heating cycle. The volume of gas generated from each heating experiment was measured and a sample was stored in a gas tight vial until analysis by gas chromatography. The pyrolyzed sediments were extracted with three 25 mL portions of methanol followed by five 50 mL portions of methylene chloride. All the solvent extracts were combined with the water from the pyrolysis experiment in a separatory funnel and the organic fraction collected. The water was extracted with two additional portions of methylene chloride and the two methylene chloride fractions were combined. The methylene chloride was dried with anhydrous sodium sulfate and the solvent was removed using a rotary evaporator at 30°C. The total extract was made up to 2 mL of methylene chloride.

The total extract (2 mL) was deasphalted using 100 mL of heptane. The asphaltenes were allowed to precipitate overnight and removed by filtration. The deasphalted fractions were fractionated on a column (30 cm x 1 cm) packed with 3.8 g alumina (fully active) over 3.8 g silica gel (fully active). Each sample was separated into three fractions by elution with 50 mL heptane (nonpolar, F1), 50 mL toluene (aromatic, F2) and 25 mL methanol (polar , F3).

Gas chromatography. The gas chromatography (GC) of the volatile hydrocarbons was performed with a Shimadzu GC-mini 3 equipped with a 1.8 m x 0.22 cm i.d. packed column (Poropak Q 50/80 mesh). The GC oven was heated using the following program : initial temperature 40°C, programmed to 180°C at 10°C/min., and isothermal at 180°C for 16 min., with the injector and detector at 225°C, and helium as the carrier gas. The GC of the sediment extracts was performed with a Hewlett Packard 5890A equipped with a 30 m x 0.25 mm i.d. DB-5 open tubular column (0.25 µm film thickness). The GC oven was heated using the following program : isothermal for 2 min. at 65°C, 4°/min. to 310°C, and isothermal for 30 min., with the injector at 290°C, detector at 325°C, and helium as the carrier gas.

Gas chromatography-mass spectrometry. The gas chromatography-mass spectrometry (GC-MS) was performed on a Finnigan 9610 gas chromatograph coupled to a Finnigan 4021 quadrupole mass spectrometer operated at 70 eV over the mass range 50-650 dalton and a cycly time of 2.0 s. The GC oven temperature was programmed at isothermal for 2 min. at 65°C, 3°/min. to 310°C, and isothermal for 30 min., with the injector at 290°C, and helium as the carrier gas. The MS data were processed with an on-line Finnigan-Incos 2300 computer data system.

RESULTS AND DISCUSSION

Volatile hydrocarbons. The gas chromatograms of the volatile hydrocarbons are shown in Fig. 4.2, and quantitative data and selected ratios are shown in Table 4.1. The production of typical thermogenic volatile hydrocarbons was confirmed by the low values (< 50) of the $C_1/(C_2 + C_3)$ molar ratios (Bernard et al., 1976; Simoneit et al., 1988). But the heating experiments also produced an unusually large amount of volatile alkenes in addition to the standard distribution of thermogenic volatile alkanes. Although the amounts of all the volatile hydrocarbons increased with increasing temperature, the proportion of volatile alkenes to volatile alkanes decreased as temperature increased. This is demonstrated by the steady drop in the ethylene to ethane ratio ($C_{2:1}/C_2$) from 6.0 in the 200°C experiment to 0.3 in the 350°C experiment.

n-Alkanes. The gas chromatograms of the total extracts are shown in Fig. 4.3. Large amounts of low molecular weight compounds were generated in the 200, 250 and 300°C experiments, but no significant n-alkane generation was observed. A major change was observed in the 350°C experiment where the n-alkanes were some of the most abundant components in the total extract. Fig. 4.4 shows the mass fragmentograms (m/z 99) representing the n-alkane distribution. Heating of the recent sediment resulted in the conversion of the n-alkane distribution from a terrestrial n-alkane signature to one more representative of an oil. The carbon preference index (CPI) progressively decreased from 6.4 in the unaltered sediment to 1.4 in the 350°C experiment. The n-alkanes in the unaltered sediment ranged from C_{15} to C_{37} with a carbon number maximum (C_{max}) at C_{29}, and a strong odd/even carbon number predominance (>C_{23}) characteristic of a significant terrestrial input (Brassell et al., 1978). Little change was observed for the 200 and 250°C experiments. The 300°C experiment resulted in a bimodal distribution ranging from C_{15} to C_{39} with a C_{max} = C_{29} and a minor maximum at C_{21}. The 350°C experiment resulted in a more uniform n-alkane distribution ranging from C_{13} to C_{33} maximizing at C_{19}.

Triterpenoid hydrocarbons. The distributions of the triterpenoid biomarkers are shown in Fig. 4.5 with biomarker concentrations listed in Table 4.2. The triterpenoid biomarker transformations can be characterized as thermally-enhanced diagenetic reactions in the lower temperature experiments to early catagenetic reactions in the 350°C experiment. The triterpenoid distribution of the unaltered sediment was characteristic of the Recent sediments from Guaymas Basin where hop-22(29)-ene (diploptene) is the major component (Simoneit et al., 1979). But diploptene could not

be detected in the extracts of the pyrolysis experiments. The loss of diploptene in the 200°C experiment was accompanied by a corresponding increase in hop-17(21)-ene suggesting a near quantitative conversion of diploptene to hop-17(21)-ene, which has been proposed as a diagenetic transformation (Ensminger, 1977; Venkatesan, 1988a). The distribution of the triterpenoid biomarkers in the 200, 250 and 300°C experiments consisted of those compounds characteristic of diagenetic transformations. There was an overall decrease in the triterpenes with the concomitant appearance of the C_{27} to C_{32} 17β(H),21β(H)-hopanes (C$_{28}$ missing) and emergence of the C_{32} and C_{33} benzohopanes. The 17β(H),21α(H)-hopanes and 17α(H),21β(H)-hopanes were formed in the 300 and 350°C experiments. The C-22 S/(S+R) epimer ratio of 17α(H),21β(H)-homohopane of 0.12 in the 300°C experiment and 0.32 in the 350°C experiment indicated a minimum of thermal stress, i.e., incomplete maturation. The benzohopanes were not detected in the 350°C experiment.

Polycyclic Aromatic Hydrocarbons. The concentrations of the major polycyclic aromatic hydrocarbons (PAH) are shown in Fig. 4.6. The major PAH in the unaltered sediment was perylene. The compound perylene, which is primarily diagenetic in origin (Louda and Baker, 1984; Venkatesan, 1988b), increased in concentration in the 200, 250 and 300°C experiments suggesting an additional production of perylene by heating. Low levels of pyrolytic PAH common in oils and sediment extracts of Guaymas Basin were also generated. The 350°C experiment resulted in the destruction of perylene with the further increase in the pyrolytic PAH. A comparison of these PAH distributions to Guaymas Basin oils and sediment extracts previously analyzed reveals that the 200 to 300°C experiments generated PAH which are very similar to thermally immature sediments, but the 350°C experiment resulted in a distribution more characteristic to sediments that have been altered by dolerite sill intrusions (Kawka, 1990; Kawka and Simoneit, 1990).

Diels' hydrocarbon. Fig. 4.7 are the mass fragmentograms of m/z 217 and m/z 231 showing the relative distributions of two series of triaromatic steroid hydrocarbons in the unaltered sediment and the heating experiments. Diels' hydrocarbon, a triaromatic steroid hydrocarbon common in Guaymas Basin petroleum and a proposed tracer of hydrothermally derived oils, was generated in the 250°C and higher temperature experiments. Fig. 4.7 shows the generation of Diels' hydrocarbon and the concomitant loss of the other long-chain steroid hydrocarbons, indicating that a possible transformation to Diels' hydrocarbon is occurring from these compounds. The concentration of Diels' hydrocarbon is shown in Fig. 4.6 relative to the polycyclic

aromatic hydrocarbons, showing that this triaromatic steroid hydrocarbon is comparable in concentration to the other PAH generated in the heating experiments.

Ketones. A survey of oils from the Guaymas Basin has revealed several homologous series of alkanones that are ubiquitous in the polar NSO fractions. The alkan-2-ones are usually in highest concentration, followed by 3-, 4-, 5- (and higher) isomers. An examination of the NSO fractions from these heating experiments detected the alkanones only in the 350°C experiment. Their pyrolytic origin was verified by the smooth homolog distribution, but the ketones were primarily the n-alkan-2-one isomers. The ketone mass fragmentogram is shown in Fig. 4.8.

These preliminary hydrous pyrolysis experiments resulted in a variety of thermally-enhanced diagenetic reactions and early catagenetic reactions. The time / temperature relationships were such that catagenetic reactions leading to hydrothermal petroleum were minimal in the 200, 250 and 300°C experiments but enhanced in the 350°C experiment. The major chemical processes with the aliphatic components observed in the heating experiments, cracking and isomerization, can be explained by a combination of radical and ionic mechanisms.

The volatile hydrocarbons generated in the heating experiments had a high proportion of alkenes, but the degree of unsaturation decreased with increasing reaction temperature. Volatile alkenes, especially ethylene, are common products formed from the thermal cleavage of aliphatic hydrocarbons by a radical cracking mechanism (Tsuchiya and Sumi, 1968). But alkenes are not present in the high temperature vent fluids of the Guaymas Basin (Simoneit, 1983b; Simoneit et al., 1988), although low levels of alkenes of biological origin have been detected in the interstitial gases of Guaymas Basin sediments (Whelan and Hunt, 1982). The large amount of volatile alkenes generated in the heating experiments is interpreted as primary cracking products that have not undergone hydrogenation. Instead they have partitioned into the headspace of the bomb and away from the catalytic surfaces which facilitate double bond reduction. Under these operating conditions, the headspace of the reaction vessel appears to affect the rates of these secondary hydrogenation reactions. A large excess of water along with the presence of a gas headspace in the reaction vessel may decrease those reaction rates that are influenced by mineral surface chemical reactions.

Another type of reactions likely to be affected by the partitioning away from the minerals and into the gas or liquid phases would be isomerization reactions, where the rates of these reactions have been found to be greatly influenced by the type of minerals present (Huizinga et al., 1987a,b; Kissin, 1987, 1990; Lu et al., 1989; Peters et al.,

1990). This may explain why decreased catalytic activity is observed when organic-mineral pyrolysis experiments are performed with an excess of water (Henderson et al., 1968; Eisma and Jurg, 1969; Huizinga et al., 1987a,b). Monthioux and co-workers (1985) have suggested that the most natural catagenetic conditions are better simulated in the laboratory by using closed-system experiments with a reduced free volume, and a minimum of any diluting gas.

Very little change in the $\underline{n}$-alkane distribution occurred in the 200°C and 250°C experiments. But greater $\underline{n}$-alkane formation from the C_{16} to C_{27} range commenced in the 300°C experiment, with a large amount of $\underline{n}$-alkane generation in the 350°C experiment. Alkenes were not found in the bitumen from these heating experiments, suggesting that the hydrogenation reactions have occurred to sufficiently reduce the alkenes of the cracking products.

The changes observed in the hopanoid biomarkers ranged from the diagenetic diploptene to hop-17(21)-ene conversion, most likely occurring by an acid catalyzed isomerization, to early catagenesis (e.g. epimerization of the $C_{31}\alpha\beta$ hopane). The biomarker changes observed in these heating experiments parallel the biomarker transformations observed in the lower sections of core PC-6 (Fig. 4.9), an eight meter long piston core which sampled a hydrothermally altered sediment column in the vicinity of active hydrothermal mounds of the Southern Trough of Guaymas Basin (Simoneit et al., 1992b).

The total extracts in the 200, 250 and 300°C experiments contained a large amount of low molecular weight polar compounds. This may be due to the fact that the pyrolysis bomb, being a closed system, cannot duplicate some of the natural hydrothermal processes such as solubilization and porewater transport or water-washing which likely affect the relative proportions of the aliphatic, aromatic and polar NSO compounds. Therefore certain constituents which may normally be transported away by porewater fluid migration are retained in the total extract.

CONCLUSIONS

The results obtained in these heating experiments show that the hydrous pyrolysis experiments can alter the surficial sediments similarly to some of the near surface reactions occurring naturally in Guaymas Basin. These reactions are a combination of radical and ionic mechanisms. It is likely that under these hydrous pyrolysis conditions, the primary pathway of releasing aliphatic components from the kerogen is by radical cracking. But secondary reactions, such as isomerizations and epimerizations, are most likely ionic reactions. Secondary radical reactions, such as double bond hydrogenation, are likely surface mediated and therefore may become diffusion controlled in large reactions vessels. Care should be taken when extrapolating the results of heating experiments performed in batch reactors with large amounts of excess water and large headspaces. Organic components typically remain in contact with mineral surfaces during natural sedimentary hydrothermal alteration. But in this experimental design, the pyrolysates can quickly be partitioned away from the mineral surfaces and remain in the gas and liquid phases.

This study simulated some of the reactions which occur during the earliest stages of hydrothermal petroleum generation. The overall process of hydrothermal petroleum generation likely occurs over a wide temperature range (warm to > 350°C).

Table 4.1. Analytical results of volatile hydrocarbon analyses for 24 hr heating experiments.

Temp. (°C)	Gas Yield mL@STP	C_1 (ppm)	$C_{2:1}$ (ppm)	C_2 (ppm)	$C_{3:1}$ (ppm)	C_3 (ppm)	$\dfrac{C_1}{(C_2+C_3)}$	$\dfrac{C_{2:1}}{C_2}$
200	39	450	108	18	77	n.d.[a]	25.0[b]	6.0
250	67	1180	426	112	380	n.d.[a]	10.5[b]	3.8
300	80	5760	1030	1060	1310	695	3.3	0.9
350	126	37750	1965	5720	2700	2925	4.4	0.3

[a] not determined due to poor resolution

[b] this ratio represents a maximum value due to lack of C_3 data

Table 4.2. Triterpenoid concentrations from the 24 hr heating experiments (ng/g sed.)

Compound	Unaltered	200°C	250°C	300°C	350°C
T_S	-	-	-	-	165
T_m	23	26	13	33	39
$C_{29}\alpha\beta$	-	-	-	68	189
Hop-17(21)-ene	43	467	74	43	-
$C_{29}\beta\alpha$	-	-	10	53	127
$C_{30}\alpha\beta$	-	-	-	39	112
Neohop-13(18)-ene	36	66	10	-	-
$C_{29}\beta\beta$	-	43	16	23	-
$C_{30}\beta\alpha$	-	-	18	67	164
$C_{31}\alpha\beta(S)$	-	-	-	4	32
$C_{31}\alpha\beta(R)$	-	-	-	29	66
$C_{30}\beta\beta$	37	95	55	87	-
$C_{31}\beta\alpha$	-	-	-	27	68
Hop-22(29)-ene	480	-	-	-	-
$C_{32}\alpha\beta(S)$	-	-	-	-	12
$C_{32}\alpha\beta(R)$	-	-	-	13	29
$C_{32}\beta\alpha$	-	-	-	12	40
$C_{31}\beta\beta$	50	83	40	47	-
$C_{32}\beta\beta$	-	11	7	16	-
C_{32} Benzohopane	-	42	88	78	-
C_{33} Benzohopane	-	-	5	14	-
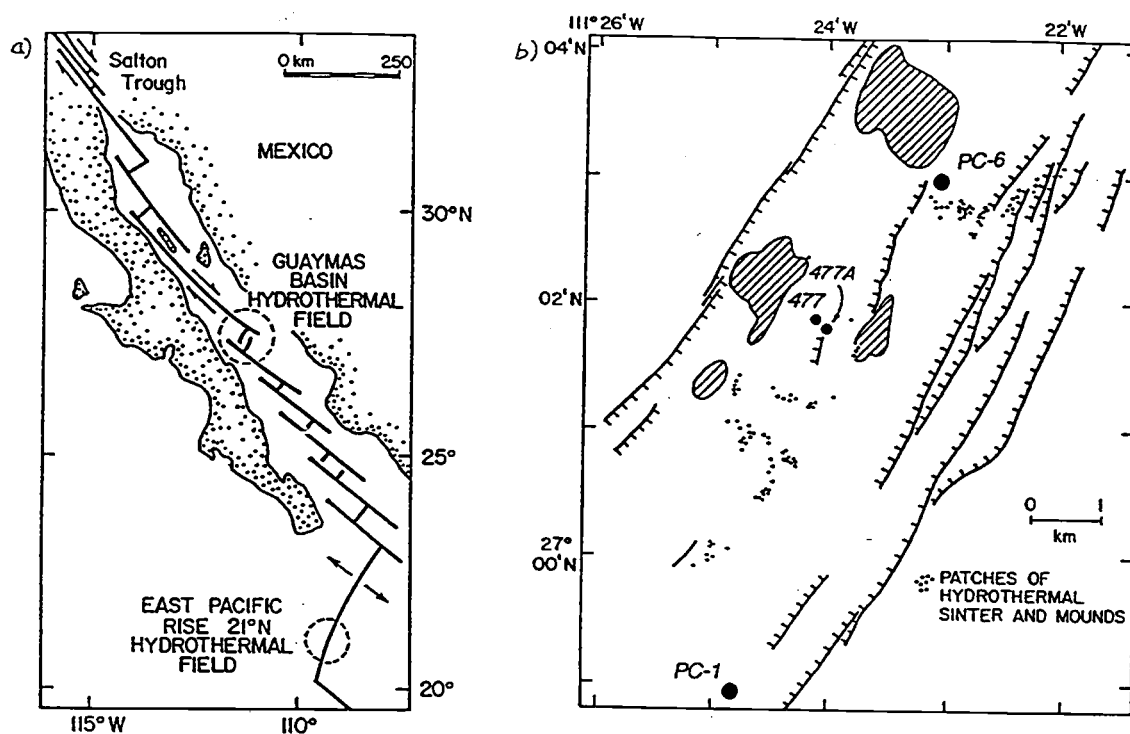
Figure 4.1. (a) Map of Gulf of California showing geographic location of the sampling area, and (b) Southern trough of Guaymas Basin.
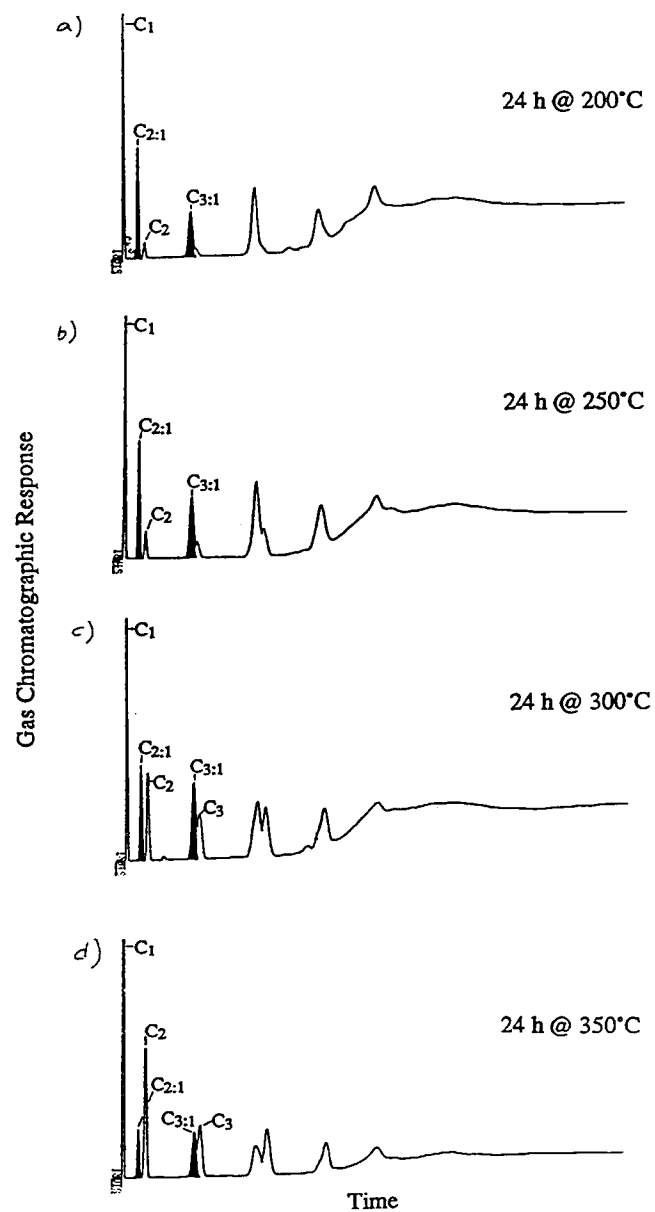
Figure 4.2. Gas chromatograms of volatile hydrocarbons : a) 24 hr @ 200°C; b) 24 hr @ 250°C; c) 24 hr @ 300°C; d) 24 hr @ 350°C.
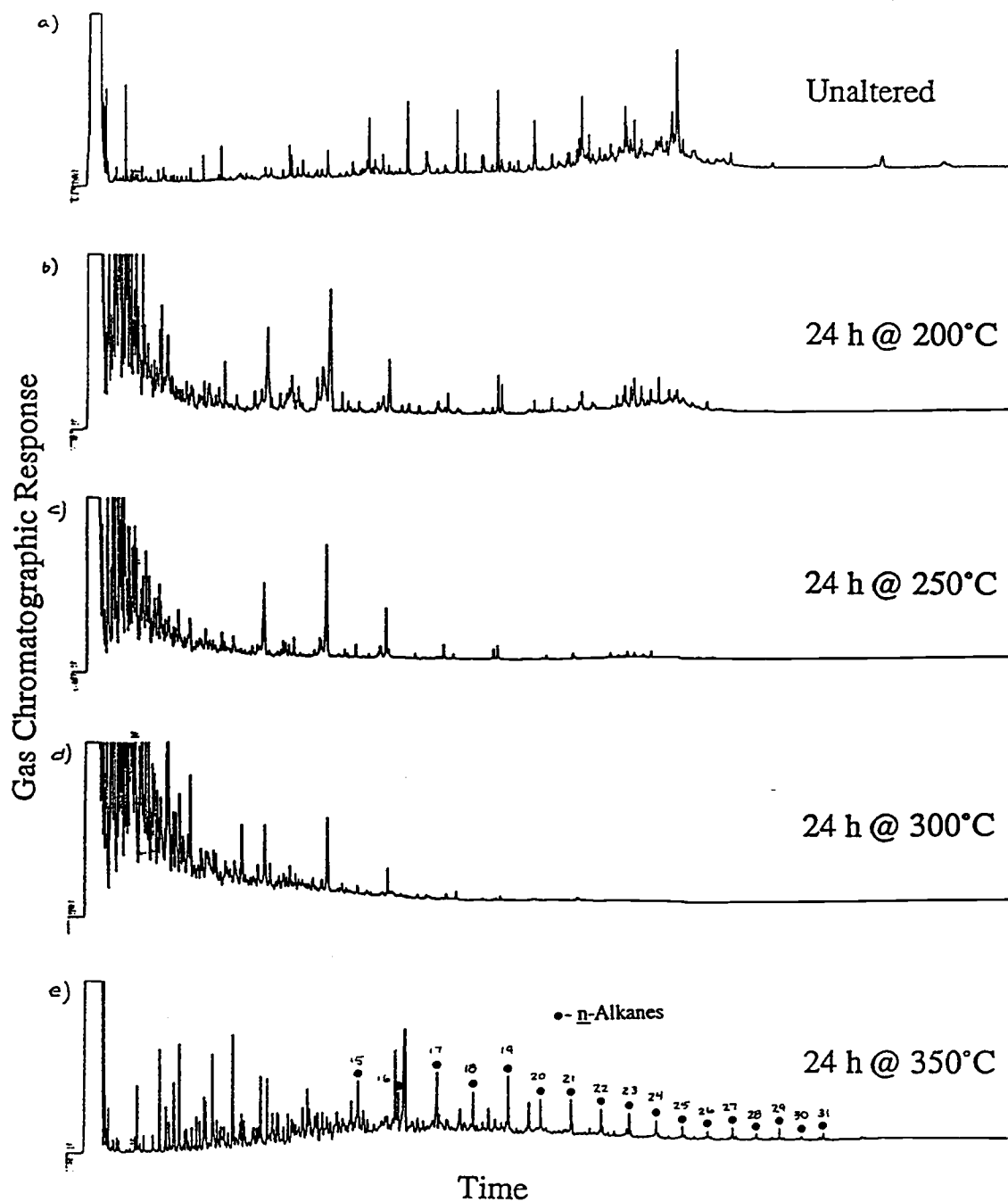
Figure 4.3. Gas chromatograms of the total extracts : a) Unaltered ; b) 24 hr @ 200°C; c) 24 hr @ 250°C; d) 24 hr @ 300°C; e) 24 hr @ 350°C. Numbers refer to carbon chain lengths of n-alkanes.
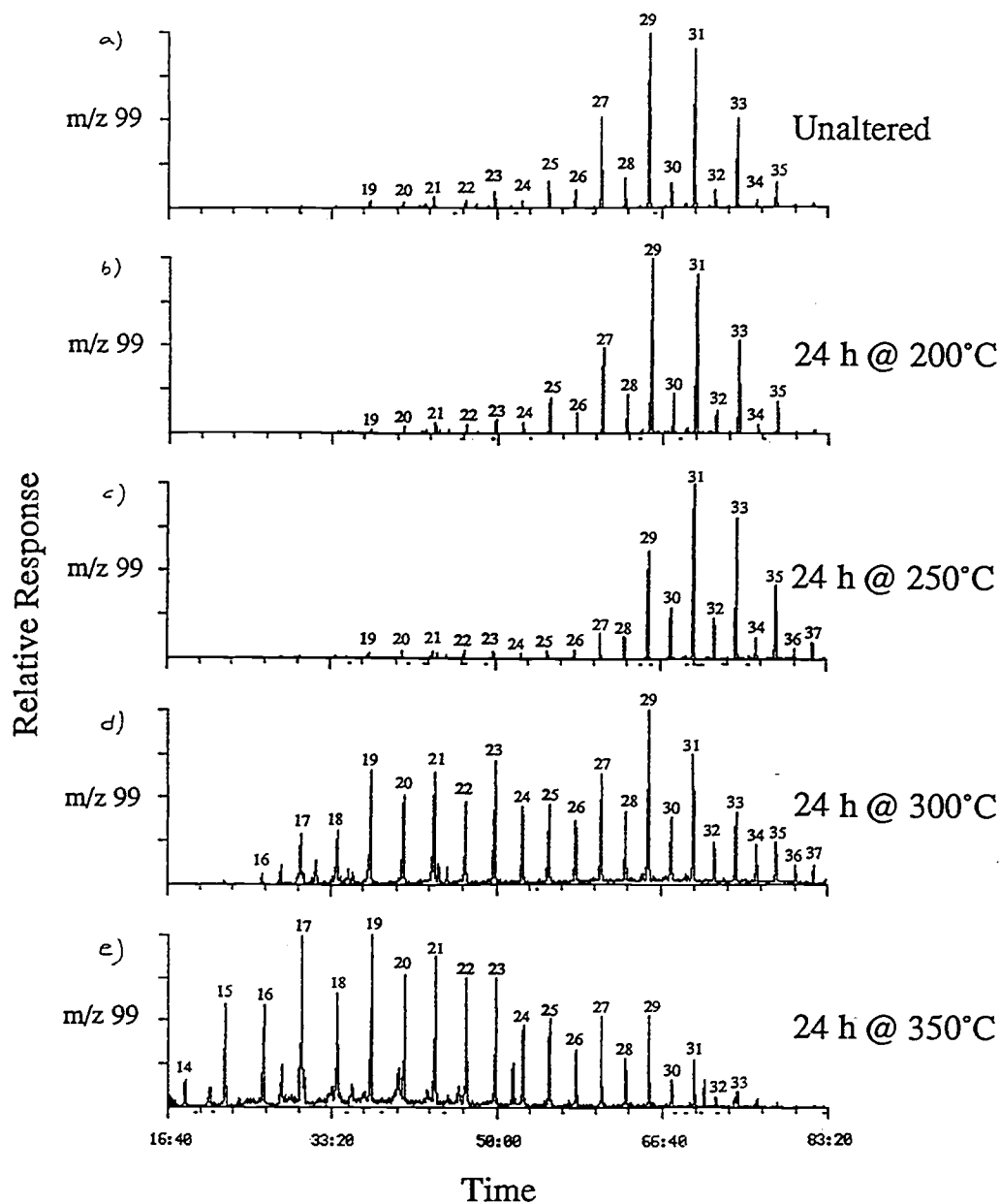
Figure 4.4. Mass fragmentograms of m/z 99, characteristic of n-alkanes : a) Unaltered ;
b) 24 hr @ 200°C; c) 24 hr @ 250°C; d) 24 hr @ 300°C; e) 24 hr @ 350°C. Numbers
refer to carbon chain lengths of n-alkanes.
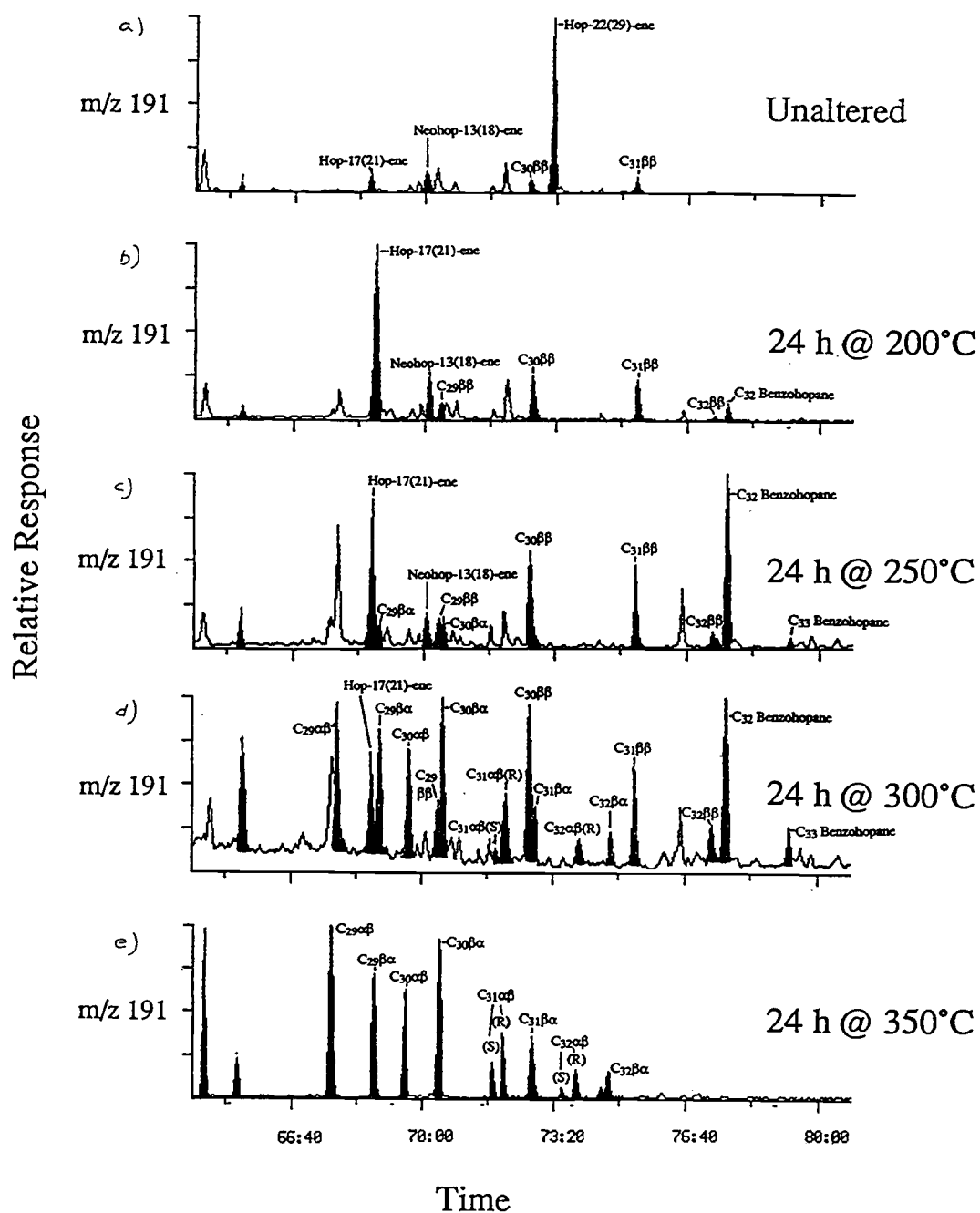
Figure 4.5. Mass fragmentograms of m/z 191, characteristic of triterpenoid hydrocarbons : a) Unaltered ; b) 24 hr @ 200°C; c) 24 hr @ 250°C; d) 24 hr @ 300°C; e) 24 hr @ 350°C. Concentrations of components are listed in Table 4.2.
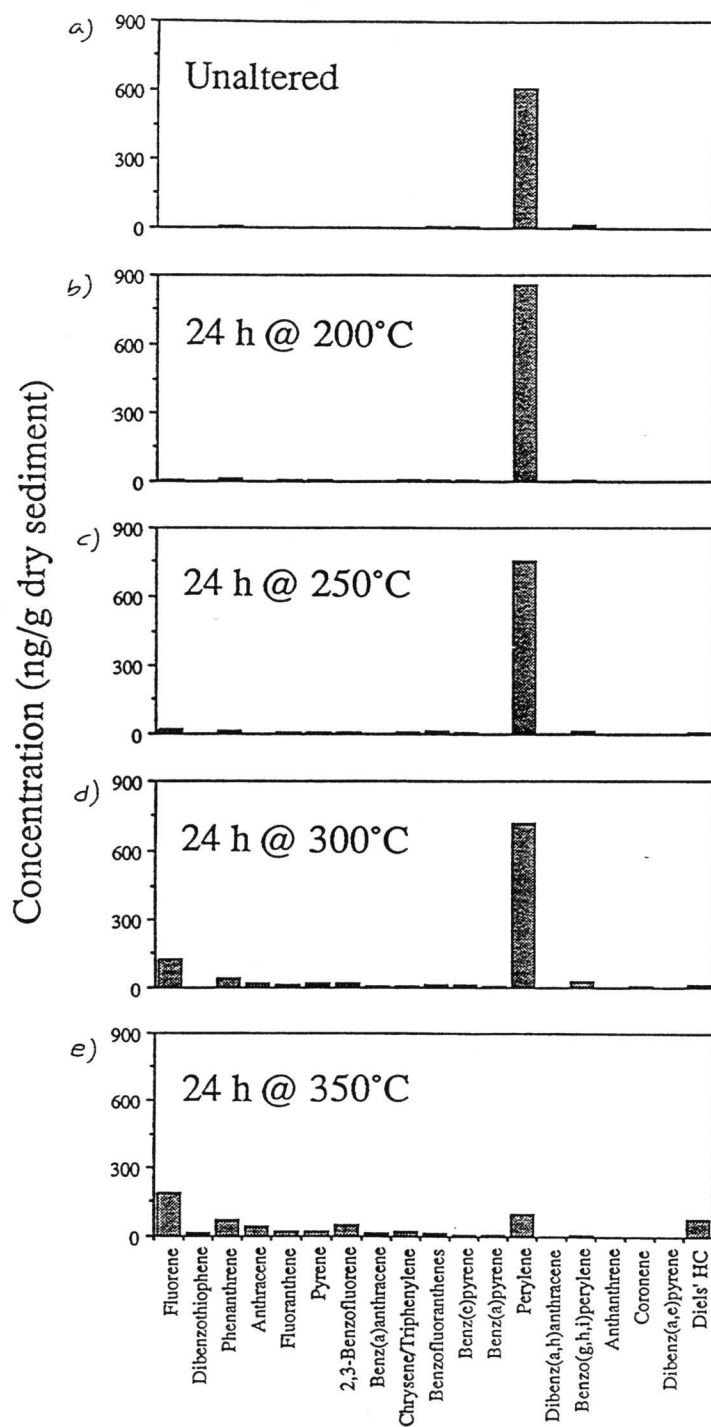
Figure 4.6. Polycyclic aromatic hydrocarbon distributions for heating experiments : a) Unaltered ; b) 24 hr @ 200°C; c) 24 hr @ 250°C; d) 24 hr @ 300°C; e) 24 hr @ 350°C.
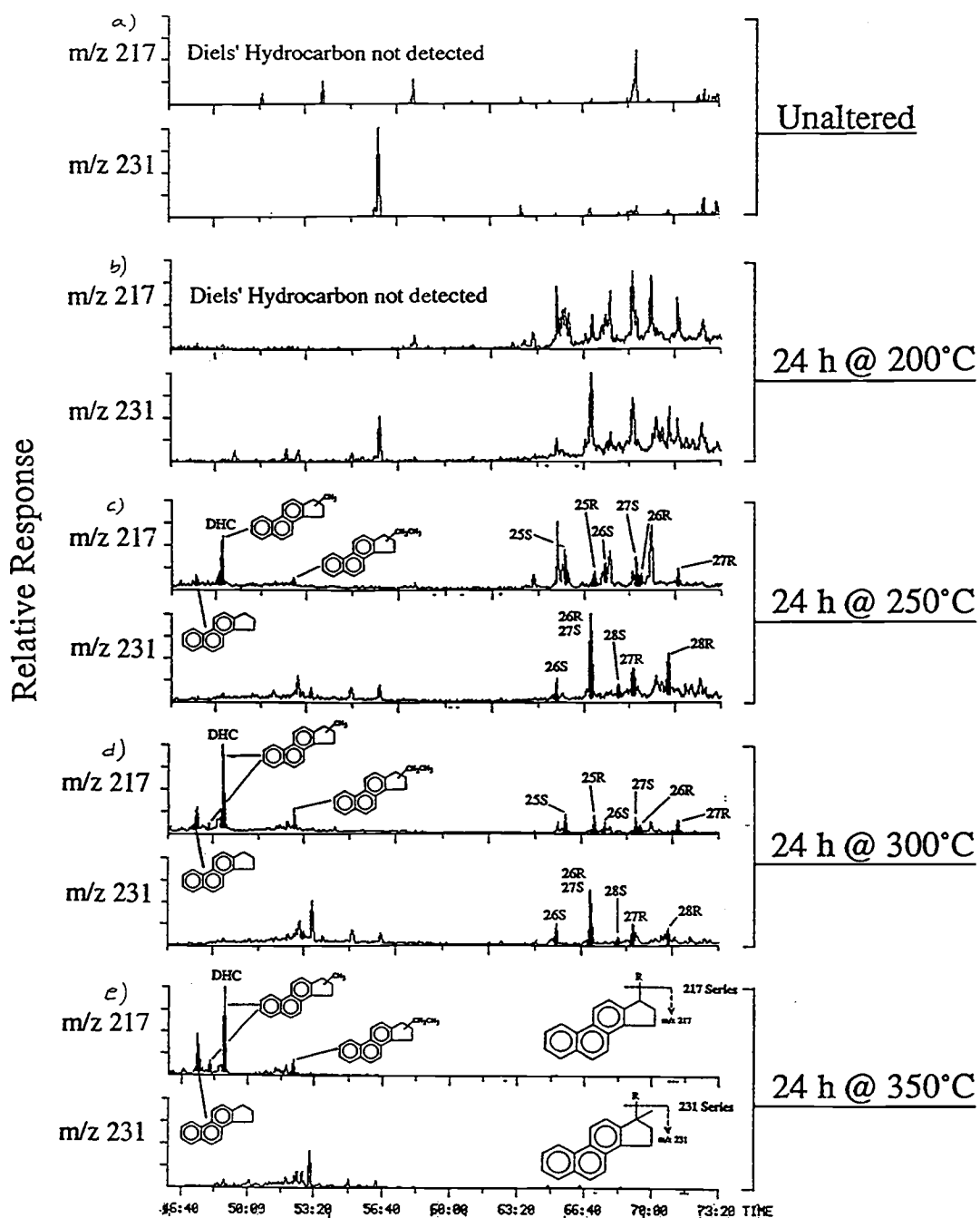
Figure 4.7. Mass fragmentograms of two series of triaromatic steroid hydrocarbons (m/z 217 and m/z 231) : a) Unaltered ; b) 24 hr @ 200°C; c) 24 hr @ 250°C; d) 24 hr @ 300°C; e) 24 hr @ 350°C. Concentrations of Diels' hydrocarbon relative to polycyclic aromatic hydrocarbons are shown in Fig. 4.6.
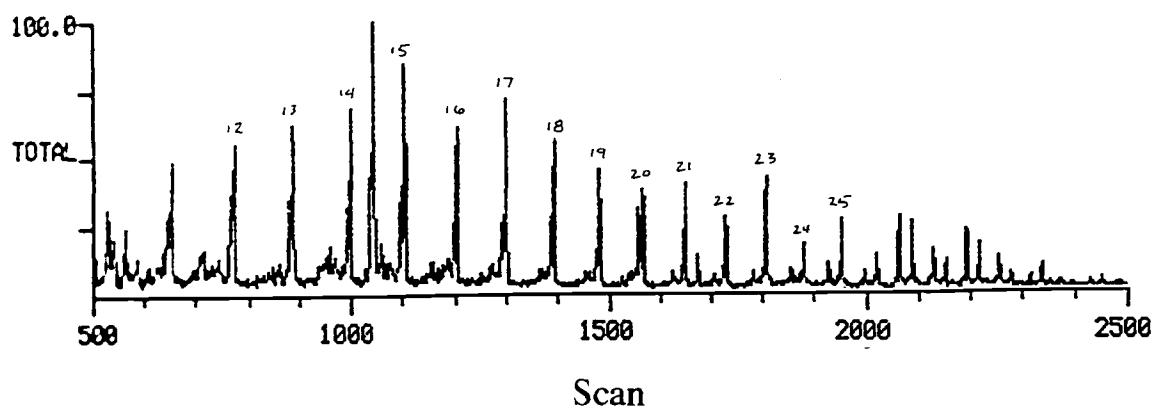
Figure 4.8. Mass fragmentogram (m/z 57, 58, 71, 72) representative of n-ketones present in the 350°C heating experiment.
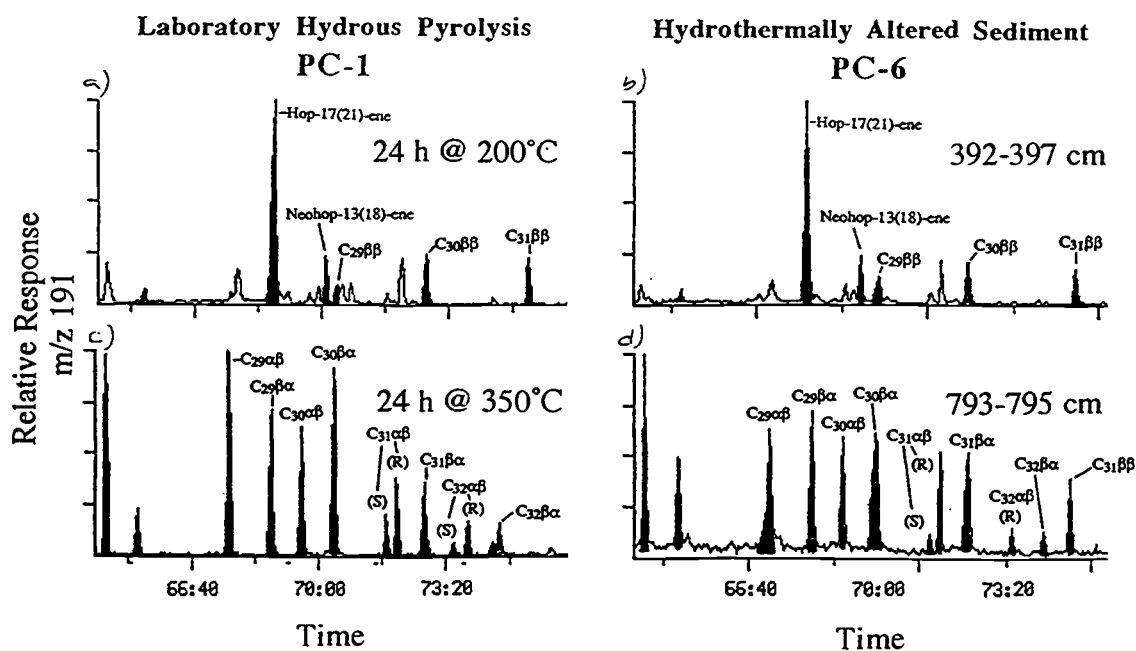
Figure 4.9. Mass fragmentograms m/z 191 representative of triterpenoid hydrocarbons: a) PC-1, 24 hr @ 200°C; b) PC-6, 392-397 cm below sea floor; c) PC-1, 24 hr @ 350°C; d) PC-6, 793-795 cm below sea floor. Distributions for heating experiments and PC-6 showing parallel transformations in the heating experiments and the naturally altered sediment.

CHAPTER 5

Simulation of Hydrothermal Catagenetic Transformations of Organic Matter in Surface and Downcore Sediments from the Northern Trough of Guaymas Basin

ABSTRACT

A series of pyrolysis experiments, using one surface sediment and two downcore sediments from the Northern Trough of Guaymas Basin, Gulf of California, was conducted to study the effects of time during the laboratory simulated hydrothermal catagenetic alteration of sedimentary organic matter. These experiments were conducted using a modified pyrolysis technique which eliminates the headspace and excess water inside the reaction vessel. Each sediment was pyrolyzed at 330°C for 24, 48 and 72 hr. The extent of alteration was measured by monitoring the n-alkanes, acyclic isoprenoids, steroid and triterpenoid biomarkers, polycyclic aromatic hydrocarbons, ketones and isoprenoid phenols. The experimental results were compared to sediment extracts which have been naturally altered by sill intrusion and accompanied hydrothermal fluid flow.

Smooth n-alkane patterns were generated with all sediments after 24 hr and full hopane and sterane maturation in 48 hr. The mature hopane ratios were altered by unequal destruction of the hopanes. The polycyclic aromatic hydrocarbons were progressively converted from a perylene- to phenanthrene-dominated pattern in the deepest sediment, and Diels' hydrocarbon was major in the upper and surface sediments. Ketones were present in the NSO fractions of all experiments.

The experimental pyrolysis experiments duplicate the natural hydrothermal alteration which has occurred by dolerite sill intrusions in the Guaymas Basin sediments. The results indicate that the extent of steroid diagenesis may be the most important factor in the formation of Diels' hydrocarbon. These experiments support the hypothesis that aliphatic ketones are common products under pyrolytic conditions.

INTRODUCTION

The production of petroleum hydrocarbons under marine hydrothermal conditions is a well documented process (Simoneit, 1988, 1990 and references within). The sedimentary organic matter associated with the Guaymas Basin hydrothermal system is pyrolyzed by the high thermal gradient of a heat source at depth and by dike and sill intrusions into the unconsolidated sediments. On Leg 64 of the DSDP drilling program, sediments from the Guaymas Basin rift system were sampled and several sills were identified which have been emplaced at different depths below the sea floor. The characteristics of these hydrothermally generated oils associated with the intrusions depends on the heating duration, heating temperature and nature of the source organic matter. The depths at which these sills were emplaced generated oils from sedimentary organic matter that had undergone different extents of diagenesis.

A set of seabed oils has been analyzed by radiochemical dating procedures and indicated that these oils have been generated from a carbon pool that is approximately 5000 years old (Peter et al., 1991). This was a broad, random selection of oils associated with the hydrothermal vents. This data indicates that most of the hydrothermal oils presently emanating from the vents are derived from relatively shallow marine sediments. The present study was a simulation of this hydrothermal generation process by laboratory pyrolyses of whole sediments from different depth horizons, and a comparison was made with the results of sediments that have been altered by a massive sill intrusion. The objective was to determine how sedimentary organic matter from different depth horizons affected the quality of the generated oils.

Experimental data on catagenetic conversions of sedimentary organic matter and petroleum source rocks have been obtained from a variety of high temperature experiments employing different experimental designs. These experiments have been performed in open or closed systems, different times, temperatures, dry or wet conditions, using diverse starting materials, sometimes with associated or added minerals. The experiments have demonstrated how time, temperature, minerals and pressure influence the organic matter conversions under the particular experimental conditions (Horsfield, 1984 and references within).

The presence of water is generally regarded as an important component of pyrolysis simulations, although ever since Lewan and co-workers (1979) used water in their experiments and named the procedure hydrous pyrolysis, the actual role of water has been a point of controversy, especially when oil-like pyrolysates have been formed

under anhydrous conditions (Comet et al., 1986). But it has been shown that under aqueous conditions, these pyrolysates resemble natural oils (Eglinton et al., 1986; Eglinton and Douglas, 1988; Lewan, 1983; Lewan et al., 1986). Water also has the important ability of facilitating the ionic mineral reactions which are primarily responsible for fixing the Eh and pH of a system (Eugster, 1986; Shock, 1990). Therefore the presence of water appears to be essential when simulation of the natural environment is desired.

In conventional hydrous pyrolysis experiments, many grams of rock chips or sediment are submerged under water so the expelled oil from the sample will float to the top of the water (Fig. 5.1). Once expelled, the oil is no longer in contact with the minerals. However, in the natural environment the organic matter remains in intimate contact with the mineral assemblage and can undergo a large number of geochemical processes in association with the mineral surfaces (Alexander et al., 1982; Goldstein, 1983; Johns, 1979). The resulting pyrolysates are similar to mature oils in many ways but biomarkers are commonly enriched in the less mature isomers. An explanation for this observation is a stronger acid than water may be needed for the isomerization of biomarkers, or any saturated chiral carbon in general (Larcher et al., 1986; Sieskind, 1979). This is where the catalytic effects of mineral surfaces are important processes. Numerous studies have shown that the mineral interactions exert considerable influence on the quality and quantity of organic matter evolution (Evans and Felbeck, 1983; Horsfield and Douglas, 1980; Huizinga et al., 1987a,b; Larcher et al., 1988; Lu et al., 1989; Peters et al., 1990; Spiro, 1984; Tannenbaum and Kaplan, 1985; Tannenbaum et al., 1986a,b).

The effects of the mineral/organic reactions will influence the rate of bitumen generation and biomarker conversion, but once removed from the mineral matrix, these reaction rates can change. The timing of the oil expelling process is unknown and therefore experimental results using the conventional hydrous pyrolysis technique may be misleading. But if the pyrolysate is confined with the minerals for the duration of the heating experiments, a more realistic set of results would be expected.

The method of aqueous confinement pyrolysis was employed to more realistically simulate the conditions found in the natural system (Fig. 5.2). This was done by confining the organic compounds to the inorganic matrix during the entire duration of the experiment. To avoid the potential problem of bitumen partitioning away form the inorganic sediment matrix, these experiments were done under hydrous but also in a confined pyrolysis system. The confined pyrolysis system eliminated the

large headspace from the reactor and also eliminated the large excess of water, thereby confining the organic pyrolysates to the bulk inorganic matrix. This principle is adapted after the confined-system pyrolysis and compaction pyrolysis methods recently used to study hydrocarbon generation (Monthioux et al., 1985; Blanc and Connan, 1992; Takeda et al., 1990). High pressure mini-reactors were adapted for this process. By combining the advances in our understanding of the actual organic chemical reactions which occur on mineral surfaces (Kissin, 1987; Lao et al., 1989; Regtop et al., 1985; Smith et al., 1989; Solomon, 1968; Weres et al., 1988; Wilson et al., 1986) and under high temperature aqueous conditions (Breslow, 1991; Blouri et al., 1981; Depeyre and Flicoteaux, 1991; Siskin and Katritzky, 1991 and references therein), a more realistic experimental procedure for hydrothermal simulations was developed .

EXPERIMENTAL

Samples. The samples used in the pyrolysis experiments were the following: AII-112-29 PC-5, a surface sediment obtained from the Northern Trough of Guaymas Basin in 1985; DSDP 481A-8-7 (top of pipe); and DSDP 481A-22-7 (top of pipe). The locations of the samples in the sediment column are shown in Fig. 5.3. The downcore samples were selected from sediments above and below a major sill intrusion that have not been thermally altered by the intrusion.

Hydrous pyrolysis experiments. Pyrolysis experiments were performed in Sno-Trik® T316 stainless steel high pressure pipes rated at 60,000 psi, sealed with end caps and heated in an air circulating oven where the temperature was set at 330° ±2°C. The reaction vessels and sediment samples were placed in a glove bag and flushed with five bag volumes of Ar. For each experiment 0.85g of dried sediment was combined with 0.250 mL of ultrapure water. Each sediment sample was homogenized and separated into three subsamples. Each sample was pyrolyzed for 24, 48 and 72 hrs.

Extraction and fractionation. The reaction vessels were removed from the oven and cooled to room temperature upon completion of the heating experiments. The reaction vessels were extracted with two 1 mL portions of methanol followed by five 1 mL portions of methylene chloride. The solvents and water from each pyrolysis experiment were combined in a centrifuge tube and the organic fraction separated and collected. The water was extracted with two additional portions of methylene chloride and the two methylene chloride fractions were combined. The methylene chloride was dried with anhydrous sodium sulfate and passed through an activated copper column to remove the elemental sulfur. The solvent was removed using a rotary evaporator at 30°C. The total extract was redissolved in 2 mL of methylene chloride and deasphalted with 100 mL of heptane. The asphaltenes were allowed to precipitate overnight and removed by filtration. The deasphalted fractions were concentrated to 2 mL and fractionated by column chromatography (30 cm x 1 cm) packed with 3.8 g alumina (fully active) over 3.8 g silica gel (fully active). The samples were separated into three fractions by elution with 50 mL heptane (nonpolar, F1), 50 mL toluene (aromatic, F2) and 25 mL methanol (polar , F3).

Gas chromatography. Gas chromatography (GC) of the pyrolysate fractions was performed with a Hewlett Packard 5890A equipped with a 30 m x 0.25 mm i.d. DB-5 open tubular column (0.25 μm film thickness). The GC oven was heated using

the following program : isothermal for 2 min. at 65°C, 4°/min. to 310°C, and isothermal for 30 min., with the injector at 290°C, detector at 325°C, and helium as the carrier gas.

Gas chromatography-mass spectrometry. The gas chromatography-mass spectrometry (GC-MS) was performed on a Finnigan 9610 gas chromatograph coupled to a Finnigan 4021 quadrupole mass spectrometer operated at 70 eV over the mass range 50-650 dalton and a cycle time of 2.0 s. The GC oven temperature was programmed at isothermal for 2 min. at 65°C, 3°/min. to 310°C, and isothermal for 30 min., with the injector at 290°C, and helium as the carrier gas. The MS data were processed with an on-line Finnigan-Incos 2300 computer data system.

RESULTS AND DISCUSSION

The gas chromatograms of the aliphatic, aromatic and NSO fractions for all of the unaltered and pyrolyzed sediment extracts are presented in Appendix 4. With the exception of the 48 hr pyrolysis of sample 481A-22-7 (top), which developed a leak during the experiment, all of the confined system pyrolysis experiments maintained a pressure tight seal. The molecular ratios of the 48 hr pyrolysis of 481A-22-7 (top) were calculated and are presented in the results section, although quantitatively there was a significant drop in the bitumen yield.

AII-112-29 PC-5. Results for the aliphatic fractions are summarized in Table 5.1. The unheated surface sediment from the Northern Trough of Guaymas Basin was characteristic of other surface sediments from that region (Simoneit et al., 1979). For example, the n-alkanes have a Carbon Preference Index (CPI) of 5.8, and the major triterpenoid was diploptene. All of the heating experiments of this sediment generated bitumen with n-alkane distributions typical of oils from the Guaymas Basin. The CPI was 1 for all three heating durations; C_{max} was 15 to 17; and the Pr/Ph ranged from 1 to 1.1. There was a progressive increase in the amount of n-alkanes relative to pristane and phytane as a function of time. Pristane and phytane were the major compounds in the 24 hr experiment but were secondary in the 72 hr experiment.

The distributions of the triterpenoid hydrocarbons for the unaltered and heating experiments for the surface sediment are shown in Fig. 5.4. The triterpane distribution of the 24 hr experiment ranges from C_{27} to C_{35} (C_{28} missing) and consists primarily of the $17\alpha(H),21\beta(H)$-hopanes and a lesser amount of the $17\beta(H),21\alpha(H)$-hopanes (moretanes). The C-22 S to R epimer ratio of the $17\alpha(H),21\beta(H)$-31-homohopane is $22S/(22S + 22R) = 0.42$, not equivalent to the maturity of a typical crude oil (equilibrium ratio = 0.60, Ensminger et al., 1974, 1977), but it is typical for some hydrothermal oils previously reported (Kawka and Simoneit, 1987). The S/(S + R) stays relatively constant for the 48 hr and 72 hr experiments, but the longer duration heating experiments resulted in a large amount of destruction of the biomarkers. Plots of the relative abundances of some triterpenoid hydrocarbons are shown in Figure 5.5. The relative amounts of the triterpenoid biomarkers indicate that the triterpenoid molecular ratios are probably affected more by preferential destruction rather than interconversion from one epimer to another.

Fragmentograms of the steroid hydrocarbons are presented in Fig. 5.6. The unaltered sample is dominated by sterenes and all three heating experiments are

dominated by C_{27} to C_{29} steranes, primarily the $5\alpha(H),14\alpha(H),17\alpha(H)$-20R isomers, with lower amounts of the $5\beta(H),14\alpha(H),17\alpha(H)$-20R isomers. There was little change in the sterane distribution as a function of heating time.

The aromatic fraction of the unaltered sample was dominated by perylene, primarily derived by diagenesis (Louda and Baker, 1984), but the distributions of the major resolved aromatic compounds were dominated by Diels' hydrocarbon (1,2-(3'-methylcyclopenteno)phenanthrene, DHC-2), with a lesser amount of a C_{18} isomer (DHC-1), in the heating experiments (Fig. 5.7). Diels' hydrocarbon, common in Guaymas Basin oils, has been used as an indicator of the rapid hydrothermal petroleum generation processes (Kawka, 1990; Simoneit et al., 1992). The rest of the aromatic compounds present in these fractions are primarily low molecular weight PAH and alkyl-PAH (i.e. phenanthrene and methyl-, dimethyl- and trimethylphenanthrenes).

Several homologous series of ketones, ranging from C_{14} to > C_{33}, were present in all of the heating experiments. They were some of the major components in the NSO fractions, with alkan-2-ones being the highest in concentrations, with lesser amounts of the 3-, 4- 5- (and higher) homologs. The isoprenoid phenols were also generated in the heating experiments, although they were minor components.

481A-8-7 (top pf pipe). The results of the aliphatic fraction are presented in Table 5.2. All of the heating experiments of this downcore sediment generated bitumen with n-alkane distributions typical of oils from the Guaymas Basin. As with the surface sediment, there was a progressive increase in the n-alkanes relative to the isoprenoid hydrocarbons pristane and phytane with respect to heating duration. The aliphatic fraction of the 48 hr experiment was characterized by the appearance of a large hump or unresolved complex mixture (UCM) in the n-C_{25} to n-C_{35} range.

The mass fragmentograms characteristic of the triterpenoid hydrocarbons for the unaltered and heating experiments are shown in Fig. 5.8. The triterpane distribution of the 24 hr experiment was similar to that of the surface sediment pyrolysis where the hopanes ranged from C_{27} to C_{35} (C_{28} missing) and consisted primarily of the $17\alpha(H),21\beta(H)$-hopanes and a lesser amount of the $17\beta(H),21\alpha(H)$-hopanes (moretanes). The C-22 S to R epimer ratio of the $17\alpha(H),21\beta(H)$-31-homohopane is 22S/(22S + 22R) = 0.46, not equivalent to the maturity of a typical crude oils, but the S/(S + R) = 0.59 in the 48 hr experiment, indicating that the epimers are in their equilibrium ratios. The 48 hr experiment resulted in a large increase in the amount of biomarkers relative to the 24 hr experiment (Fig. 5.9), corresponding to the

formation of the large UCM in the aliphatic fraction. There was significant destruction of the biomarkers in the 72 hr experiment. The reversal in the C_{31}-homohopane S/(S + R) ratio in the 72 hr experiment is the result of hopane destruction.

Fragmentograms of the steroid hydrocarbons are presented in Fig. 5.10. The unaltered sample is dominated by C_{27} to C_{29} sterenes. The 24 hr experiment consists of C_{27} to C_{29} steranes, primarily the $5\alpha(H),14\alpha(H),17\alpha(H)$-20R isomers, with lower amounts of the $5\beta(H),14\alpha(H),17\alpha(H)$-20R isomers. Extensive isomerization of the steranes occurred in the 48 hr experiment resulting in a pattern representative of a fully mature oil. Destruction of the steranes occurred in the 72 hr experiment, a loss of sterane hydrocarbons analogous to the destruction of the triterpanes. The remaining steranes were primarily the $5\alpha(H),14\alpha(H),17\alpha(H)$-20R isomers, with lower amounts of the $5\beta(H),14\alpha(H),17\alpha(H)$-20R isomers.

A summary of the PAH quantitation is shown in Fig. 5.11. The aromatic fraction of the unaltered sample was dominated by perylene, and there was a trend of perylene destruction accompanied by pyrolytic PAH formation as a function of time in the heating experiments. Diels' hydrocarbon was also formed in relatively high amounts, but in lower amounts compared to the concentrations obtained by the pyrolyses of the surface sediment PC-5. The pyrolyses of this sediment formed Diels' hydrocarbon in concentrations approximately 30% of the surface sediment pyrolyses.

The multiple homologous series of ketones were all present in the heating experiments and were well resolved and in high amounts in the NSO fractions. As with the pyrolysis of the surface sediment, the alkan-2-ones were in highest concentrations, with lesser amounts of the 3-, 4- 5- (and higher) homologs. The isoprenoid phenols were also generated in the heating experiments, although they were minor components.

481A-22-7 (top of pipe). The results of the aliphatic fraction are presented in Table 5.3. All of the heating experiments of this sediment generated bitumen with n-alkane distributions typical of those found in oils of Guaymas Basin. The relative amounts of n-alkanes to pristane and phytane were much higher in these experiments than in the previous experiments. The 48 hr experiment developed a leak some time during the experiment, which resulted in an overall decrease in extactable organic matter.

The mass fragmentograms characteristic of the triterpenoid hydrocarbons for the unaltered and heating experiments are shown in Fig. 5.12. The triterpane

distribution of the unaltered sediment consisted of hop-17(21)-ene and the C_{29} to C_{31} $\beta\beta$-hopanes. The pyrolysis experiments formed hopanes ranging from C_{27} to C_{35} (C_{28} missing) in their fully mature configurations, the C-22 S to R epimer ratio of the $17\alpha(H),21\beta(H)$-31-homohopane is 22S/(22S + 22R) = 0.59 in the 48 hr experiment and 0.58 in the 72 hr experiment. Fig. 5.13 shows the relative amounts of the selected hopane biomarkers. The minimum values of the 48 hr experiment correspond to the pressure vessel that leaked during the experiment.

The sterane plots are shown in Fig. 5.14. Conversion from the sterene pattern of the unaltered to the oil-like pattern occurred in only 24 hr, indicating that the extensive isomerization to the fully mature signature is rapid. This pattern remained unchanged for the 48 and 72 hr experiments.

The histograms from the PAH quantitation are shown in Fig. 5.15. The aromatic fraction of the unaltered sample was dominated by perylene, and there was a large amount of perylene destruction accompanied by pyrolytic PAH formation as a function of time in the heating experiments. Diels' hydrocarbon was formed in only trace levels in the 24 and 72 hr experiments.

The homologous series of ketones were the major compounds of the NSO fractions of the 24 and 72 hr experiments, with only trace amounts in the 48 hr experiment. The low amount of ketones in the 48 hr experiment is likely an artifact due to the leak in the reaction vessel. The isoprenoid phenols were not formed in any of the heating experiments of sediment 481A-22-7 (top).

The results clearly show that there are significant catagenetic changes as a result of the heating experiments, demonstrating that under these experimental conditions pyrolysates very similar to hydrothermal oils can be generated by confinement pyrolysis.

Effects of time on the pyrolysates. Increasing the duration of the experiments from 24 to 72 hr resulted in the general trend of increasing the amount of n-alkanes relative to the isoprenoids pristane and phytane. Isoprenoids can be derived from several sources such as the phytyl side chain of chlorophyll (Cox et al., 1970; Maxwell et al., 1972), from tocopherols (Goosens et al., 1984), as well as from ether lipids from Archaebacteria (Michaelis and Albright, 1979). It is possible that these isoprenoids are released from the kerogen earlier than the n-alkanes due to slightly weaker chemical bonds linking the isoprenoids to the bound matrix.

The triterpenoid biomarker distribution in the pyrolysis of the surface sediment AII-112-29 PC-5 is probably the result of the simultaneous generation, isomerization

and destruction of the compounds in this series. The distribution after 24 hr closely resembles that of an oil, although the C_{31}-homohopane S/(S + R) ratio did not indicate full maturation. The 48 and 72 hr experiments appear to be post-mature, due to the destruction of the biomarkers.

A similar trend was observed in the 481A-8-7 (top) sediment, but this sample reached full maturation after 48 hr, both in the hopane and sterane biomarkers. The reversal in the C_{31}-homohopane S/(S + R) ratio after 72 hr was a result of a preferential loss of the R isomer from the extensive loss of the biomarkers due to thermal destruction.

Sample 481A-22-7 (top) also reached full maturation in both the steranes and hopanes after 48 hr and maintained these biomarker distributions through to the 72 hr experiment. Considering that the 48 hr experiment leaked, a comparison of the 24 hr to the 72 hr experiment suggests little change, or even a slight increase in the amount of hopanes for the 72 hr duration.

Using the hopane and sterane biomarkers as a measure, the "oil window" was reached within 72 hr of heating for all three sediments. This demonstrates that maturation of the sedimentary organic matter accompanied by full hopane and sterane isomerization can be achieved from recent, thermally-unaltered sedimentary organic matter. These biomarker conversions match closely those changes observed in sediments from DSDP Site 481A, where the sedimentary organic matter in the proximity of a dolerite sill was thermally altered and resulted in maturation of the biomarker signatures (see Ch. 2, Figs. 2.17 and 2.18).

The PAH distributions reflect the destruction of perylene coupled with the generation of lower molecular weight aromatic compounds. This trend was also seen in the sediments that were naturally altered in DSDP Site 481A (see Ch 2. Fig. 2.19). The experimental set that most closely matched the natural trend was the 481A-22-7 (top) sediment. But in the experiments a large amount of anthracene was also formed, a PAH which is commonly found in hydrothermal oils (Kawka and Simoneit, 1990). Anthracene was in very low concentrations or not detected in the naturally altered sediments of Site 481A.

Effects of depth on the pyrolysates. The most striking trend observed as a function of sediment depth was in the polycyclic aromatic hydrocarbons. Both the surface sediment and sample 481A-8-7 (top), a sample from the hydrothermally unaltered sediments above the sill, generated a large amount of Diels' hydrocarbon, but this compound was present in only trace amounts in the pyrolysates of 481A-22-7

(top). This compound has been proposed as a tracer of high temperature alteration of sedimentary organic matter, but its absence suggests that the formation of Diels' hydrocarbon is more than just temperature dependent, that its formation is a function of the nature of the organic matter. A plot showing the relative amounts of Diels' hydrocarbon as a function of temperature for the three samples is shown in Fig. 5.16. Diels' hydrocarbon is thought to be primarily derived from functionalized steroid compounds in the sediments, and under hydrothermal conditions the steroid is rapidly dehydrogenated to the triaromatic steroid hydrocarbon. The results indicate that the extent of diagenesis affects the yield of Diels' hydrocarbon. It is possible that as diagenesis progresses, the functionalized steroid natural products slowly become defunctionalized and reduced to saturated sterane hydrocarbons. Hydrothermal alteration of saturated steranes favors epimerization and destruction reactions rather than aromatization reactions. This would explain the lack of Diels' hydrocarbon in the pyrolysis of the deepest sediments. The present seabed oils, which contain high amounts of Diels' hydrocarbon (Kawka, 1990), are likely derived from sedimentary organic matter that has not undergone extensive diagenesis, in agreement with the young ^{14}C ages of the oils (Peter et al., 1991).

The series of ketones present in all of the pyrolysates have also been found in hydrothermal oils, extracts of hydrothermally-altered sediments, and simulated pyrolysis experiments. The ubiquitous presence of these compounds in the bitumen and oils of high temperature origin (Leif et al., 1992; George and Jardine, 1993) suggests that these compounds may be good indicators of high temperature hydrothermal alterations of organic matter. The isoprenoid phenols, previously identified as common constituents in the NSO fractions of hydrothermal oils, were generated in all of the heating experiments. Their concentrations were low, but the distributions of these compounds in the heating experiments matched those in the seabed oils.

The procedure of confinement pyrolysis was successful in converting the recent, immature sedimentary organic matter to products resembling mature oils or sedimentary organic matter that has been extensively altered by high temperature hydrothermal activity. Parallel experiments using the conventional hydrous pyrolysis technique were not performed. Therefore, it cannot be concluded that these conversions would have occurred at different rates under hydrous pyrolysis conditions. Although, numerous experiments have been carried out on Guaymas

Basin sediments using conventional hydrous pyrolysis conditions under similar time and temperature conditions, full biomarker isomerization was never observed.

CONCLUSIONS

The procedure of confinement pyrolysis has been performed using whole, unconsolidated sediments from the Guaymas Basin hydrothermal system. Thermal alteration of immature sedimentary organic matter to a fully mature extractable bitumen has been achieved using three different sediments from the Guaymas Basin hydrothermal system, with full maturation occurring after 48 hr. Comparison of the major compounds in the aliphatic, aromatic and NSO fractions generated in the heating experiments with those in naturally-altered sediment sequences indicates a reasonable match in the quality and quantity of those components.

Application of these experimental results to oil generation in the Guaymas Basin indicates that diagenesis may play an important role in altering the nature of the source organic matter, especially the steroids and their derivatives. The aliphatic ketones appear to be good universal indicators for high temperature catagenetic processes.

Table 5.1. Selected parameters for the aliphatic fractions of AII-112-29 PC-5.

Parameter	AII-112-29 PC5			
	Unaltered	24 hr @ 330°C	48 hr @ 330°C	72 hr @ 330°C
$\underline{n}$-alkane range	15-35	12-39	12-39	11-39
CPI	5.8	1.0	1.0	1.0
C_{max}	31	17	15	15
Pr/Ph	n.d.	1	1.06	1.12
Pr/$\underline{n}$-C_{17}	n.d.	1.16	0.98	0.81
Ph/$\underline{n}$-C_{18}	n.d.	1.33	1.04	0.87
S/(S+R) C_{31}	-	0.42	0.37	0.45
S/(S+R) C_{32}	-	0.46	0.38	0.44
$\underline{29,30,31H}$ 29,30,31M	-	2.48	1.75	2.03
27R/29R	-	1.96	2.40	3.60
27R/28R	-	2.48	2.48	4.50
28R/29R	-	0.79	0.97	0.80

n.d. = not determined

S/(S+R) = C-22 S and R epimer ratios for C_{31} and C_{32} α-homohopanes

$$\frac{29,30,31 \text{ H}}{29,30,31 \text{ M}} = \frac{C_{29} + C_{30} + C_{31} \text{ } \alpha\text{-hopanes}}{C_{29} + C_{30} + C_{31} \text{ moretanes}} \qquad \frac{27R}{28R} = \frac{C_{27} \text{ 20 R } \alpha\alpha\alpha\text{-sterane}}{C_{28} \text{ 20 R } \alpha\alpha\alpha\text{-sterane}}$$

$$\frac{27R}{29R} = \frac{C_{27} \text{ 20 R } \alpha\alpha\alpha\text{-sterane}}{C_{29} \text{ 20 R } \alpha\alpha\alpha\text{-sterane}} \qquad \frac{28R}{29R} = \frac{C_{28} \text{ 20 R } \alpha\alpha\alpha\text{-sterane}}{C_{29} \text{ 20 R } \alpha\alpha\alpha\text{-sterane}}$$

Table 5.2. Selected parameters for the aliphatic fractions of 481A-8-7 (top of pipe).

Parameter	481A-8-7 (top of pipe)			
	Unaltered	24 hr @ 330°C	48 hr @ 330°C	72 hr @ 330°C
$\underline{n}$-alkane range	12-32	10-39	10-38	12-38
CPI	3.6	1.0	1.0	1.0
C_{max}	29	15	15	15
Pr/Ph	0.47	2.3	2.0	2.2
Pr/$\underline{n}$-C_{17}	0.31	1.10	0.85	0.80
Ph/$\underline{n}$-C_{18}	1.04	0.56	0.50	0.40
S/(S+R) C_{31}	-	0.46	0.59	0.46
S/(S+R) C_{32}	-	0.49	0.55	0.48
$\dfrac{29,30,31H}{29,30,31M}$	-	2.04	3.30	1.64
27R/29R	-	1.44	1.05	3.79
27R/28R	-	2.4	1.86	4.34
28R/29R	-	0.60	0.56	0.87

S/(S+R) = C-22 S and R epimer ratios for C_{31} and C_{32} α-homohopanes

$$\frac{29,30,31\ H}{29,30,31\ M} = \frac{C_{29} + C_{30} + C_{31}\ \alpha\text{-hopanes}}{C_{29} + C_{30} + C_{31}\ \text{moretanes}} \qquad \frac{27R}{28R} = \frac{C_{27}\ 20\ R\ \alpha\alpha\alpha\text{-sterane}}{C_{28}\ 20\ R\ \alpha\alpha\alpha\text{-sterane}}$$

$$\frac{27R}{29R} = \frac{C_{27}\ 20\ R\ \alpha\alpha\alpha\text{-sterane}}{C_{29}\ 20\ R\ \alpha\alpha\alpha\text{-sterane}} \qquad \frac{28R}{29R} = \frac{C_{28}\ 20\ R\ \alpha\alpha\alpha\text{-sterane}}{C_{29}\ 20\ R\ \alpha\alpha\alpha\text{-sterane}}$$

Table 5.3. Selected parameters for the aliphatic fractions of 481A-22-7 (top of pipe).

	481A-22-7 (top of pipe)			
Parameter	Unaltered	24 hr @ 330°C	48 hr @ 330°C	72 hr @ 330°C
n-alkane range	13-31	10-37	13-38	12-38
CPI	4.13	1.1	1.0	1.1
C_{max}	29	19	16	17
Pr/Ph	0.44	2.3	-	2.4
Pr/n-C_{17}	1.17	0.44	-	0.29
Ph/n-C_{18}	4.43	0.20	-	0.13
S/(S+R) C_{31}	-	0.47	0.59	0.58
S/(S+R) C_{32}	-	0.57	0.56	0.48
$\frac{29,30,31H}{29,30,31M}$	-	2.40	3.81	3.56
27R/29R	-	0.68	0.50	0.57
27R/28R	-	2.63	1.71	1.37
28R/29R	-	0.26	0.29	0.41

S/(S+R) = C-22 S and R epimer ratios for C_{31} and C_{32} α-homohopanes

$$\frac{29,30,31\ H}{29,30,31\ M} = \frac{C_{29} + C_{30} + C_{31}\ \alpha\text{-hopanes}}{C_{29} + C_{30} + C_{31}\ \text{moretanes}}$$

$$\frac{27R}{28R} = \frac{C_{27}\ 20\ R\ \alpha\alpha\alpha\text{-sterane}}{C_{28}\ 20\ R\ \alpha\alpha\alpha\text{-sterane}}$$

$$\frac{27R}{29R} = \frac{C_{27}\ 20\ R\ \alpha\alpha\alpha\text{-sterane}}{C_{29}\ 20\ R\ \alpha\alpha\alpha\text{-sterane}}$$

$$\frac{28R}{29R} = \frac{C_{28}\ 20\ R\ \alpha\alpha\alpha\text{-sterane}}{C_{29}\ 20\ R\ \alpha\alpha\alpha\text{-sterane}}$$

Before Heating   During Heating   After Heating

Expelled Oil
Water
Reaction Vessel
Sample

Figure 5.1. Diagram showing expulsion of pyrolysates during conventional hydrous pyrolysis.

Before Heating   During Heating   After Heating

Sample/Water
Reaction Vessel
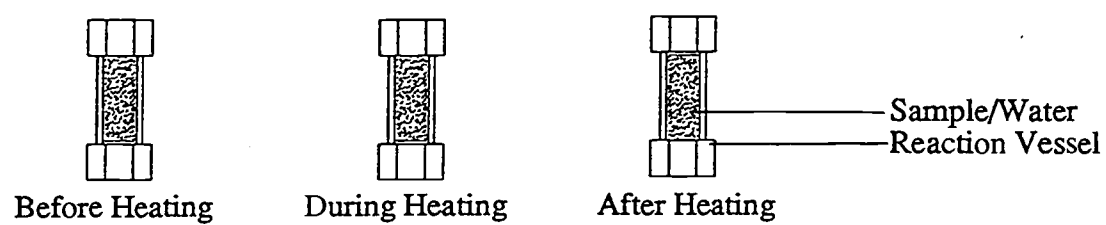
Figure 5.2. Diagram showing the principle of confinement pyrolysis.
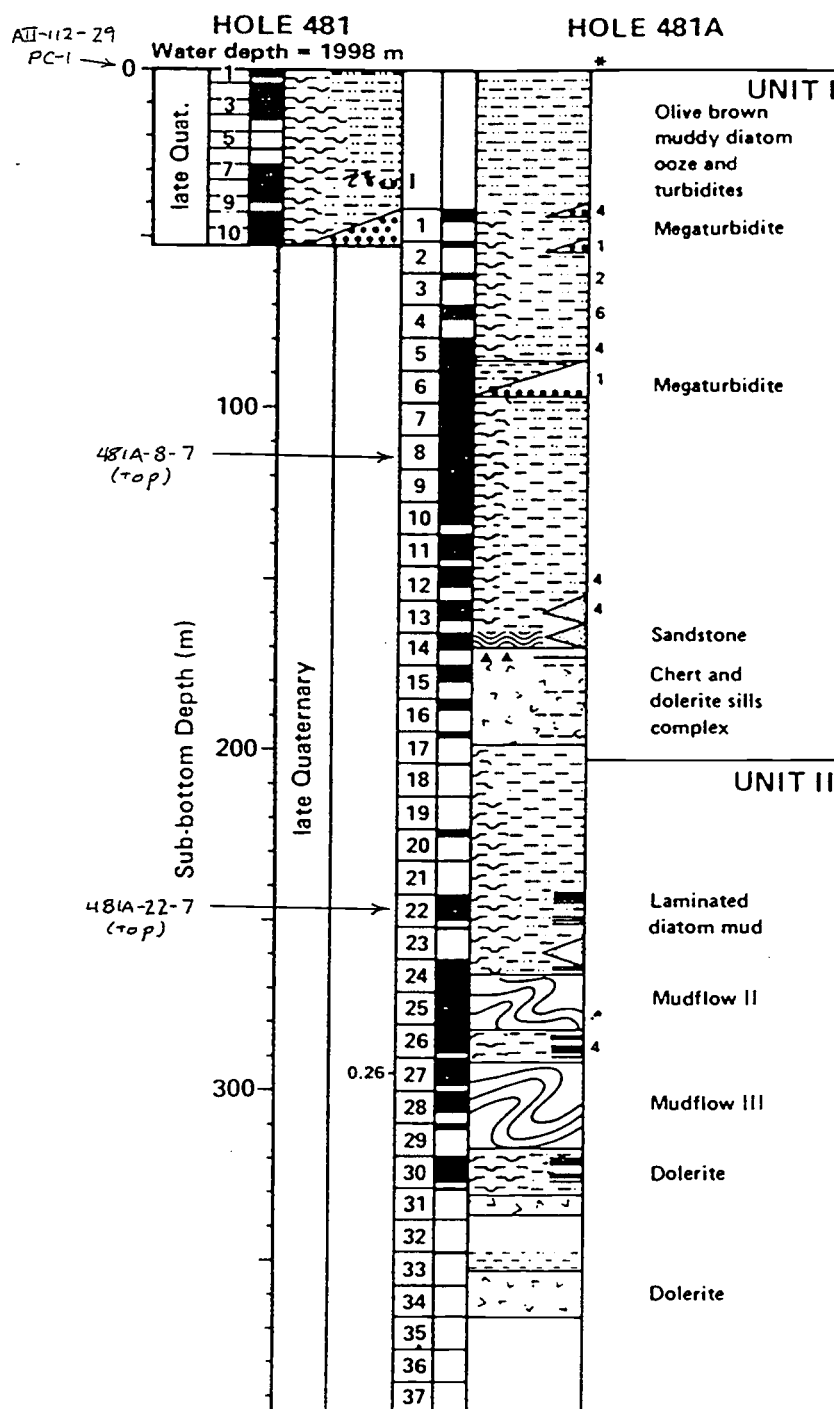
Figure 5.3. Lithologic column for DSDP Site 481A, location of samples for pyrolysis are shown (Curray et al., 1982).
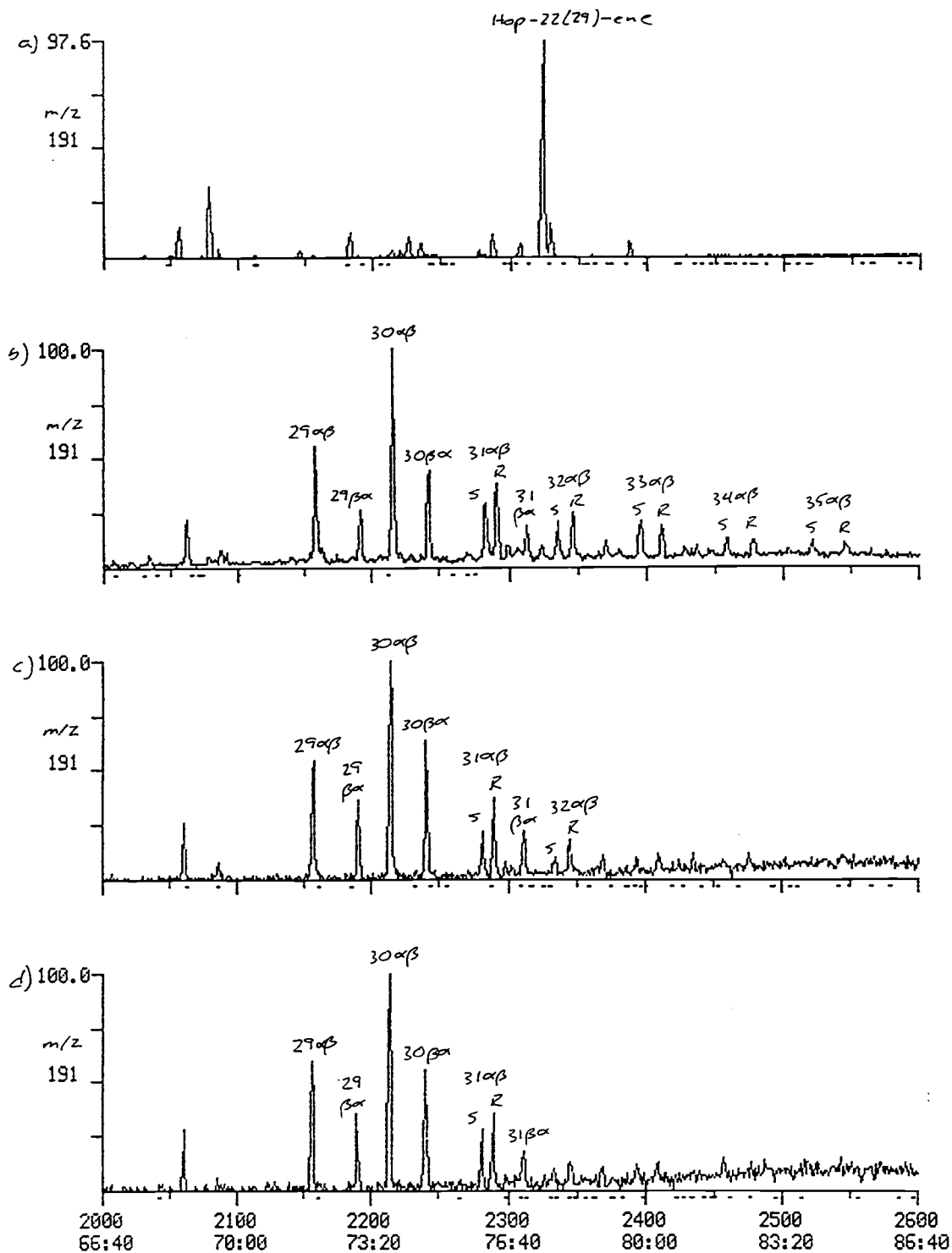
Figure 5.4. Representative mass fragmentograms m/z 191 for the triterpenoid hydrocarbons in the extracts of sediment AII-112-29 PC1: a) Unaltered; b) 24 hr @ 330°C; c) 48 hr @ 330°C; d) 72 hr @ 330°C.
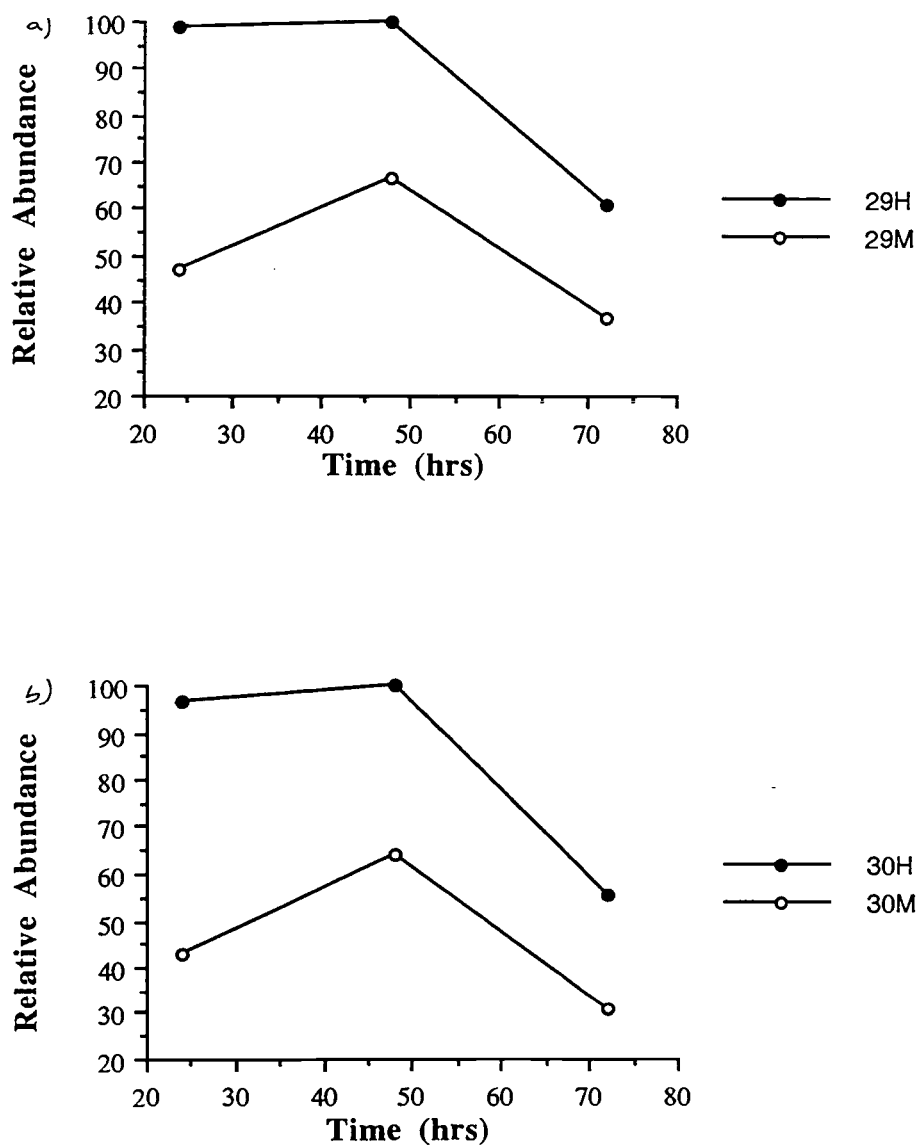
Figure 5.5. Relative abundance of selected triterpane biomarkers in the heating experiments of sediment AII-112-29 PC-5: a) 17α(H),21β(H)-29-hopane and 17β(H),21α(H)-29-hopane vs. time, and b) 17α(H),21β(H)-30-hopane and 17β(H),21α(H)-30-hopane vs. time.
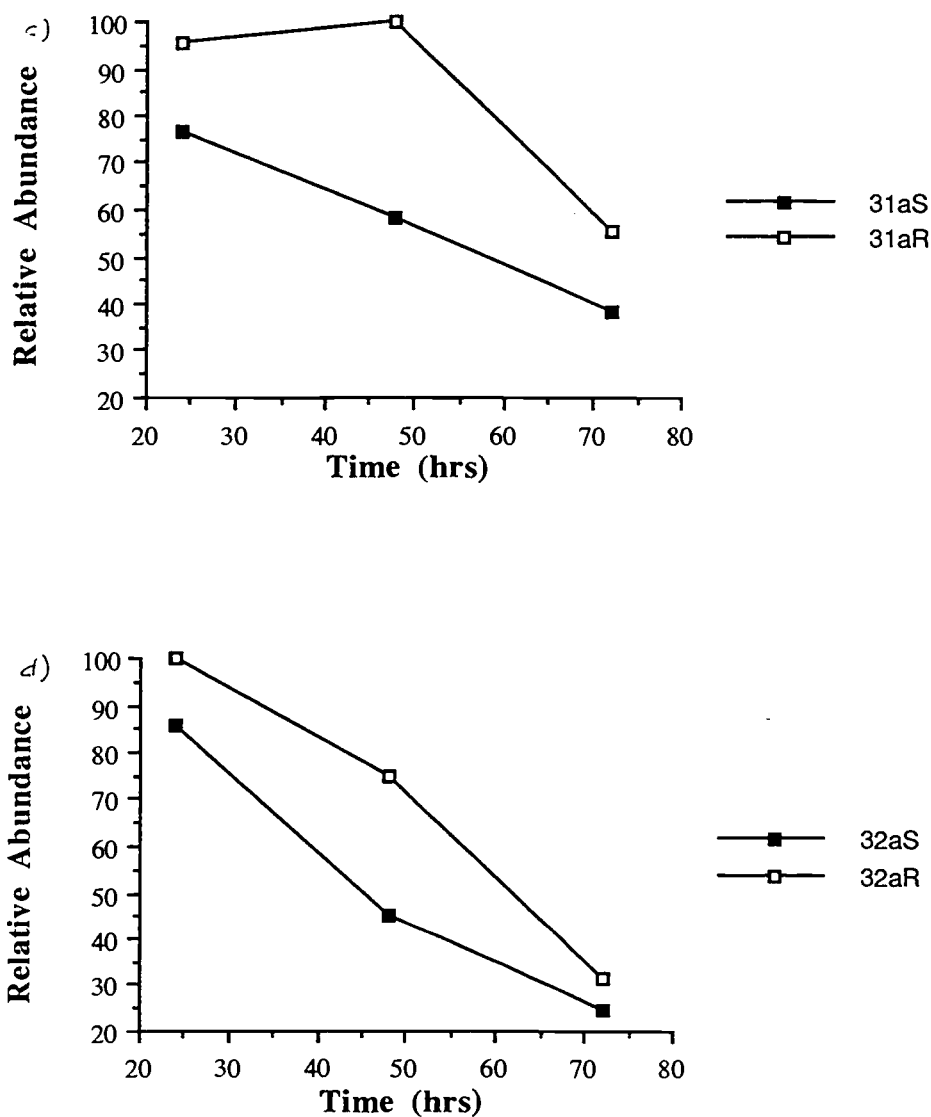
Figure 5.5. Relative abundance of selected triterpane biomarkers in the heating experiments of sediment AII-112-29 PC-5: c) 17α(H),21β(H)-31-hopane (22S) and 17β(H),21α(H)-31-hopane(22R) vs. time, and d) 17α(H),21β(H)-32-hopane (22S) and 17β(H),21α(H)-32-hopane(22R) vs. time.
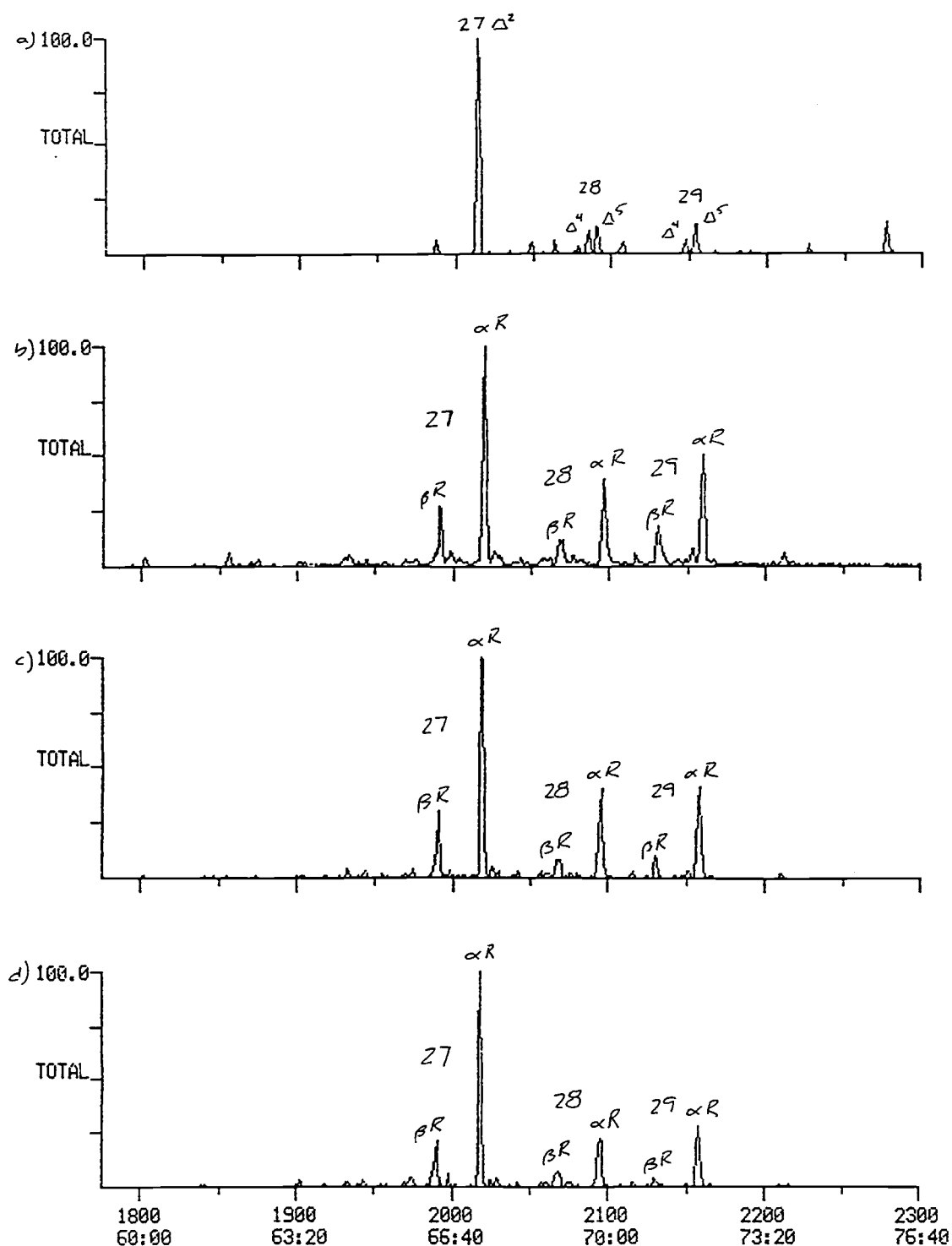
Figure 5.6. Representative mass fragmentograms (m/z 215, 217, 218, 257, 259) for the steroid hydrocarbons in the extracts of sediment AII-112-29 PC1: a) Unaltered; b) 24 hr @ 330°C; c) 48 hr @ 330°C; d) 72 hr @ 330°C.
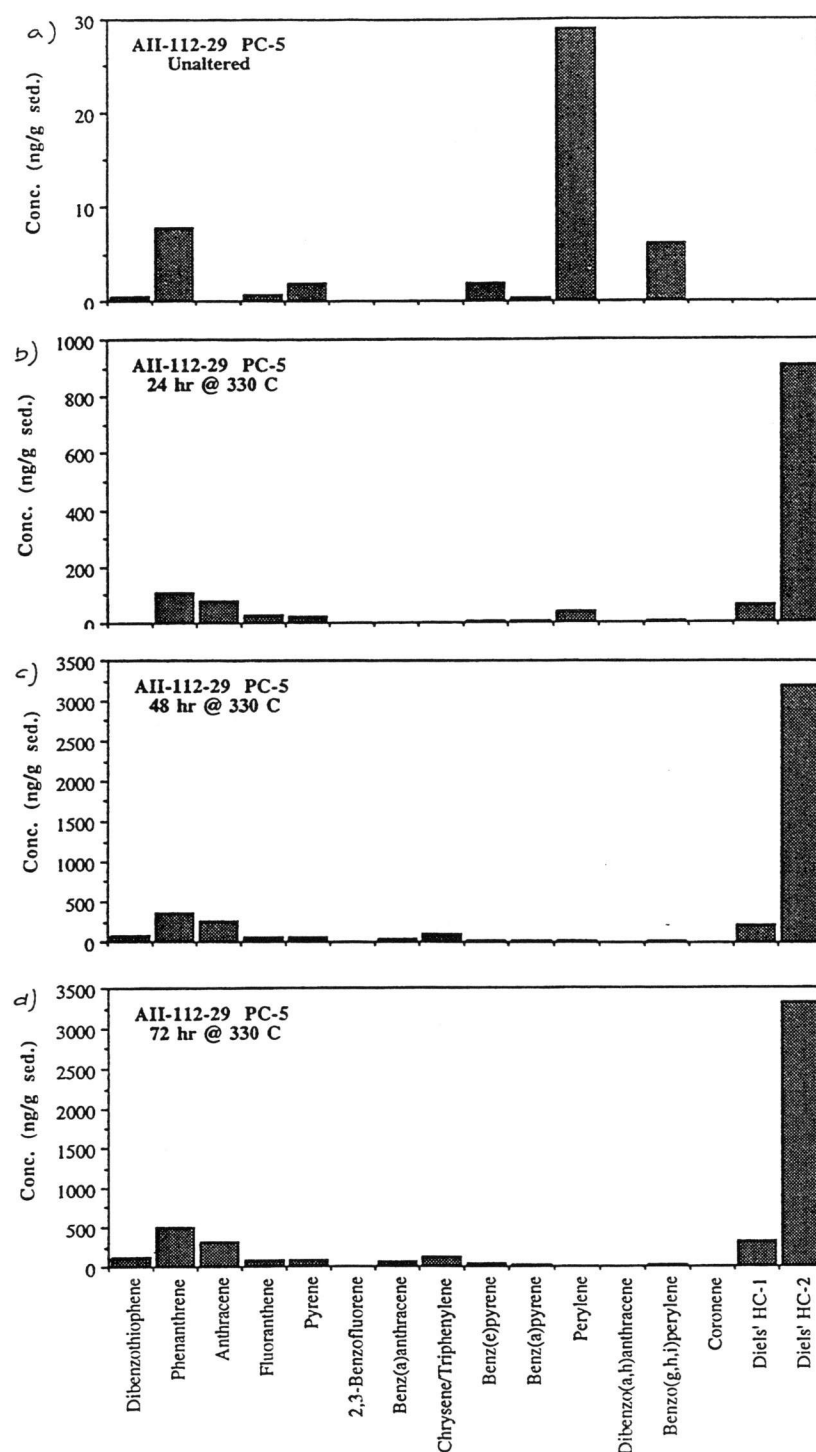
Figure 5.7. Histograms of the major aromatic compounds present in the extracts of sediment AII-112-29 PC1: a) Unaltered; b) 24 hr @ 330°C; c) 48 hr @ 330°C; d) 72 hr @ 330°C.
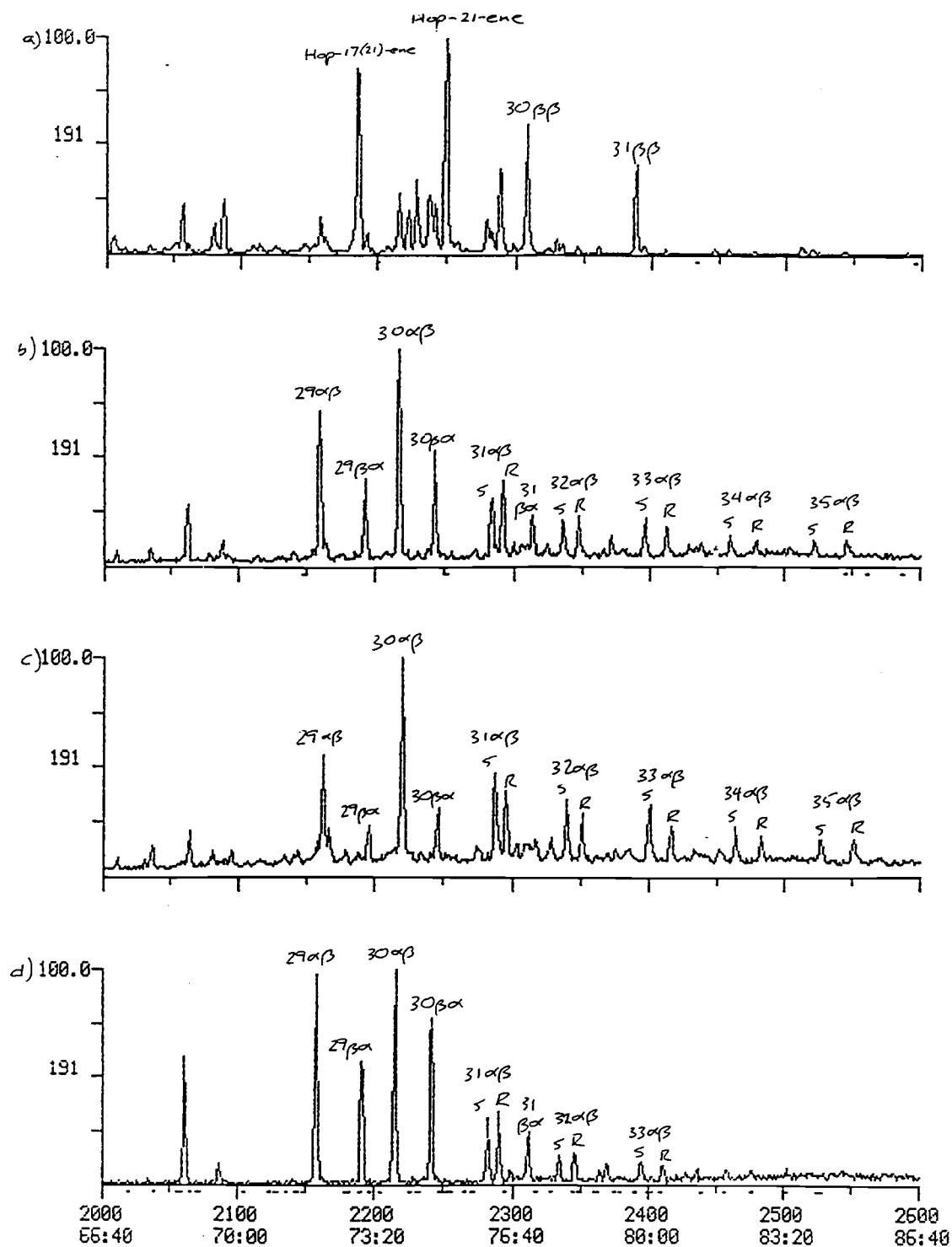
Figure 5.8. Representative mass fragmentograms m/z 191 for the triterpenoid hydrocarbons in the extracts of sediment 481A-8-7 (top): a) Unaltered; b) 24 hr @ 330°C; c) 48 hr @ 330°C; d) 72 hr @ 330°C.
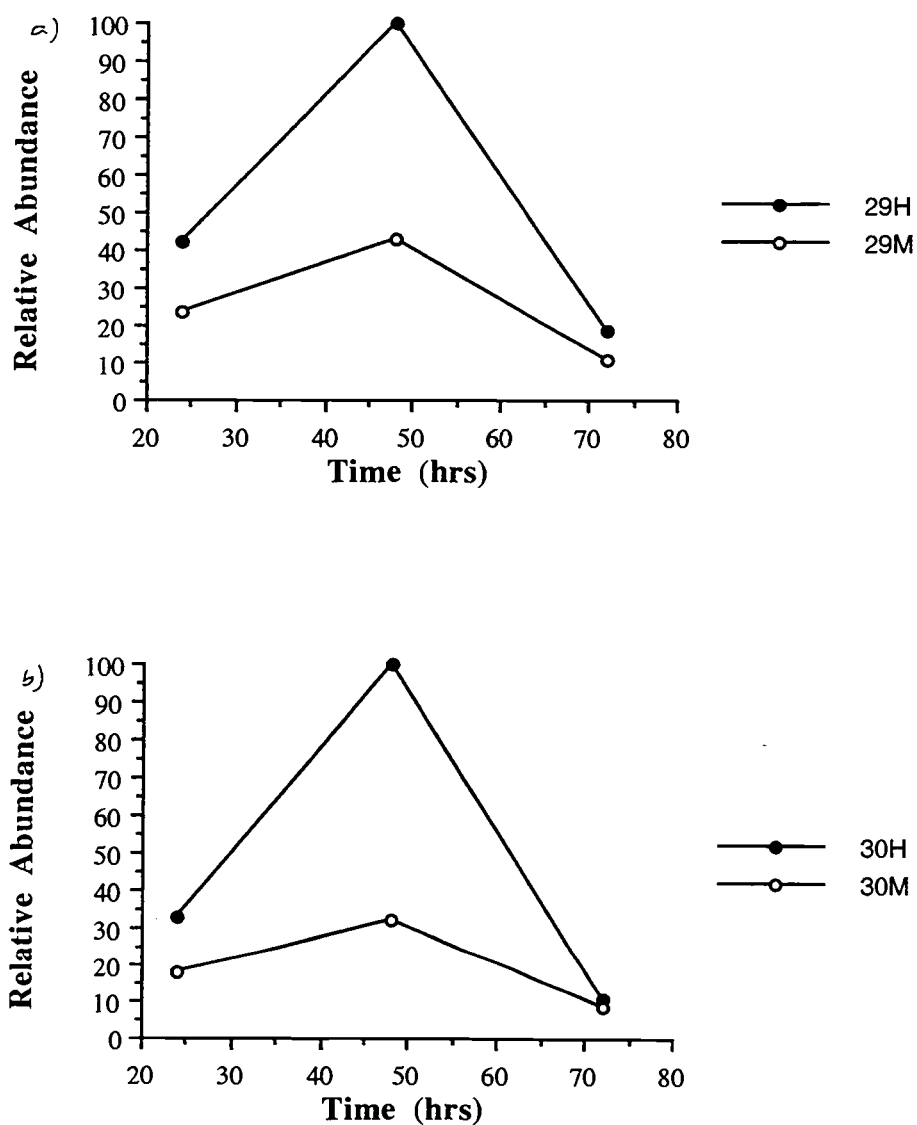
Figure 5.9. Relative abundance of selected triterpane biomarkers in the heating experiments of sediment 481A-8-7 (top): a) 17α(H),21β(H)-29-hopane and 17β(H),21α(H)-29-hopane vs. time, and b) 17α(H),21β(H)-30-hopane and 17β(H),21α(H)-30-hopane vs. time.
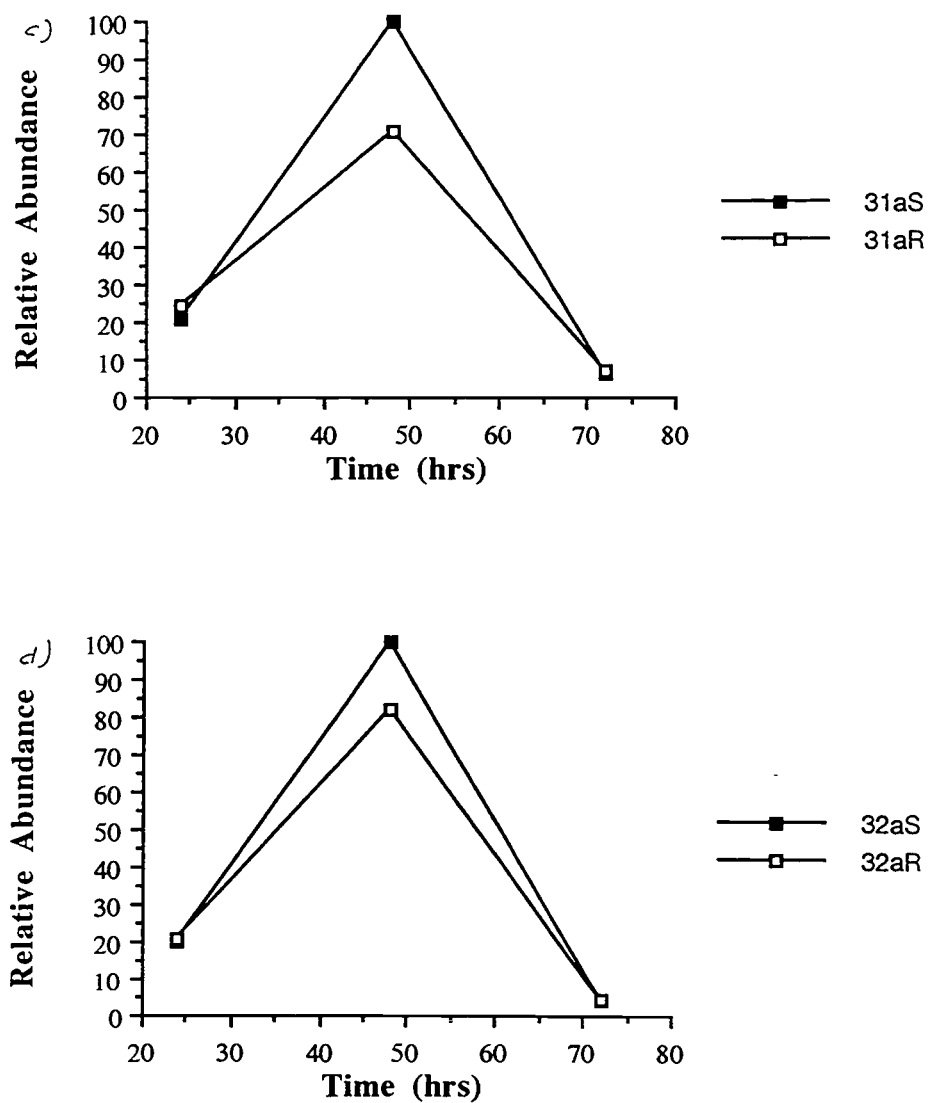
Figure 5.9. Relative abundance of selected triterpane biomarkers in the heating experiments of sediment 481A-8-7 (top): c) 17α(H),21β(H)-31-hopane (22S) and 17β(H),21α(H)-31-hopane(22R) vs. time, and d) 17α(H),21β(H)-32-hopane (22S) and 17β(H),21α(H)-32-hopane(22R) vs. time.
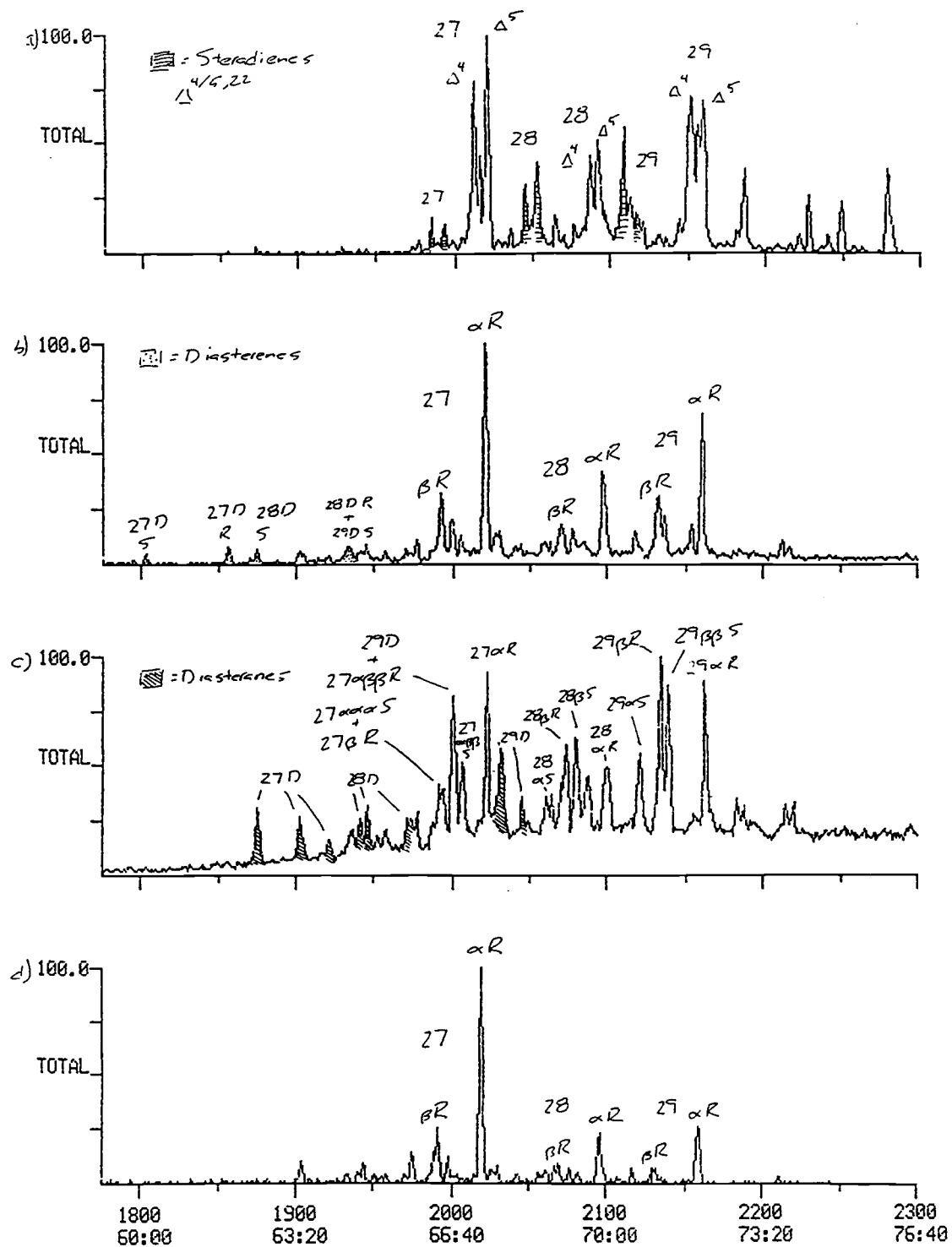
Figure 5.10. Representative mass fragmentograms (m/z 215, 217, 218, 257, 259) for the steroid hydrocarbons in the extracts of sediment 481A-8-7 (top): a) Unaltered; b) 24 hr @ 330°C; c) 48 hr @ 330°C; d) 72 hr @ 330°C.
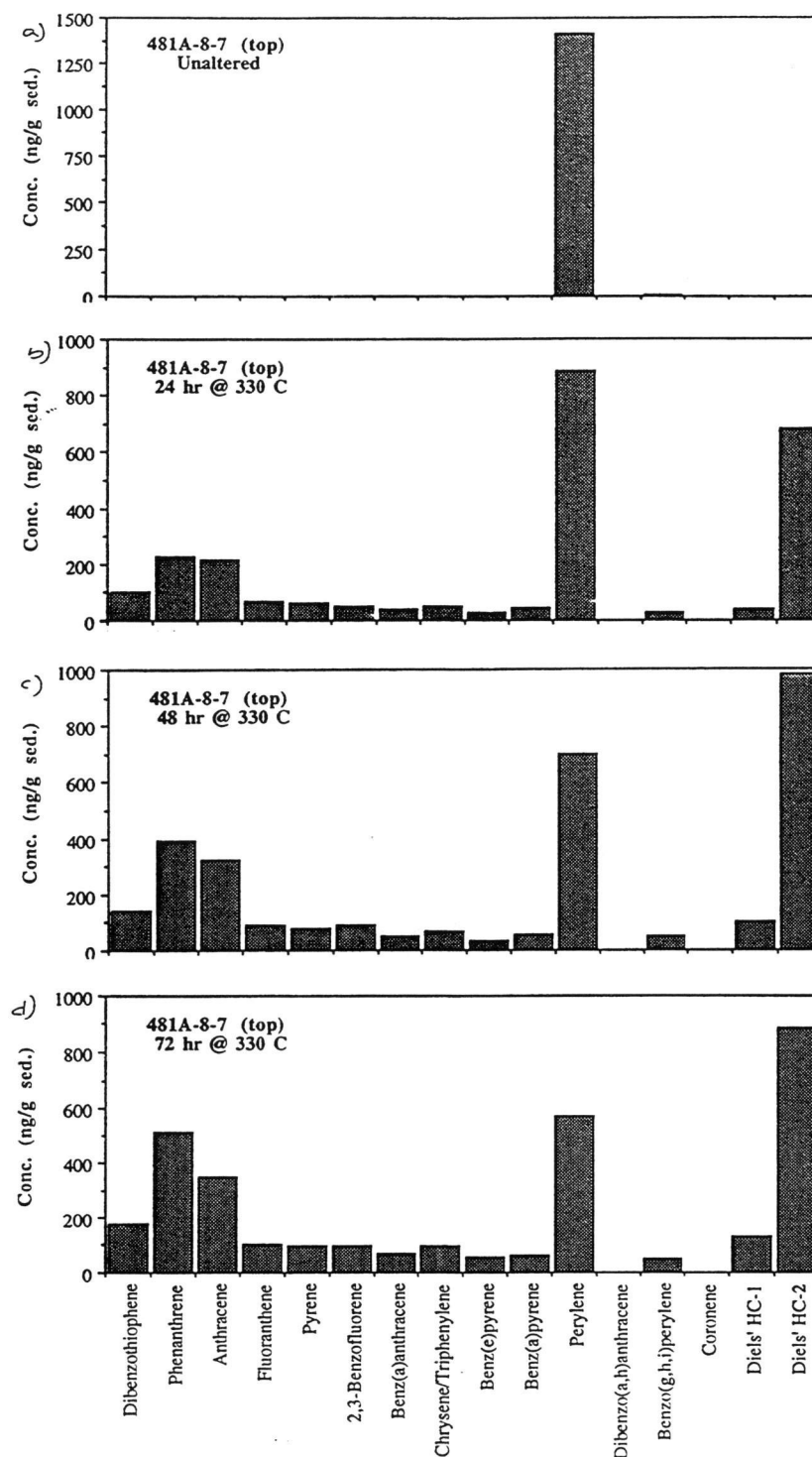
Figure 5.11. Histograms of the major aromatic compounds present in the extracts of sediment 481A-8-7 (top): a) Unaltered; b) 24 hr @ 330°C; c) 48 hr @ 330°C; d) 72 hr @ 330°C.
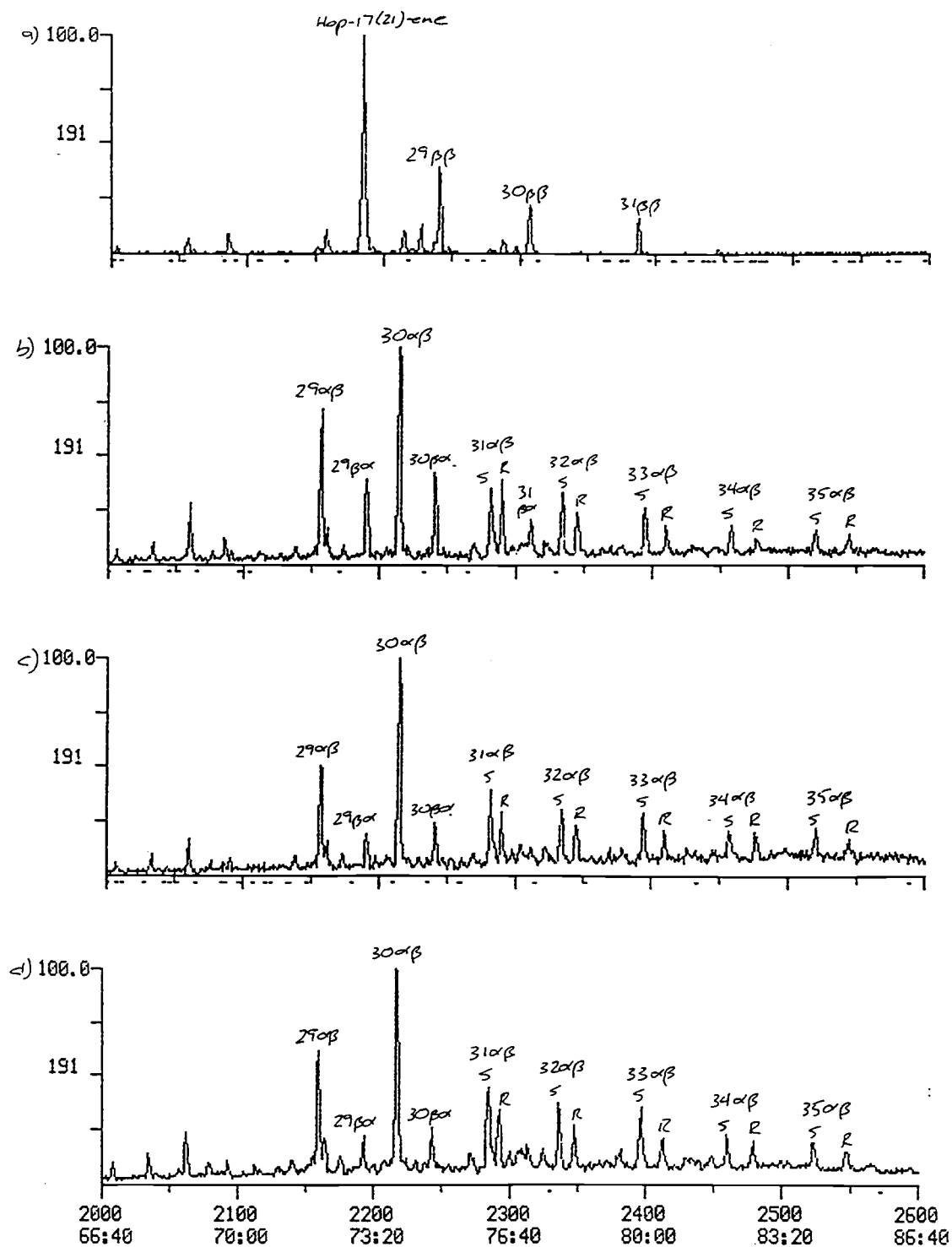
Figure 5.12. Representative mass fragmentograms m/z 191 for the triterpenoid hydrocarbons in the extracts of sediment 481A-22-7 (top): a) Unaltered; b) 24 hr @ 330°C; c) 48 hr @ 330°C; d) 72 hr @ 330°C.
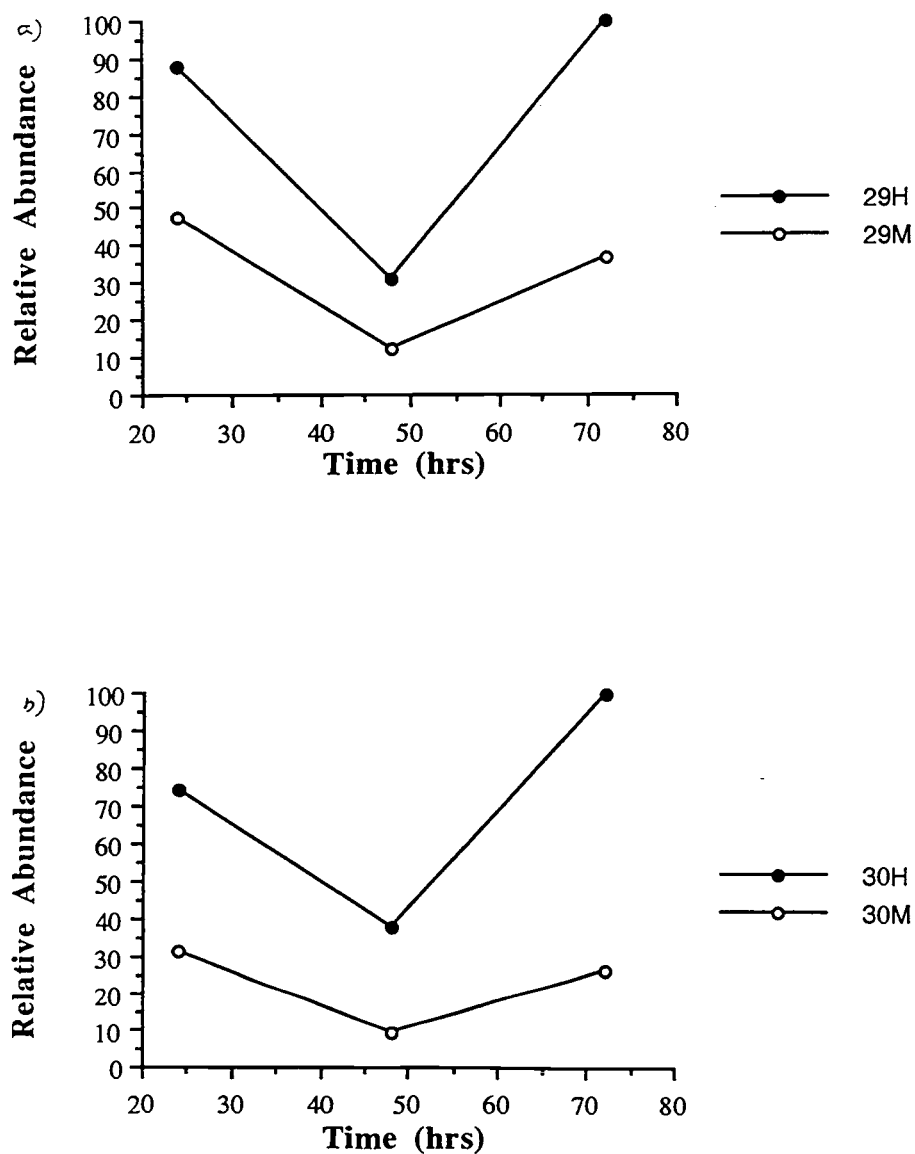
Figure 5.13. Relative abundance of selected triterpane biomarkers in the heating experiments of sediment 481A-22-7 (top): a) 17α(H),21β(H)-29-hopane and 17β(H),21α(H)-29-hopane vs. time, and b) 17α(H),21β(H)-30-hopane and 17β(H),21α(H)-30-hopane vs. time.
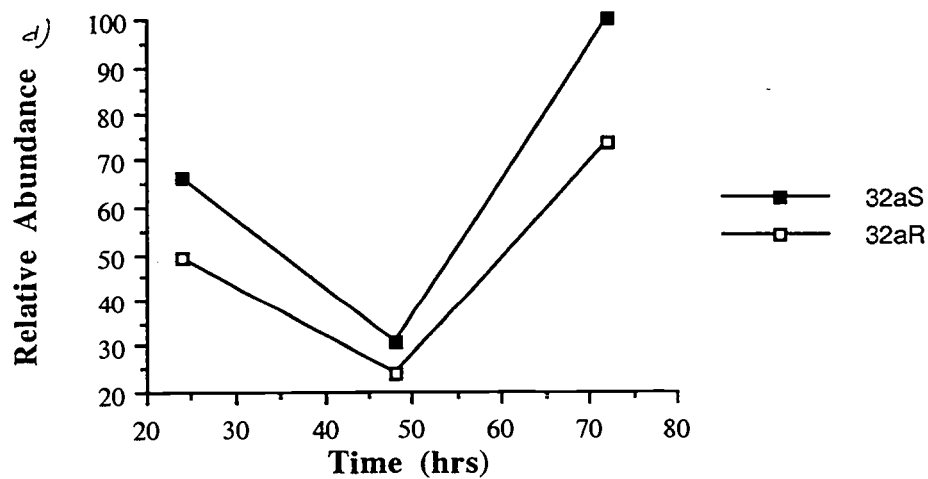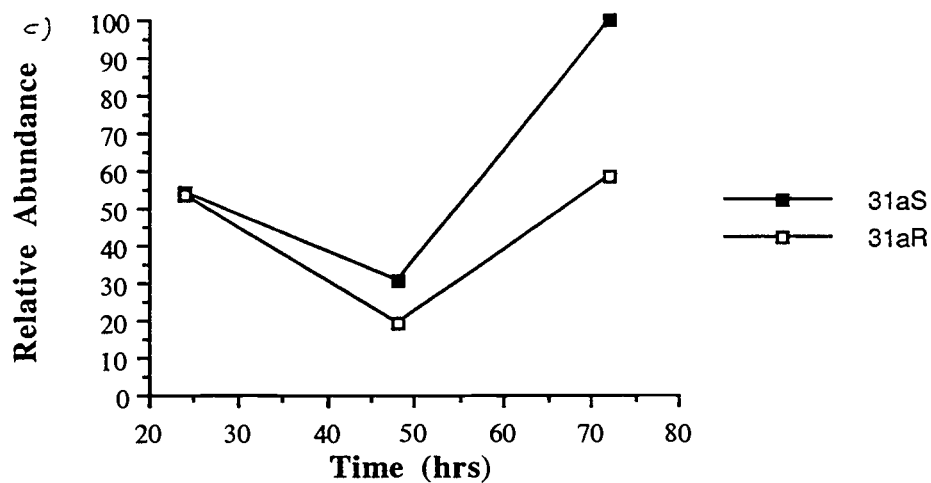
Figure 5.13. Relative abundance of selected triterpane biomarkers in the heating experiments of sediment 481A-22-7 (top): c) 17α(H),21β(H)-31-hopane (22S) and 17β(H),21α(H)-31-hopane(22R) vs. time, and d) 17α(H),21β(H)-32-hopane (22S) and 17β(H),21α(H)-32-hopane(22R) vs. time.
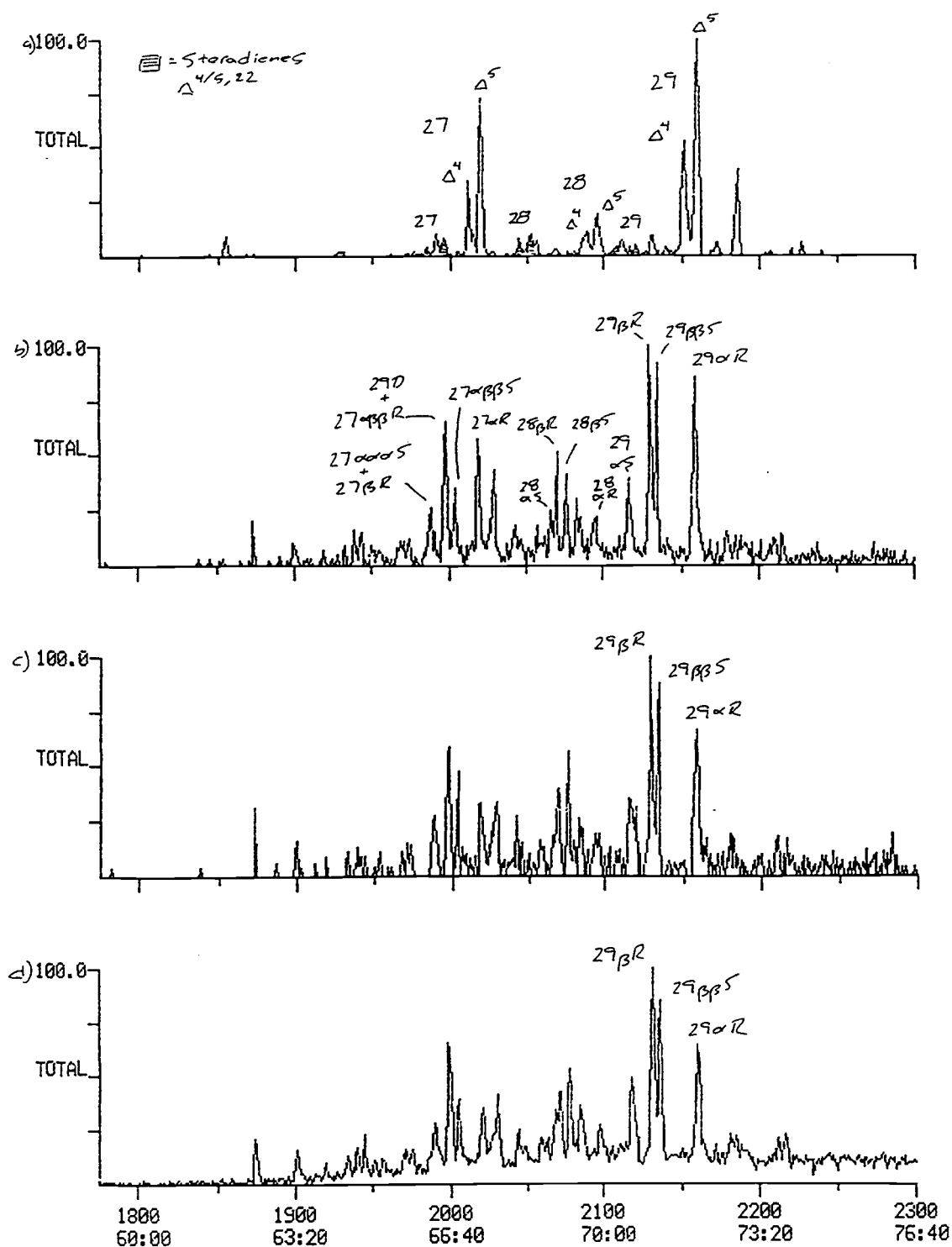
Figure 5.14. Representative mass fragmentograms (m/z 215, 217, 218, 257, 259) for the steroid hydrocarbons in the extracts of sediment 481A-22-7 (top): a) Unaltered; b) 24 hr @ 330°C; c) 48 hr @ 330°C; d) 72 hr @ 330°C.
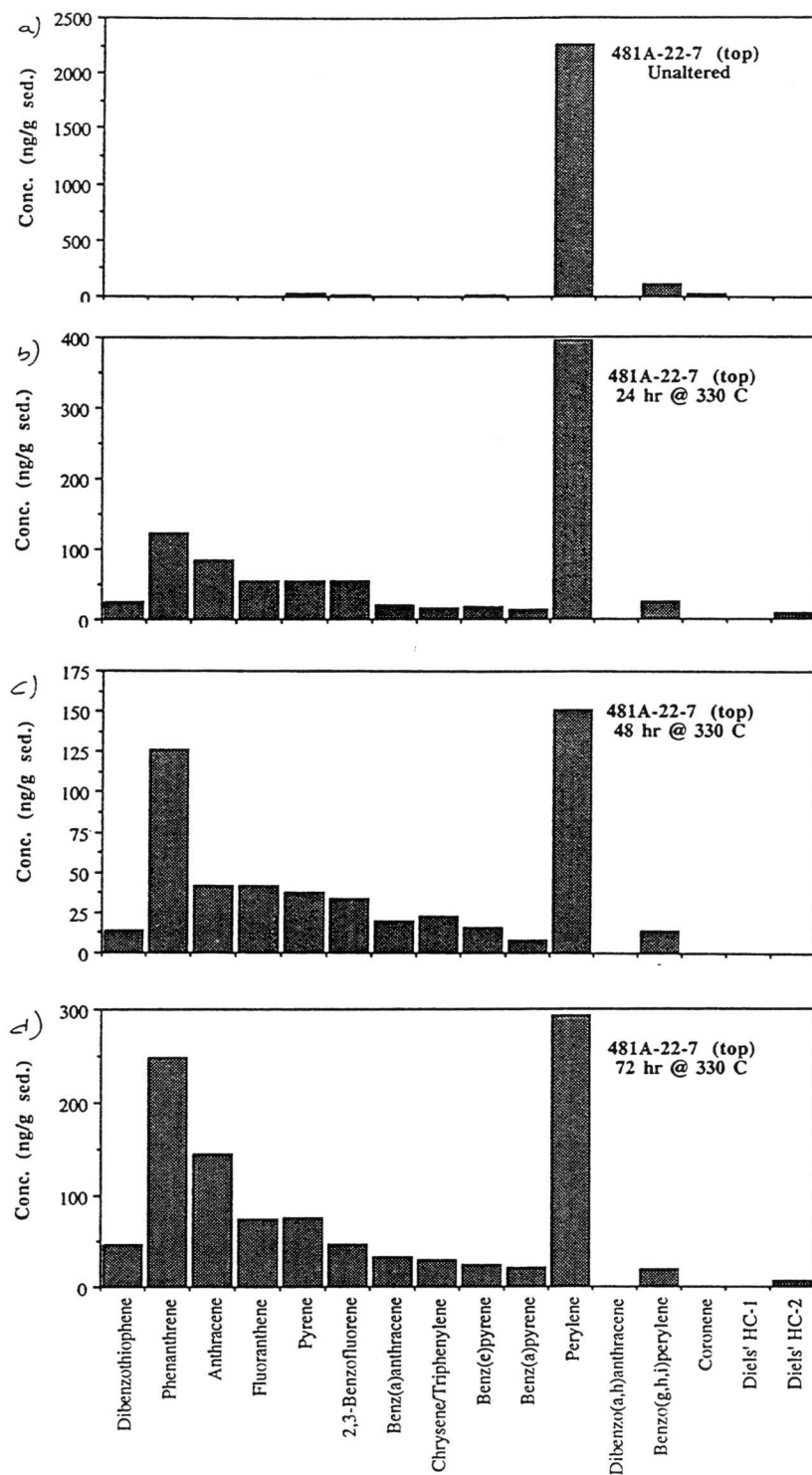
Figure 5.15. Histograms of the major aromatic compounds present in the extracts of sediment 481A-22-7 (top): a) Unaltered; b) 24 hr @ 330°C; c) 48 hr @ 330°C; d) 72 hr @ 330°C.
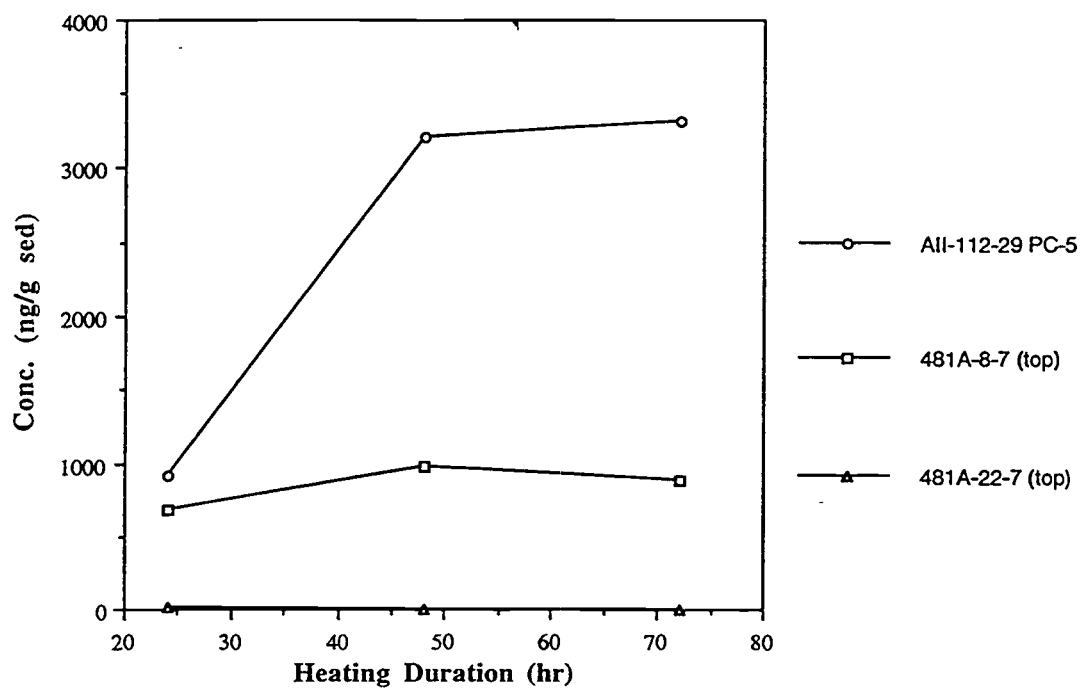
Figure 5.16. Plot showing the yields of Diels' hydrocarbon (DHC-2) in the heating experiments for the three sediment samples.

CHAPTER 6

A Proposed Chemical Pathway for the Origin of Ketones in Oils and Sediment Extracts from the Guaymas Basin Hydrothermal System

ABSTRACT

Hydrothermal oils and extracts of hydrothermally altered sediments contain ketones that appear to be uniquely associated with a high temperature hydrothermal mode of formation. Oils associated with hydrothermal vents contain several homologous series of alkanones, ranging in carbon number from C_{11} to C_{30} with a C_{max} from C_{15} to C_{23}. The large variation in C_{max} is probably a function of the vent fluid temperatures which range from 250° to 350°C. These oils contain alkan-2-ones in highest concentrations with slightly lower amounts of 3-, 4-, 5-, (and higher) alkanones. These compounds are enriched in the interiors of the hydrothermal vent spires or in downcore hydrothermally-altered sediments, indicating an origin at depth or in the hydrothermal fluids and not from external biogenic deposition.

Simulation of the natural hydrothermal pyrolysis process by laboratory hydrous pyrolysis techniques provides information regarding the mode of alkanone formation. Hydrous pyrolysis of $\underline{n}$-$C_{32}H_{66}$ at 330 and 350°C for 72 hr with water only or water with inorganic additives has been studied using a stainless steel reaction vessel. In each experiment a similar distribution of alkanones was formed from the cracking of the $\underline{n}$-alkane. The product distributions indicate a reaction pathway consisting of $\underline{n}$-alkanes and α-olefins as primary cracking products with internal olefins, alkanones and alkanals as secondary reaction products of the α-olefins. The product compositions were modified by ionic strength, pH and reactive species such as sulfate, elemental sulfur and sulfide.

Hydrous pyrolyses of Messel shale spiked with molecular probes have been performed under similar time and temperature constraints to produce alkanone distributions like those found in the hydrothermal vent oils.

INTRODUCTION

Numerous reports have identified aliphatic ketones in the extractable portion of sedimentary organic matter. This homologous series of alkan-2-ones occurs with an odd carbon number predominance and its source is most likely being microbial (Cranwell, 1977; Simoneit, 1978, 1979; Brassell et al., 1980; Albaigés et al., 1984). Alkanones with an odd/even predominance produced from the incomplete combustion of n-alkanes or n-alkanols have been identified in aerosols (Simoneit et al., 1991). Aliphatic ketones with no carbon number predominance have only recently been reported (Leif et al., 1992; George and Jardine, 1993), with both occurrences being associated with dolorite sill intrusions into sedimentary sections. Oil shale pyrolyses generate alkan-2-ones and lesser amounts of 3-, 4-, 5- and 6-ketones (Regtop et al., 1982, 1985; Rovere et al., 1983). Other products generated in the oil shale pyrolyses include n-alkanes and terminal and internal n-alkenes. The origin of the aliphatic ketones must be related to the high temperature conditions encountered in all the previous studies. The mechanism by which they are formed is still not understood. George and Jardine (1993) suggest that the ketones originate by the thermal fission of alkyl chains linked by ether groups at a variety of chain positions, from 3 to at least 7.

Experiments have been performed which were designed to understand the chemistry of high temperature hydrothermal systems. Using the procedure of hydrous pyrolysis, aliphatic ketones have been found to be common pyrolysis products, no matter what the beginning source material is. This paper presents some results of the heating experiments and proposes a chemical pathway by which these compounds are formed.

EXPERIMENTAL

Sample. The seabed oil for this study was sampled from the interior of a hydrothermal vent collected during Deep Submergence Vessel (D.S.V.) *Alvin* dives of March, 1988 (sample 1972-CH1 Interior).

Hydrous pyrolysis experiments. Pyrolysis experiments were performed in Sno-Trik® T316 stainless steel high pressure pipes rated at 60,000 psig (4080 bar), sealed with end caps and heated in an air circulating oven set at 330° ±2°C. Burdick and Jackson ultrapure water was used in all experiments. Aliphatic compounds used in pyrolysis experiments were 1,13-tetradecadiene (purity > 97%), 1-hexadecene (purity > 97%), eicosane (purity 99%), and dotriacontane ($\underline{n}$-$C_{32}H_{66}$, purity > 97%). The Messel shale used in the experiments was powdered and Soxhlet extracted with methanol/methylene chloride for 72 hr prior to the pyrolysis studies. The reaction vessels with reactant mixtures were placed in a glove bag and flushed with five volumes of argon. Deoxygenated H_2O or D_2O, prepared by bubbling with argon gas for 45 minutes, was added and the vessels sealed. Durations of the heating experiments ranged from 1 hr to 72 hr.

Extraction and fractionation. The frozen hydrothermal vent sample was brought to room temperature and an oil sample was removed from the interior of the vent matrix. The oil was diluted in chloroform and filtered to remove any debris and passed through an activated copper column to remove the elemental sulfur. The sample was reduced to 2 mL by rotary evaporation.

The reaction vessels were removed from the oven and cooled to room temperature upon completion of the heating cycles. The reaction vessels were extracted with two 1 mL portions of methanol followed by five 1 mL portions of methylene chloride. The solvents and water from each pyrolysis experiment were combined in a centrifuge tube and the organic fraction separated and collected. The water was extracted with two additional portions of methylene chloride and the two extract fractions were combined. The methylene chloride extract was dried with anhydrous sodium sulfate and passed through an activated copper column to remove the elemental sulfur.

The whole oils and pyrolysis extracts were deasphalted with 100 mL heptane. The asphaltenes were allowed to precipitate for 24 hrs and removed by filtration. The deasphalted fractions were fractionated by column chromatography (30 cm x 1 cm) packed with 3.8 g alumina (fully active) over 3.8 g silica gel (fully active). The

samples were separated into three fractions by elution with 50 mL heptane (aliphatic, F1), 50 mL toluene (aromatic, F2) and 25 mL methanol (polar NSO, F3).

Further fractionation was performed by thin layer chromatography (TLC). The polar NSO fraction was loaded on a silica gel plate (fully active , 20 x 20 cm, 250 μm), and eluted with a solution of heptane:diethyl ether (20:1). The band corresponding to R_f 0.25 to 0.50 was the ketone band. The ketones were eluted with methylene chloride and concentrated by rotary evaporation. Quantitation was by the addition of $\underline{n}$-$C_{24}D_{50}$ and $\underline{n}$-$C_{32}D_{66}$.

Gas chromatography. Gas chromatography (GC) of the oil fractions was performed with a Hewlett Packard 5890A equipped with a 30 m x 0.25 mm i.d. DB-5 open tubular column (0.25 μm film thickness). The GC oven was heated using the following program : isothermal for 2 min. at 65°C, 4°/min. to 310°C, and isothermal for 30 min., with the injector at 290°C, detector at 325°C, and helium as the carrier gas.

Gas chromatography-mass spectrometry. The gas chromatography-mass spectrometry (GC-MS) was performed on a Finnigan 9610 gas chromatograph coupled to a Finnigan 4021 quadrupole mass spectrometer operated at 70 eV over the mass range 50-650 dalton and a cycle time of 2.0 s. The GC oven temperature was programmed at isothermal for 2 min. at 65°C, 3°/min. to 310°C, and isothermal for 30 min., with the injector at 290°C, and helium as the carrier gas. The MS data were processed with an on-line Finnigan-Incos 2300 computer data system.

RESULTS and DISCUSSION

We have been interested in identifying compounds that could be used as markers to distinguish hydrothermally derived oils from conventional reservoir oils. Progress has been made in understanding the hydrothermal generation process and formation of certain oxygenated compounds.

Chromatographic behavior of aliphatic ketones. The gas chromatographic behavior of several ketone isomers is shown in Fig. 6.1. Tetradecan-2-one and tetradecan-3-one are completely resolved by gas chromatography on a DB-5 column, but tetradecan-4-one is on a shoulder of a peak formed by the coelution of the 5-,6- and 7-tetradecanones. The mass spectra of the pure ketone standards are shown in Fig. 6.2 and mass spectra of the four peaks in the ketone mixture are shown in Fig. 6.3.

Ketones in hydrothermal oils. Aliphatic ketones are ubiquitous in unbiodegraded oils associated with high temperature hydrothermal vents in the Guaymas Basin. Fig. 6.4a shows a gas chromatogram of the polar NSO fraction of a representative hydrothermally-generated oil. Fig. 6.4b is the ketone fraction isolated by thin layer chromatography. There was some loss of the alkan-2-one series in another fraction. These ketones in hydrothermal oils possess a smooth distribution, analogous to the $\underline{n}$-alkane distributions in mature oils. The aliphatic ketones are enriched in the interiors of the high temperature vents, suggesting a pyrolytic source. The alkan-2-ones are usually in highest concentrations, with lesser amounts of 3-, 4-, 5- (and higher) ketones. The same series of ketones has been identified in the hydrothermally-altered sediments in the proximity of a dolorite sill. The association of the ketones with sill intrusions, with the exception of the contribution of George and Jardine (1993), has not been described before in geological samples.

Ketones from the hydrous pyrolysis of n-$C_{32}H_{66}$. The aqueous high temperature organic chemistry of $\underline{n}$-$C_{32}H_{66}$ was investigated by pyrolyzing the hydrocarbon with water only or water with several selected inorganic components (Leif et al., 1992). The products consisted of a broad distribution of cracking products with a large amount of unreacted starting material. The cracking products were $\underline{n}$-alkanes, $\underline{n}$-alkenes, and a polar fraction containing $\underline{n}$-ketones as the major components. It appears that the primary products are the $\underline{n}$-alkanes and terminal $\underline{n}$-alkenes, generated by radical cracking, and secondary reactions produce internal $\underline{n}$-alkenes and oxygenated compounds. It is possible that the alkenes are intermediates to the

formation of the ketones. Fig. 6.5 shows gas chromatograms of one pyrolysis experiment conducted in the presence of iron sulfides. Fig. 6.5a is the nonpolar aliphatic fraction, containing n-alkanes, and Fig. 6.5b is the polar fraction, consisting of ketones. The alkan-2-ones are highest, with lesser amounts of 3-, 4- (and higher) ketones. Even under strong reducing conditions the ketones were formed by the hydrous pyrolysis conditions.

Ketones from the pyrolysis of aliphatic molecular probes with Messel shale. A series of hydrous pyrolysis experiments was performed by spiking 1,13-tetradecadiene, 1-hexadecene and eicosane on Messel shale and heating at 330°C. The products were analyzed after 1, 5, 10, 36 and 72 hr. Fig. 6.6 shows the gas chromatograms of the polar fractions. It was shown that at the termination of the heating experiments (72 hr), the major compounds were ketones. The distribution of the ketone isomers is shown in Fig. 6.7. Fig. 6.7a shows the ketones from the reaction of 1,13-tetradecadiene and Fig. 6.7b shows the products from 1-hexadecene. Both of these product distributions are dominated by the alkan-2-one, with lesser amounts of the other ketones. Fig. 6.7c shows the ketones generated from eicosane. The distribution closely matches the ketone distribution found in the hydrothermal oils (Fig. 6.8). These experiments indicate that under high temperature hydrothermal conditions, ketones can be formed from alkenes and alkanes.

Proposed origin of ketones under natural and simulated hydrothermal conditions. Aliphatic ketones have been shown to be synthesized under natural and simulated hydrothermal conditions, especially under reducing conditions. A chemical pathway is proposed where the ketones derive from a short-lived aliphatic alcohol. Fig. 6.9 shows the general reaction scheme, analogous to the set of reactions proposed to occur during the thermal degradation of jet fuels (Coleman et al., 1992). It is suggested that alkanes are first oxidized, and can subsequently form alkenes or ketones. As shown in Fig. 6.9, catalytic dehydrogenation of alcohols occurs in two ways depending on the presence or absence of oxygen (Haines, 1988). But reaction I is favored at high temperatures. In pyrolysis experiments, very often the alkan-2-ones are highest in concentration and often their predominance occurs together with terminal n-alkenes, in agreement with the proposed mechanism.

CONCLUSIONS

Aliphatic ketones are commonly formed under reducing hydrothermal conditions from alkenes, alkanes and/or aliphatic-rich sedimentary organic matter. These results indicate that a high temperature chemical reaction is responsible is for their formation. A mechanism is proposed where aliphatic alkanes and alkenes proceed through an alcohol intermediate, which can then proceed to the ketone with or without the presence of oxygen.
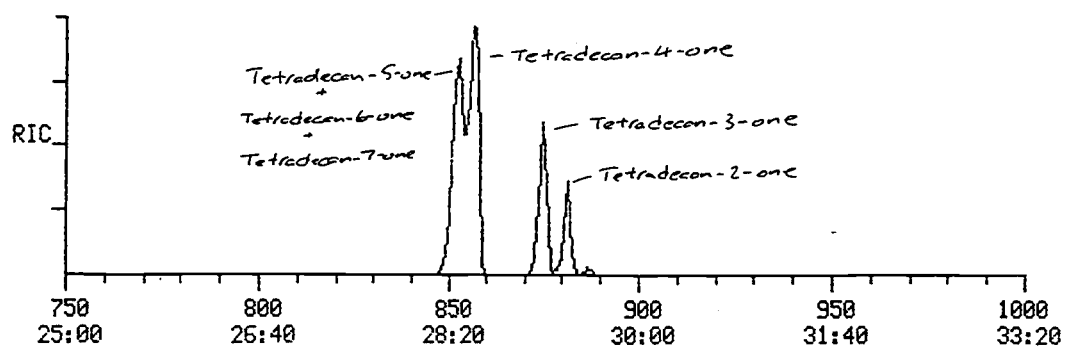
Figure 6.1. Portion of a gas chromatogram showing the elution order of six C_{14} ketone isomers.
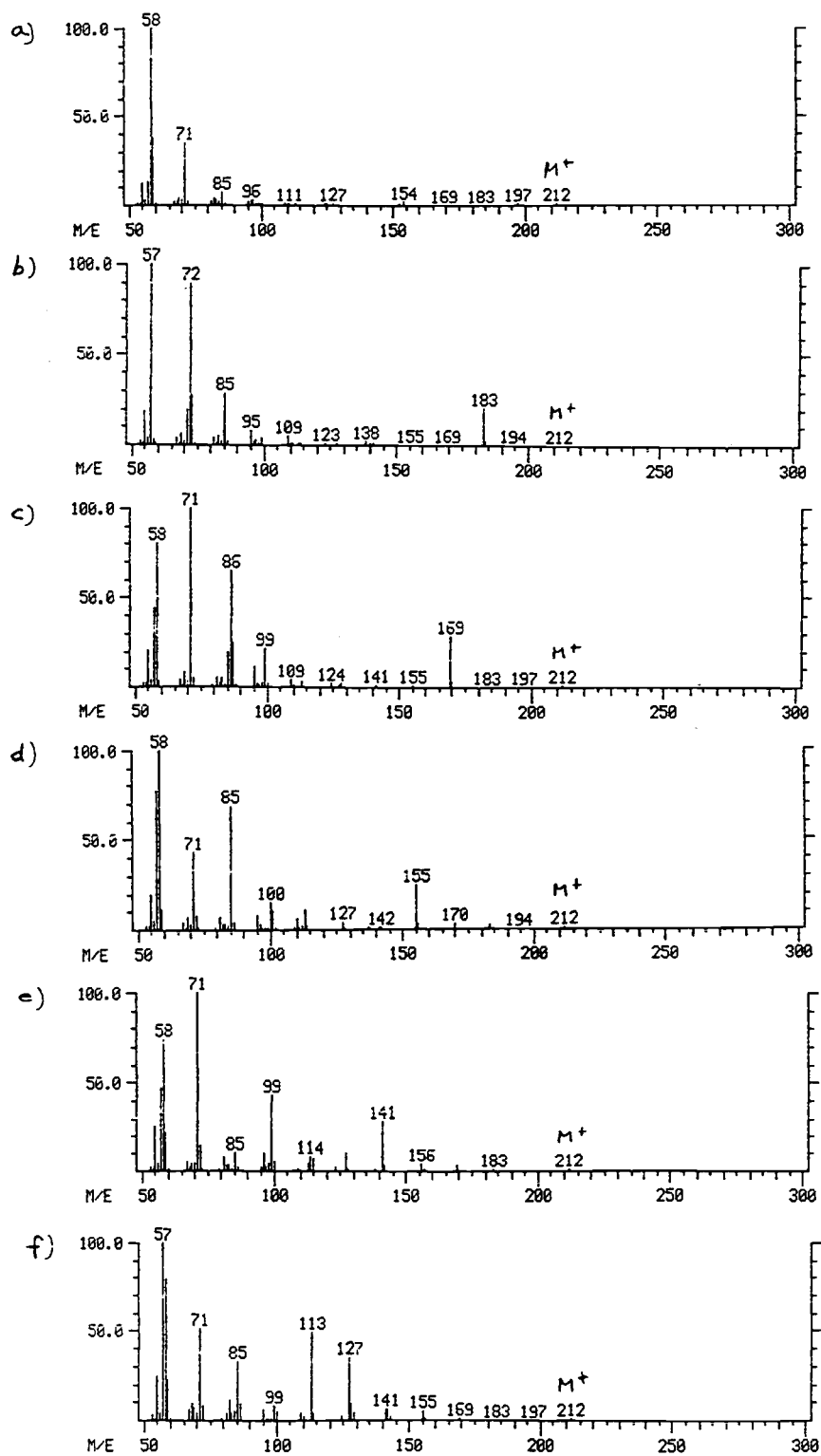
Figue 6.2. Mass spectra of aliphatic ketone standards ; a) tetradecan-2-one; b) tetradecan-3-one; c) tetradecan-4-one; d) tetradecan-5-one; e) tetradecan-6-one; f) tetradecan-7-one.
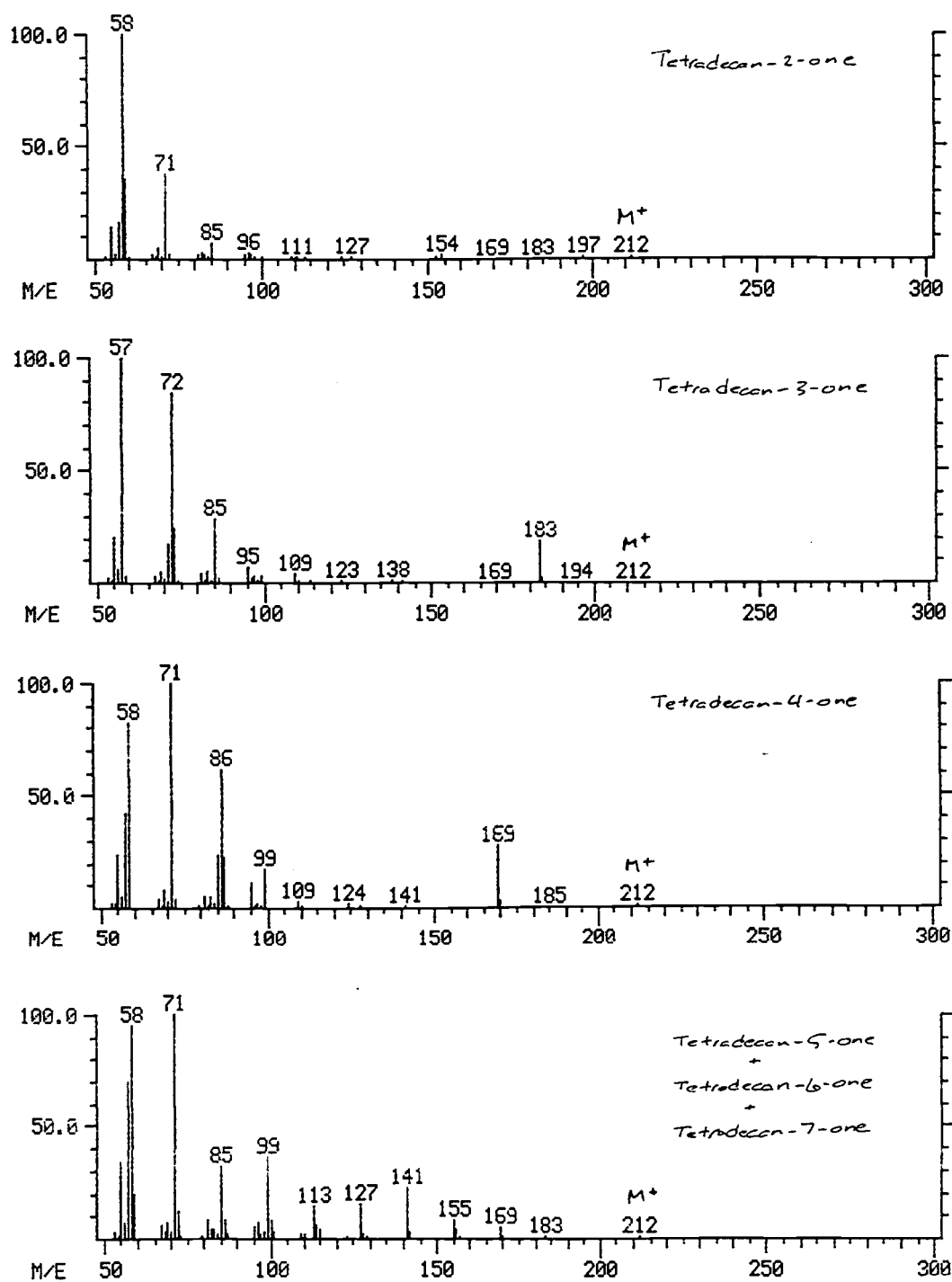
Figure 6.3. Mass spectra corresponding to the peaks in Fig. 6.1.
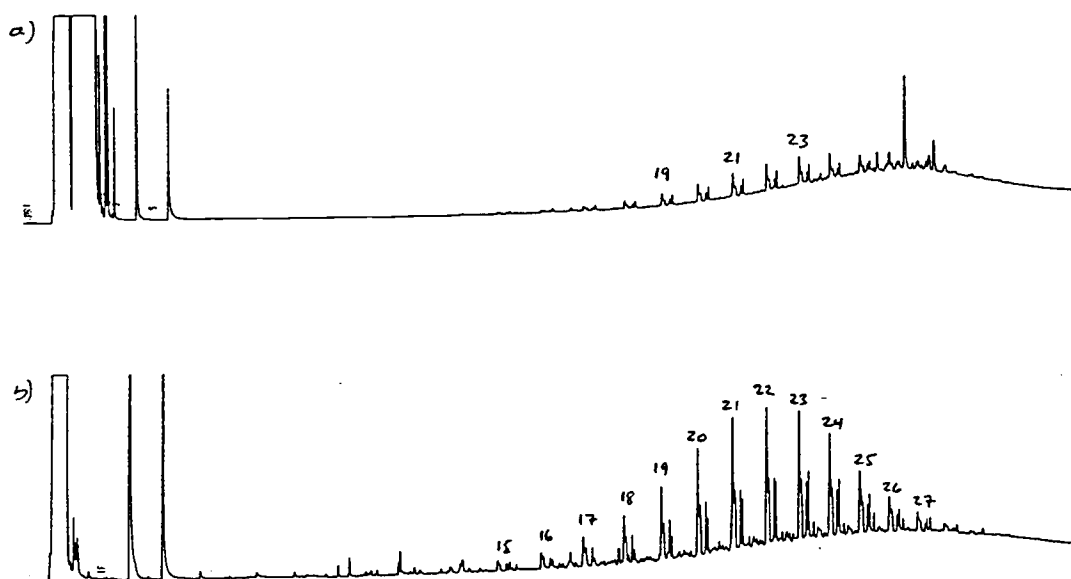
Figure 6.4. Gas chromatograms of the hydrothermal oil 1972-CH1 Interior: a) polar NSO fraction and b) isolated ketone fraction of the NSO fraction.
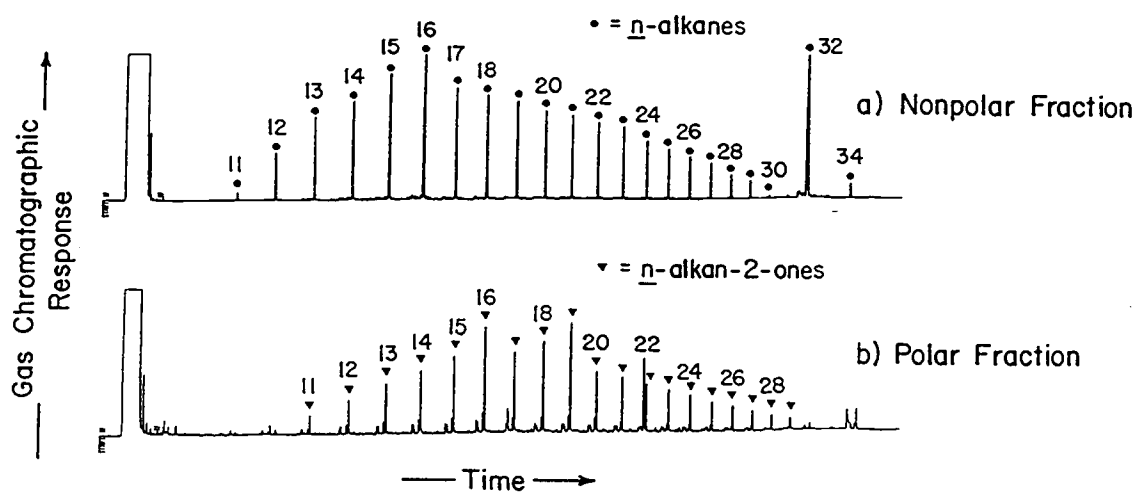
Figure 6.5. Gas chromatograms of the H_2O - n-$C_{32}H_{66}$ - Sulfide system (72 hr @ 350°C): a) nonpolar aliphatic fraction and b) polar NSO fraction.
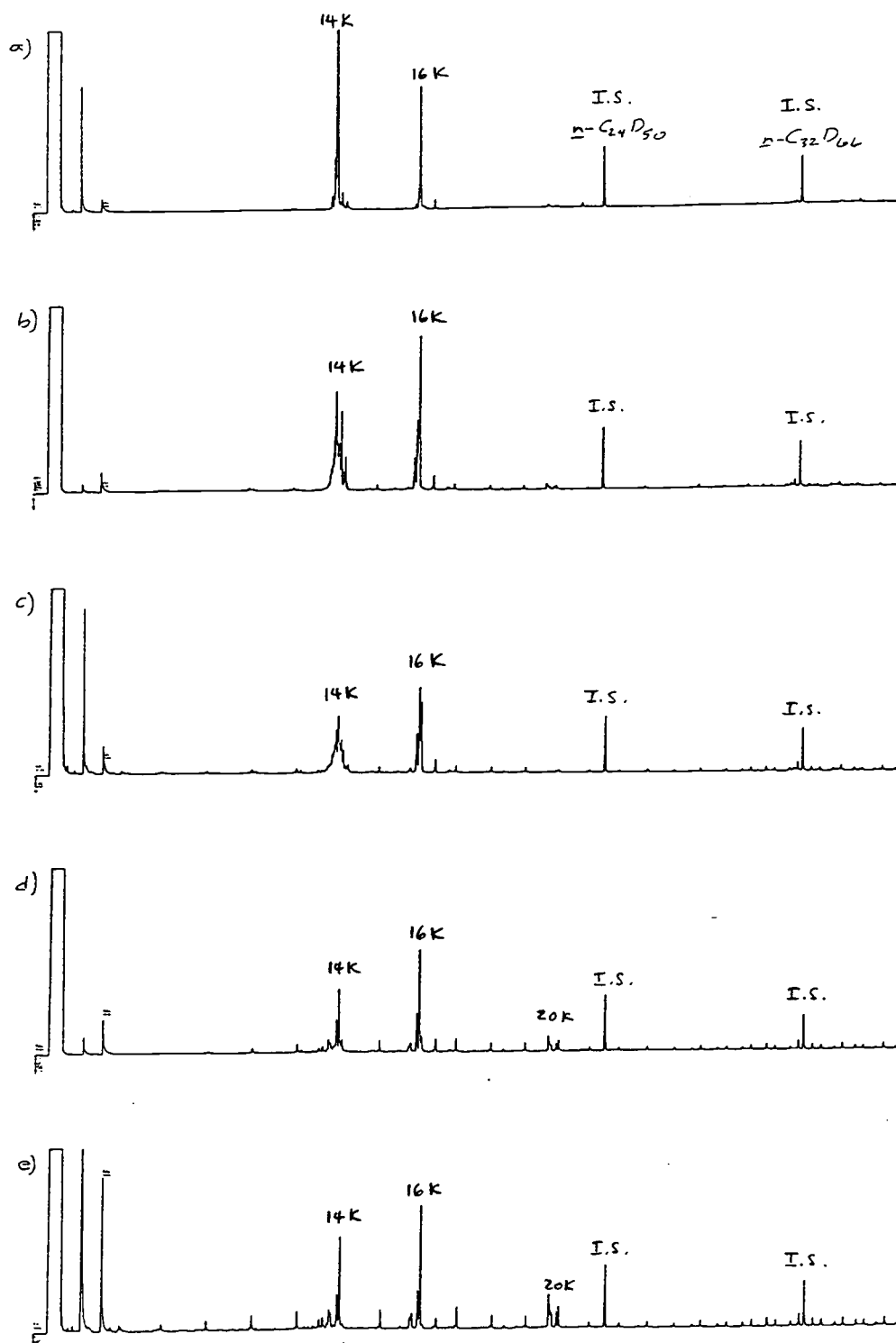
Figure 6.6. Gas chromatograms of the polar NSO fractions obtained by hydrous pyrolysis of 1,13-tetradecadiene, 1-hexadecene and eicosane on Messel shale: a) 1 hr @ 330°C; b) 5 hr @ 330°C; c) 10 hr @ 330°C; d) 36 hr @ 330°C; e) 72 hr @ 330°C. Internal standards : $\underline{n}$-$C_{24}D_{50}$ and $\underline{n}$-$C_{32}D_{66}$.
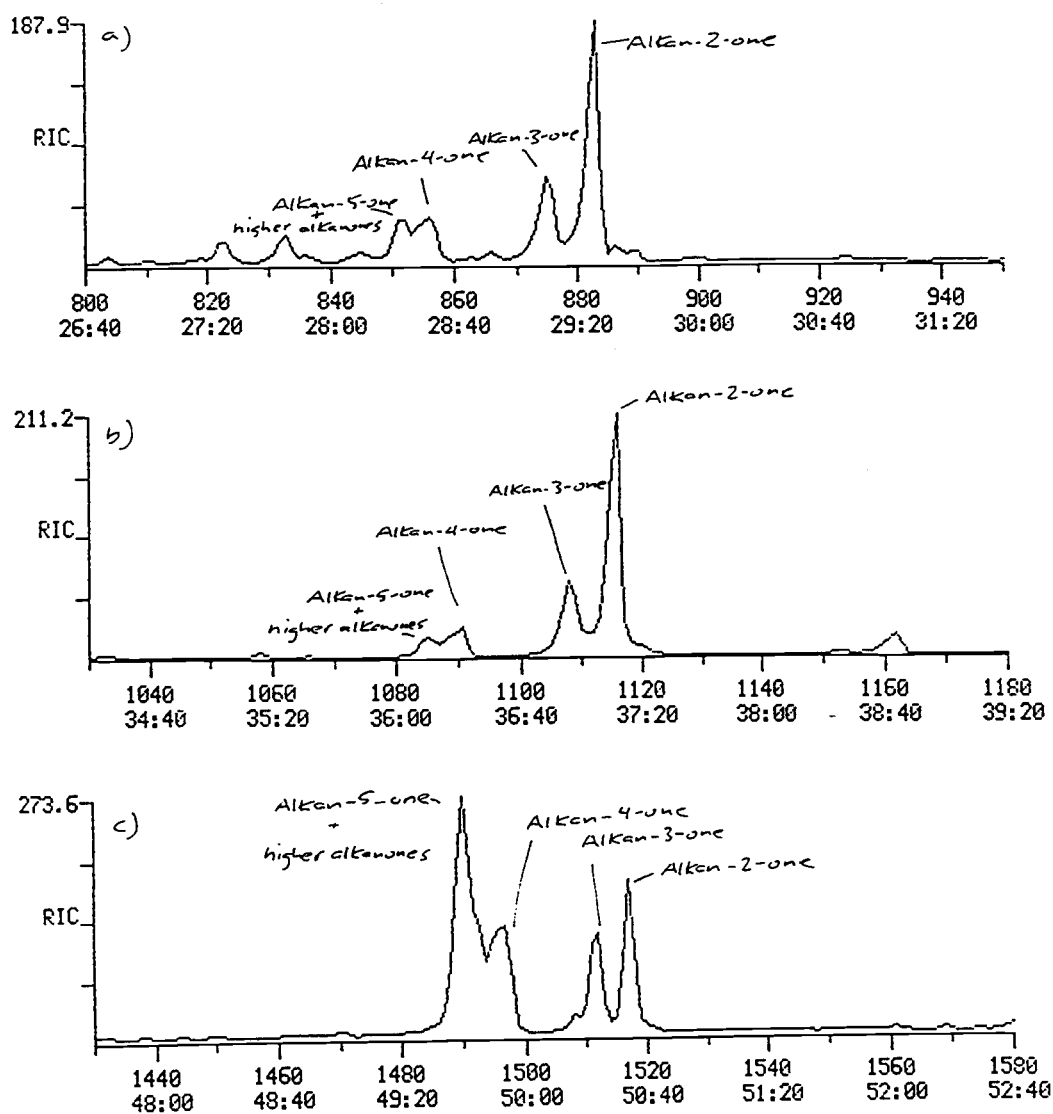
Figure 6.7. Reconstructed ion chromatograms (RIC) representative of the aliphatic ketones generated during the molecular probe experiments pyrolyzed with Messel shale : a) ketones from 1,13-tetradecadiene; b) ketones from 1-hexadecene; c) ketones from eicosane.
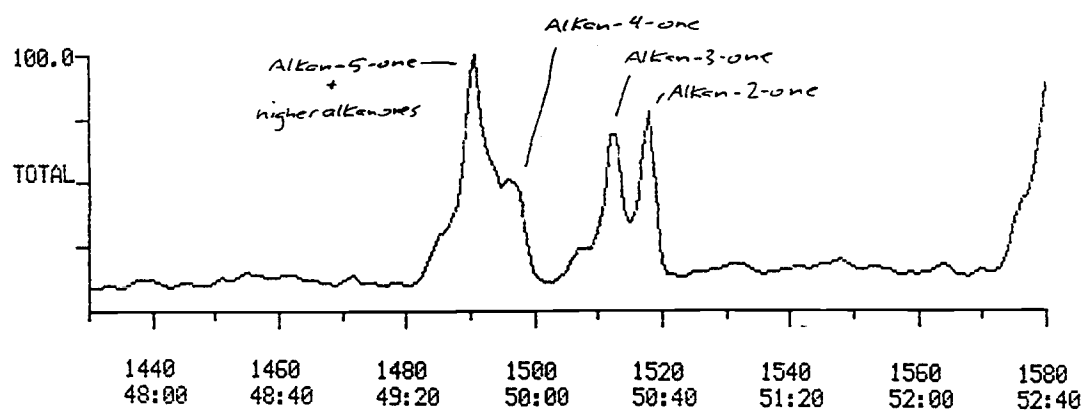
Figure 6.8. Mass fragmentogram (m/z 57, 58, 71; 72) representative of the aliphatic ketones present in a hydrothermally-derived oil (1972-CH1 Interior).
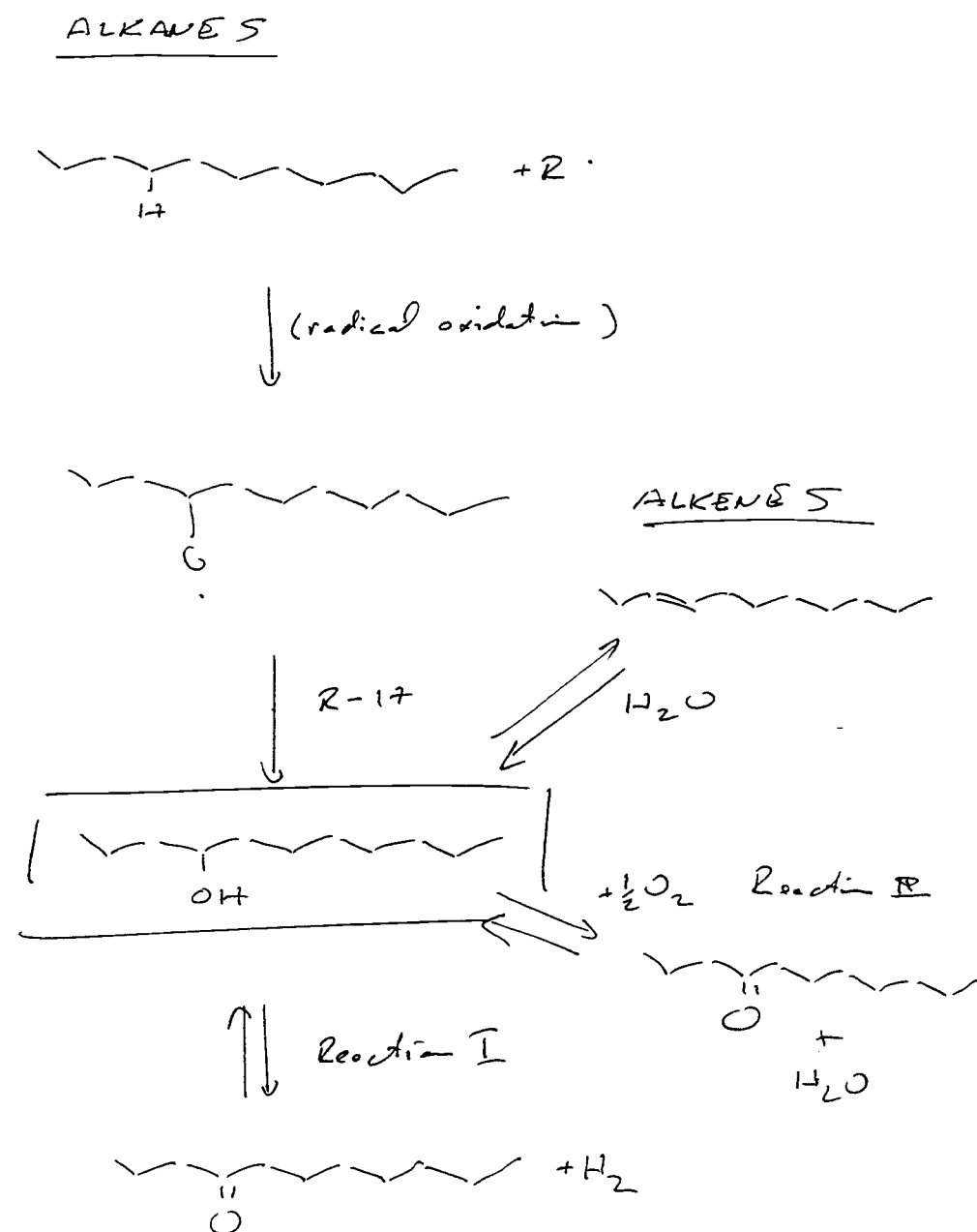
Figure 6.9. Proposed reaction scheme for the generation of ketones during the pyrolysis of aliphatic-rich organic matter.

CHAPTER 7

Conclusions

Hydrothermal alteration of sedimentary organic matter in the Guaymas Basin transforms the insoluble organic matter into petroleum by high temperature aqueous pyrolysis. The results obtained in this dissertation demonstrate the utility of applying pyrolysis techniques such as hydrous pyrolysis and confinement pyrolysis to simulate and study the organic geochemical processes occurring under extreme hydrothermal conditions such as those found in the Guaymas Basin hydrothermal system. A survey of the oils and sediment extracts from this system and the application of pyrolysis techniques to duplicate the natural hydrous pyrolysis process has resulted in the following :

- several homologous series of aliphatic ketones were found to be ubiquitous in the oils associated with high temperature hydrothermal vents, and in the extracts of sediments that have been thermally altered by sill intrusions, their smooth distributions indicate a pyrolytic origin;

- novel isoprenoid phenols are the major compounds in the polar NSO fractions of hydrothermal oils and their distributions indicate an origin from natural product precursors in the sedimentary organic matter;

- several series of alkylphenol isomers are present in the oils, their smooth distributions indicate that they are hydrothermal synthesis products;

- the rapid hydrothermal oil generation process at high temperature is suited for simulation by pyrolysis methods such as hydrous pyrolysis;

- a series of experiments using the hydrous pyrolysis technique resulted in a re-evaluation of the Hoering (1984) paper, proposing a combination of ionic and radical reactions to explain the extent of deuterium incorporation observed when pyrolysis experiments are carried out in D_2O;

- the application of a standard hydrous pyrolysis technique duplicated some of the thermally-enhanced diagenetic conversions documented under natural conditions;

- evaluation of the hydrous pyrolysis technique indicated that mineral-catalyzed reactions may be preferentially decreased relative to the radical cracking reactions when applying the method to the pyrolysis of unconsolidated marine sediments;

- the procedure of confinement pyrolysis was developed and successfully applied to the simulation of catagenetic transformations occurring by hydrothermal alteration;

- reaction pathways were proposed to explain the origin of the aliphatic ketones common in the hydrothermal oils.

The proposed reaction pathways presented in this thesis are based on both experimental results and evidence reported in the literature. The hypothesized role of clays as active sites for ionic chemistry is supported by numerous reports in the literature on the catalytic effects of clay minerals. Further research into specific reaction pathways of model organic compounds is required before conclusions can be drawn about the relative contributions of ionic and radical reactions.

REFERENCES

Albaigés J., J. Algaba and J. Grimalt (1984) Extractable and bound neutral lipids in some lacustrine sediments. Org. Geochem. 6, 223-236.

Alexander R., R. I. Kagi and A. V. Larcher (1982) Clay catalysis of aromatic hydrogen-exchange reactions. Geochim. Cosmochim. Acta 46, 219-222.

Anderson R. N., M. G. Angseth and J. G. Sclater (1977) The mechanisms of heat transfer through the floor of the Indian Ocean. J. Geophys. Res. 82, 3391-3409.

Blanc P. and J. Connan (1992) Generation and expulsion of hydrocarbons from a Paris Basin Toarcian source rock: An experimental study by confined-system pyrolysis. Energy Fuels 6, 666-677.

Bernard B. B., J. M. Brooks and W. M. Sackett (1976) Natural gas seepage in the Gulf of Mexico. Earth Planet. Sci. Lett. 31, 48-54.

Blouri B., J. Giraud, S. Nouri and D. Herault (1981) Steam cracking of high-molecular-weight hydrocarbons. Ind. Eng. Chem. Process Des. Dev. 20, 307-313.

Brassell S. C., P. A. Comet, G. Eglinton, P. J. Isaacson, J. McEvoy, J. R. Maxwell, I. D. Thompson, P. J. C. Tibbetts and J. K. Volkman (1980) The origin and fate of lipids in the Japan trench. In Advances in Organic Geochemistry 1979 (Eds. A. G. Douglas and J. R. Maxwell), pp. 375-392, Pergamon Press, Oxford.

Brassell S. C., G. Eglinton, J. R. Maxwell and R. P. Philp (1978) Natural background of alkanes in the aquatic environment. In Aquatic Pollutants: Transformation and Biological Effects (Eds. O. Hutzinger, T. H. van Lelyveld and B. C. J. Zoeteman), pp. 69-86, Pergamon Press, New York.

Breslow R. (1991) Hydrophobic effects on simple organic reactions in water. Acc. Chem. Res. 24, 159-164.

Burlingame A. L., P. A. Haug, H. K. Schnoes and B. R. T. Simoneit (1969) Fatty acids derived from the Green River formation oil shale by extraction and oxidations - A review. In Advances in Organic Geochemistry 1968 (Eds. P. A. Schenck and I. Havenaar), pp. 85-129, Pergamon-Vieweg, Oxford.

Calvert S. E. (1966) Accumulation of diatomaceous silica in the sediments of the Gulf of California. GSA Bulletin 77, 569-596.

Coleman M. M., L. Selvaraj, M. Sobkowiak and E. Yoon (1992) Potential stabilizers for jet fuels subjected to thermal stress above 400°C. Energy Fuels 6, 535-539.

Comet P. A., J. McEvoy, W. Giger and A. G. Douglas (1986) Hydrous and anhydrous pyrolysis of DSDP Leg 75 kerogens - A comparative study using a biological marker approach. Org. Geochem. 9, 171-182.

Connan J., A. Restle and P. Albrecht (1980) Biodegradation of crude oil in the Aquitaine Basin. In Advances in Organic Geochemistry 1979 (Eds. A. G. Douglas and J. R. Maxwell), pp. 1-17, Pergamon Press, Oxford.

Corliss J. B., J. Dymond, L. I. Gordon, J. M. Edmond, R. P. von Herzen, R. D. Ballard, K. Green, D. Williams, A. Bainbridge, K. Crane and T. H. van Andel (1979) Submarine thermal springs on the Galapagos Rift. Science 203, 1073-1083.

Cox R. E., J. R. Maxwell, G. Eglinton, C. T. Pillinger, R. G. Ackman and S. N. Hooper (1970) The geological fate of chlorophyll: The absolute stereochemistry of acyclic isoprenoid acid in a 50-million year old lacustrine sediment. Chem. Comm. pp. 1639-1641.

Cranwell P. A. (1977) Organic geochemistry of Cam Loch (Sutherland) sediments. Chem. Geol. 20, 205-221.

Curray J. R. et al. (1982) Initial Reports of the Deep Sea Drilling Project, Leg 64. pp. 1313, Washington D. C., U. S. Government Printing Office.

Depeyre D. and C. Flicoteaux (1991) Modeling of thermal steam cracking of n-hexadecane. Ind. Eng. Chem. Res. 30, 1116-1130.

Djuricic M., R. C. Murphy, D. Vitorovic and K. Biemann (1971) Organic acids obtained by alkaline permanganate oxidation of kerogen from the Green River (Colorado) shale. Geochim. Cosmochim. Acta 35, 1201-1207.

Eglinton T. I. and A. G. Douglas (1988) Quantitative study of biomarker hydrocarbons released from kerogens during hydrous pyrolysis. Energy Fuels 2, 81-88.

Eglinton T. I., S. J. Rowland, C. D. Curtis and A. G. Douglas (1986) Kerogen-mineral reactions at raised temperatures in the presence of water. In Advances in Organic Geochemistry 1985 (Eds. D. Leythaeuser and J. Rullkötter), Org. Geochem. 10, 1041-1052.

Einsele G. and K. Kelts (1982) Pliocene and Quaternary mud turbidites in the Gulf of California: Sedimentology, mass physical properties and significance. In Initial Reports of the Deep Sea Drilling Project, Vol. 64, Pt. 2 (Eds. J. R. Curray, D. G. Moore et al.), pp. 511-526, U.S. Govt. Printing Office, Washington.

Einsele G. et al. (1980) Intrusion of basaltic sills into highly porous sediments, and resulting hydrothermal activity. Nature 283, 441-445.

Eisma E. and J. W. Jurg (1969) Fundamental aspects of the generation of petroleum. In Organic Geochemistry (Eds. G. Eglinton and M. T. J. Murphy), pp. 676-698. Springer, Berlin.

Ensminger A. (1977) Evolution de composes polycycliques sedimentaires. These de docteur en Sciences, Universite Louis Pasteur, Strasbourg, France.

Ensminger A., P. Albrecht, G. Ourisson and B. Tissot (1977) Evolution of polycyclic alkanes under the effect of burial (Early Toarcian shales, Paris Basin). In Advances in Organic Geochemistry 1975 (Eds. R. Campos and J. Goni), pp. 45-52, Enadimsa, Madrid.

Ensminger A., A. van Dorsselaer, C. Spyckerelle, P. Albrecht and G. Ourisson (1974) Pentacyclic triterpanes of the hopane type as ubiquitous geochemical markers: Origin and significance. In Advances in Organic Geochemistry 1973 (Eds. B. Tissot and F. Bienner), pp. 245-260, Editions Technip, Paris.

Eugster H. P. (1986) Minerals in hot water. Am. Mineral. 71, 655-673.

Evans R. J. and G. T. Felbeck, Jr. (1983) High temperature simulation of petroleum formation - II. Effect of inorganic sedimentary constituents on hydrocarbon formation. Org. Geochem. 4, 145-152.

George S. C. and D. R. Jardine (1993) Ketones in a Proterozoic dolerite sill. Org. Geochem., In press.

Gieskes J. M., H. Elderfield, J. R. Lawrence, J. Johnson, B. Meyers and A. Campbell (1982a) Geochemistry of interstitial waters and sediments, Leg 64, Gulf of California. In Initial Reports of the Deep Sea Drilling Project, Vol. 64, Pt. 2 (Eds. J. R. Curray, D. G. Moore et al.), pp. 675-694, U.S. Govt. Printing Office, Washington.

Gieskes J. M., M. Kastner, G. Einsele, K. Kelts and J. Niemitz (1982b) Hydrothermal activity in the Guaymas Basin, Gulf of California: A synthesis. In Initial Reports of the Deep Sea Drilling Project, Vol. 64, Pt. 2 (Eds. J. R. Curray, D. G. Moore et al.), pp. 1159-1168, U.S. Govt. Printing Office, Washington.

Gieskes J. M., B. R. T. Simoneit, T. Brown, T. Shaw, Y.-C. Wang and A. Magenheim (1988) Hydrothermal fluids and petroleum in surface sediments of Guaymas Basin, Gulf of California: A case study. Can. Mineral. 26, 589-602.

Goldhaber M. B. (1974) Equilibrium and dynamic aspects of the marine geochemistry of sulfur. Ph. D. Thesis, University of California at Los Angeles, California.

Goldstein T. P. (1983) Geocatalytic reactions in formation and maturation of petroleum. Amer. Assoc. Petrol. Geol. Bull. 67, 152-159.

Goosens H., J. W. de Leeuw, P. A. Schenck and S. C. Brassell (1984) Tocopherols as likely precursors of pristane in ancient sediments and crude oils. Nature 312, 440-442.

Goth K., J. W. de Leeuw, W. Püttman and E. W. Tegelaar (1988) Origin of Messel Oil Shale kerogen. Nature 336, 759-761.

Haines A. H. (1988) Methods for the Oxidation of Organic Compounds. Academic Press, London.

Henderson W., G. Eglinton, P. Simmonds and J. E. Lovelock (1968) Thermal alteration as a contributory process to the genesis of petroleum. Nature 219, 1012-1016.

Hoering T. C. (1984) Thermal reactions of kerogen with added water, heavy water and pure organic substances. Org. Geochem. 5, 267-278.

Horsfield B. (1984) Pyrolysis studies and petroleum exploration. In Advances in Petroleum Geochemistry, Vol. 1 (Eds. J. Brooks and D. Welte), pp. 247-298, Academic Press, New York.

Horsfield B. and A. G. Douglas (1980) The influence of minerals on the pyrolysis of kerogens. Geochim. Cosmochim. Acta 44, 1119-1131.

Huang W.-Y. and W. G. Meinschein (1979) Sterols as ecological indicators. Geochim. Cosmochim. Acta 43, 739-745.

Huizinga B. J., E. Tannenbaum and I. R. Kaplan (1987a) The role of minerals in the thermal alteration of organic matter - III. Generation of bitumen in laboratory experiments. Org. Geochem. 11, 591-604.

Huizinga B. J., E. Tannenbaum and I. R. Kaplan (1987b) The role of minerals in the thermal alteration of organic matter - IV. Generation of n-alkanes, acyclic isoprenoids, and alkenes in laboratory experiments. Geochim. Cosmochim. Acta 51, 1083-1097.

Johns W. D. (1979) Clay mineral catalysis and petroleum generation. Ann. Rev. Earth. Planet. Sci. 7, 183-198.

Kastner M. (1982) Evidence for two distinct hydrothermal systems in the Guaymas Basin. In Initial Reports of the Deep Sea Drilling Project, Vol. 64, Pt. 2 (Eds. J. R. Curray, D. G. Moore et al.), pp. 1143-1157, U.S. Govt. Printing Office, Washington.

Kawka O. E. (1990) Hydrothermal alteration of sedimentary organic matter in Guaymas Basin, Gulf of California. Ph. D. Thesis, Oregon State University, Corvallis, Oregon.

Kawka O. E. and B. R. T. Simoneit (1987) Survey of hydrothermally-generated petroleums from the Guaymas Basin spreading center. Org. Geochem. 11, 311-328.

Kawka O. E. and B. R. T. Simoneit (1990) Polycyclic aromatic hydrocarbons in hydrothermal petroleums from the Guaymas Basin spreading center. Appl. Geochem. 5, 17-27.

Kissin Y. V. (1987) Catagenesis and composition of petroleum: Origin of n-alkanes and isoalkanes in petroleum crudes. Geochim. Cosmochim. Acta 51, 2445-2457.

Kissin Y. V. (1990) Catagenesis of light cycloalkanes in petroleum. Org. Geochem. 15, 575-594.

Kvenvolden K. A. and B. R. T. Simoneit (1990) Hydrothermally derived petroleum: Examples from Guaymas Basin, Gulf of California, and Escanaba Trough, Northeast Pacific Ocean. AAPG Bulletin 74, 223-237.

Kvenvolden K. A., J. B. Rapp, F. D. Hostettler, J. L. Morton, J. D. King and G. E. Claypool (1986) Petroleum associated with metallic sulfide in sediment from Gorda Ridge. Science 234, 1231-1234.

Kvenvolden K. A., J. B. Rapp, F. D. Hostettler, J. D. King and G. E. Claypool (1988) Organic geothermometry of petroleum from Escanaba Trough, offshore northern California. In Advances in Organic Geochemistry 1987 (Eds. L. Mattavelli and L. Novelli), Org. Geochem. 13, 351-355.

Lao Y., J. Korth, J. Ellis and P. T. Crisp (1989) Hetergeneous reactions of 1-pristene catalysed by clays under simulated geological conditions. Org. Geochem. 14, 375-379.

Larcher A. V., R. Alexander and R. I. Kagi (1988) Differences in reactivities of sedimentary hopane diastereomers when heated in the presence of clays. In Advances in Organic Geochemistry 1987 (Eds. L. Mattavelli and L. Novelli), Org. Geochem. 13, 665-669.

Larcher A. V., R. Alexander, S. J. Rowland and R. I. Kagi (1986) Acid catalysis of alkyl hydrogen exchange and configurational isomerisation reactions: Acyclic isoprenoid acids. In Advances in Organic Geochemistry 1985 (Eds. D. Leythaeuser and J. Rullkötter), Org. Geochem. 10, 1015-1021.

Leif R. N., B. R. T. Simoneit and K. A. Kvenvolden (1992) Hydrous pyrolysis of n-$C_{32}H_{66}$ in the presence and absence of inorganic components. Am. Chem. Soc., Div. Fuel Chem. Preprints, 37(4), 1748-1753.

Lewan M. D. (1983) Effects of thermal maturation on stable organic carbon isotopes as determined by hydrous pyrolysis of Woodford Shale. Geochim. Cosmochim. Acta 47, 1471-1479.

Lewan M. D. (1992) Nomenclature for pyrolysis experiments involving H_2O. Am. Chem. Soc., Div. Fuel Chem. Preprints, 37(4), 1545-1547.

Lewan M. D. (1993) Laboratory simulation of petroleum generation: Hydrous pyrolysis. In Organic Geochemistry (Eds. M. H. Engel and S. A. Macko), Plenum Publishing Corp., in press.

Lewan M. D., M. Bjorøy and D. L. Dolcater (1986) Effects of thermal maturation on steroid hydrocarbons as determined by hydrous pyrolysis of Phosphoria Retort Shale. Geochim. Cosmochim. Acta 50, 1977-1987.

Lewan M. D., J. C. Winters and J. H. McDonald (1979) Generation of oil-like pyroysates from organic-rich shales. Science 203, 897-899.

Lonsdale P. (1985) A transform continental margin rich in hydrocarbons, Gulf of California. AAPG Bulletin 69, 1160-1180.

Lonsdale P. and L. Lawver (1980) Immature plate boundary zones studied with a submersible in the Gulf of California. GSA Bulletin 91, 555-569.

Lonsdale P. and K. Becker (1985) Hydrothermal plumes, hot springs, and conductive heat flow in the Southern Trough of Guaymas Basin. Earth Planet. Sci. Lett. 73, 211-225.

Louda J. W. and E. W. Baker (1984) Perylene occurrence and possible sources in deep-ocean sediments. Geochim. Cosmochim. Acta 48, 1043-1058.

Lu S.-T., E. Ruth and I. R. Kaplan (1989) Pyrolysis of kerogens in the absence and presence of montmorillonite - I. The generation, degradation and isomerization of steranes and triterpanes at 200 and 300°C. Org. Geochem. 14, 491-499

Maxwell J. R., R. E. Cox, R. G. Ackman and S. N. Hooper (1972) The diagenesis and maturation of phytol. The stereochemistry of 2,6,10,14-tetramethylpentadecane from an ancient sediment. In Advances in Organic Geochemistry 1971 (Eds. H. R. von Gaertner and H. Wehner), pp. 177-191.

Michaelis W. and P. Albrecht (1979) Molecular fossils of Archaebacteria in kerogen. Naturwiss. 66, 420-422.

Monthioux M., P. Landais and J.-C. Monin (1985) Comparison between natural and artificial maturation series of humic coals from the Mahakam delta, Indonesia. Org. Geochem. 8, 275-292.

Moore D. G. (1973) Plate edge deformation and crustal growth in the Gulf of California. GSA Bulletin 84, 1883-1905.

Peter J. M., P. Peltonen, S. D. Scott, B. R. T. Simoneit and O. E. Kawka (1991) ^{14}C ages of hydrothermal petroleum and carbonate in Guaymas Basin, Gulf of California: Implications for oil generation, expulsion, and migration. Geology 19, 253-256.

Peters K. E., J. M. Moldowan and P. Sundararaman (1990) Effects of hydrous pyrolysis on biomarker thermal maturity parameters: Monterey Phosphatic and Siliceous members. Org. Geochem. 15, 249-265.

Regtop R. A., P. T. Crisp and J. Ellis (1982) Chemical characterization of shale oil from Rundle, Queensland. Fuel 61, 195-192.

Regtop R. A., J. Ellis, P. T. Crisp, A. Ekstrom and C. J. R. Fookes (1985) Pyrolysis of model compounds on spent oil shales, minerals and charcoal. Fuel 64, 1640-1646.

Ross D. (1992a) Comments on the source of petroleum hydrocarbons in hydrous pyrolysis. Org. Geochem. 18, 79-81.

Ross D. (1992b) Hydrothermal media, oil shale, and coal. Am. Chem. Soc., Div. Fuel Chem. Preprints, 37(4), 1555-1561.

Rovere C. E., P. T. Crisp, J. Ellis and P. D. Bolton (1983) Chemical characterization of shale oil from Condor, Australia. Fuel 62, 1274-1282.

Seifert W. K. and J. M. Moldowan (1978) Applications of steranes, terpanes and monoaromatics to the maturation, migration and source of crude oils. Geochim. Cosmochim. Acta 42, 77-95.

Shock E. L. (1990) Geochemical constraints on the origin of organic compounds in hydrothermal systems. Origins of Life 20, 331-367.

Sieskind O., G. Joly and P. Albrecht (1979) Simulation of the geochemical transformations of sterols: Superacid effect of clay minerals. Geochim. Cosmochim. Acta 43, 1675-1679.

Simoneit B. R. T. (1978) Organic geochemistry of terrigenous muds and various shales from the Black Sea, DSDP Leg 42B. In Initial Reports of the Deep Sea Drilling Project, Vol. 42, Pt. 2 (Eds. D. Ross, Y. Neprochnov et al.), pp. 749-753, U.S. Government Printing Office, Washington, D.C.

Simoneit B. R. T. (1979) Organic geochemistry of the shales from the Northwestern Proto-Atlantic, DSDP Leg 43. In Initial Reports of the Deep Sea Drilling Project, Vol. 43 (Eds. B. Tucholke, P. Vogt et al.), pp. 643-649, U.S. Government Printing Office, Washington, D.C.

Simoneit B. R. T. (1983) Organic matter maturation and petroleum genesis: geothermal versus hydrothermal. In Proc. Symp., The Role of Heat in the Development of Energy and Mineral Resources in the Northern Basin and Range Province, Geotherm. Res. Council, Special Report No. 13, pp. 215-241, Davis, California.

Simoneit B. R. T. (1984a) Hydrothermal effects on organic matter - high versus low temperature components. In Advances in Organic Geochemistry 1983 (Eds. P.A. Schenck, J.W. deLeeuw and G.W.M. Lijmbach), Pergamon Press, Oxford, Org. Geochem. 6, 857-864.

Simoneit B. R. T. (1984b) Effects of hydrothermal activity on sedimentary organic matter: Guaymas Basin, Gulf of California - petroleum genesis and protokerogen degradation. In Hydrothermal Processes at Seafloor Spreading Centers (Eds. P. A. Rona et al.), pp. 451-471, Plenum Publishing Corp., New York.

Simoneit B. R. T. (1985) Hydrothermal petroleum: Genesis, migration, and deposition in Guaymas Basin, Gulf of California. Can. J. Earth Sci. 22, 1919-1929.

Simoneit B. R. T. (1988) Petroleum generation in submarine hydrothermal systems: An update. Can. Mineral. 26, 827-840.

Simoneit B. R. T. (1990) Petroleum generation, an easy and widespread process in hydrothermal systems: An overview. Appl. Geochem. 5, 3-15.

Simoneit B. R. T. (1991) Hydrothermal effects on Recent diatomaceous sediments in Guaymas Basin - generation, migration and deposition of petroleum. In The Gulf and Peninsular Province of the Californias (Eds. J.P. Dauphin and B.R.T. Simoneit), Amer. Assoc. Petrol. Geologists, Tulsa, OK, Memoir 47, Chapt. 38, pp. 793-825.

Simoneit B. R. T. (1992) Natural hydrous pyrolysis - Petroleum generation in submarine hydrothermal systems. In Productivity, Accumulation and Preservation of Organic Matter in Recent Sediments and Ancient Sediments (Eds. J. K. Whelan and J. W. Farrington), pp. 368-402, Columbia University Press, New York.

Simoneit B. R. T. (1993) Lipid/bitumen maturation by hydrothermal activity in sediments of Middle Valley, ODP Leg 139. In Proceedings of the Ocean Drilling Program, Leg 139, Scientific Results, in press.

Simoneit B. R. T. and A. L. Burlingame (1973) Carboxylic acids derived from Tasmanian tasmanite by extractions and kerogen oxidations. Geochim. Cosmochim. Acta 37, 595-610.

Simoneit B. R. T. and K. A. Kvenvolden (1993) Comparison of [14]C Ages of hydrothermal petroleums. Org. Geochem., in press.

Simoneit B. R. T. and P. F. Lonsdale (1982) Hydrothermal petroleum in mineralized mounds at the seabed of Guaymas Basin. Nature 295, 198-202.

Simoneit B. R. T., O. E. Kawka and M. Brault (1988) Origin of gases and condensates in the Guaymas Basin hydrothermal system (Gulf of California). Chem. Geol. 71, 169-182.

Simoneit B. R. T., O.E. Kawka and G.-M. Wang (1992a) Biomarker maturation in contemporary hydrothermal systems, alteration of immature organic matter in zero geological time. In Biological Markers in Sediments and Petroleum, Seifert Memorial Volume (Eds. J.M. Moldowan, P. Albrecht and R.P. Philp), pp. 124-141, Chapt. 7, Prentice Hall, Englewood Cliffs, NJ.

Simoneit B. R. T., R. N. Leif, A. A. Sturz, A. E. Sturdivant and J. M. Gieskes (1992b) Geochemistry of shallow sediments in Guaymas Basin, Gulf of California: Hydrothermal gas and oil migration and effects of mineralogy. Org. Geochem. 18, 765-784.

Simoneit B. R. T., M. A. Mazurek, S. Brenner, P. T. Crisp and I. R. Kaplan (1979) Organic geochemistry of Recent sediments from Guaymas Basin, Gulf of California. Deep-Sea Res. 26A, 879-891.

Simoneit B. R. T., R. P. Philp, P. D. Jenden and E. M. Galimov (1984) Organic geochemistry of Deep Sea Drilling Project sediments from the Gulf of California - Hydrothermal effects on unconsolidated diatom ooze. Org. Geochem. 7, 173-205.

Simoneit B. R. T., G. Sheng, X. Chen, J. Fu, J. Zhang and Y. Xu (1991) Molecular marker study of extractable organic matter in aerosols from urban areas of China. Atmosph. Environ. 25A, 2111-2129.

Sinninghe Damsté J. S., A. C. Kock-Van Dalen, J. W. de Leeuw, P. A. Schenck, G. Sheng and S. C. Brassell (1987) The identification of mono-, di- and trimethyl 2-methyl-2-(4,8,12-trimethyltridecyl)chromans and their occurrence in the geosphere. Geochim. Cosmochim. Acta 51, 2393-2400.

Siskin M., G. Brons, A. R. Katritzky and M. Balasubramanian (1990) Aqueous organic chemistry. 1. Aquathermolysis: Comparison with thermolysis in the reactivity of aliphatic compounds. Energy Fuels 4, 475-482.

Siskin M. and A. R. Katritzky (1991) Reactivity of organic compounds in hot water: Geochemical and technological implications. Science 254, 231-237.

Smith J. W., B. D. Batts and T. D. Gilbert (1989) Hydrous pyrolysis of model compounds. Org. Geochem. 14, 365-373.

Solomon D. H. (1968) Clay minerals as electron acceptors and/or electron donors in organic reactions. Clays Clay Miner. 16, 31-39.

Spiro B. (1984) Effects of the mineral matrix on the distribution of geochemical markers in thermally affected sedimentary sequences. Org. Geochem. 6, 543-559.

Sugimura Y. and S. Tsuge (1978) Fundamental splitting conditions for pyrogram measurements with glass capillary gas chromatography. Anal. Chem. 50, 1968-1972.

Takeda N., S. Sato and T. Machihara (1990) Study of petroleum generation by compaction pyrolysis - I. Construction of a novel pyrolysis system with compaction and expulsion of pyrolyzate from source rock. In Advances in Organic Geochemistry 1989 (Eds. B. Durand and F. Behar), Org. Geochem. 16, 143-153.

Tannenbaum E. and I. R. Kaplan (1985) Role of minerals in the thermal alteration of organic matter - I: Generation of gases and condensates under dry conditions. Geochim. Cosmochim. Acta 49, 2589-2604.

Tannenbaum E., B. J. Huizinga and I. R. Kaplan (1986a) Role of minerals in thermal alteration of organic matter - II: A material balance. Am. Assoc. Pet. Geol. Bull. 70, 1156-1165.

Tannenbaum E., E. Ruth and I. R. Kaplan (1986b) Steranes and triterpanes generated from kerogen pyrolysis in the absence and presence of minerals. Geochim. Cosmochim. Acta 50, 805-812.

Tegelaar E. W., J. W. de Leeuw, S. Derenne and C. Largeau (1989a) A reappraisal of kerogen formation. Geochim. Cosmochim. Acta 53, 3103-3106.

Tegelaar E. W., R. M. Matthezing, J. B. H. Jansen, B. Horsfield and J. W. de Leeuw (1989b) Possible origin of n-alkanes in high crude oils. Nature 342, 529-531.

Tegelaar E. W., J. W. de Leeuw, C. Largeau, S. Derenne, H.-R. Schulten, R. Muller, J. J. Boon, M. Nip and J. C. M. Sprenkels (1989c) Scope and limitations of several pyrolysis methods in the structural elucidation of a macromolecular plant constituent in the leaf cuticle of agave americana L. J. Anal. Appl. Pyrol. 15, 29-54.

Tissot B. P. and D. H. Welte (1984) Petroleum Formation and Occurrence: A New Approach to Oil and Gas Exploration, 2nd edn., pp. 699, Springer, Berlin.

Tsuchiya Y. and K. Sumi (1968) Thermal decomposition products of polyethylene. J. Polymer Sci. 6, 415-424.

van Andel T. (1964) Recent marine sediments of Gulf of California. In Marine Geology of the Gulf of California (Eds. T. van Andel and G. Shor), AAPG Memoir 3, pp. 260.

Venkatesan M. I. (1988a) Diploptene in Antarctic sediments. Geochim. Cosmochim. Acta 52, 217-222.

Venkatesan M. I. (1988b) Occurrence and possible sources of perylene in marine systems - a review. Mar. Chem. 25, 1-27.

Vitorovic D. (1980) Structure elucidation of kerogen by chemical methods. In Kerogen (Ed. B. Durand), pp. 301-338, Editions Technip, Paris.

Volkman J. K., R. Alexander, R. I. Kagi, R. A. Noble and G. W. Woodhouse (1983) A geochemical reconstruction of oil generation in the Barrow Sub-basin of Western Australia. Geochim. Cosmochim. Acta 47, 2091-2106.

Von Damm K. L. (1990) Seafloor hydrothermal activity: Black smoker chemistry and chimneys. Annu. Rev. Earth Planet. Sci. Lett. 18, 173-204.

Wampler T. P. (1989) Thermometric behavior of polyolefins. J. Anal. Appl. Pyrol. 15, 187-195.

211

Wampler T. P. and E. J. Levy (1987) Effects of slow heating rates on products of polyethylene pyrolysis. Analyst. 111, 1065-1067.

Weres O., A. S. Newton and L. Tsao (1988) Hydrous pyrolysis of alkanes, alkenes, alcohols and ethers. Org. Geochem. 12, 433-444.

Whelan J. K. and J. M. Hunt (1982) C_1-C_8 in Leg 64 sediments, Gulf of California. In Initial Reports of the Deep Sea Drilling Project, Vol. 64 (Eds. J. R. Curray et al.), pp. 763-779, U.S. Government Printing Office, Washington, D.C.

Williams D., K. Becker, L. A. Lawver and R. P. von Herzen (1979) Heat flow at the spreading centers of the Guaymas Basin, Gulf of California. J. Geophys. Res. 84, 6757-6769.

Wilson M. A., S. A. McCarthy, P. J. Collin and D. E. Lambert (1986) Alkene transformations catalysed by mineral matter during oil shale pyrolysis. Org. Geochem. 9, 245-253.

Wilt J. W. (1973) Free radical rearrangements. In Free Radicals (Ed. J. K. Kochi), pp. 333-501, Wiley, New York.

Wingert W. S. (1992) GC-MS analysis of diamondoid hydrocarbons in Smackover petroleums. Fuel 71, 37-43.

APPENDICES

Appendix 1

The Gas Chromatograms for the Seabed Oils from the Hydrothermal Vents of Guaymas Basin, Gulf of California

In this Appendix the gas chromatograms of the aliphatic , aromatic and NSO fractions for the interior and exterior oils collected during the 1988 Alvin dive series are presented.

1972-CH1 Interior
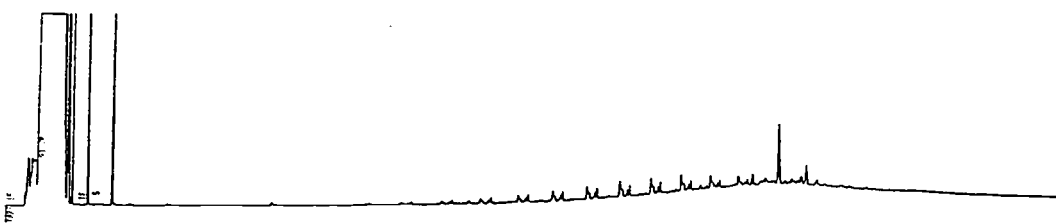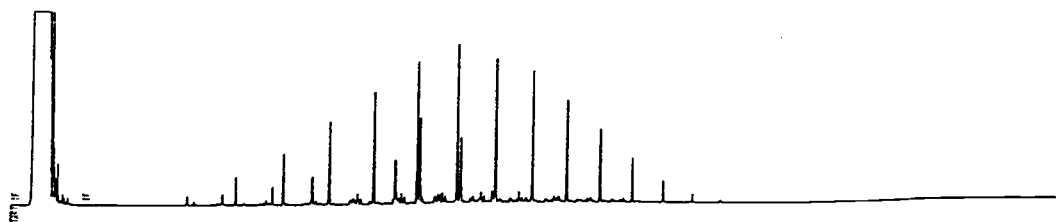
1972-CH1 Exterior
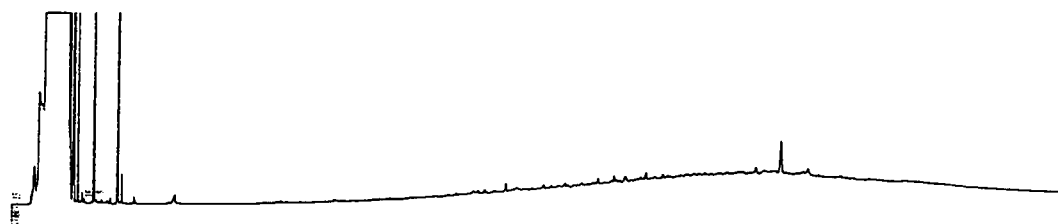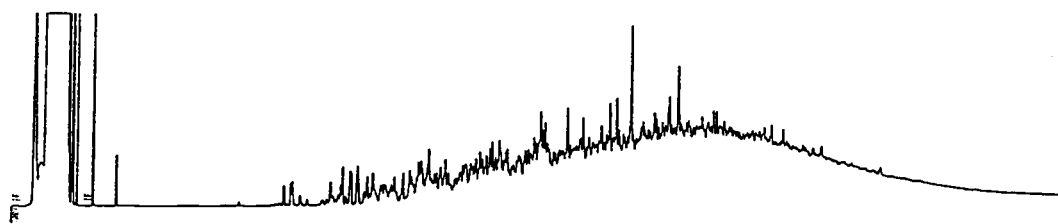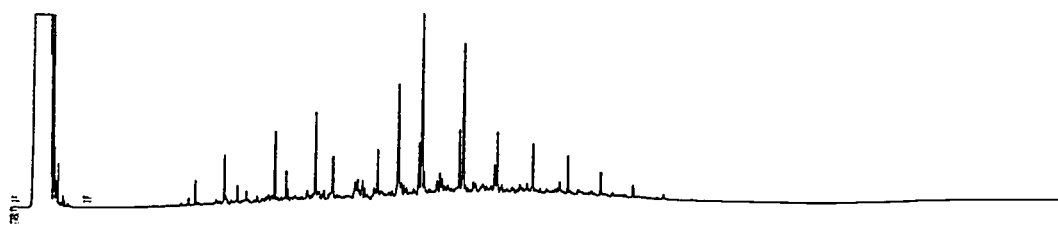
1983-CH1 Interior
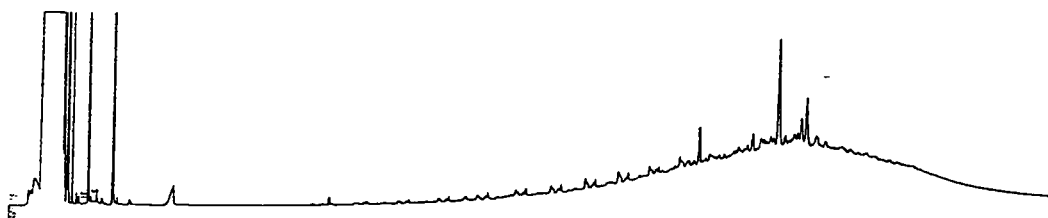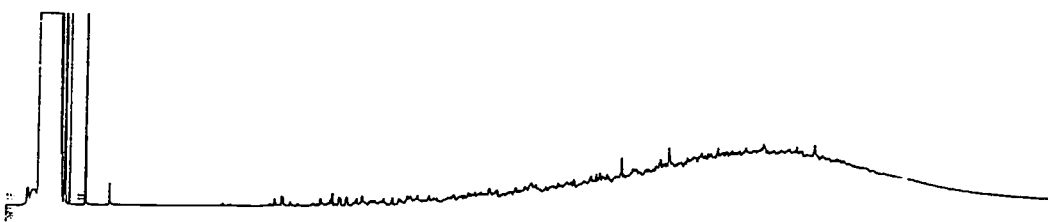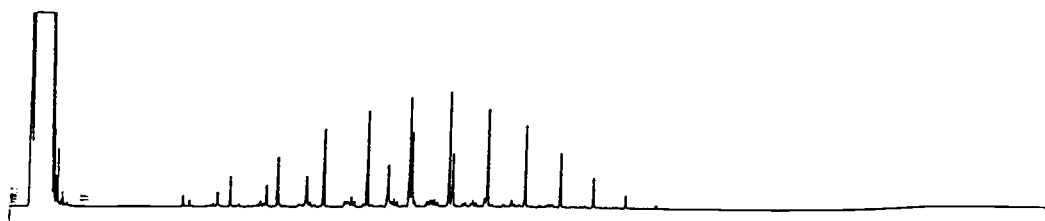
1983-CH1 Exterior
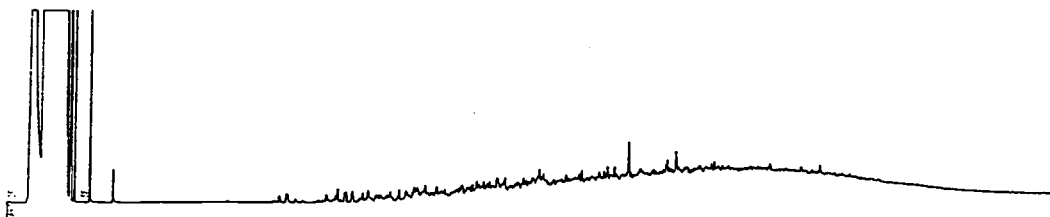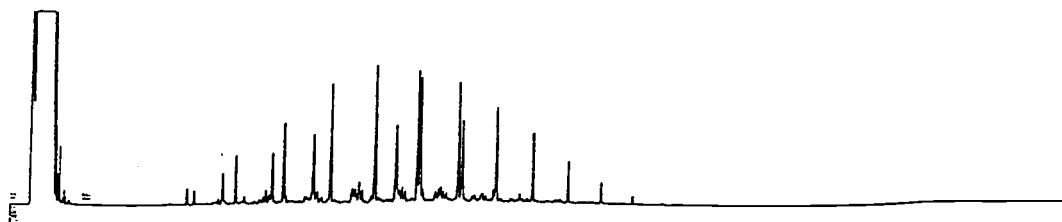
1984-CH1 Interior
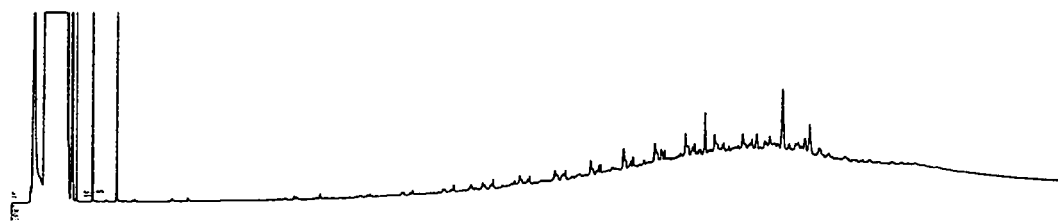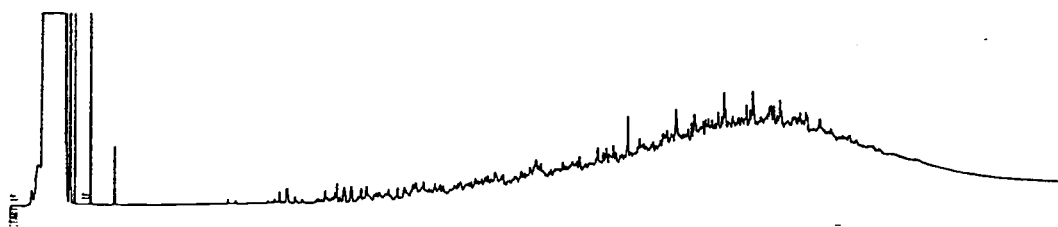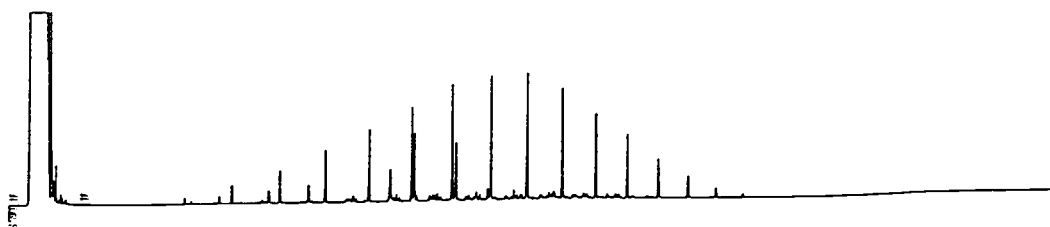
1984-CH1 Exterior
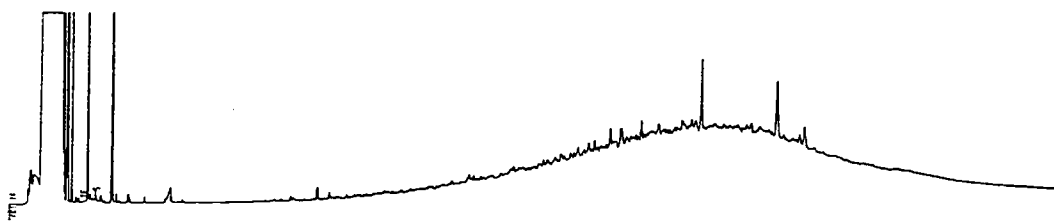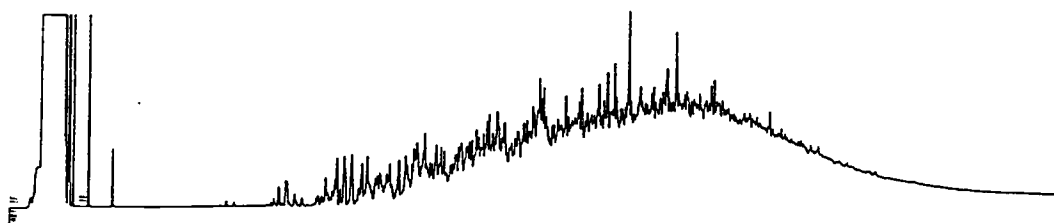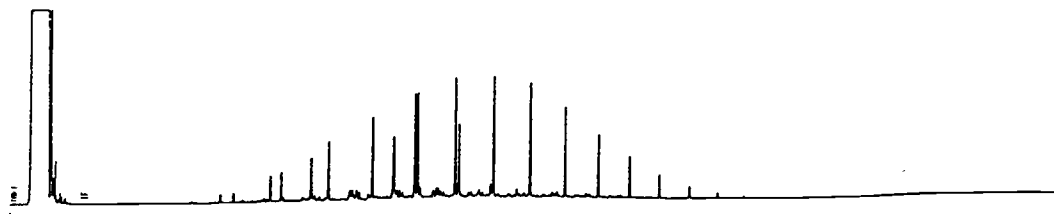
1984-CH2 Interior
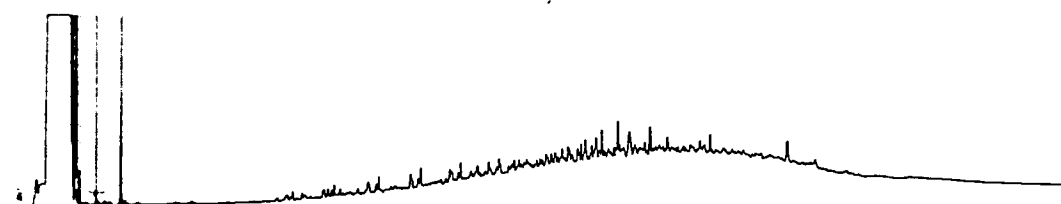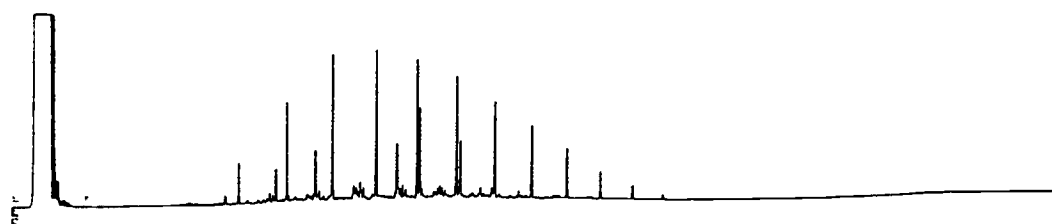
1984-CH2 Exterior
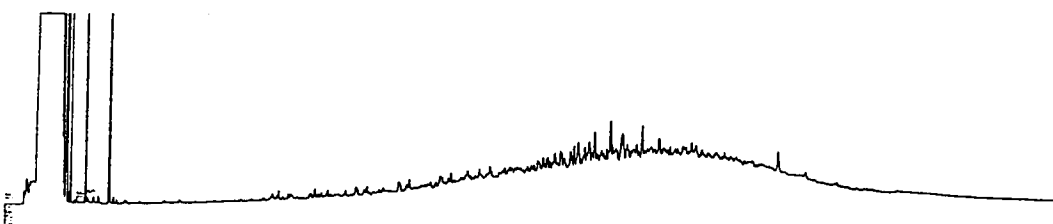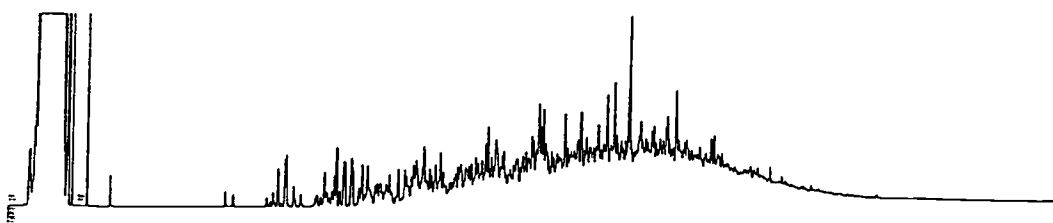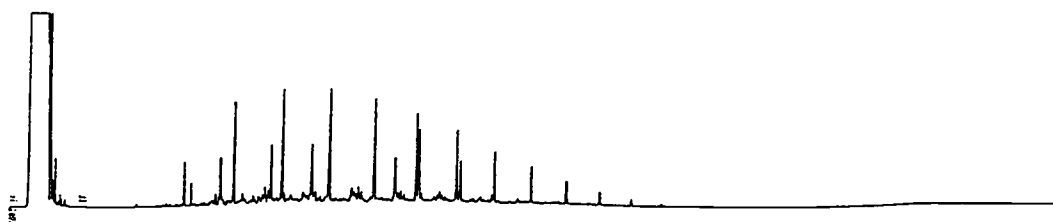
Appendix 2

The Gas Chromatograms for the Downcore Sediment Extracts from DSDP Site 477 of Guaymas Basin, Gulf of California

In this Appendix the gas chromatograms of the total extracts, aliphatic , aromatic and NSO fractions for the sediment extracts from DSDP Site 477 used in this thesis are presented.

477-2-2 (145-150)
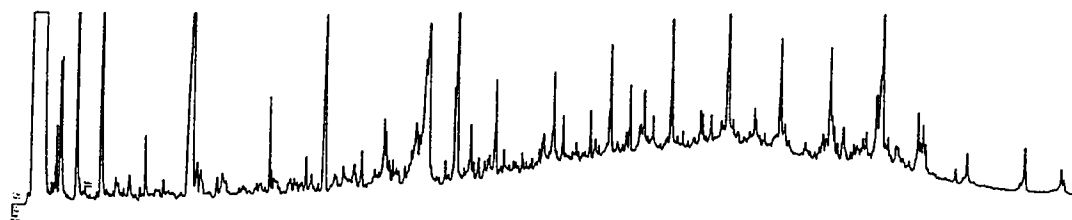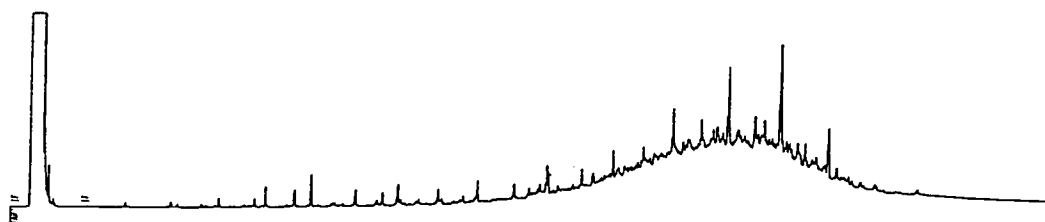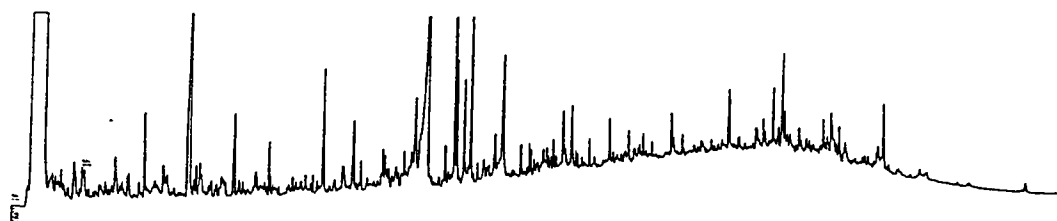
477-7-1 (88-90)
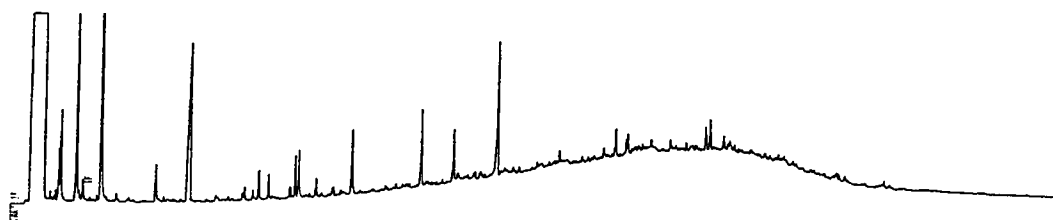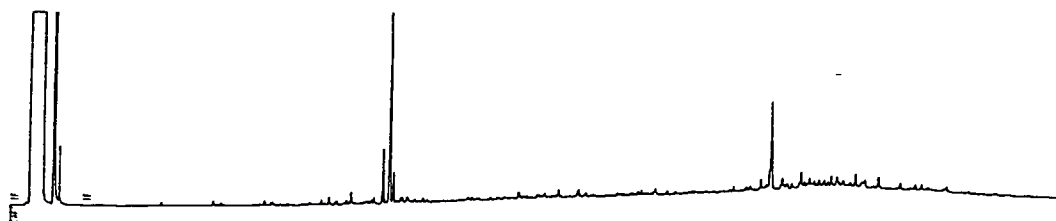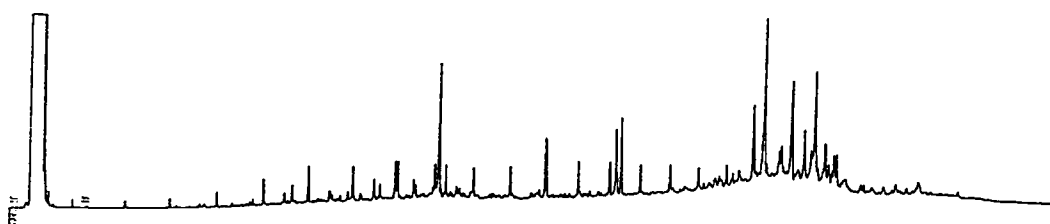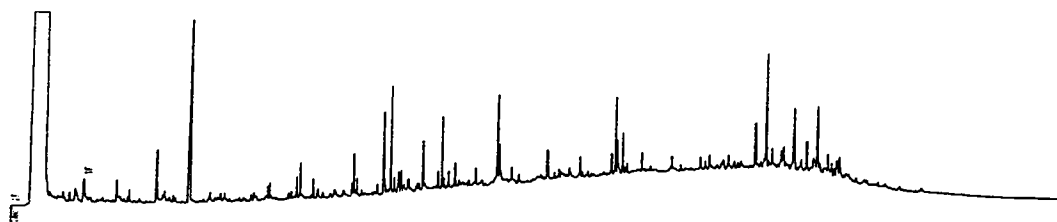
477-7-1 (106-108)
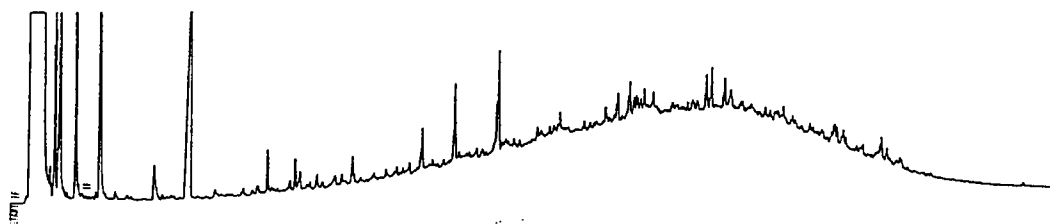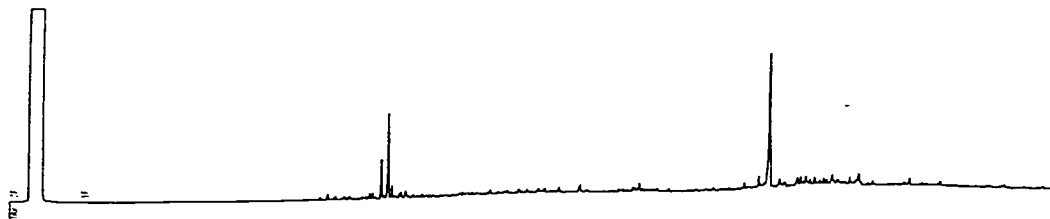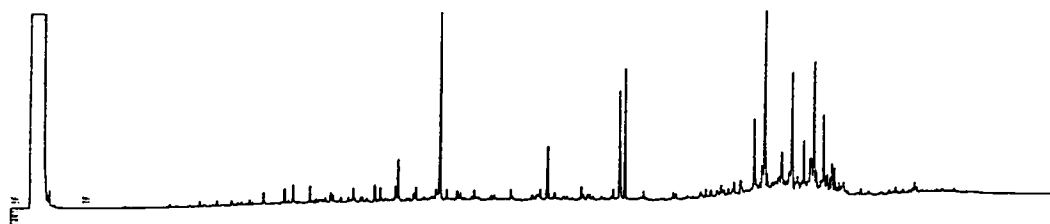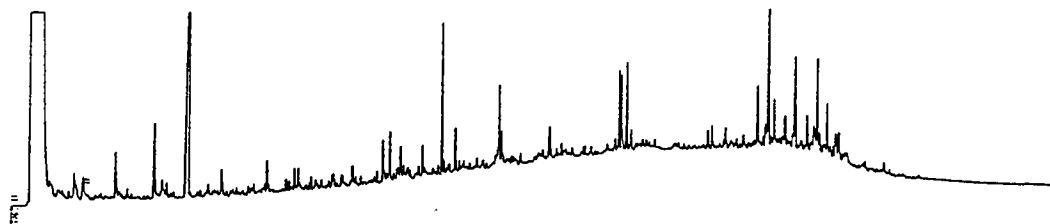
477-16-2 (140-145)
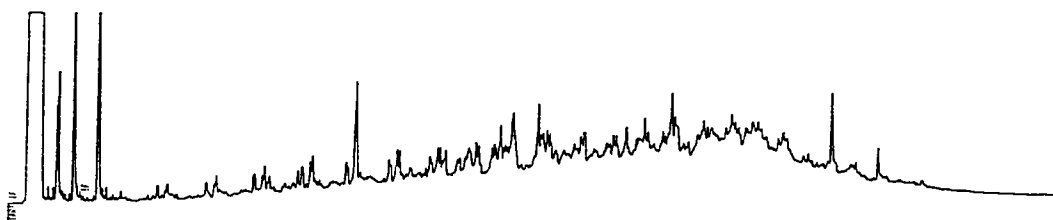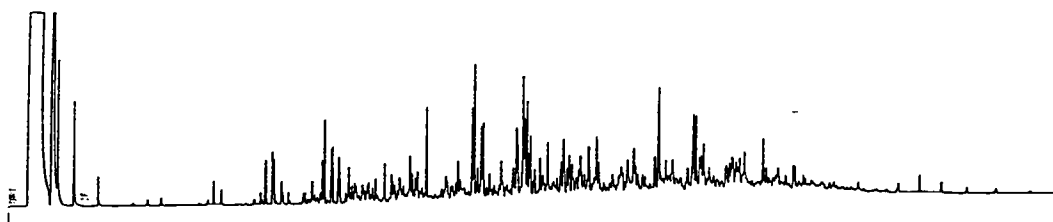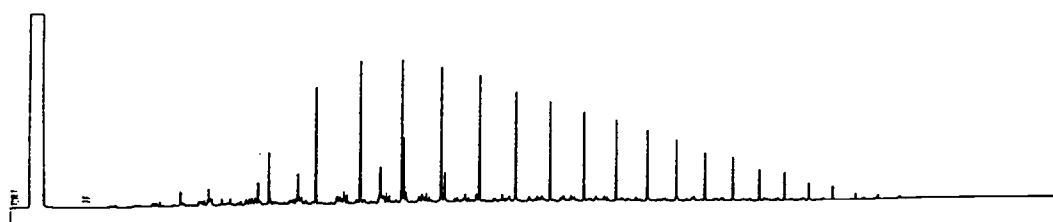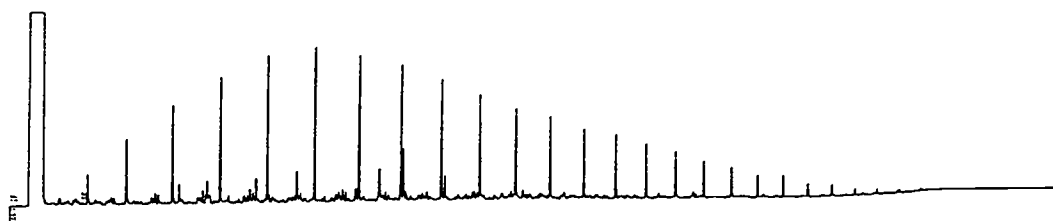
477-16-2 (145-150)
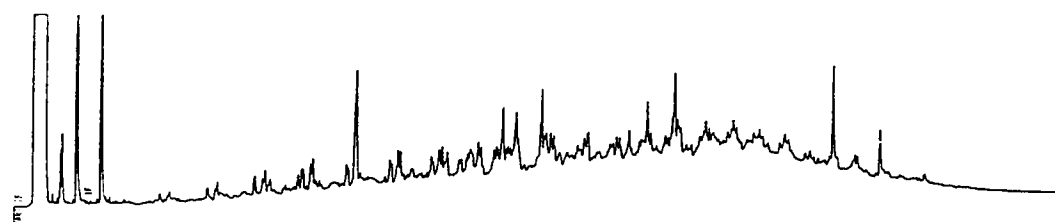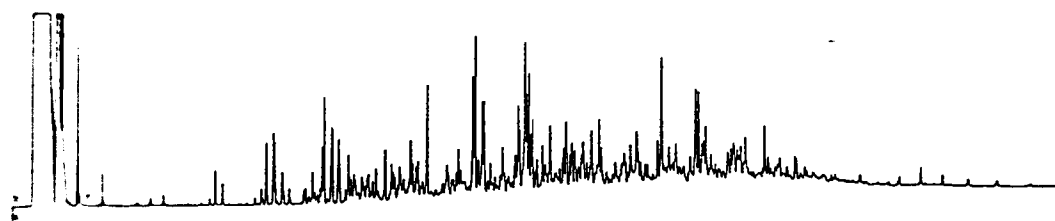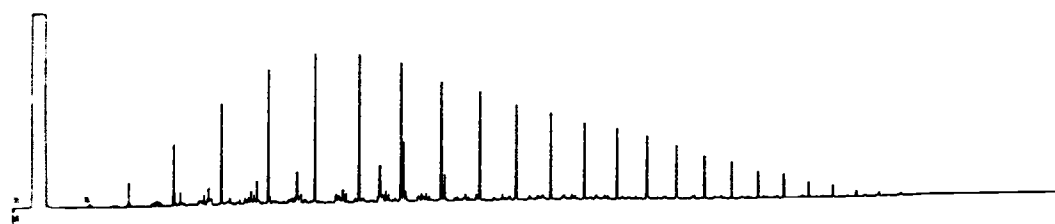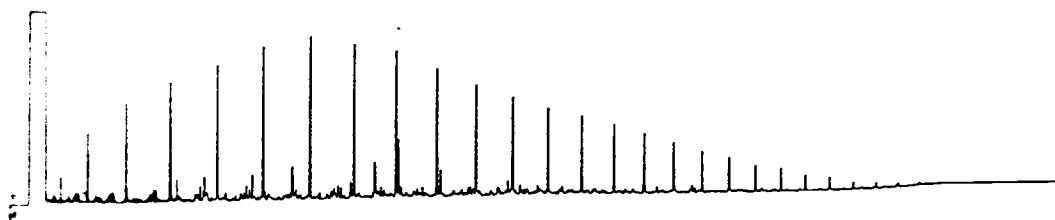
477-16-4 (130-135)
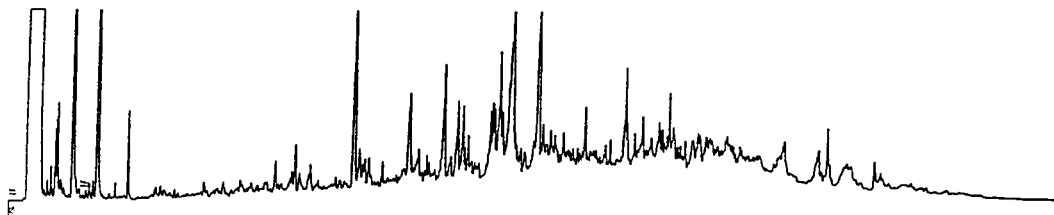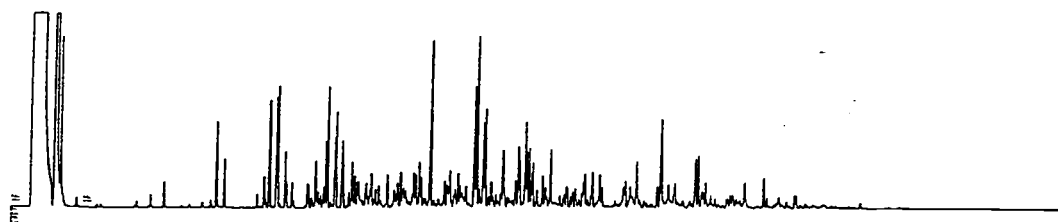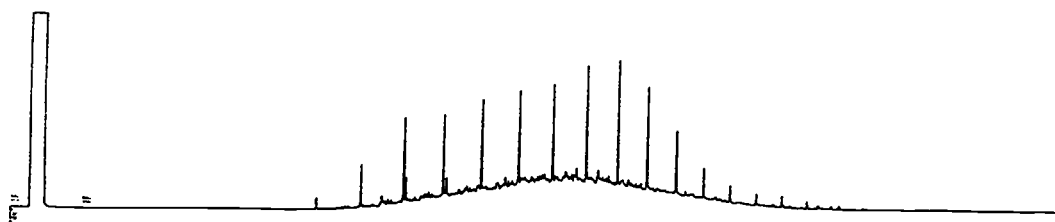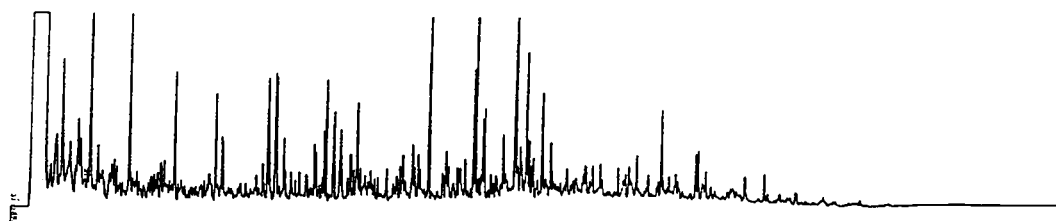
477-16-4 (135-140)
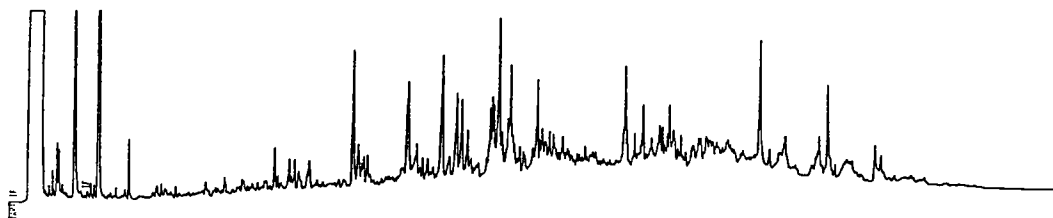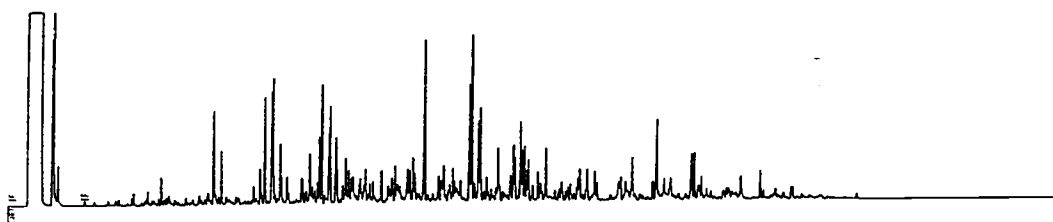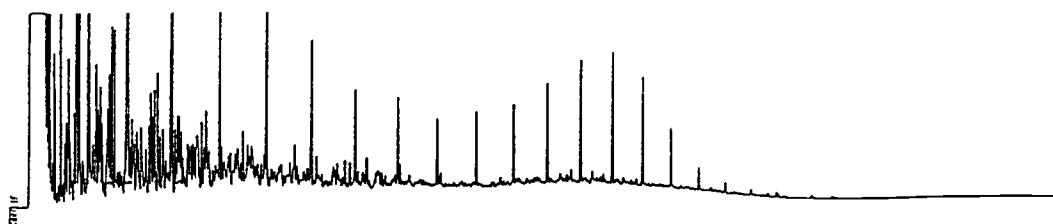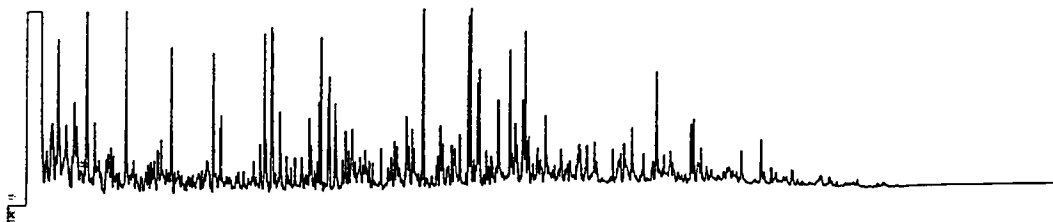
477-17-1 (145-150)
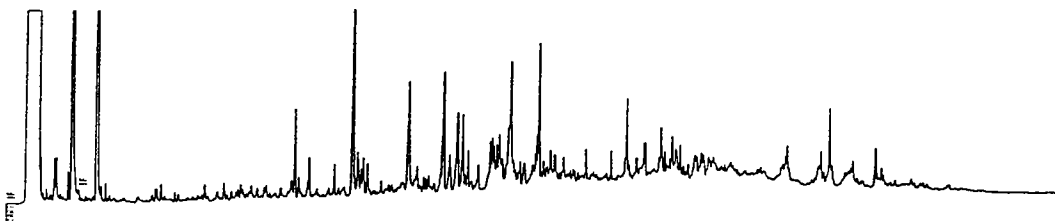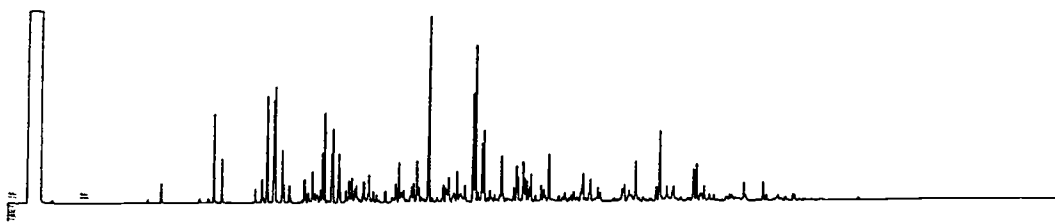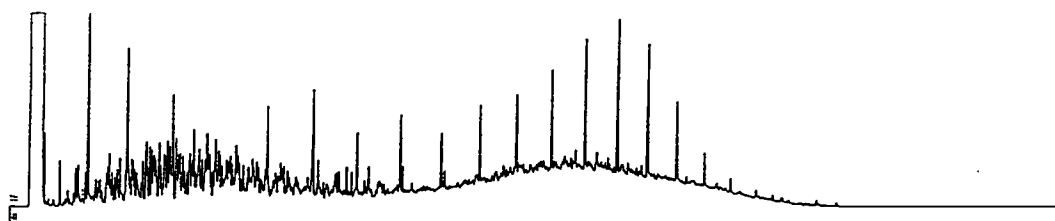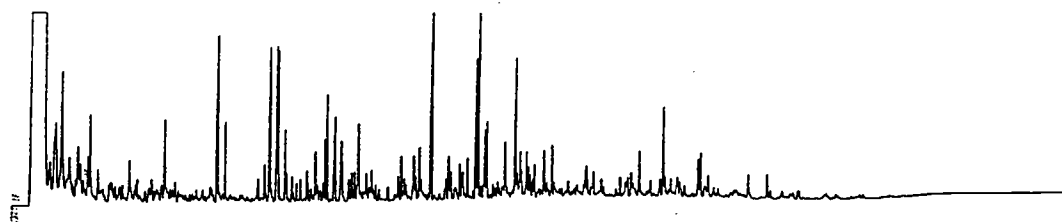
477-19-1 (130-135)
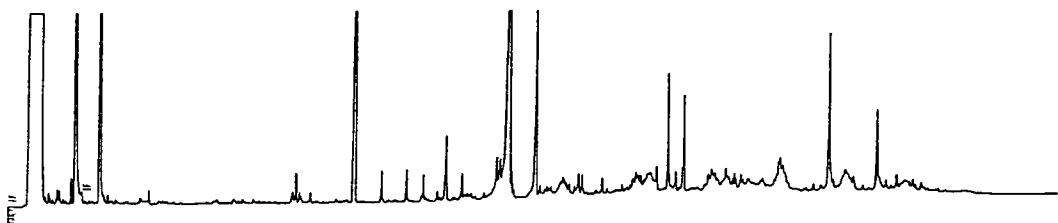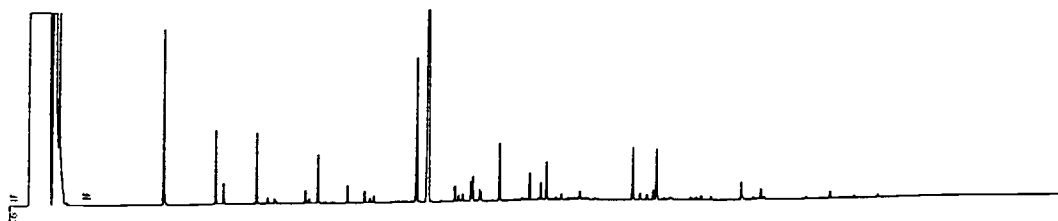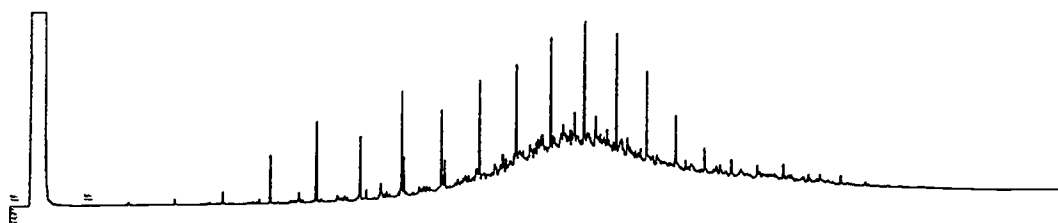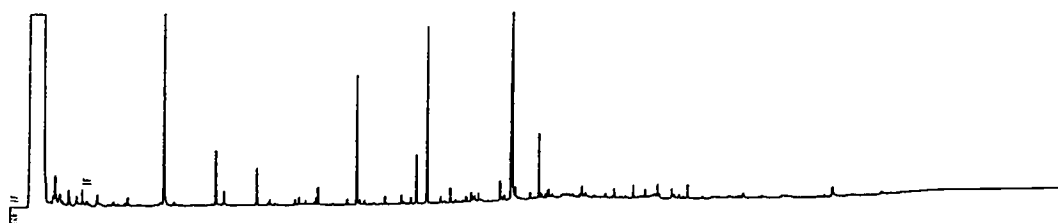
477-19-1 (135-140)
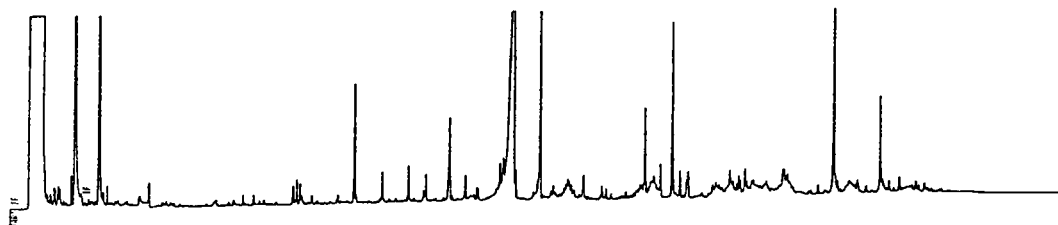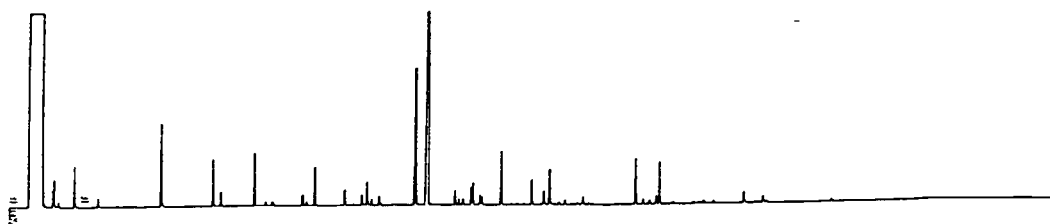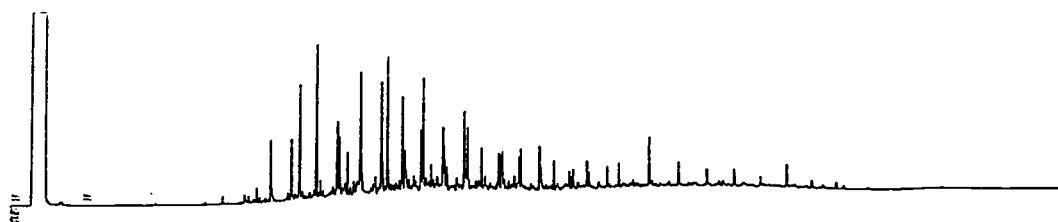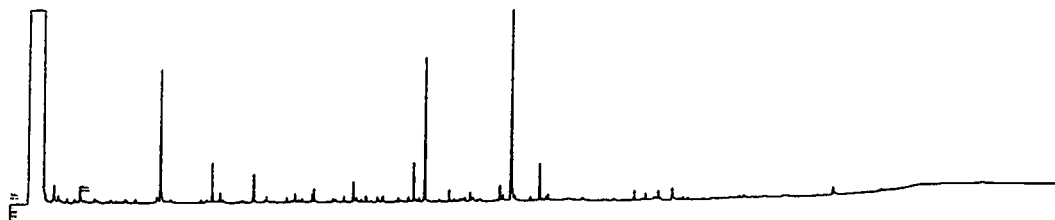
477-20-1 (135-140)
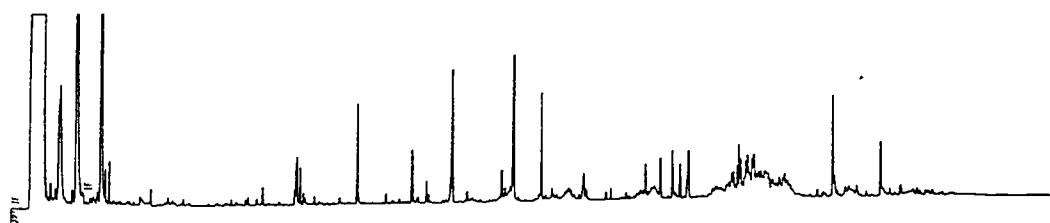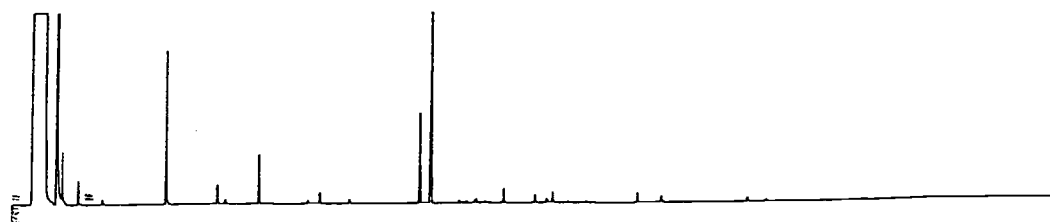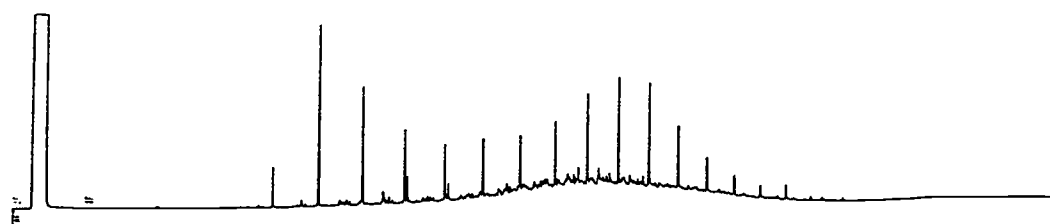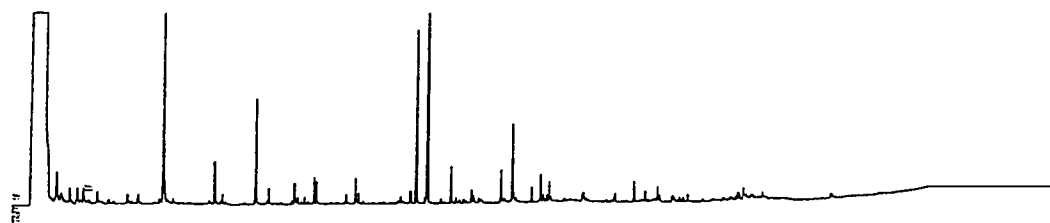
477-21-1 (52-57 + 91-96)
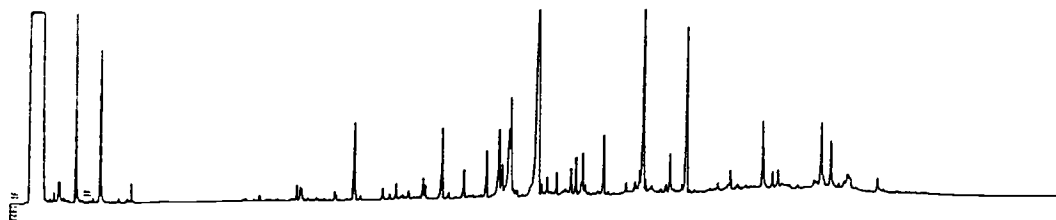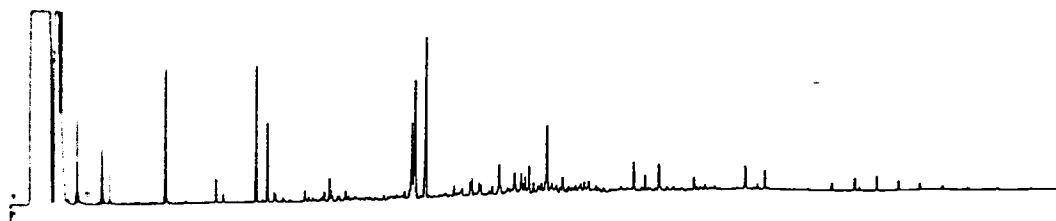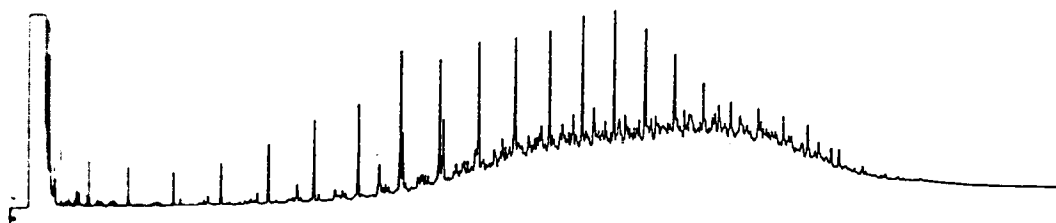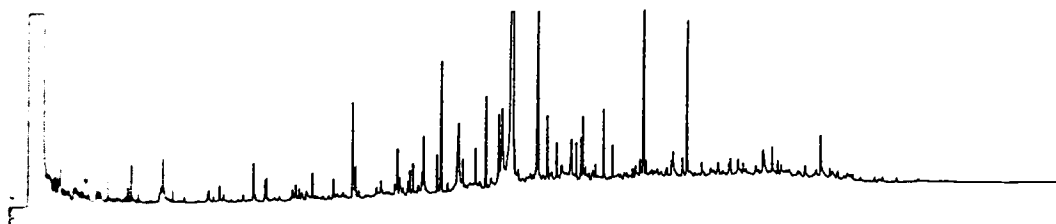
477-22-1 (110-115)
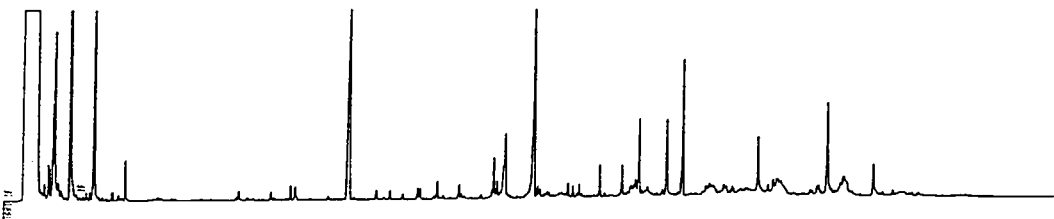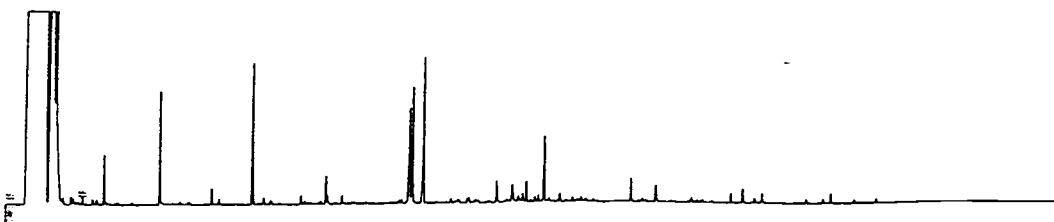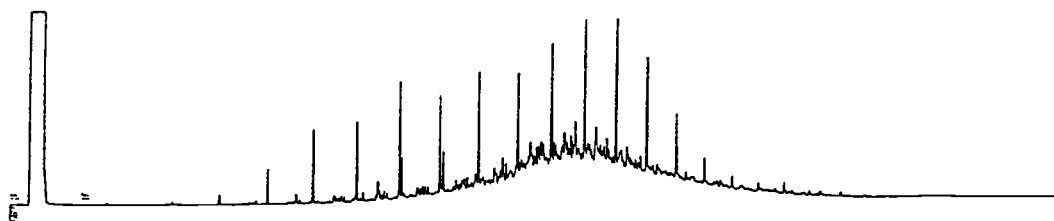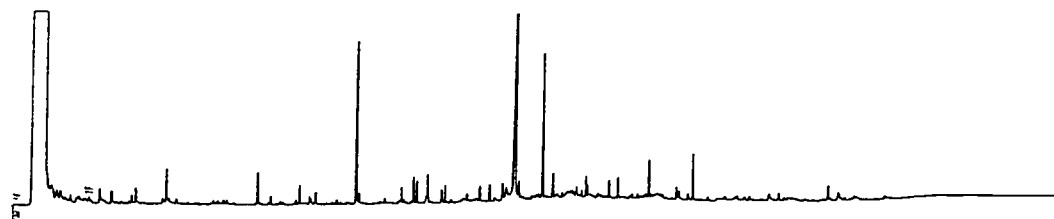
477-23-1 (90-95)
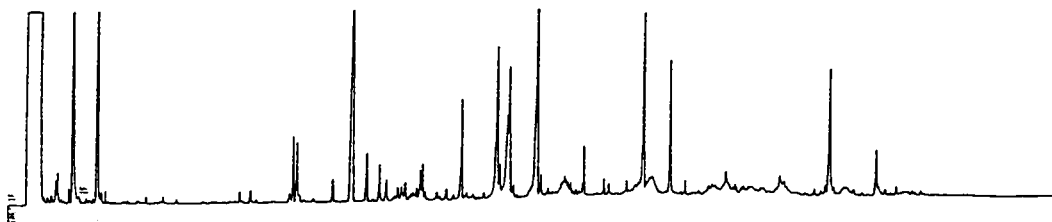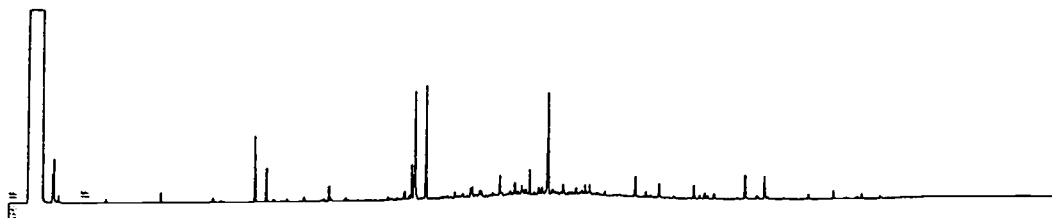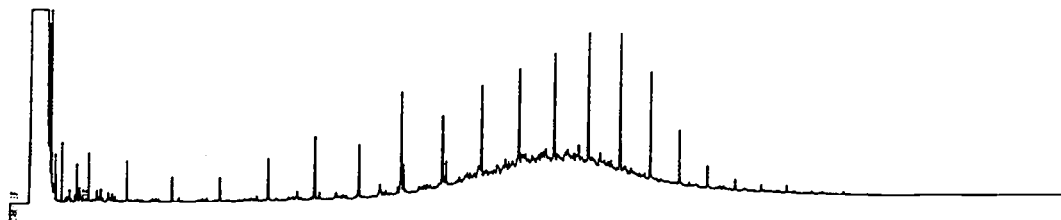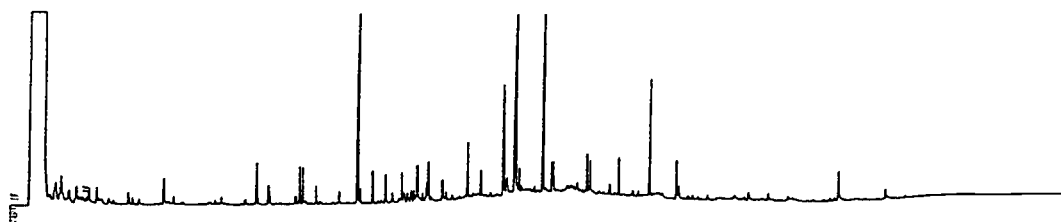
477-23-1 (CC)
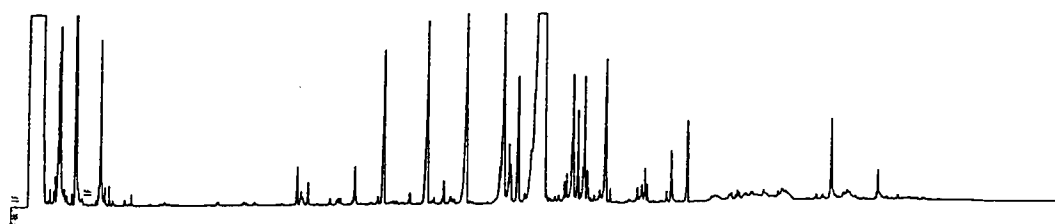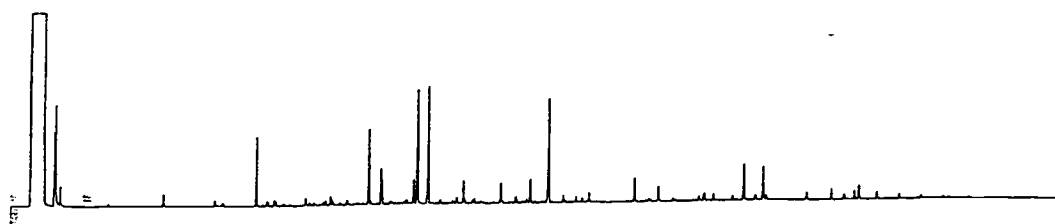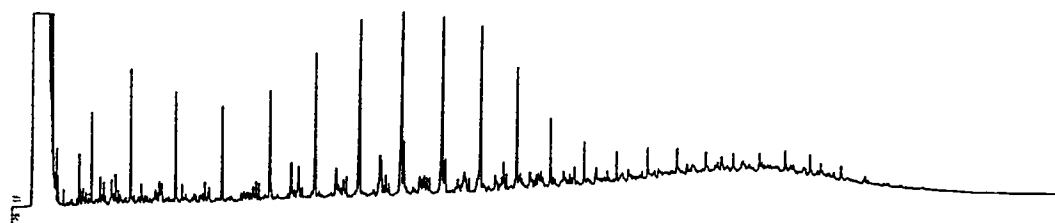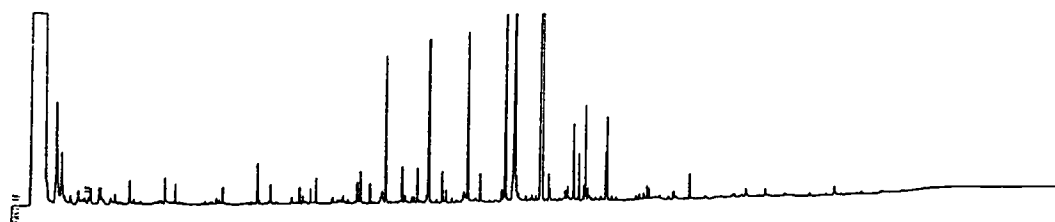
Appendix 3

The Gas Chromatograms for the Downcore Sediment Extracts from DSDP Site 481A of Guaymas Basin, Gulf of California

In this Appendix the gas chromatograms of the total extracts, aliphatic , aromatic and NSO fractions for the sediment extracts from DSDP Site 481A used in this thesis are presented.

481A-4-2 (93-98)
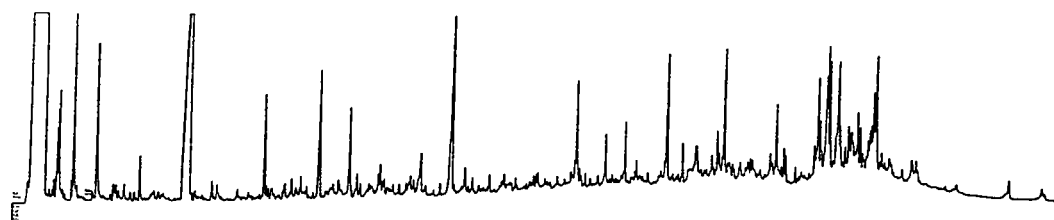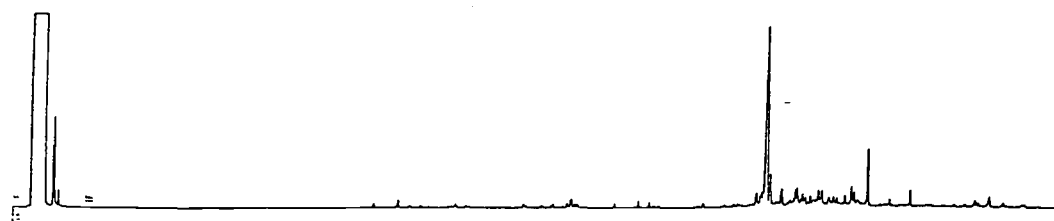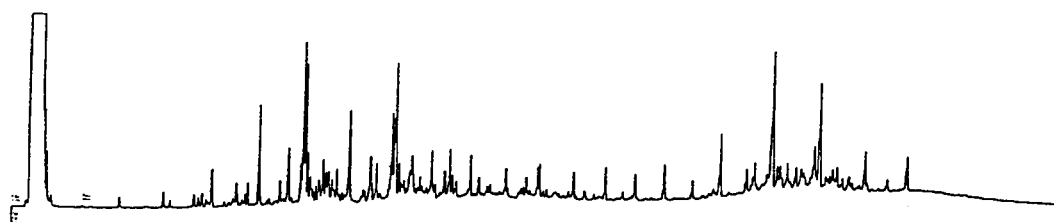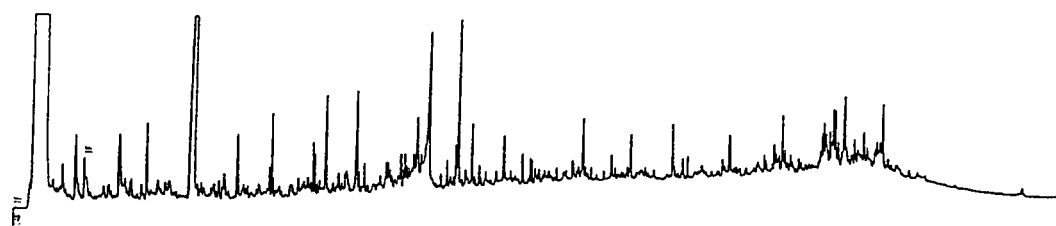
481A-6-5 (118-120)
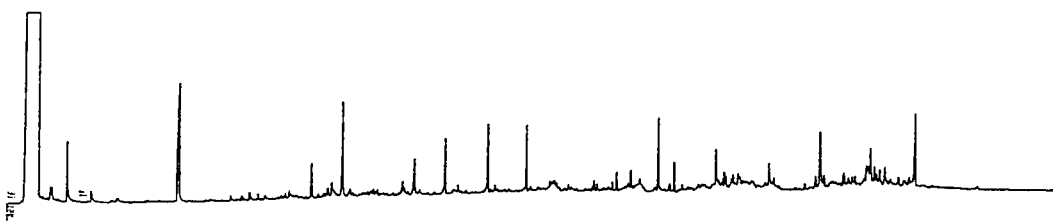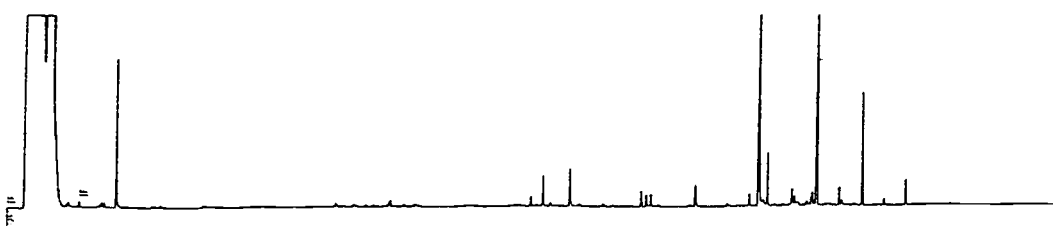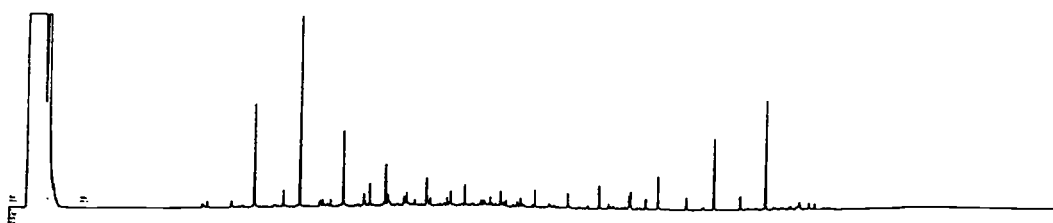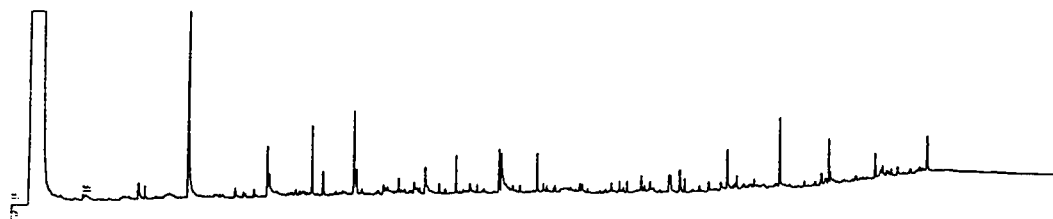
481A-6-5 (124-135)
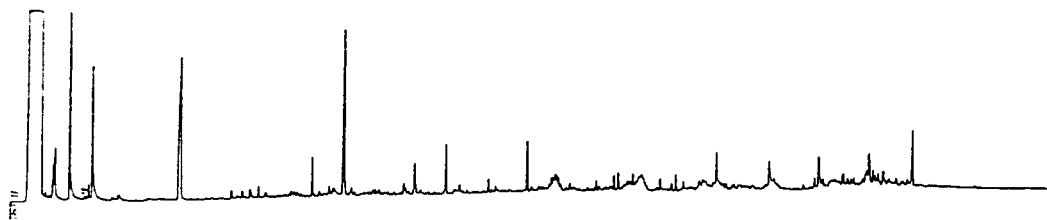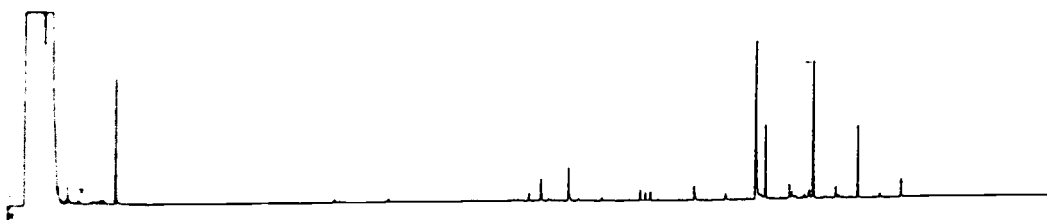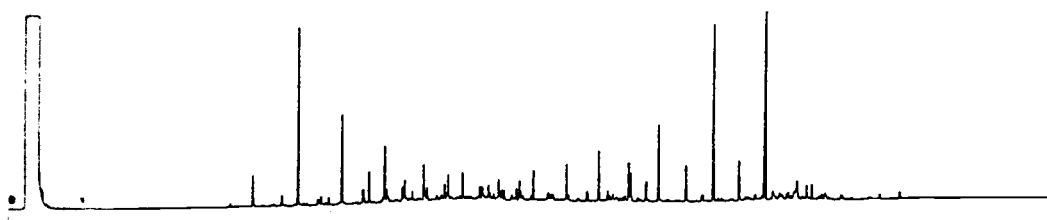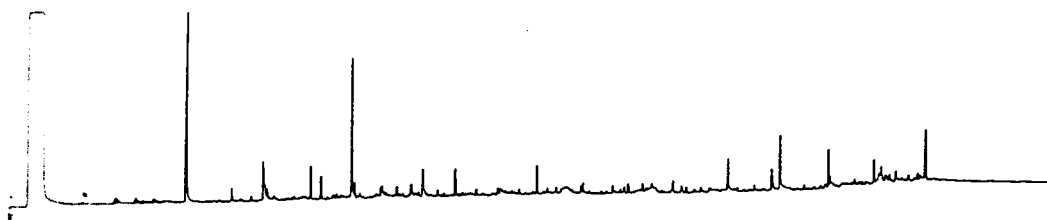
481A-7-6 (71-80)
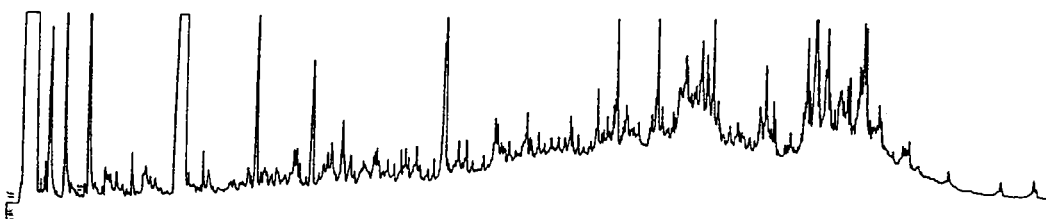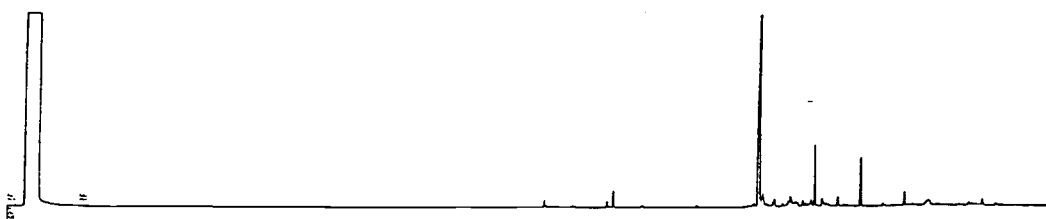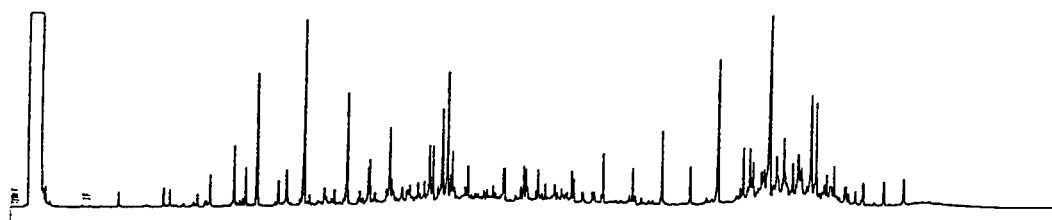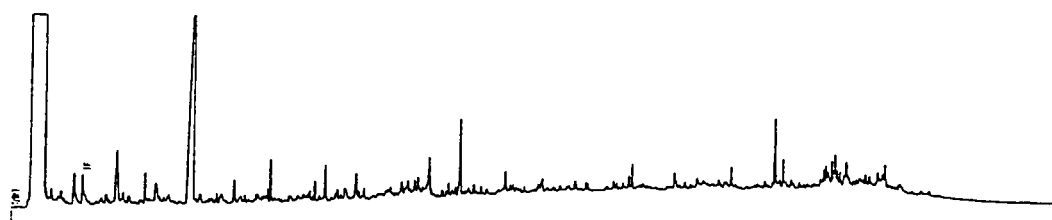
481A-8-7 (top of pipe)
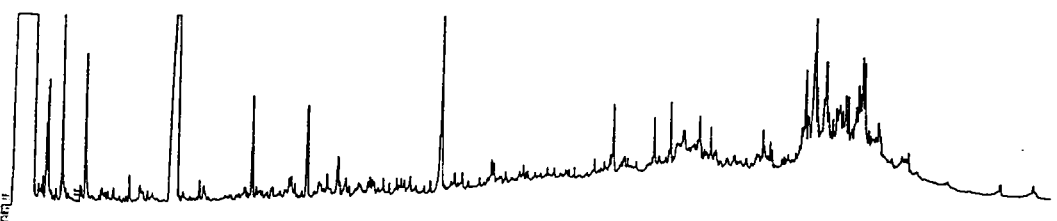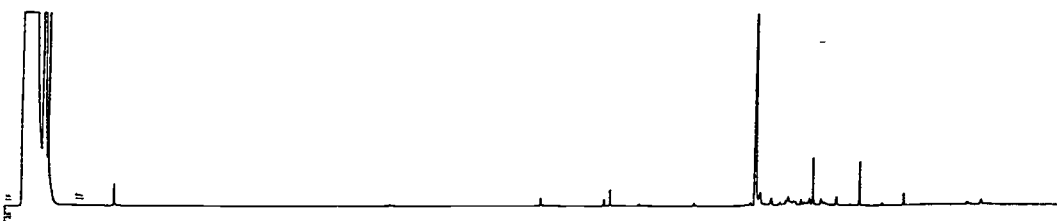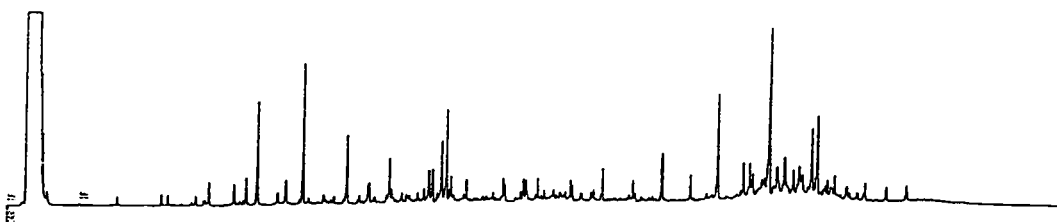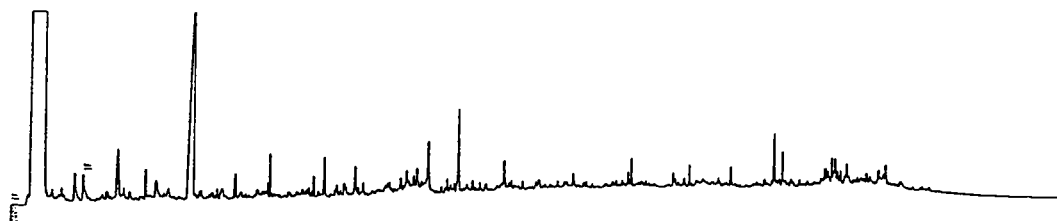
481A-12-4 (55-65)
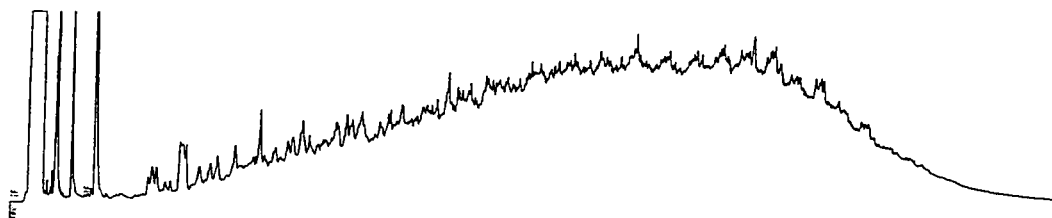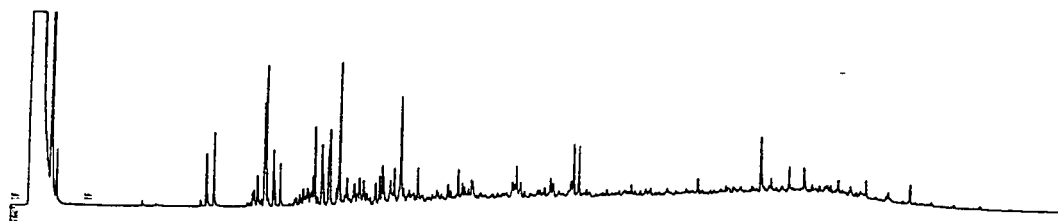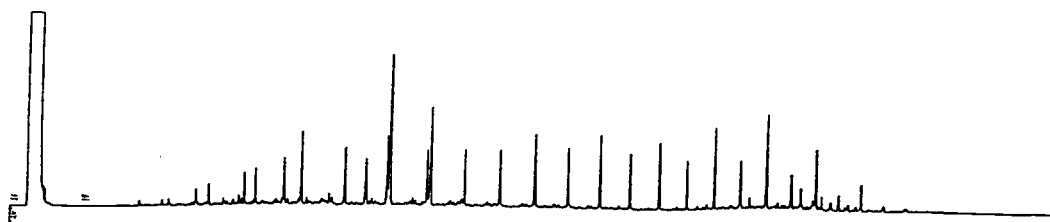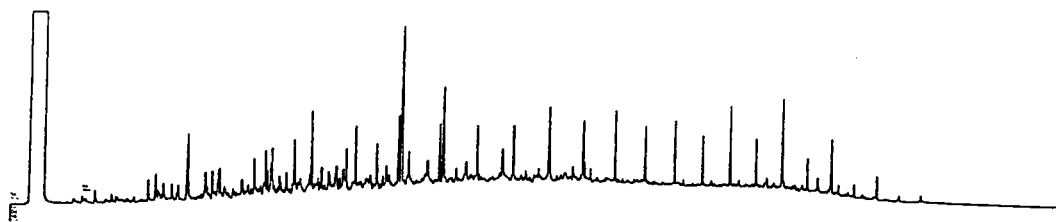
481A-13-2 (118-127)
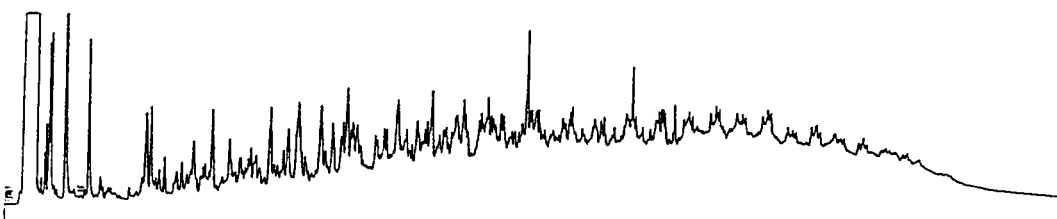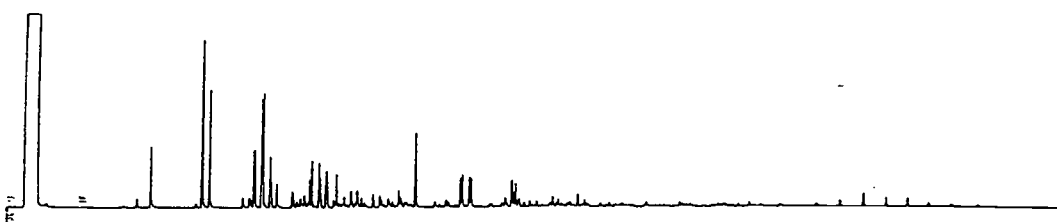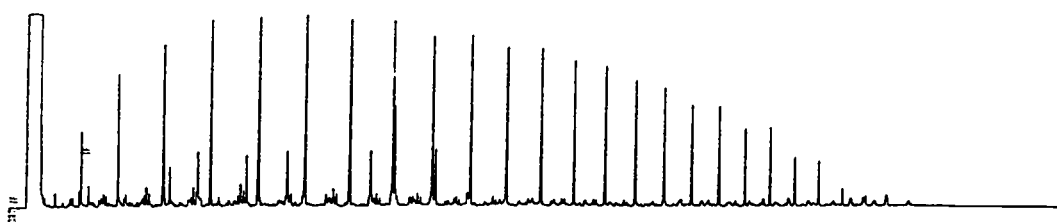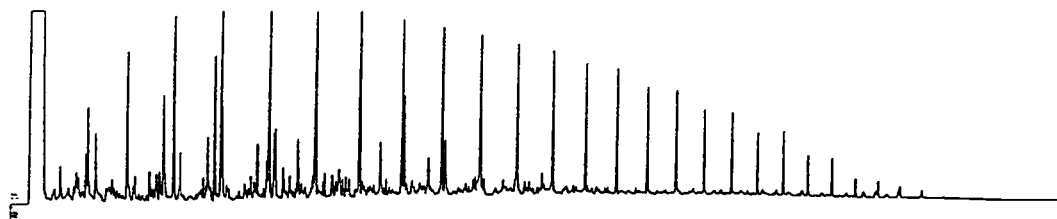
481A-18-1 (30-32)
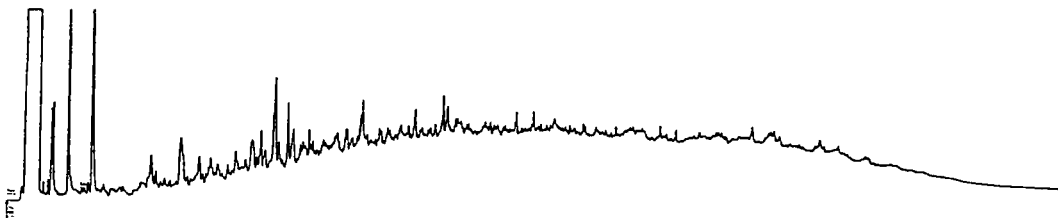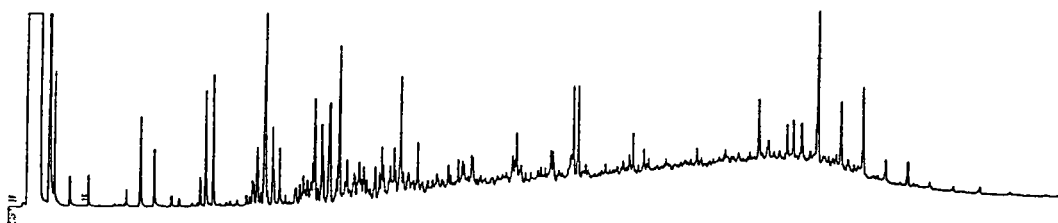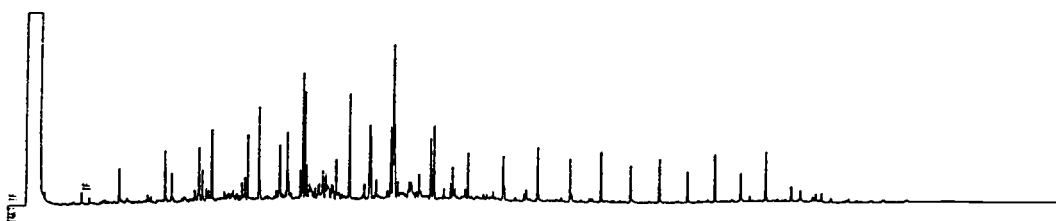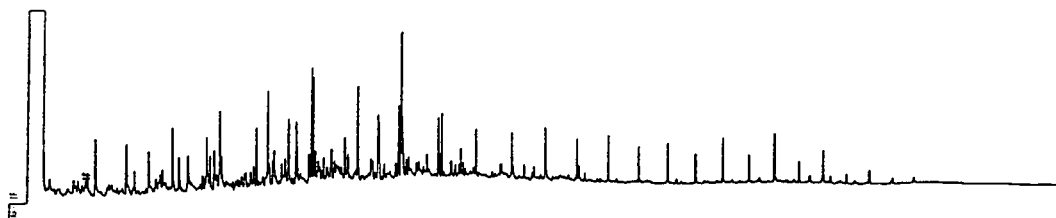
481A-18-1 (CC)
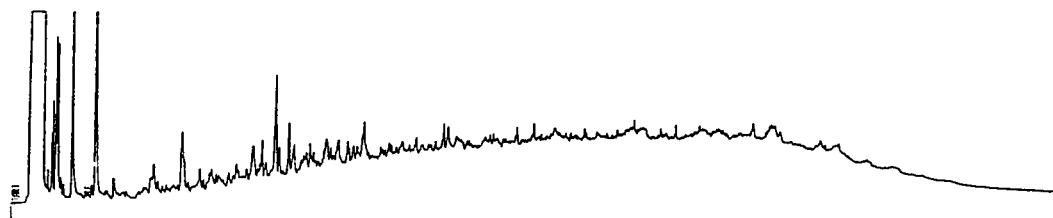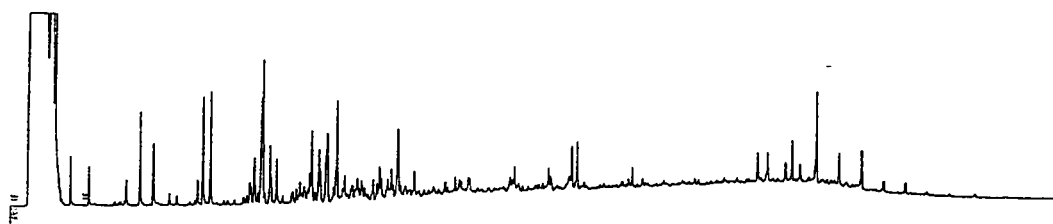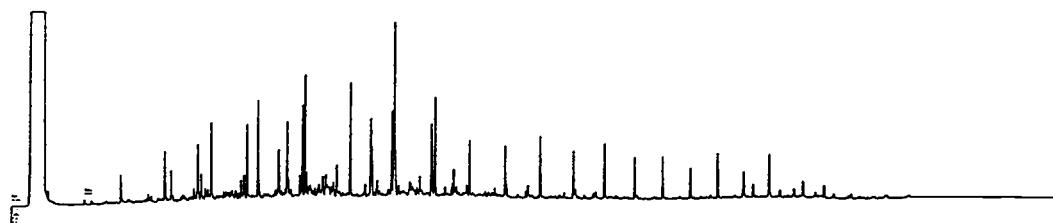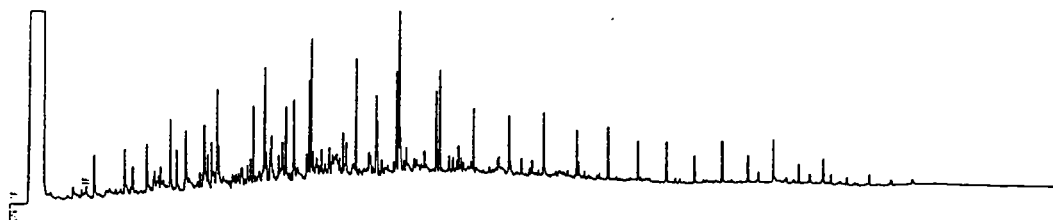
481A-20-1 (110-115)
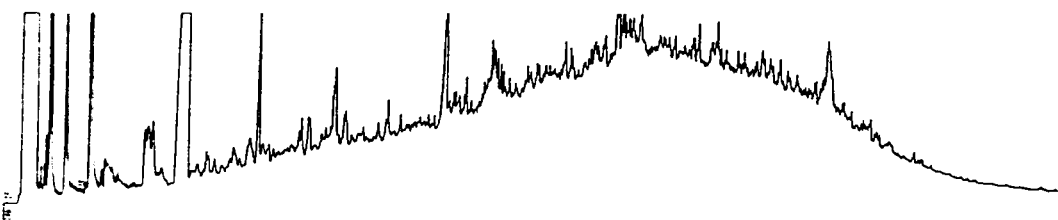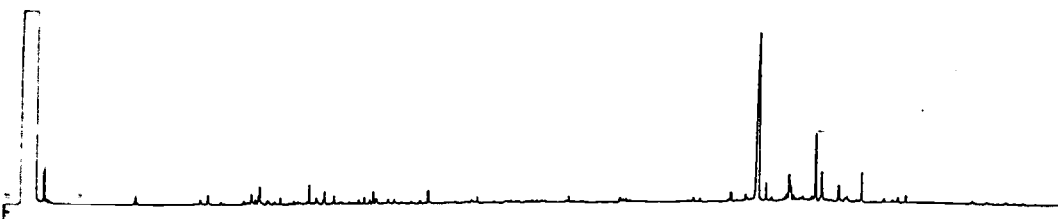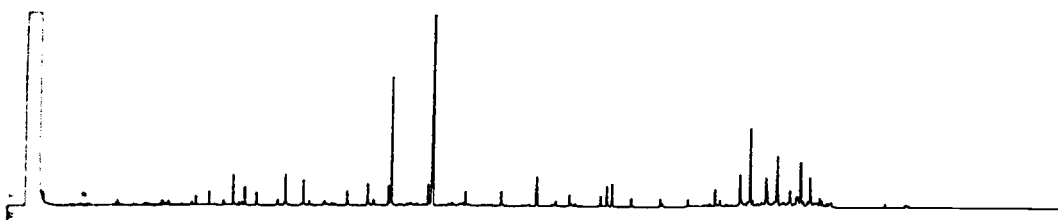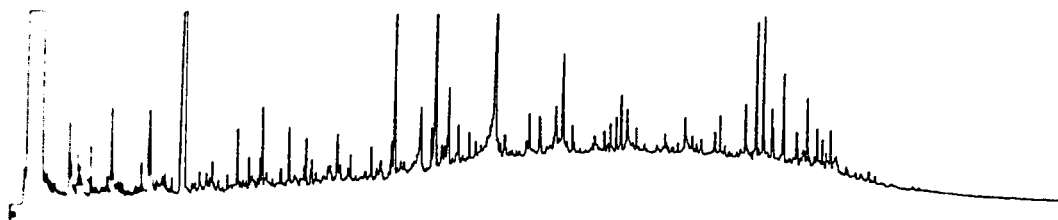
481A-22-1 (65-70)
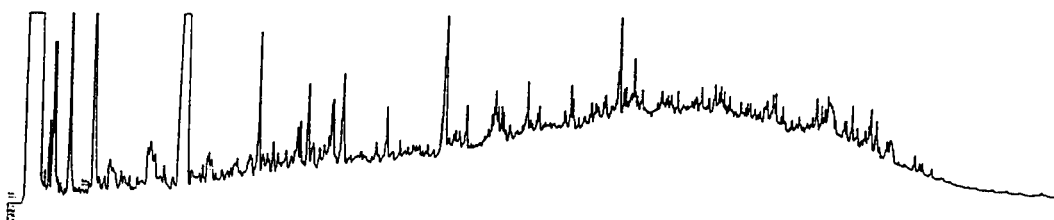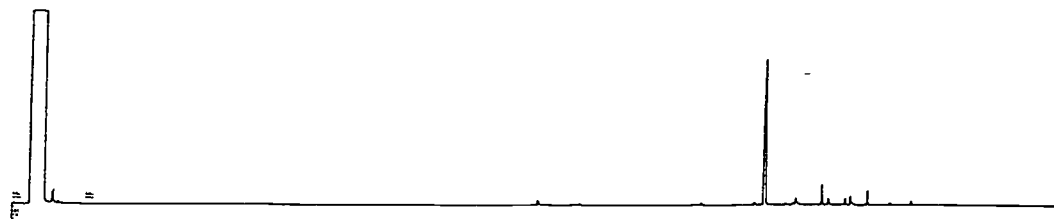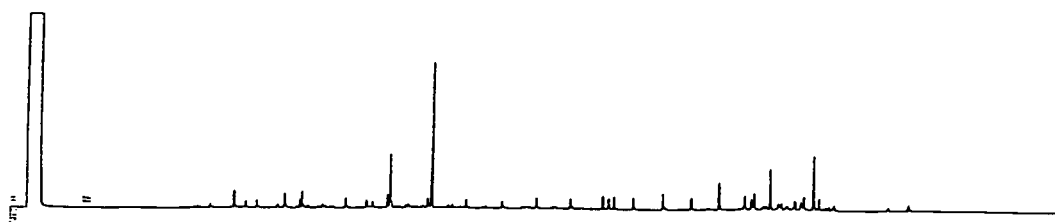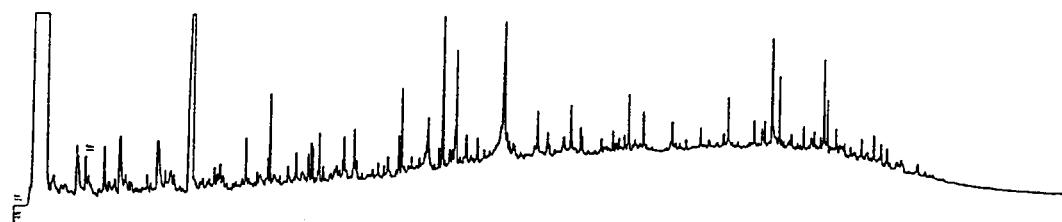
481A-22-7 (top of pipe)
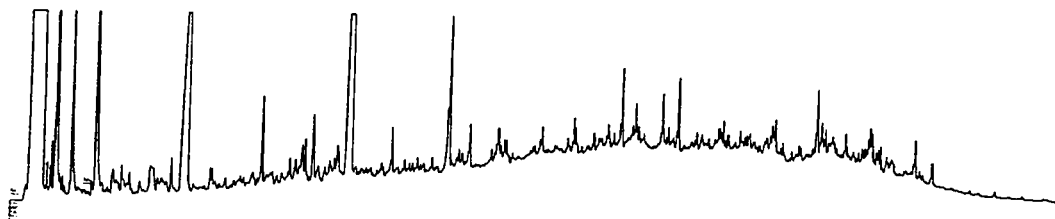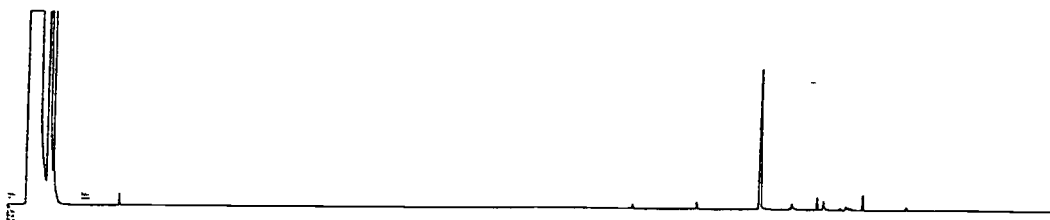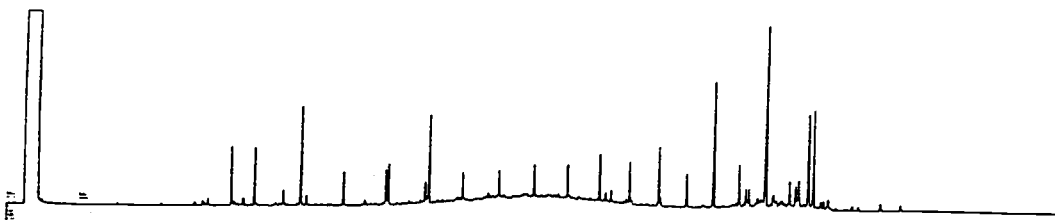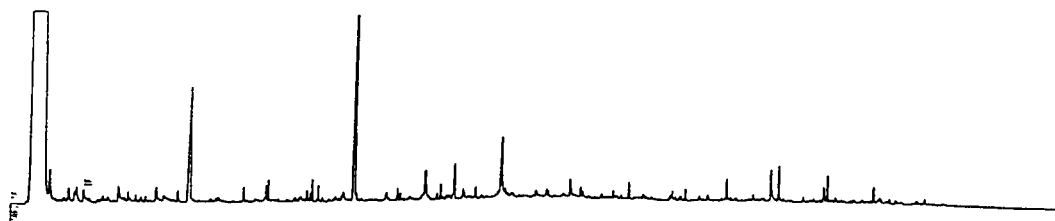
481A-22-7 (97-101)
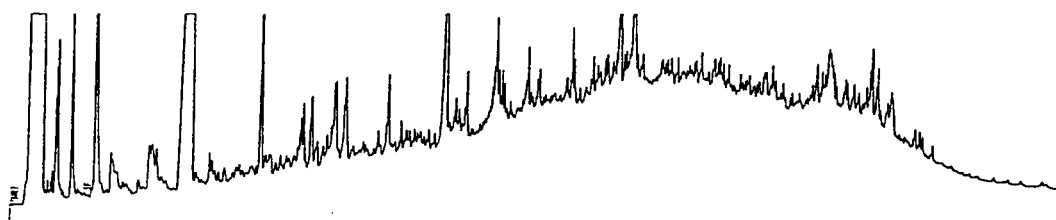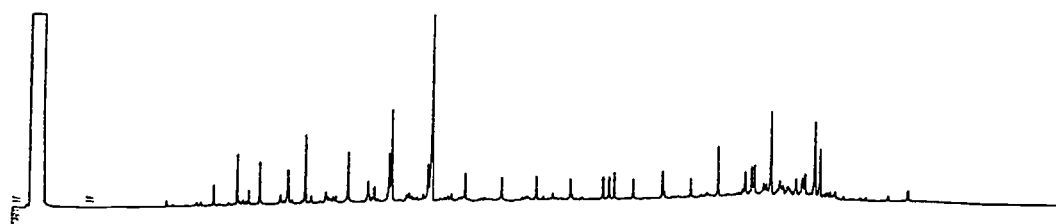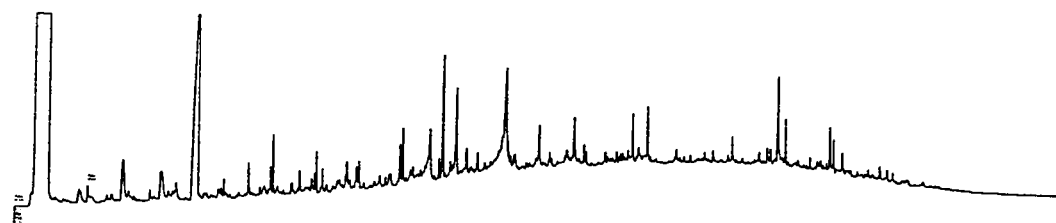
481A-24-CC
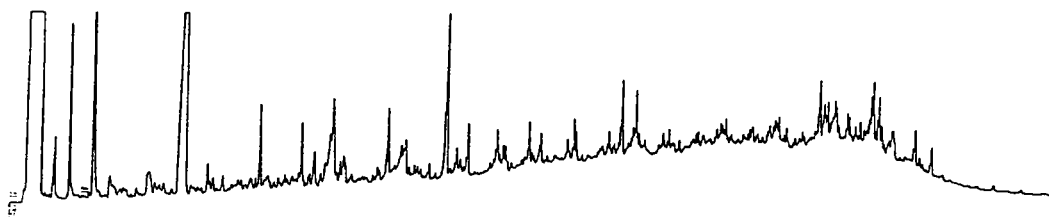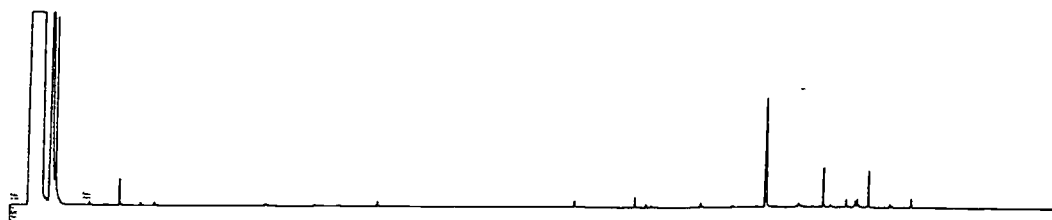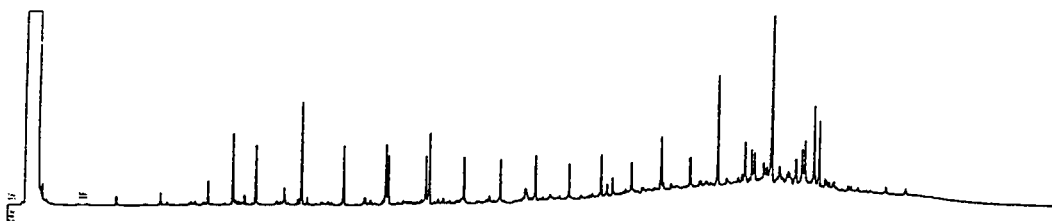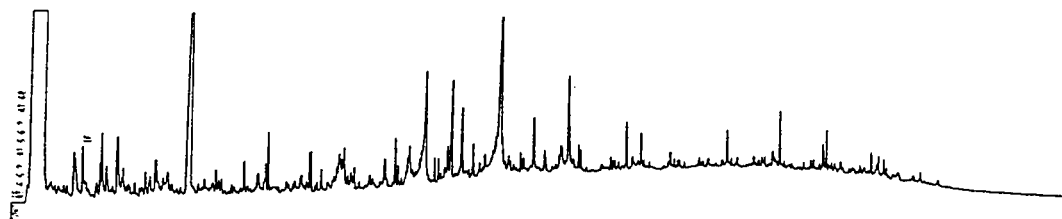
481A-25-CC
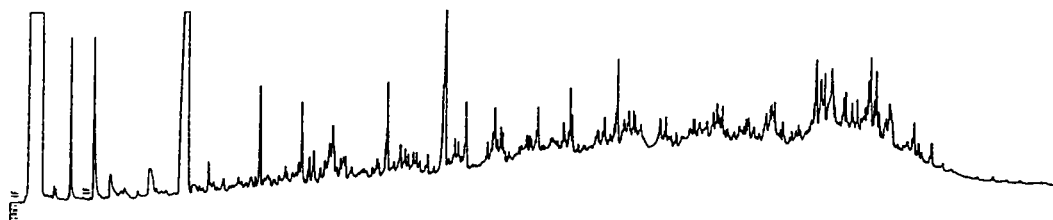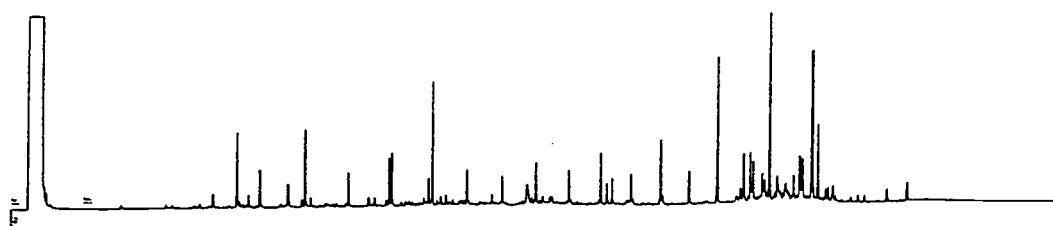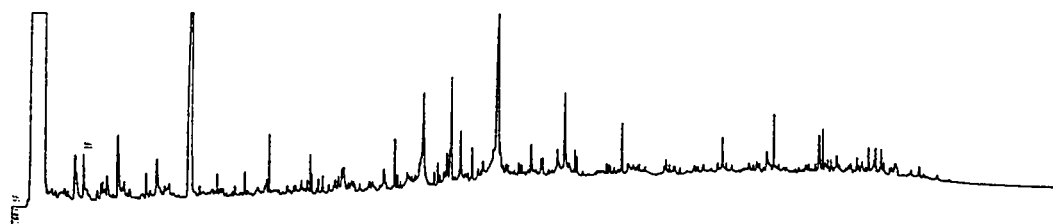
481A-26-CC
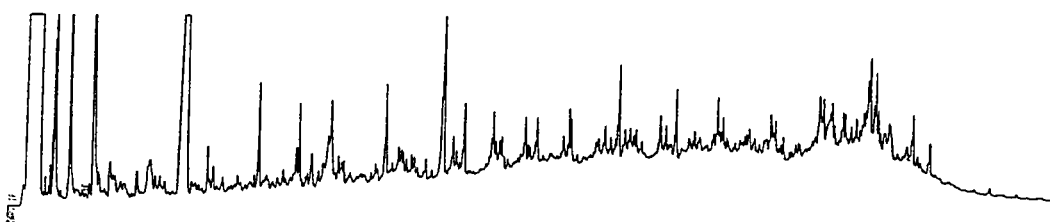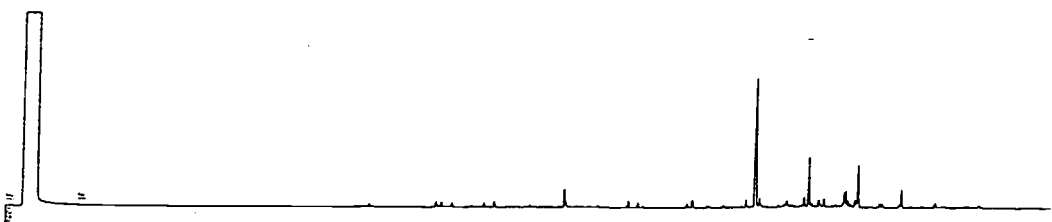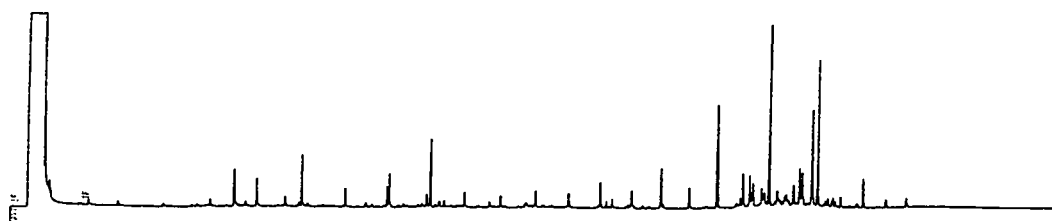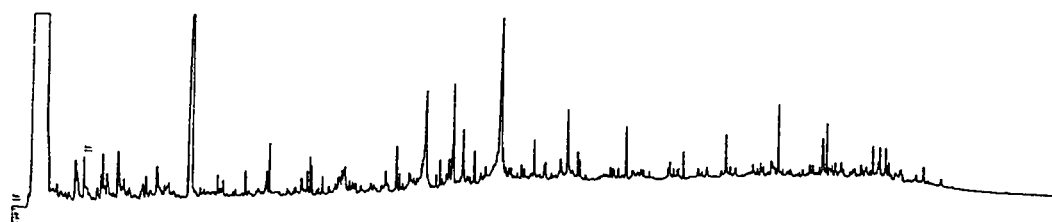
Appendix 4

The Gas Chromatograms from the Pyrolysis Experiments on the North Rift Surface Sediment and Downcore Sediments of DSDP Site 481A, Guaymas Basin, Gulf of California

In this Appendix the gas chromatograms of the aliphatic , aromatic and NSO fractions of the unaltered sediment extracts and the pyrolyzed sediment extracts used in Chapter 5 of this thesis are presented.

AII-112-29 PC-5
(Unaltered)
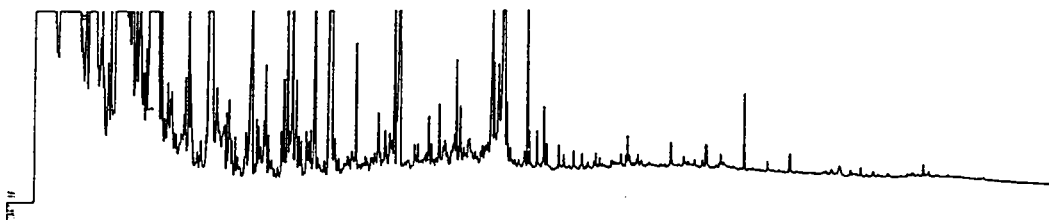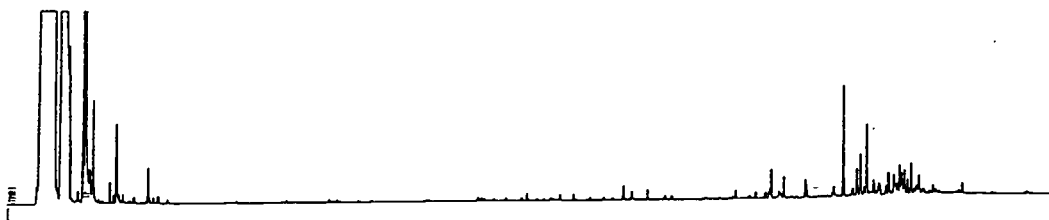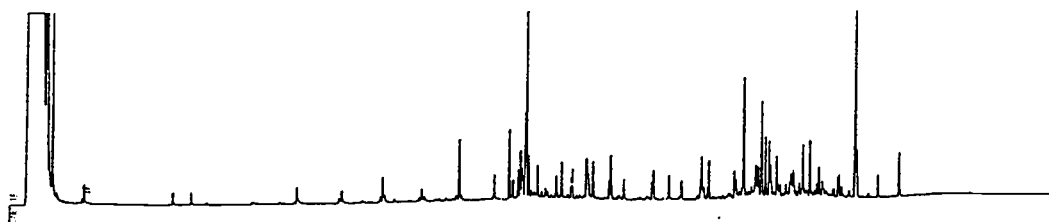
AII-112-29 PC-5
(24 hr at 330°C)
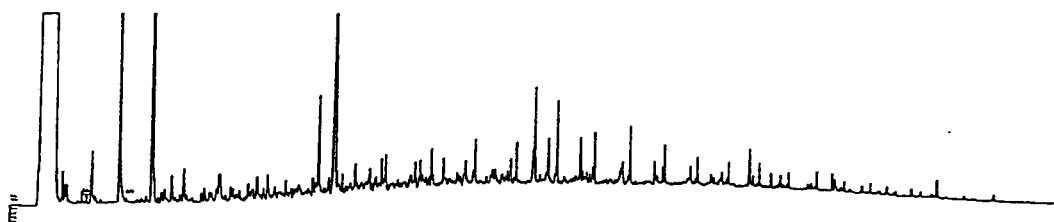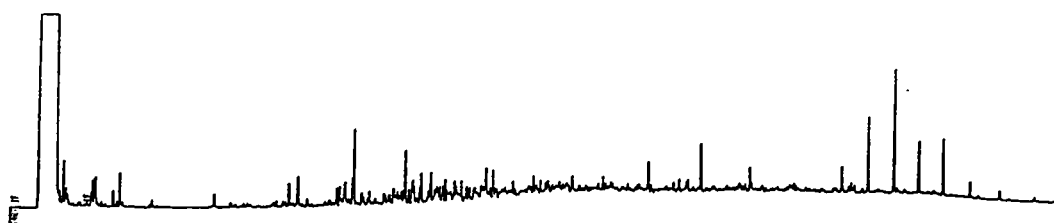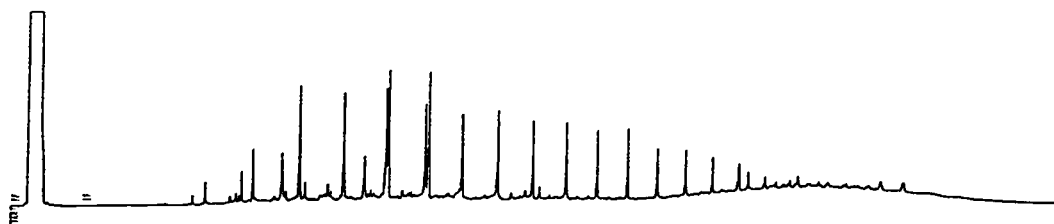
AII-112-29 PC-5

(48 hr at 330°C)
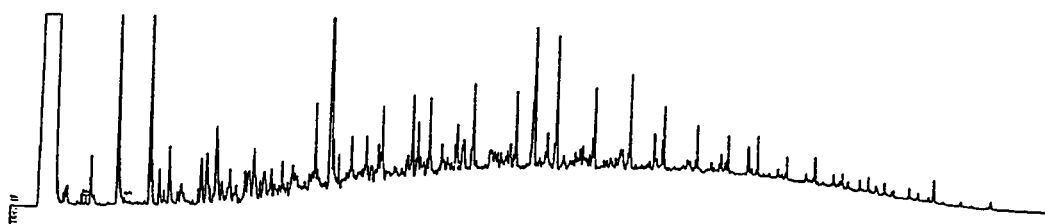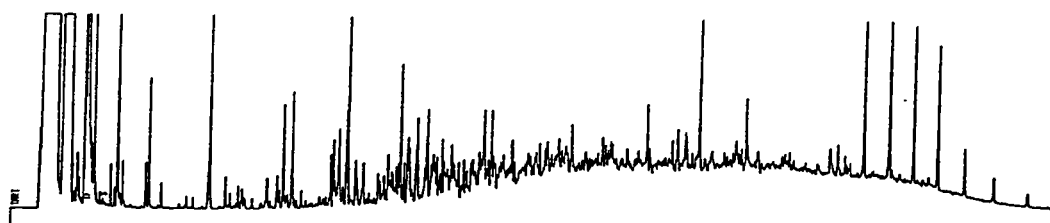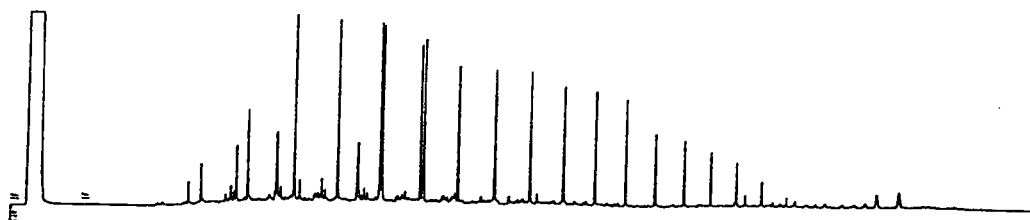
AII-112-29 PC-5
(72 hr at 330°C)
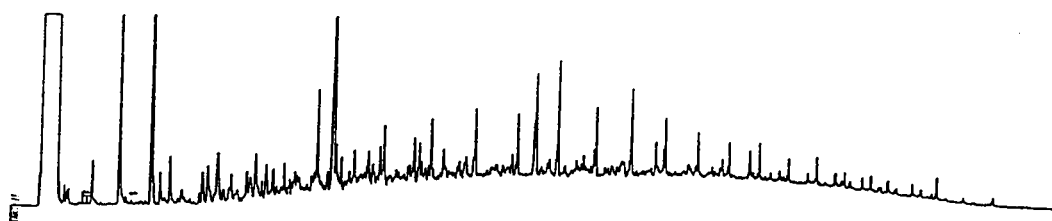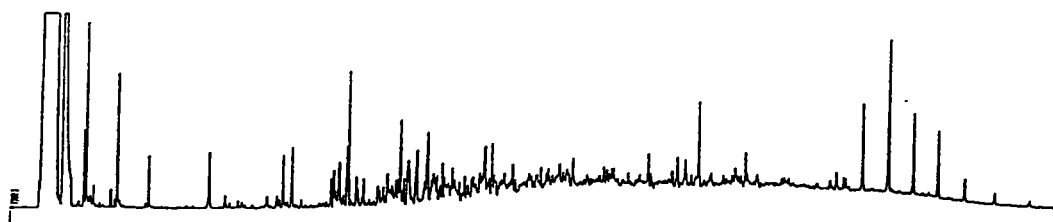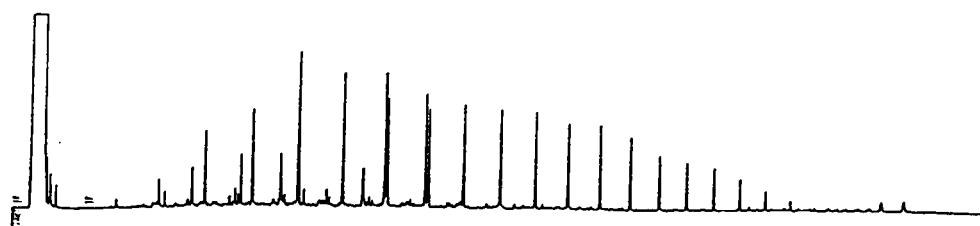
481A-8-7 (top of pipe)
(Unaltered)
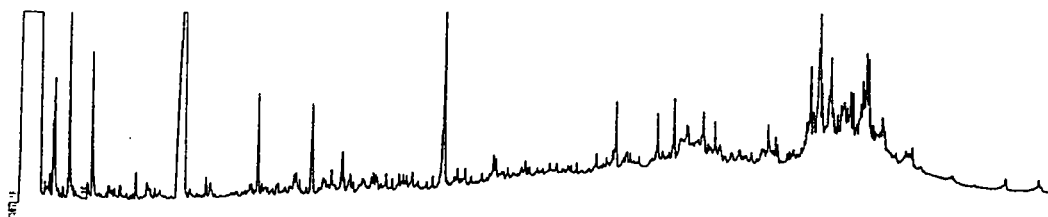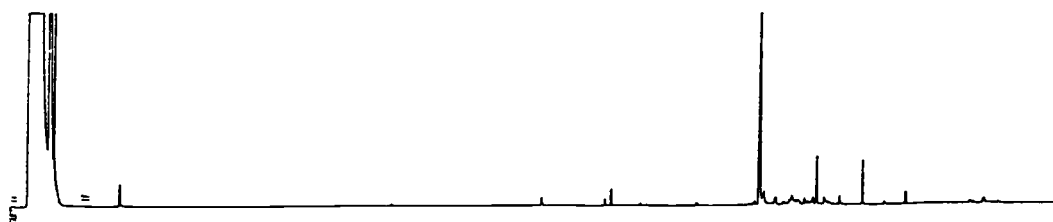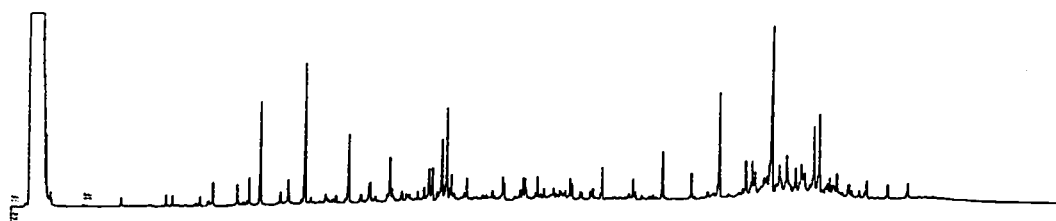
481A-8-7 (top of pipe)
(24 hr at 330°C)
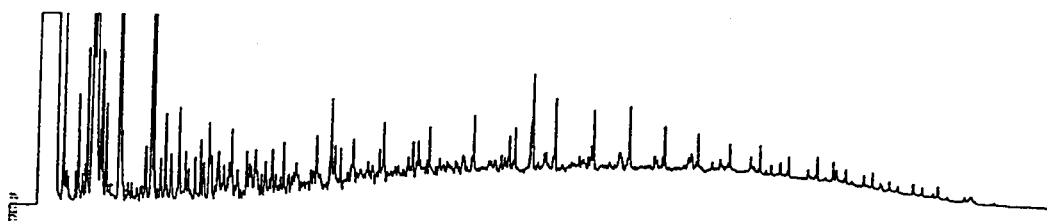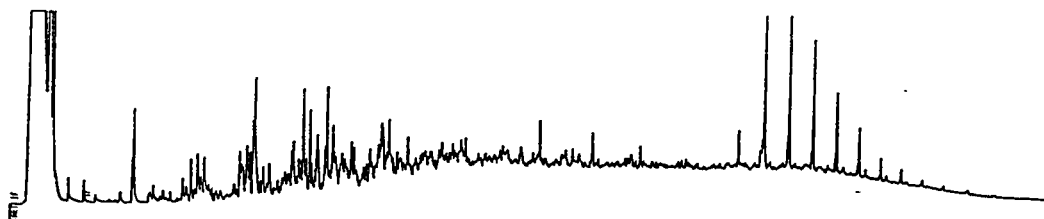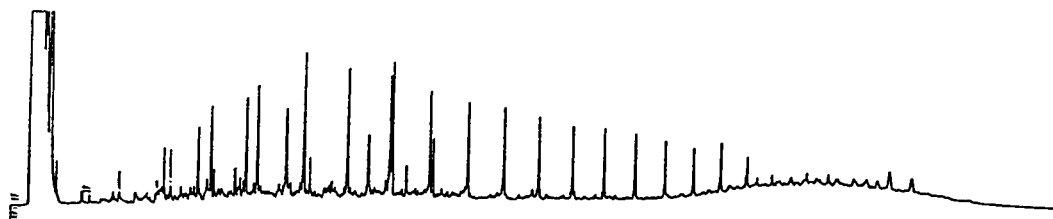
481A-8-7 (top of pipe)
(48hr at 330°C)
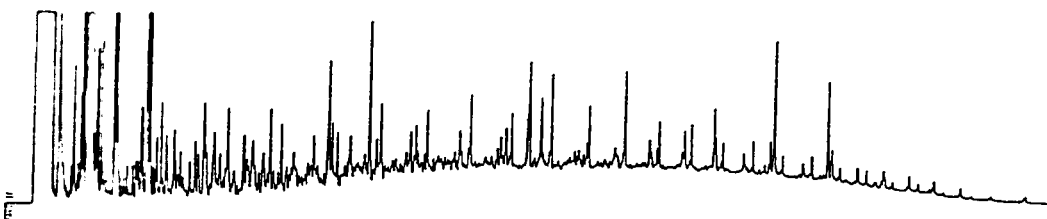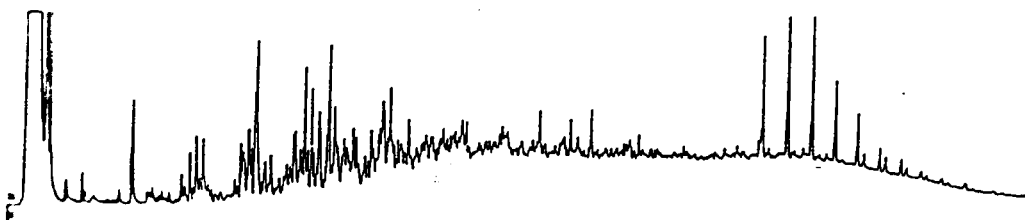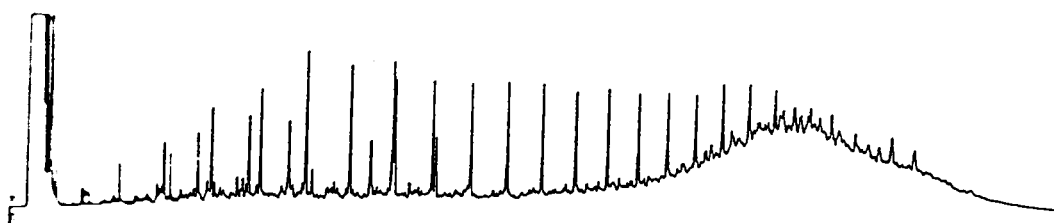
481A-8-7 (top of pipe)
(72hr at 330°C)
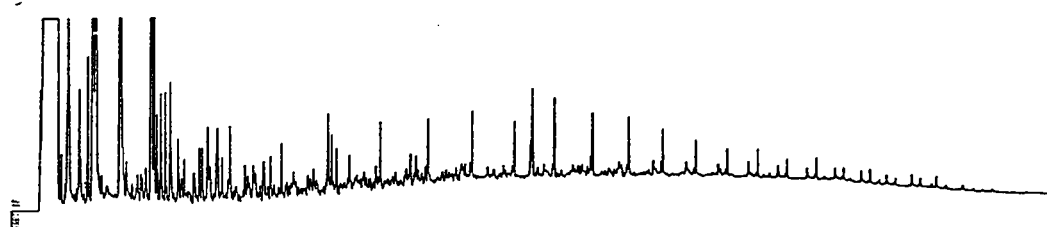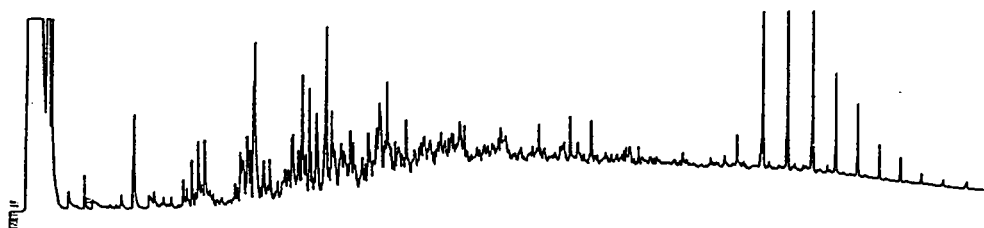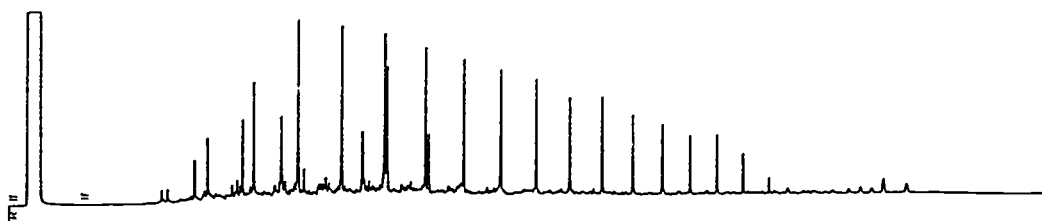
481A-22-7 (top of pipe)

(Unaltered)
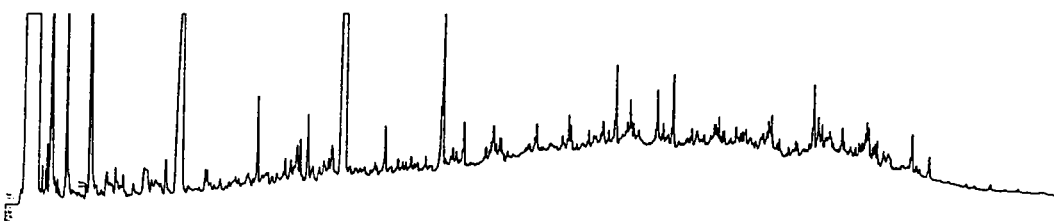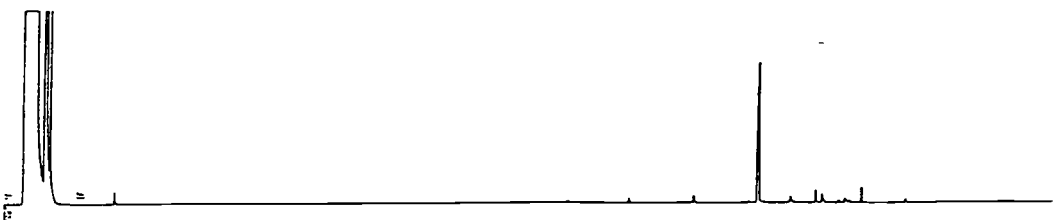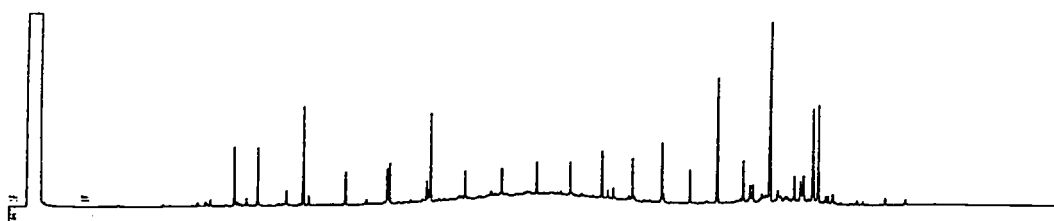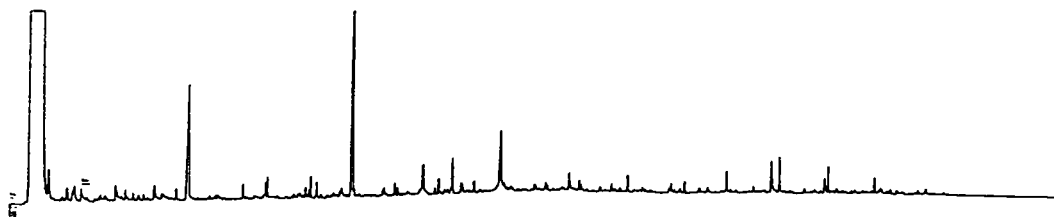
481A-22-7 (top of pipe)
(24 hr @ 330°C)
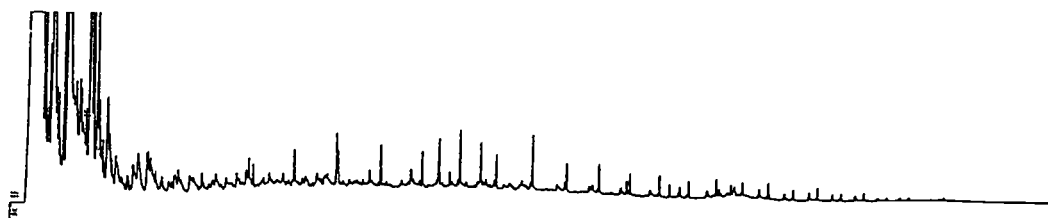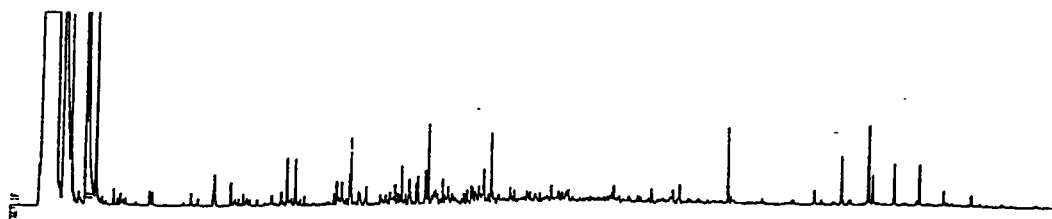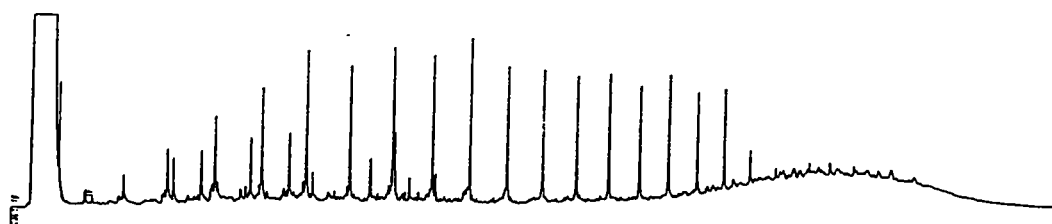
481A-22-7 (top of pipe)
(48hr @ 330°C)
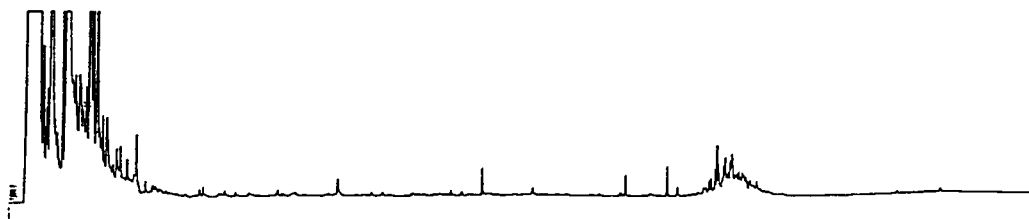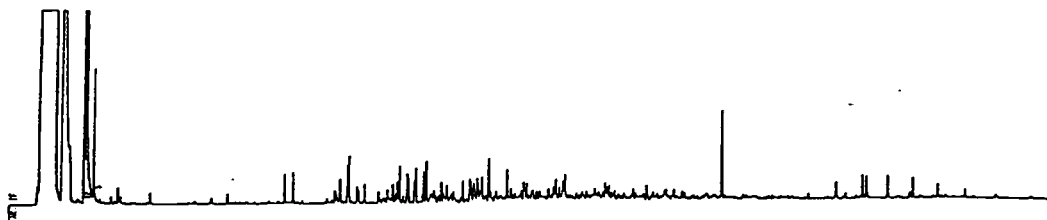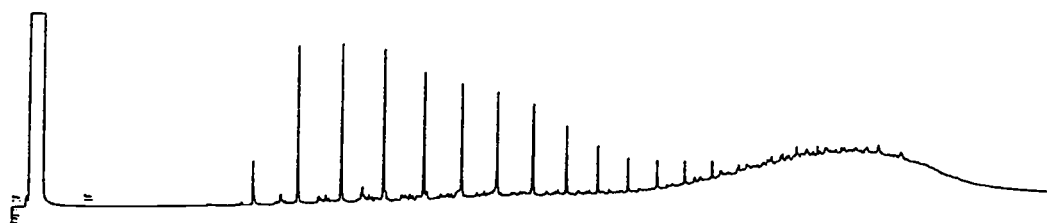
481A-22-7 (top of pipe)
(72hr @ 330°C)